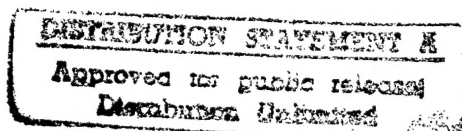VOLUME III
SYSTEMS PHASE

CHAPTER 5
ELECTRO-OPTICAL
SYSTEMS

19970117 019

30 JUNE 1995

USAF TEST PILOT SCHOOL
EDWARDS AFB, CALIFORNIA

TABLE OF CONTENTS

SECTION III - OPTICS

SECTION IV - LASER FUNDAMENTALS AND SYSTEMS

SECTION V - OPTICAL DETECTORS

SECTION VI - DISPLAYS

SECTION VII - HUDS

SECTION VIII - ELECTRO-OPTICAL SYSTEM PERFORMANCE TEST AND EVALUATION

SECTION I

INTRODUCTION TO ELECTRO-OPTICS

1.1 INTRODUCTION. Electro-optical (E-O) systems encompass the range of wavelengths from the ultraviolet to the infrared portions of the electromagnetic spectrum. The systems are termed optical because optical techniques are employed in differentiating and detecting the various signals even though the wavelengths are not always visible to the human eye. The signals generated by the optical detector are processed using electronic techniques and hence the term electro. The systems or subsystems normally considered to be electro-optical are:

a. Television. Operates in the visible spectrum in both daylight and low light level (LLL) conditions. TV can also operate into the near IR region.

b. Infrared. IR operates in the longer wavelength, nonvisible portion of the spectrum.

c. Lasers. Lasers operate at a single wavelength individually, but can be selected from a broad spectrum area covering the visible through the IR sections.

Optical systems have seen military applications for centuries. Refinements over the years have led to system functions in gunnery, bombing, navigation, and search/identifications instruments viewed directly by the operator. Electronic sensing of the light permitted remote placement of sensors, light amplification, and sensing wavelengths not visible to the eye.

Television sensors were used in the late 1940's for pilotless aircraft and quickly expanded to daylight applications in the remote control of tail guns and remote surveillance. Further sensor development, aimed at decreasing size and increasing sensitivity to provide low light level capability, led to new applications. Early feasibility systems for television with both day and night capability were flown in the USAF ADO-53 program to provide a developmental base. These tests led to operational systems such as helicopter TV and Tropic Moon II.

The helicopter TV was a LLLTV with limited elevation pointing capability mounted on a UH-1 helicopter. The system was deployed to SEA in 1967 and demonstrated limited success as a locator system. Tropic Moon II was a pod mounted gimballed mirror system using a LLLTV and a laser ranger for weapons delivery. The system

was deployed on a B-57 and demonstrated the utility and accuracy of E O systems.

Infrared systems development actually began before TV but lagged due to inadequate IR detectors. In 1957 Texas Instruments developed the induim-antimonide (InSb) detector which led to the first practical airborne infra-red sensor. This eventually led to forward looking infrared (FLIR) which became feasible for airborne systems in the late 1960s.

The first successful multispectral system was Tropic Moon III installed in that old work horse - the B-57. It contained LLLTV, FLIR, and a laser mounted on a single gimbal. These elements were tied to the digital computer and gave the aircraft a precision weapon delivery capability. Tropic Moon III was proven in SEA and was particularly effective against soft targets.

Precision munitions guided by EO systems were extremely successful during the gulf war. Both laser guided bombs (LGB) and maverick air-to-surface missiles were used to destroy military targets with minimal collateral damage. The laser guided bomb (LGB) detects the reflected laser light from an illuminated target and homes in on it. The target can be illuminated by systems ranging from a hand-held unit with a boresight telescope to a complex airborne tracker and designator. In high performance aircraft the designator must be stabilized to compensate for aircraft movement. Pave Spike (TV tracker) and Pave Tack (Imaging Infrared (IIR) tracker) are representative laser designator/ranging systems using a pointable, stabilized gimballed mirror.

The Low Altitude Navigation and Targeting Infrared System for Night (LANTIRN) was developed on the F-16 during the 1980s. LANTIRN used a navigation pod and a targeting pod to allow night, low level air-to-ground operations under the weather. The navigation pod contained terrain following radar (TFR) and a FLIR. The TFR provided HUD symbology which the pilot could follow for manual terrain following or the navigation pod could be coupled with the flight control system for automatic terrain following. The FLIR generated a infrared image for raster display on a CRT or HUD. The targeting pod contained a gimballed targeting infrared with point or area track capability. The target pod could automatically handoff previously locked targets to infrared maverick missiles and also had a laser for ranging and LGB designation.

1.2 EO vs. RADIO FREQUENCY (RF) COMPARISON.

Electro-optical systems offer certain advantages in comparison with RF systems. Perhaps the greatest advantage of an infrared (IR) sensor is its ability to passively detect a target utilizing the radiation emitted by a target's heat signature. It is difficult to conceal targets from an infrared sensor since almost all militarily significant targets dissipate energy in the form of heat. Another important advantage is the improved accuracy in position determination which results from the narrow beamwidths possible with EO sensors. A third advantage is the greater information bandwidth afforded by the extremely high EO carrier frequencies. The narrow beamwidth and wide bandwidth make it very difficult to intercept and/or jam the emissions from an EO sensor.

The principal disadvantage of EO systems, in comparison with RF systems, is the presence of greater atmospheric absorption at EO frequencies. This absorption greatly reduces the effective range of terrestrial EO systems. Range is also limited in EO systems by line-of-sight propagation. Another important disadvantage of EO systems is the prevalence of natural clutter and noise in the infrared region. Just as all targets above zero degrees absolute temperature emit infrared radiation, so do all non-targets above absolute zero.

FIGURE 1.1. GENERALIZED ELECTRO-OPTIC SENSOR

Display

Electronics (Processor)

Detector

Field Lens

Reticle

Objective Lens

(Cold Stop for I/R Shield)

Disp

Elec

Dat

Scattering and Absorbing Medium

Target Radiation

Background Clutter
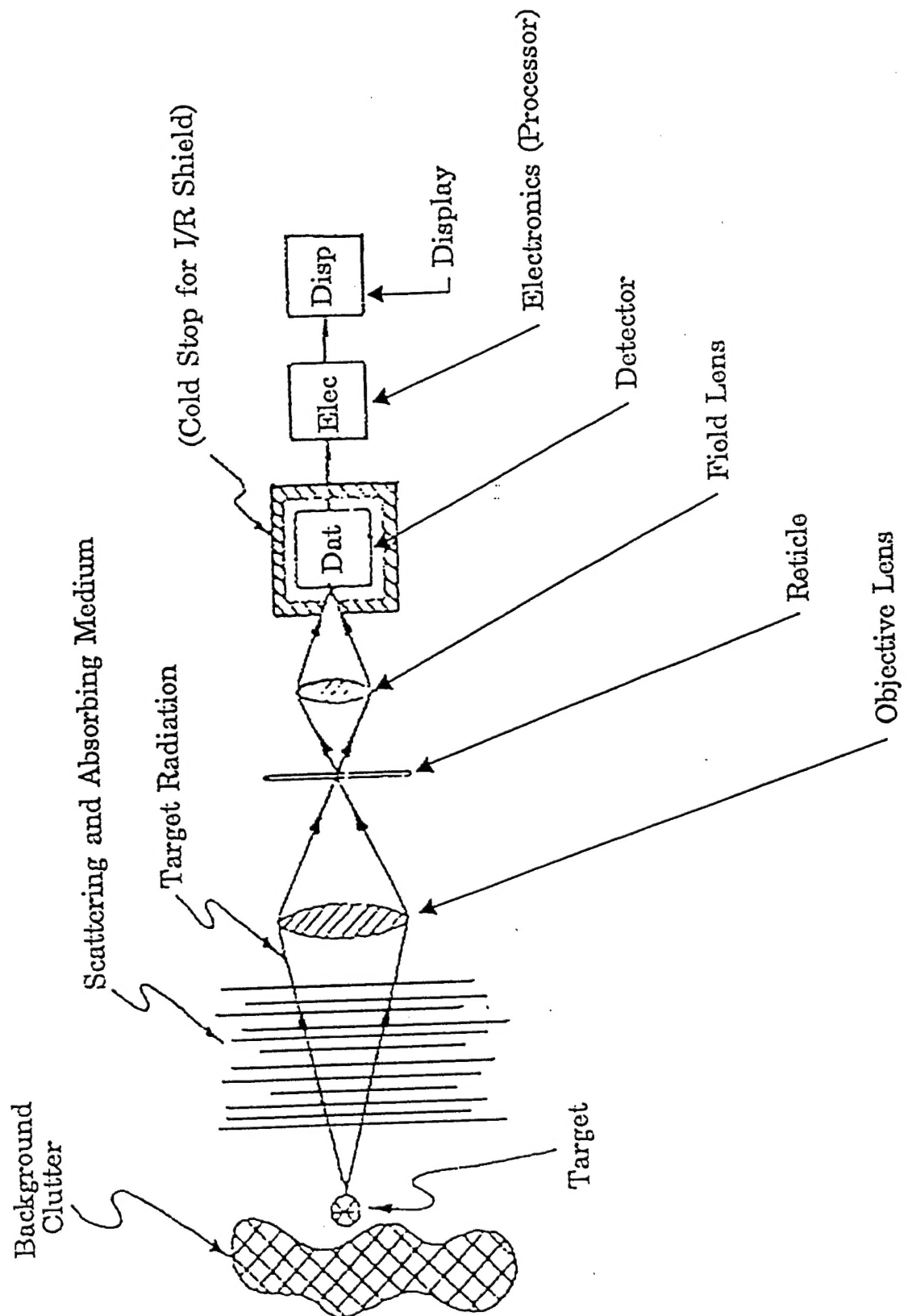
Target

1.3 GENERALIZED ELECTRO-OPTIC SENSOR. The common features
of all electro-optical systems (except direct-radiation laser weapons) are represented
by the generalized radiation sensor depicted in Figure 1.1. Referring to Figure 1.1,
a target and surrounding objects (clutter) emit or reflect radiation in the optical
frequency range. This radiation passes through a propagating medium (the
atmosphere), and suffers from absorption and scattering losses. The radiation
typically is collected by an objective lens or mirror, passed through a reticle, and
directed onto a radiation detector by a field lens or mirror. The reticle is a
multipurpose optical element designed to improve the signal-to-noise ratio of the
radiation by discriminating between target, clutter, or noise on the basis of position,
size and shape (spatial filtering); radiation frequency (chromatic filtering); and/or time
(optical modulation or chopping). The radiation detector is an energy transducer that
converts electromagnetic energy into an electrical signal that is more easily processed.
The output signal from the detector is electronically processed and sent to a display.

The principles of operation, operating characteristics, and test and evaluation of
electro-optical systems are the subject of this text. The necessary information will be
provided to allow you to design tests which will reveal the significant characteristics
of the EO system being evaluated. Sufficient theoretic background will be provided
to allow you to analyze the design of the system under test and thereby anticipate its
likely performance characteristics (strengths and weaknesses). Only in this manner
can an adequate test plan be devised. The difficulties in designing an adequate test
are due, in large part, to the ever-present funding and time limitations. The tester
virtually never has enough time or funding to perform exhaustive testing. For that
reason, you must concentrate on those tests which reveal the likely performance
weaknesses of the subject system. Only by understanding the system design and its
implications can you identify the appropriate areas of concentration.

(THIS PAGE INTENTIONALLY LEFT BLANK)

SECTION II

VISIBLE AND IR RADIATION

2.1 ELECTROMAGNETIC SPECTRUM. Communication, radar, and electro-optical (E-O) systems are all related in basic principles: each requires a source of electromagnetic (EM) energy, a transmission medium (the atmosphere), and a receiver. The systems differ only in the particular type of signal processing within the receiver which is dictated by the radiation frequency. Atmospheric effects are also a strong function of frequency and often establish the particular frequency band used for a specific application. In this chapter we will examine the EM spectrum and some of the problems associated with atmospheric transmission and absorption.

Electromagnetic radiation covers a continuous spectrum from DC to well over 10^{22} Hertz (cycles per seconds). The lower frequencies include power, radio, and microwaves and are best handled using electronic techniques (transmission lines, active and passive elements, etc.). The highest frequencies include x-rays, gamma rays, and cosmic waves and are best treated using atomic particle techniques (electrons zapping nuclei, etc.). The optical region of the spectrum lies between these extremes, starting in the far infrared $(10^{12}\,\text{Hz})$ and extending through the ultraviolet (10^{18}Hz). Electromagnetic radiation in this region is commonly referred to as light because optical techniques are employed even though only a portion of the energy is visible to the human eye. The EM spectrum is summarized in Figure 2.1.

FIGURE 2.1. THE ELECTROMAGNETIC SPECTRUM
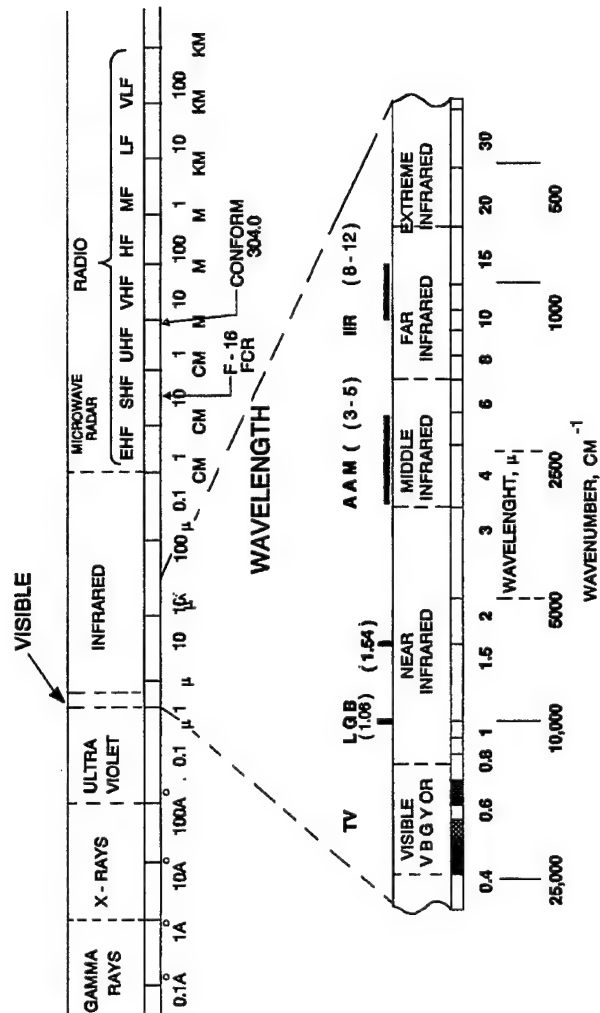
2.1.1   FREQUENCY AND WAVELENGTH.   Electromagnetic radiation can be specified by frequency, wavelength, wavenumber, or energy and a measure of its intensity. Wavelength (λ) is related to frequency (υ) by

$$\lambda = c / \upsilon \qquad\qquad (2.1)$$

where c is the speed of light (2.997925×10^{8} m/s in free space). The most common units associated with each portion of the EM spectrum are listed in Table 2.1.

Table 2.1
The Common Units for the Electromagnetic Spectrum

PORTION OF SPECTRUM	NAME	SYMBOL	VALUE
Power & Audio	Hertz	Hz	1 cps
Radio	Kilohertz	KHz	10^{3} Hz
	Megahertz	MHz	10^{6} Hz
Microwaves (Radar)	Gigahertz	GHz	10^{9} Hz
Far Infrared	Wavenumber	CM^{-1}	$1/\lambda$ (reciprocal centimeters)
Near Infrared	Micron	μ	10^{-6} Meters (M)
Optical & Ultraviolet	Angstrom	$\overset{.}{A}$	10^{-10} Meters
X-Rays & Beyond	Electron-Volt	eV	1.60210 $\pm\ 7 \times 10^{-19}$ J

Frequencies in the infrared are very high ($\geq 10^{12}$ Hz) and consequently become rather cumbersome to work with. Wavelength is more convenient in this area with the micron being the most common unit in the near infrared. One micron falls just below visible light and several hundred microns is in the far infrared. The angstrom unit ($1\overset{\circ}{A} = 10^{-4}\mu$) is often used with visible and ultraviolet light; 6000 Å falls in the red portion of the visible spectrum whereas 4000Å is in the ultraviolet. The energy of the

radiation is generally specified in electron volts for the higher frequencies beginning with x-rays, where the energy and frequency relationship is $E = h\nu$.

Another division within the electromagnetic spectrum is also possible when dealing with EO sensors. This division is according to the type of radiation predominant at the receiver at a given wavelength and is either reflected or emitted radiation. When a scene is irradiated by an external source such as the sun, the scene is observed primarily by <u>reflected</u> light. This holds true for near ultraviolet, visible, and near IR wavelengths. However, as we proceed further into the infrared, beyond wavelengths of 3.5 microns, the thermal <u>emitted</u> radiation exceeds the reflected radiation. Thus television systems, which operate in the visible and near infrared to approximately 0.8 microns, are dependent almost entirely on reflected light and therefore require scene illumination. IR photography can be accomplished at wavelengths up to 1.3 microns and also requires illumination, which may not be visible to the naked eye.

2.2 ELECTROMAGNETIC ENERGY.

The study of mechanics is founded on three basic concepts: space, time, and mass. In the theories of electromagnetism, the additional concept of charge is introduced. Due to the many varied and seemingly unrelated characteristics displayed by electromagnetic radiation, two theories are currently required to describe all of the observed phenomena. To the electrical engineer, EM waves are composed of electric and magnetic fields with an associated Poynting vector (Field Theory). On the other hand a quantum physicist sees little bodiless particles called photons zipping along at the speed of light (Photon Theory).

2.2.1 FIELD THEORY.

Field theory describes the interaction of charges and currents in terms of fields of electric intensity (E) and magnetic induction (B). The theory was pioneered by Hygens, mathematically formulated by Maxwell, and experimentally verified by Hertz. The electromagnetic field in a given region of space depends on the kind of matter occupying the region as well as on the distribution of charge giving rise to the field.

2.2.2 PHOTON THEORY.

Hallwachs observed that zinc irradiated with ultraviolet light lost negative charge. In 1899 Lenard showed that the radiation caused the metal to emit electrons, a phenomenon known as the photoelectric effect. Physicists immediately took to the task of explaining the effect in terms of classical theories of the day with interesting results.

One can calculate the time required for an electron to absorb sufficient energy to escape from the surface of a photoelectric material using Maxwell's field theory. The time works out to be about 100 seconds. However, there is no observable delay between the application of the radiation and emission of photoelectrons, as they are called. In 1905 Einstein proposed that light is composed of energy bundles called photons. The energy in the photon is proportional to the frequency of the radiation ($E = h\nu$). According to his theory a photon would collide with an electron, passing all of its energy to the electron while pulling the old disappearance trick. The transfer was thus immediate without delay. Einstein received the Nobel prize in 1921 for this explanation (not relativity theory as most people think).

A light beam according to this theory is composed of packets of photons, each traveling at the speed of light. Each photon is then described in terms of a frequency and wave vector which specifies the spatial and phase information. A beam composed of identical photons (frequency and wave vector) is said to have spatial and temporal coherence.

Both the field theory and photon theory of radiation are essentially correct. In some phenomena such as interference, field theory must be employed. In other phenomena, the photon theory is necessary. In other words, photon theory does not destroy the validity of field theory. All it does is demolish a small sector of physics called classical (Newtonian) mechanics!

2.3 INTERACTION OF LIGHT AND MATTER.

The interaction of radiation with matter is a function of the wavelength of the radiation compared to inter atomic size and spacing of the particle. Significant interactions are also noted when the photon energy of the radiation is approximately equal to one of the quantized energy levels of the matter. The most important interactions in the optical region are reflectance, refraction (transmission), diffraction, scattering, absorption, and emission. These processes are summarized in Table 2.2 and diagramed in Figure 2.2.

TABLE 2.2

INTERACTION OF RADIATION WITH MATTER

REFLECTANCE (ρ)	Radiation which is turned back into the first medium when striking a boundary between two different media, where ($\varepsilon_1 \neq \varepsilon_2$)
REFRACTION (τ) (transmission)	Radiation which passes into the second medium
ABSORPTION (α)	Process in which radiative energy is changed into some form(s) of molecular energy
where ($\alpha + \tau + \rho = 1$)	
SCATTERING	Change in direction of radiation due to interference from suspended particles within the medium
EMISSION	Reverse of absorption - molecular emission
DIFFRACTION	Spreading of radiation as it passes through an aperture.

2.3.1 REFLECTANCE.   When light strikes a boundary between two media with different refractive indices, such as scotch and water, some or all of the incident radiation is turned back into the first medium by reflection. Reflection from a smooth polished surface such as a mirror is called specular reflection. However, a surface may be highly polished at one wavelength but to a higher frequency it may look like sandpaper. Reflection from a rough or granular surface is called diffuse reflectance.

FIGURE 2.2 INTERACTION OF RADIATION AND MATTER

REFLECTANCE

INCIDENT
(E_i)

NORMAL

REFLECTED
(E_r)

θ_i θ_r

POLISHED
SURFACE

SPECULAR $(E_r = E_i)$

INCIDENT
(E_i)

NORMAL

TRUE
NORMAL

θ_i θ_r

REFLECTED
(E_r)

DIFFUSE $(E_r = E_i \rho \cos\theta/\pi)$

REFRACTION

INCIDENT
(E_i)

μ_1 $\mu_2 > \mu_1$ (INDEX OF REFRACTION)

θ_1

NORMAL

θ_r

θ_2

TRANSMITTED
(E_t)

REFLECTED
(E_r)

ABSORPTION (ELECTRONIC)

ATOM
(GAINS ENERGY)

PHOTON

$E_p = h_\nu$

ELECTRON ABSORBS PHOTON
IF $E_p \simeq E_1 - E_1$ BY
TRANSITION TO E_1 LEVEL

NUCLEUS AND
INNER ELECTRON
SHELLS

ENERGY LEVEL E_2

ENERGY LEVEL E_1

FIGURE 2.2 INTERACTION OF RADIATION AND MATTER(cont.)

SCATTERING

INCIDENT   LARGE PARTICLE
                  (DUST)

θ_i
θ_r r

REFLECTED

$r \gg \lambda_{inc}$

MIE $(\theta_i = \theta_r)$

ELECTRIC
DIPOLE
$(N_2, O_2, etc.)$

INCIDENT

                    −   REFLECTED

$r \sim \lambda_{inc}$ r + θ_s

RAYLEIGH $(\theta_s = f(\lambda))$

EMISSION

ATOM
(LOSES ENERGY)

E_2

E_1

                                        PHOTON

$E_p = E_1 - E_2$

PHOTON 1   ATOM
                  (LOSES ENERGY)

$E_{p1} = E_1 - E_2$

                                        PHOTON 2

$E_{p2} = E_{p1}$

PHOTON 1 CAUSES IDENTICAL PHOTON
        (2) TO BE EMITTED

SPONTANEOUS   STIMULATE

DIFFRACTION

                  APERTURE   SPREADING
                                              OF
                                              WAVEFRONTS

INCOMING
WAVEFRONTS

The diffuse reflectance of targets at various wavelengths is an important factor in the range equation for optical systems. Table 2.3 summarizes the data obtained by the University of Michigan under USAF contract for diffuse reflectance. In some cases over 250 sources of information were used to obtain the results.

TABLE 2.3

DIFFUSE REFLECTANCE

Wavelength, Microns (μ)	Vehicles	Concrete	Soil	Brush
.3371	----	----	0.12	0.05
.4480	0.05	0.20	0.11	0.05
.5145	0.09	0.22	0.14	0.09
.6328	0.05	0.28	0.22	0.13
.844	----	0.26	0.30	0.57
1.06	----	0.28	0.33	0.63
3.39	0.53	----	0.13	0.07
3.5	0.54	----	0.15	0.07
10.6	0.48	----	0.03	0.07

A 1.06 micron laser is used for LGB laser designation. Notice the high diffuse reflectivity at this frequency.

2.3.2 REFRACTION. When light strikes the boundary between two media, some of the radiation may pass into the second medium. This process is termed refraction and the refracted radiation usually experiences a change in the direction of propagation. The refracted light is bent toward the normal when the index of refraction of the second medium is higher than the first (example: trying to locate the olive looking into the top of a martini). The angle of incidence for which the angle of refraction is 90° is called the critical angle. The incident radiation is totally reflected for angles greater than the critical angle.

The angle of refraction is governed by Snell's law which states

$$\mu_1 \; SIN \; \theta_1 = \mu_2 \; SIN \; \theta_2 \qquad\qquad (2.2)$$

where μ is the index of refraction of the medium and θ is the incident angle of the radiation measured to the normal. The index of refraction is a function of wavelength. Consequently light can be dispersed (separated into component wavelengths such as a rainbow) by diffraction as with a prism. Shorter wavelengths are diffracted more than longer wave-lengths. What is the color in the top band of a rainbow?

2.3.3 ABSORPTION.

Absorptivity is the fraction of radiant energy falling on a given body which is absorbed or transferred to heat; or the ratio of the radiation absorbed to that absorbed under identical conditions by a blackbody. Absorption can be given by

$$I = I_o \, e^{-Kx} \qquad\qquad\qquad (2.3)$$

where: I_o is the original intensity

I is the intensity after passing through a material of thickness x

$K = 4\pi K'n / \lambda$

where K' is the index of absorption and n is the refractive index

2.3.4 SCATTERING.

As radiation propagates through the atmosphere, some of the light is scattered in different directions. Large particles such as dust or smog scatter the radiation by reflectance. This process is called Mie scattering and results when the wavelength of the light is much smaller than the diameter of the particle. A refractive process called Rayleigh scattering occurs when the diameter of the particle is comparable with the wavelength of the incident radiation. Gas molecules (N_2, O_2, CO_2) meet this requirement for visible light. Each particle in the light path behaves as if it were a secondary light source. The intensity of the scattered light varies inversely as the fourth power of the wavelength, thus short wavelengths are scattered more than longer wavelengths. When white light passes through the atmosphere, the light observed at 90° from the direction of propagation appears bluish as a result of Rayleigh scattering. Why does a sunset appear red?

Backscattering becomes extremely important when considering detection range of active optical systems. Mie scattering is the most significant contributor. The atmospheric scattering coefficient at 1.04μ has been reported as 0.048/km with the Raleigh component contributing only 2% of the total. Consequently, backscattering increases as visibility decreases, reducing the operational range of the system.

2.3.5 DIFFRACTION.   When light passes through an aperture it spreads to some extent into regions that would not be reached by rays drawn from the original incoming wavefront. The spreading becomes very pronounced when the opening is on the order of magnitude of the incoming wavelengths. This process is termed diffraction and leads to interference patterns because the phase angle of the light at some distant point is a function of the optical path.

Diffraction becomes important in optical systems when considering resolving powers. The condition for resolving two targets with angular separation α is known as the Rayleigh criterion and is expressed

$$\alpha \approx \lambda / D \qquad\qquad (2.4)$$

where D is the diameter of the lens. If the angular separation is smaller than λ / D the system will not be capable of differentiating between the two targets (they look like one big blob). For good angular resolution we require small wavelengths and large apertures. How would the resolving power of a radar compare with a ladar (laser radar system)?

2.4 BLACKBODY RADIATION.   One of the most useful concepts employed when working with infrared radiation is the "blackbody". A blackbody is defined as an object which absorbs all radiation incident on it. To maintain thermo equilibrium the blackbody must then be a perfect source of IR, emitting its radiation at any given temperature with the greatest and most uniform intensity possible. We will now review the basic laws which characterize blackbody radiation.

The most important parameter in determining the IR characteristics of any body it its temperature. Temperature is a measure of the energy stored within the body which in order of importance is nuclear, electronic, vibrational, rotational, and magnetic.

Now, let's start warming a cold body. As the temperature of the body increases, the wavelength of the peak radiation decreases (higher frequency) and the total energy radiated increases. These fundamental relationships are given by two laws: Stefan-Boltzmann's Law and Wein's Displacement Law.

2.4.1 STEFAN-BOLTZMANN LAW.   The radiant emittance (power / unit are) of a blackbody is directly proportional to the fourth power of the absolute temperature:

$$W = \sigma \, T^4 \qquad\qquad\qquad (2.5)$$

where σ is the Stefan-Boltzmann constant with a value of
5.67×10^{-3} W / °K cm^2

If the temperature of a body is doubled, the emitted radiation will increase 16 fold. This relationship is shown in Figure 2.3.   For a graybody with emissivity (ε) less than one, Stefan-Boltzmann's law can be expressed as $W = \varepsilon \, \sigma \, T^4$.

FIG 2.3 RADIANT EMITTANCE OF A PERFECT BLACKBODY

RADIANT EMITTANCE OF A PERFECT BLACKBODY
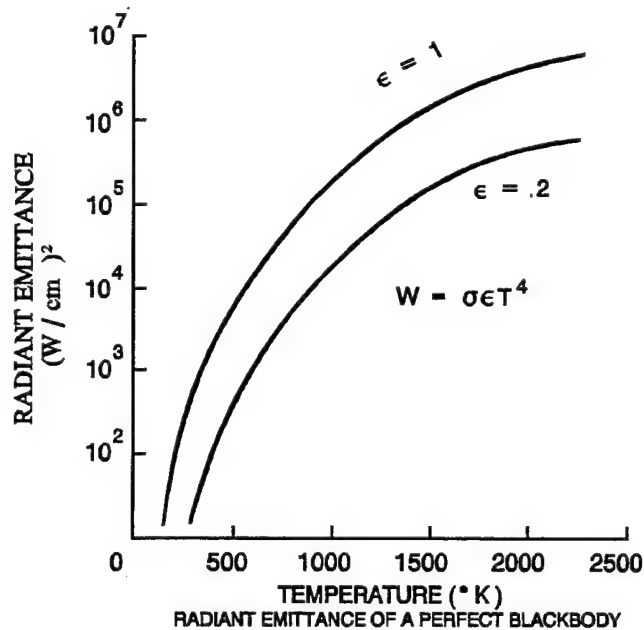
2.4.2 WIEN'S DISPLACEMENT LAW. The wavelength of the maximum radiation (λ_M) is inversely proportional to the absolute temperature of the body (°K):

$$\lambda_M \; = \; K/T \hspace{4cm} (2.6)$$

Where K ~ 2900 °Kμ.   A block of ice (273°K) emits its peak radiation around 10 microns. Stick a knife blade into the fire on a gas range and watch the color change. First the blade turns red, then whitish yellow, then blue and finally you realize you forgot to use a potholder - ouch! This relationship is shown in Figure 2.4.

FIG. 2.4 λ OF MAXIMUM RADIATION vs BLACKBODY TEMPERATURE

BLACKBODY WAVELENGTH
VARIATION

$$\lambda_m = \frac{2900}{T} \text{ MICRONS}$$

EARTH

TEMPERATURE (°K)

WAVELENGTH (MICRONS)

VARIATION IN WAVELENGTH OF PEAK RADIATION WITH
TEMPERATURE FOR A PERFECT BLACKBODY SOURCE.
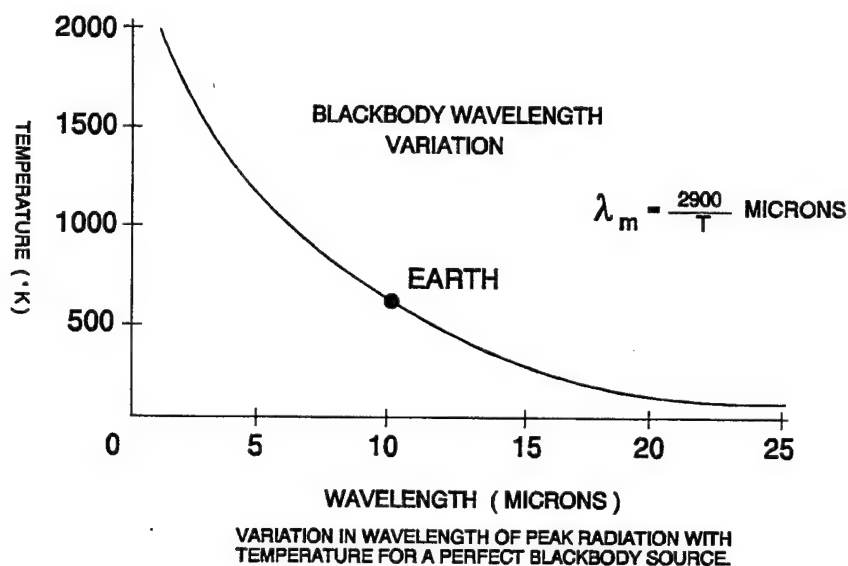
2.4.3   PLANCK'S LAW.   Wein's Law and Stefan-Boltzmann's Law were first determined experimentally.   While their formulas were a "pretty good fit" to experimental observation, Max Planck was able to accurately derive the correct formula for energy density radiated by a blackbody.

$$U_\lambda = \frac{8\pi ch\ \lambda^{-5}\ d\lambda}{e^{\,ch/\lambda K_B T}-1} \qquad\qquad (2.7)$$

where U_λ is the energy density in Joules per cm^3 in the wavelength range λ to λ + $d\lambda$. The value of h is experimentally determined from the photoelectric effect, c is the speed of light, and k_B is Boltzman constant with a value 1.38×10^{-23}J/°K. The curves is shown in Figure 2.5.

FIG 2.5 IDEAL BLACKBODY RADIATION CURVES FROM PLANCK'S LAW
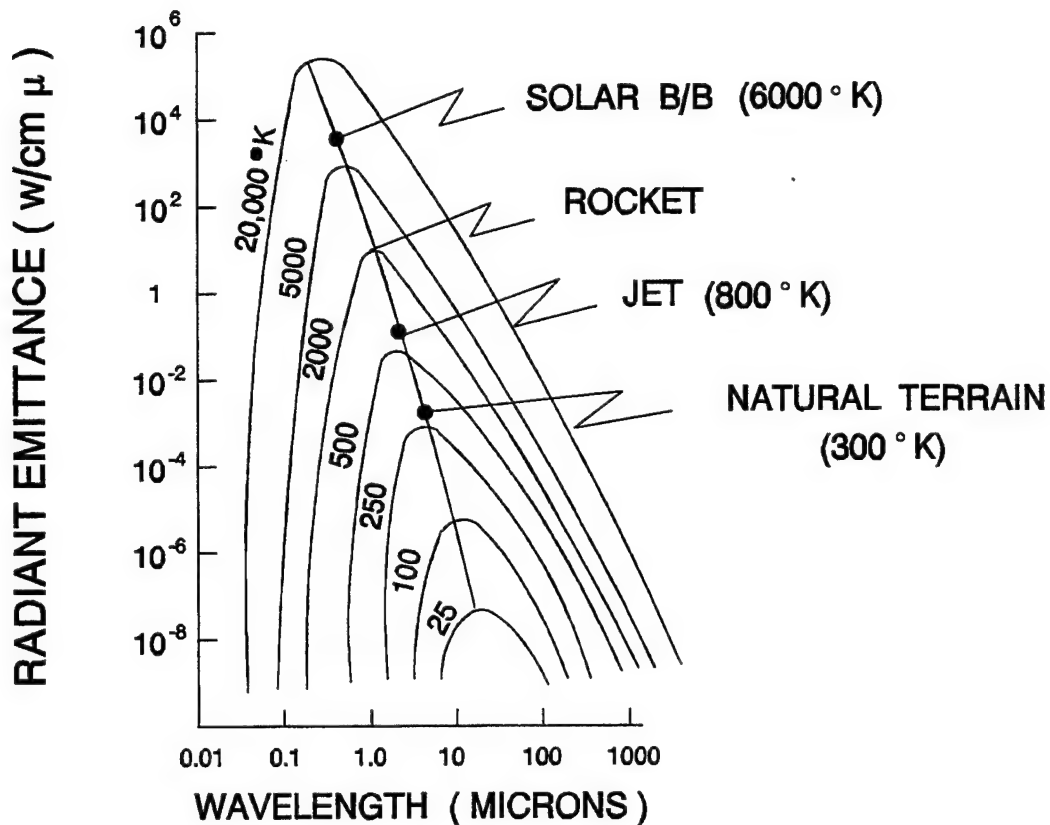
2.4.4 SPECTRAL DISTRIBUTION. In summary, electromagnetic energy from a source will be distributed over a good part of the spectrum, but the maximum radiation occurs at some specific wavelength. It was shown mathematically from Planck's Law that the energy radiated at this wavelength varies with the fifth power of the absolute temperature. In other words, doubling the temperature of an object will increase the radiation emitted at the peak wavelength by 32 times.

As an example, radiation from jet and rocket engine exhaust is primarily due to the molecular excitation of water vapor and carbon dioxide which are characteristic by-products of combustion. This molecular radiation peaks at 2.7 microns (due to water vapor and carbon dioxide) and 4.3 microns (due to carbon dioxide alone). In a practical situation, however, this radiation is almost negligible in comparison to the total black body radiation from the aircraft, as the tail-pipe surfaces contribute the greater part of the total radiation when viewed from a tail aspect.

2.5 EMISSIVITY. Black bodies occur very rarely in nature. In order to compare the radiation emitted by an actual source with that of a perfect radiator, the concept of emissivity is employed. Emissivity is defined as the ratio of the total radiation emitted by any solid object at a temperature T to the total radiation emitted by an ideal black body at the same temperature. The emissivity of any object depends on the amount of energy its surface can absorb. If the surface absorbs most of the infrared radiation striking it, then it will emit a relatively high amount and the emissivity of the object will be comparatively large. By the same reasoning, if the surface reflects most of the incident radiation, the object will have a relatively small emissivity. By definition, a black body has an emissivity of unity. Therefore, any other object will have an emissivity of less than one. Table 2.4 shows the emissivity of various surfaces.

TABLE 2.4

EMISSIVITIES OF VARIOUS SURFACES

SURFACE	EMISSIVITY
Black Body	1.00
Lampblack	0.95
Painted	0.90
Steel, cold-rolled	0.60
Aluminum paint	0.25
Steel, stainless	0.09
Aluminum aircraft skin	0.08
Aluminum foil	0.04
Silvered mirror	0.02

The Stefan-Boltzmann Law can be modified to include the emissivity factor, and by using the right units, the total radiation can be obtained by: $W = \varepsilon \sigma T^4$ where ε is the emissivity factor of the radiating surface. With these figures, a black body at an absolute temperature of 300°K (81°F) will radiate 46 milliwatts of power per square centimeter of its surface. A painted surface, such as the skin of a commercial airliner, at the same absolute temperature will radiate 41 milliwatts per square centimeter. If this aluminum aircraft skin were not painted, the emissivity factor would be considerably smaller, and the radiation would be less than four milliwatts of power per square centimeter.

2.6 INFRARED BACKGROUND SOURCES.
Regardless of the nature of the target source, a certain amount of background or interfering radiation will be present in the detection system in the form of unwanted noise. In general, natural sources are always present, and in most IR applications will constitute background sources. These natural sources may be broadly classified into 3 categories: terrestrial, atmospheric, and celestial (the last 2 combine into the single background, the sky).

2.6.1 TERRESTRIAL SOURCES.   Whenever an IR system is looking below the horizon, it encounters the terrestrial background radiation.   Every object with a temperature above absolute zero radiates IR energy including trees, bushes, rocks, earth, sand, water, etc.   A further source of terrestrial background radiation is reflected sunlight. The sun is a strong IR source and surface such as rock, sand, metal, and green foliage (due to chlorophyll effect) are excellent IR energy reflectors.

2.6.2 SKY SOURCES.   Whenever the IR device looks above the horizon, the sky provides the background radiation. The prime IR sources in the sky are celestial and atmospheric sources.   The radiation characteristics of celestial sources depend primarily on the source's temperature, and the characteristics undergo modification by the earth's atmosphere.   Additionally, the received radiation characteristically changes depending on the altitude of an observer.

2.6.2.1   THE SUN.   The sun being an approximate blackbody radiator at a temperature of 6000°K, has its radiant energy peak at 0.5μ. Half of its radiant power occurs in the infrared wavelengths, as shown in Figure 2.6, and the distribution of radiant power falls off as the wavelength increases.   Studies of the spectral appearance of sunlight, reflected from clouds, terrain, and sea, show that this reflected radiation is quite similar to direct sunlight. Another consideration which must be accounted for is the effect of the earth's atmosphere. As shown in Figure 2.6, the solar spectrum (as viewed from the earth's surface) is radically changed by absorption and scattering. Although peaking still occurs in the visible spectrum, the shorter wavelength ultraviolet disappears and, by a percentage comparison, the longer wavelength IR proportionally remains the same, or makes up more of the total solar power. As an ascent is made through the atmosphere, the solar spectral distribution approaches that of the 6000°K blackbody.

Figure 2.6
Spectral Distribution of
Solar Radiation
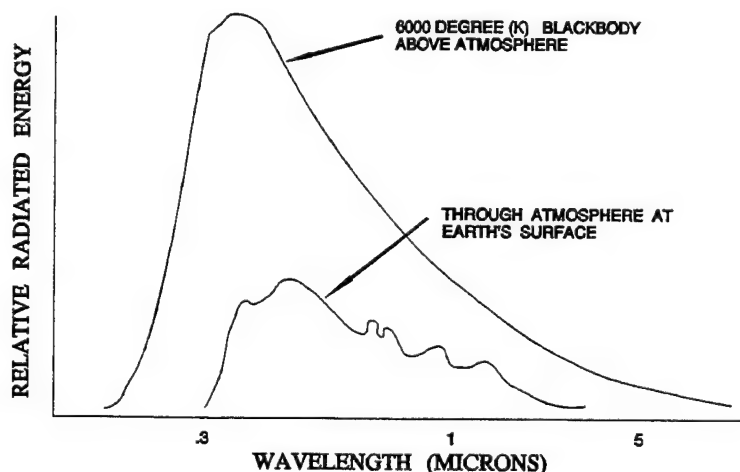
2.6.2.2 THE MOON. The next most important celestial source of IR is the moon. The bulk of the energy received from the moon is solar radiation, modified by reflection from the lunar surface, slight absorption by any lunar atmosphere and the earth's atmosphere. The moon is also a natural radiating source. During the lunar day its surface is heated to as high as 373°K and during the lunar night the surface temperature falls to 120°K. Other celestial sources are very weak point sources of IR radiation, when compared to the sun and moon, and can be disregarded except in special astronomical applications.

2.6.3 NIGHT vs DAY. Because the sun is such an intense source of radiation, the background of the sky has to be considered separately for day or night. The primary differences between night sky background radiation normal to the earth's surface are shown in Figure 2.7, which is a plot of the spectral distribution of energy for clear night and clear day skies. At night, the short wavelength background radiation caused by the scattering of sunlight by air molecules, dust, and other particles disappears. In fact, at night there is a tendency for the earth's surface and the atmosphere to blend with a loss of the horizon, since both are at the same ambient temperature and both have approximately the same high emissivity factor. Radiation from the clear night sky approximates that of a blackbody at 273°K, with the peak intensity occurring at a wavelength of about 10.5μ, and, as Figure 2.7 illustrates, the overall energy level is slightly lower than that of a clear daytime sky.

Figure 2.7 Spectral Energy Distribution of Background Radiation from the Sky
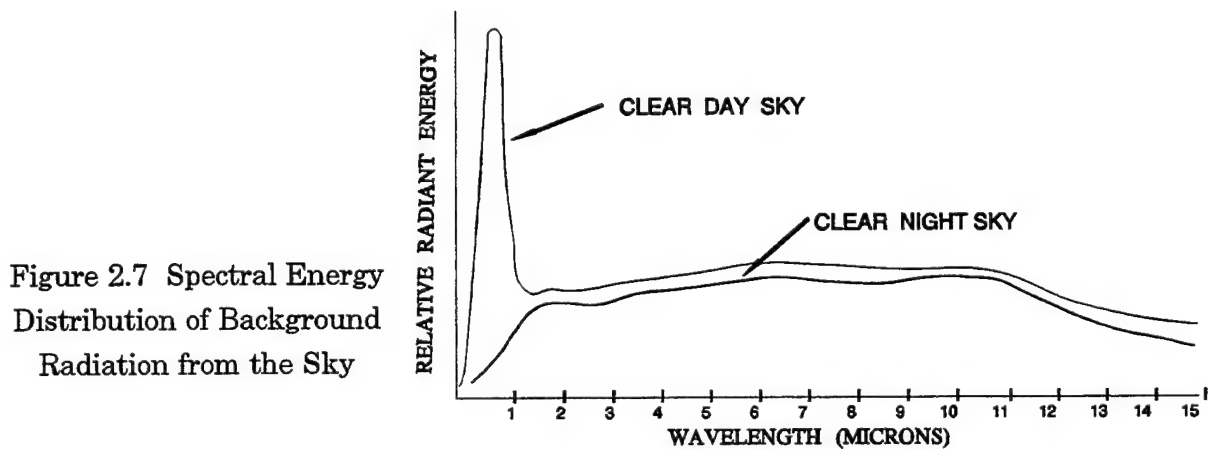
2.6.4 CLOUD EFFECTS. One of the main constituents of the lower regions of the atmosphere is water vapor, and a special effect on background radiation occurs when the water vapor condenses into cloud. Clouds product considerable variation in sky background with the greatest effect occurring at wavelengths shorter than 3μ. This

is caused by solar radiation reflected from the cloud surfaces. Early IR homing missiles showed a greater affinity for cumulus clouds than the target aircraft. Discrimination from this background effect requires the use of not only spectral filtering, which eliminates the shorter wavelengths, but also spatial filtering, which distinguishes the smaller area of the target from the larger area of the cloud edge.

2.6.5 TERRAIN vs SKY. Terrain produces a higher background-energy distribution than that of the clear sky. This is caused by reflection of sunlight in the short-wavelength region and by natural thermal emission at the longer wavelengths. The absence of sharp thermal discontinuities, that is breaks in the radiation pattern between an object and its surroundings, complicates the problem of the detection of terrestrial targets.

2.6.6 THERMAL CROSSOVER. Occasionally objects with different emissivities and temperatures produce the same radiant emittance, and thus there is no contrast in the picture. This is known as thermal crossover and results in a loss of picture information. Thermal crossover is likely to occur a couple of hours after either sunrise or sunset as objects with different emissivities change temperatures at different rates.

2.7 ATMOSPHERIC TRANSMISSION.

In military applications of optical systems, the transmitting medium is generally the atmosphere. Consequently, the effect of the atmospheric attenuation on the transmission of radiation is of prime importance in considering the overall effectiveness of the system. There are three primary causes of atmospheric attenuation: absorption by free molecules, scattering by suspended solids, and scintillation caused by refraction. The influences are additive but absorption is the most important factor. The transmission of IR radiation through the earth's atmosphere is dependent on the concentration and distribution of the atmospheric constituents. These atmospheric constituents are dependent upon meteorological considerations, particularly in the lower atmosphere where the water vapor, various gases, and dust contents may vary continuously with changes in altitude and the local weather.

2.7.1 ABSORPTION. One form of attenuation of radiation, found throughout the IR region, results from the resonance-absorption bands of the atmospheric constituents. The complete absorption spectrum of the atmosphere is the sum of the absorption-band spectra of the individual atmosphere constituents. Figure 2.8 shows the IR

absorptions-bands and the associated IR-transmission "windows" caused by the primary atmospheric constituents at sea level and higher altitudes.

There are two substances of interest in the atmosphere which absorb most of the radiation: water vapor and carbon dioxide. For both of these substances, there are several wavelength bands where the absorption is relatively large. At low altitudes, where the atmosphere is more dense, this absorption is so great that in some wavelength bands the percentage of radiation transmitted drops rapidly to zero. Transmittance increases with altitude because the less dense and cooler air holds less water vapor. Between the absorption bands are areas where the atmospheric attenuation is not so great. These transmission bands are called windows. The transmission windows in the atmosphere are shown in Table 2.5. The atmospheric transmission characteristics for three different altitudes are shown in Figure 2.8.

Table 2.5
Atmospheric Transmission Windows

0.9 - 1.05 microns	2.1 - 2.4 microns
1.20 - 1.30	3.0 - 5.0
1.50 - 1.80	8.0 - 12.0

2.7.2 SCATTERING. The effects of scattering by haze and fog in the atmosphere are mainly of concern in the visible spectrum, and, with the exception of fog, are of minor concern in the IR spectrum. Surprisingly perhaps, IR transmission through mist is very good. The amount of scattering depends on the particle size; particles in the atmosphere are rarely bigger than 0.5 microns and thus they have little effect on wavelengths of 3 microns or greater. However, once moisture condenses on the particles to form fog, the droplet size can be anything from 0.5 to 80 microns, and the peak of their distribution curve is between 5 and 15 microns. Thus fog particles are comparable to IR wavelengths, and the transmittance becomes very poor. The same reasoning applies to clouds, and movement to another part of the spectrum does not usually help because of the limited extent of the "windows" in the absorption bands. As raindrops are so much bigger than the wavelength, there is less effect in that it tends to even out the temperature difference between a target and its surroundings.

FIGURE 2.8 ATMOSPHERIC TRANSMISSION CHARACTERISTICS
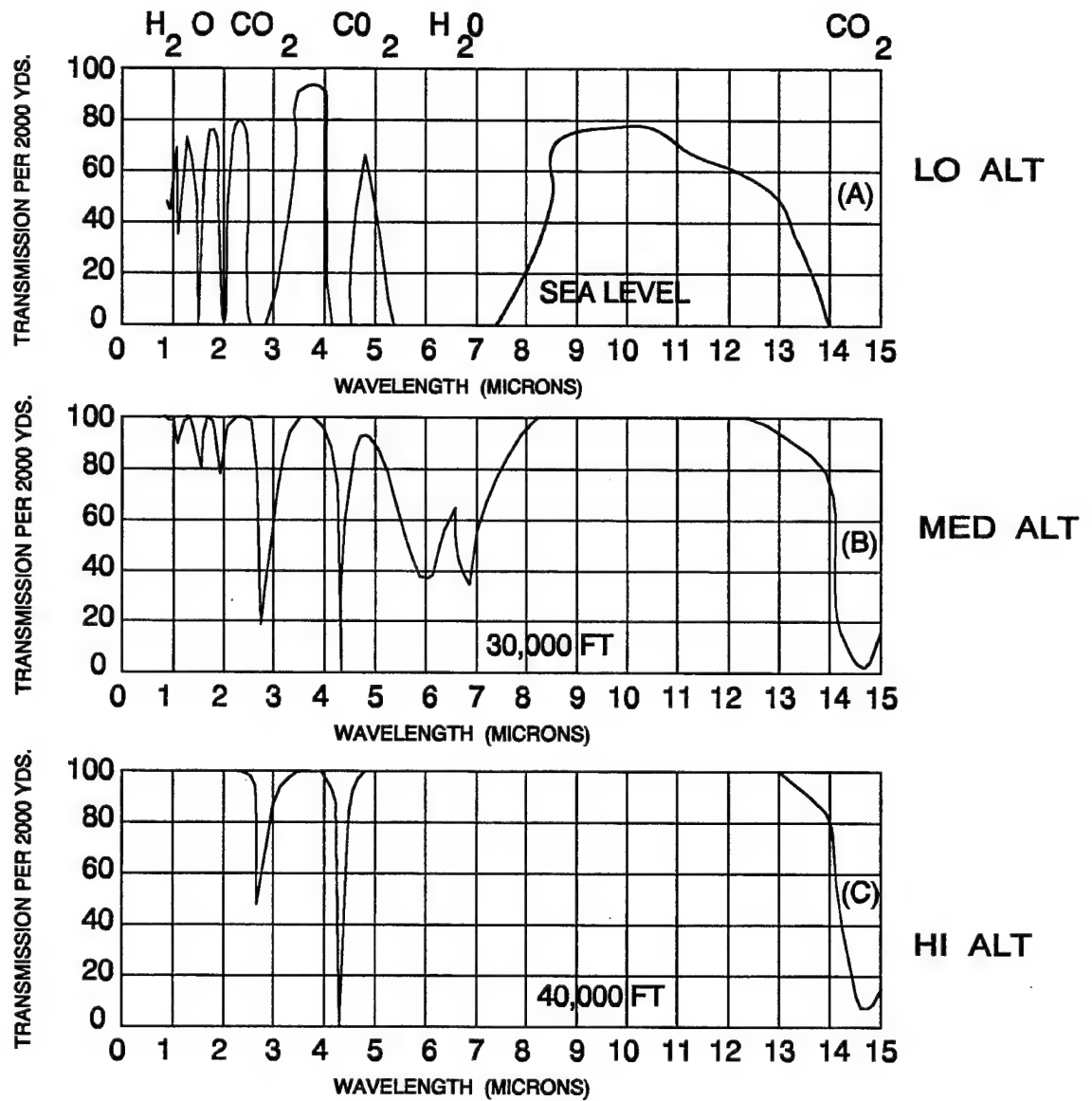
2.7.3 ATMOSPHERIC SCINTILLATION. Scintillation is the effect which causes the stars to appear to twinkle. When a beam of light passes through regions of temperature variation (such as a road heated by sunlight) it is refracted from its original direction. Since such regions of air are unstable, the deviation of the beam is a random, time varying quantity. The effect is most pronounced when the line of sight passes close to the earth and gives rise to unwanted modulations of the signal, and incorrect direction information for distant targets.

(THIS PAGE INTENTIONALLY LEFT BLANK)

SECTION III

OPTICS

3.0 Basic Optics

The laws of optics are essentially the same for both the visible and the infrared spectrum. However, differences in optical technique do in practice arise due to the materials used. Because ordinary glass is opaque to infrared much beyond 3 microns, the tendency in the past has been to use reflective optics as opposed to refractive optics for IR. With the advent of IR transparent materials such as silicon, germanium, and the "IRtran" range, lens systems as well as mirror systems will be increasingly used for IR work. Refractive optics are almost invariably used for LLTV systems. The size and design of an optical system influences the overall size and performance of the sensor, and both reflective and refractive systems used the same parameters, the most important being:

   a. Focal length.
   b. Relative aperture.
   c. Depth of focus.
   d. Depth of field.
   e. Field of view.

3.0.1 Focal Length. Assume a series of parallel light rays, all focused to one point as shown in Figure 8.2.1. The distance from the center of the lens to the focal point is called the focal length, (f). There is a corresponding
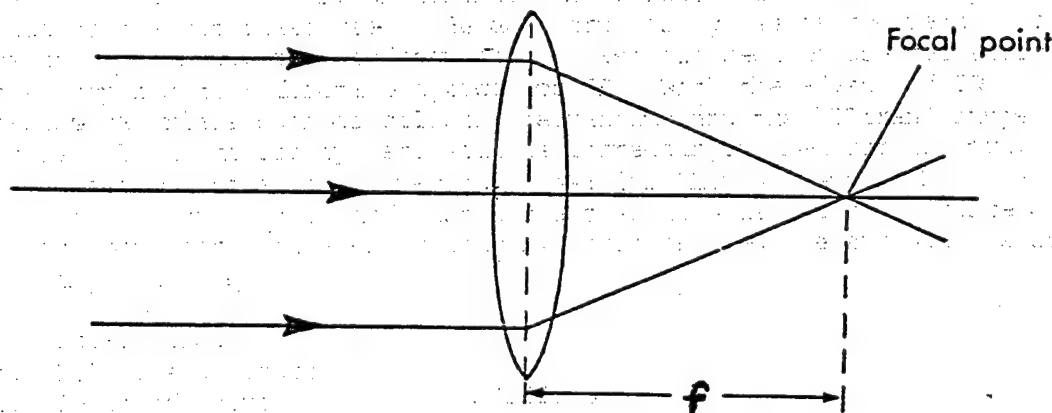
Figure 8.2.1. Focal Point of a Lens

focal point in front of the lens. The image of an object can be drawn using
the focal points as shown in Figure 8.2.2. The magnification, (m), of this
lens is defined as the ratio of the height of the image to the height of the
object and, for a remote object (the usual reconnaissance case), is easily
shown to be:

$$m = \frac{f}{S} \qquad (2\text{-}1)$$

where S is the distance from the object to the lens. It can be seen from this
that increasing the focal length of a lens increases its ability to magnify.
The inverse of the magnification ratio is more commonly used in reconnaissance
and is called scale factor.

$$\text{Scale factor} = \frac{S}{f} \qquad (2\text{-}2)$$

Figure 8.2.2. Imaging Geometry

3.0.2 Relative Aperture (F-number). The ratio of focal length to the
diameter of a lens (f/D) is called the relative aperture, or F-number (f_N) of
the lens. This ratio determines the irradiance of the image (irradiance is
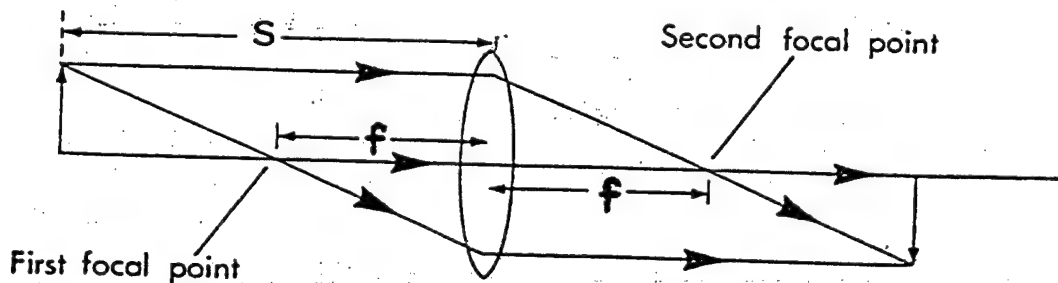the radiant flux striking a surface of unit area). A lower F-number means a
brighter image. Theoretically, the F-number also determines the resolving
power of the lens. Lenses tend to give the sharpest image when they have been
stopped down from their maximum aperture. This is because lens quality is
imperfect at maximum aperture due to the difficulty in correcting the lens
over its entire surface. The larger the diameter of a lens, the better the
angular resolution. However, the linear separation in the image plane (image
resolution) depends on the F-number. Thus, for best resolution, both the
focal length and the lens diameter must be chosen with care (but see "depth of
focus" below).

3.0.3 Depth of Focus. The F-number also determines another important
property of a lens: depth of focus. If a lens images a point on a screen, as
in Figure 8.2.3, the screen can be moved a distance Δf without any apparent
change in the size or sharpness of the image. The image of the point is
called the "circle of confusion". It exists because the focal point differs
for different wavelengths of light and IR, and because of other imperfections
in the lens. From geometry, the depth of focus is:

$$\Delta f = \pm \ d \ (f/D) \qquad\qquad\qquad (2\text{--}3)$$
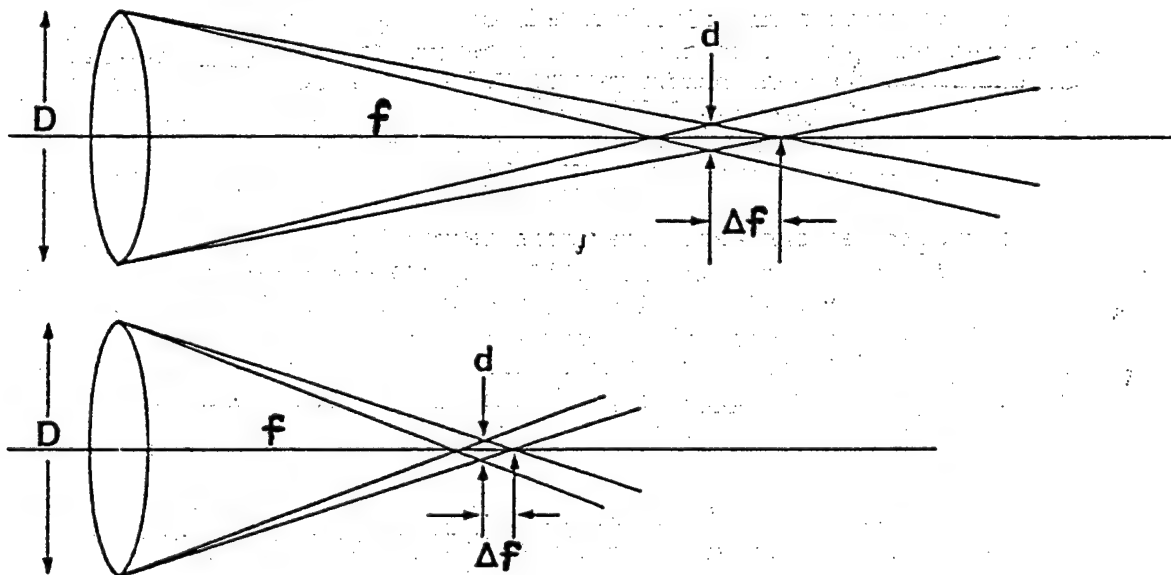

Figure 8.2.3. Depth of Focus Depends on the F-Number of the Lens

where d is the diameter of the circle of confusion. It can be seen that focusing is more critical for lower F-numbers than for higher F-numbers. Thus although a low F-number is good from the point of view of a bright image and good resolution, a critical depth of focus imposes problems on the designer of optical systems for reconnaissance purposes, in that he may be forced into employing automatic focusing systems, thus increasing the complexity. It is apparent that the design of optical systems is necessarily a compromise between conflicting parameters.

3.0.4 <u>Depth of Field</u>. Analogous to the depth of focus, there is a depth of field. Only objects within the depth of field are imaged within the depth of focus of the lens. When a sensor optical system is focused at infinity, the closest distance in acceptable focus is called the hyper-focal distance. Airborne systems are generally focused on infinity, so the hyper-focal distance corresponds to the minimum altitude or range for which the optics remain in focus.

3.0.5 <u>Field of View</u>. The field of view of a lens is established by the focal length of the lens and the dimensions of the sensor area. If the field of view is ϕ, the relationship is, from Figure 8.2.4:

$$\tan \frac{\phi}{2} = \frac{W}{2f} , \qquad \text{or} \qquad \phi = 2 \tan^{-1} \frac{(W)}{(2f)} \qquad\qquad (2\text{-}4)$$

where W is the corresponding width or diagonal of the sensor. It can be seen from the formula that increasing the focal length reduces the field of view. Thus it is impossible to have both a long focal length and a wide field of view, unless the dimensions of the sensor are greatly increased, which is usually not practicable. An increased field of view introduces its own problems of curvature of the field, reduced illumination and vignetting (obstruction of the field of view by lens mounts and other interior surfaces).
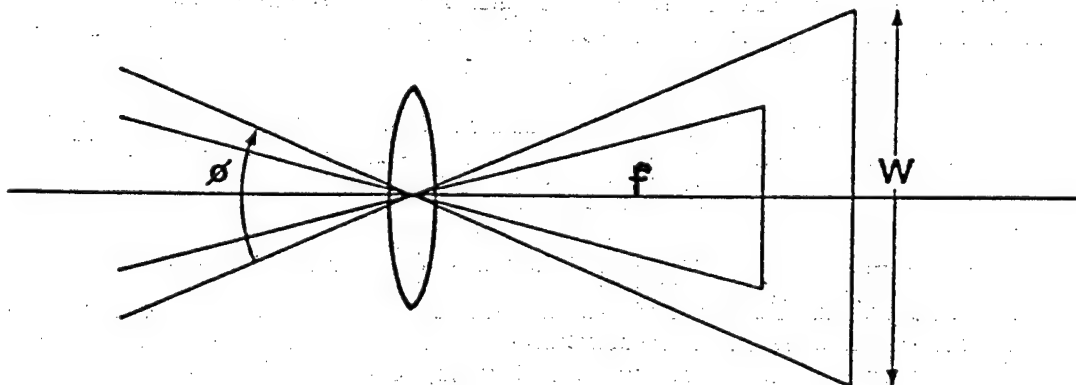

Figure 8.2.4. Field of View Depends on Focal Length and Sensor Size

3.1 **The Lens.** The lens is an optical element that utilizes the phenomenon of refraction to collect, concentrate, redirect, and focus electromagnetic wave radiation. The lens generally is characterized by curved surfaces (faces) and may consist of two or more lens elements, in tandem, with different geometries or indices of refraction.

A lens is considered a "thin lens" when its thickness is small in comparison with the radii of curvature of its surfaces, its focal length, and the object and image distances. When such is not the case, the lens must be considered a "thick lens". As will be seen, the same imaging formulae apply to thin and thick lenses provided that the object and image distances for a thick lens are measured from the principal points of the lens rather than from its center as for a thin lens.

3.1.1 **The Lens Maker's Formula.** The focal length of a thin lens is determined by its index of refraction and the radii of curvature of its surfaces (see Figure 8.2.5), and is given by the equation:

$$f = (\frac{1}{n-1}) \; (\frac{r_2 r_1}{r_2 - r_1}) \quad (cm) \qquad\qquad (2\text{-}5)$$

where it is assumed that the medium on both sides of the lens has an index of refraction equal to unity and:

n = Index of Refraction of Lens Material (N.D.)

r_1 = Radius of Curvature of Left Hand Surface of Lens in cm.

r_2 = Radius of Curvature of Right Hand Surface of Lens in cm.

(A radius of curvature is positive if the surface is concave to the left in the figure.)

$$f = \left(\frac{1}{n-1}\right)\left(\frac{r_1 \, r_2}{r_2 - r_1}\right)$$
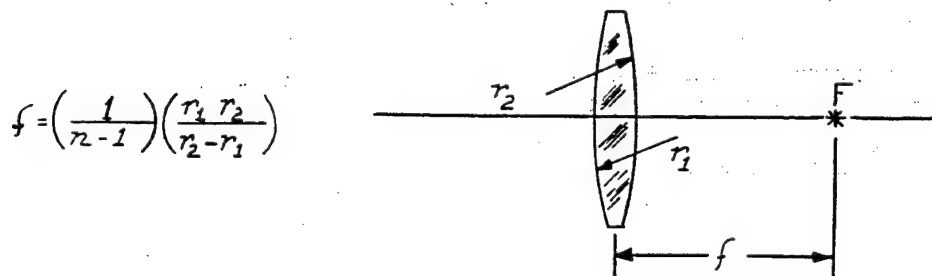
n =   Lens Index of Refraction (N.D.)

r_1, r_2 = Lens Radii of Curvature (cm)   (A Radius is Positive if Surface is Concave to the left).

When f > 0, the lens is said to be positive.

When f < 0, the lens is said to be negative.

Figure 8.2.5. Focal Length of a Lens

Note that is is possible for a lens to have a negative focal length, indicating that the focal point is located on the opposite side of the lens to that shown in the figure.

3.1.2 Object/Image Geometric Construction (Ray Tracing). The image produced by a positive lens (f > 0) may be geometrically determined from the object by utilizing the following ray tracing rules:

   a. A ray entering the lens parallel to its optical axis passes through the focal point on the far side of the lens.

   b. A ray entering the lens after having passed through the focal point on the near side of the lens exits from the lens parallel to the optical axis.

   c. A ray passing through the geometric center of a (thin) lens is undeflected by the lens.

Rays illustrating the three rules are shown in Figure 8.2.6 emanating from the head of an arrow (the object) and converging on the head of the image of the arrow. Using this method, each point in an object can be traced to the corresponding point in its image.
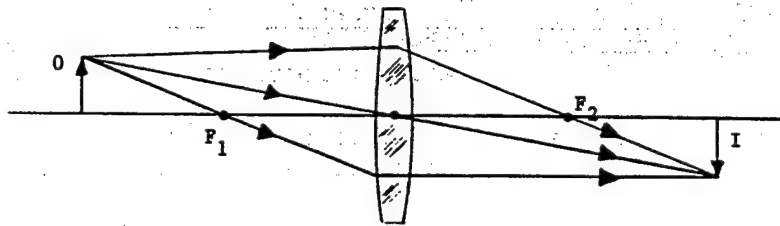
Figure 8.2.6. Geometric Method of Object-to-Image Construction
for a Positive Lens (f > 0)

3.1.3 The Virtual Image. When the rays forming an image actually emanate from the apparent position of that image, the image is termed "real". When the rays only appear to emanate from the image, as shown in Figure 8.2.7, the image is termed "virtual". When the focal length of a lens is negative (f < 0), it creates a virtual image of an object beyond its focal point. P' Q' is the virtual image in Figure 8.2.7. If a screen were placed at the position of an image, only a real image would appear on the screen. The rays to the right of the lens in the figure are, however, exactly as they would be if P' Q' were a "real" image. Thus, P' Q' forms the "object" for other optical elements to the right of the lens.
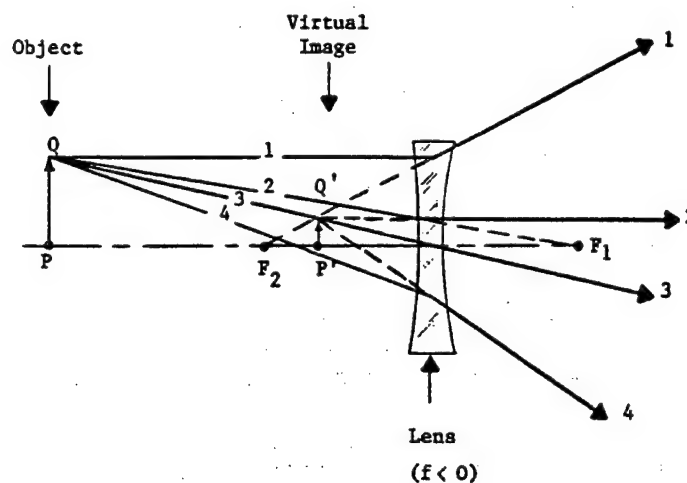
Figure 8.2.7.   The Virtual Image Produced by a Negative
               Lens (f < 0)

The virtual image produced by a negative lens, (f < 0), may be
geometrically determined from the object by utilizing the following ray
tracing rules:

   a.   A ray entering the lens parallel to the optical axis is refracted so
        that it appears to emanate from the focal point on the near side of
        the lens.

   b.   A ray entering the lens after having passed through the focal point
        on the near side of the lens exits from the lens parallel to the
        optical axis.

   c.   A ray passing through the center of a (thin) lens is undeflected by
        the lens.

Rays illustrating these three rules are shown in Figure 8.2.7.

When the object is beyond the focal point of a lens with positive focal
length (f > 0), a real image is formed, as shown in Figure 8.2.8(a). When the
object is at the focal point, the image is formed at infinite distance
($d_i = \infty$) as shown in Figure 8.2.8(d). When the object is inside the focal
point, a virtual image is formed, as shown in Figure 8.2.8(c).

(a) Real Image $(|d_o| > |f|)$

(b) Image at Infinity $(|d_o| = |f|)$

I at Infinity

(c) Virtual Image $(|d_o| < |f|)$
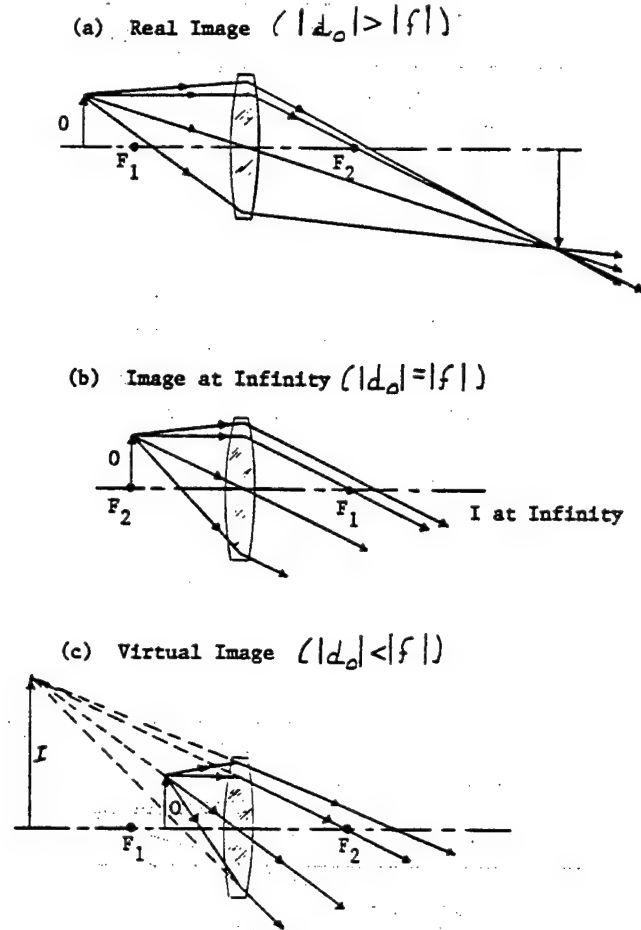
Figure 8.2.8. Effect of Object Location on Image

3.1.4 Multi-Lens Image Construction. Figure 8.2.9 shows a four-lens optical system with the geometric construction used to determine the successive images (P, Q, R, and I) from the object (O). As can be seen from the figure, the real image from lens 1, (P), is inside the focal point of lens 2, thus producing a virtual image from lens 2, (Q). The virtual image from lens 2, (Q), forms the object for lens 3, producing an image from lens 3, (R), which would be real except for lens 4. Since R is beyond lens 4, the graphical construction yields a real final image from lens 4, (I), on the same side of lens 4 as the image from lens 3.

3.1.5 Lens Imaging Characteristics. The position and magnification of the image produced by a lens depend only upon the focal length of the lens and the position of the object with respect to the lens, as shown in Figure 8.2.10. Specifically:

$$d_i = \frac{d_o f}{d_o - f} \qquad \text{(cm)} \qquad\qquad\qquad (2\text{-}6)$$

$$m = \frac{f}{f - d_o} \qquad \text{(N.D.)} \qquad\qquad\qquad (2\text{-}7)$$

where: d_i = Image Distance (cm)

d_o = Object Distance (cm)

f = Focal Length of Lens (cm)

m = Magnification

If d_i is positive, the image is real. If d_i is negative, the image is virtual.
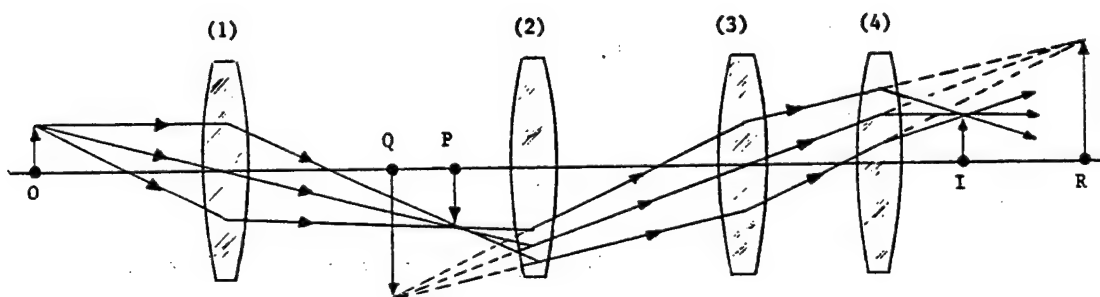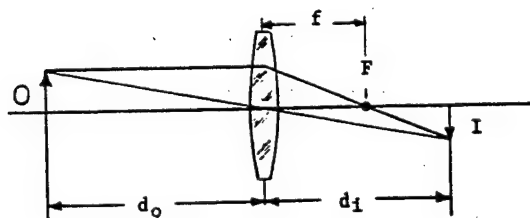
Figure 8.2.9. Multi-Lens Image Construction

$$d_i = \frac{d_o\, f}{d_o - f} \quad \text{(cm)}$$

$$m = \frac{f}{f - d_o} \quad \text{(N.D)}$$

When $d_i > 0$, the image is real.

When $d_i < 0$, the image is virtual.

Figure 8.2.10. Lens Imaging Characteristics

The sign conventions for object, image, and optical element parameters are dictated by the following rules:

a. All distances are measured along the optical axis from the refracting or reflecting element to the object or image.

b. An object distance (d_o) is positive if its direction is opposite to that of the incident ray.

c. An image distance (d_i) is positive if its direction is the same as that of the refracted or reflected ray.

d. A radius of curvature is positive if the direction from the surface to the center of the optical element is the same as that of the refracted or reflected ray.

e. An object or image dimension above the optical axis is positive.

.1.6 The Thick Lens. As previously stated, a "thick lens" is one for which its thickness (distance between surfaces) is not small in comparison with the radii of curvature of its surfaces, its focal length, and the object and image distances. Multiple lens systems also can be considered to be thick lenses. As indicated in Figure 8.2.11, the focal point, image, and object distances must be measured with respect to the Principal Points, H_1 and H_2. When these distances are taken in this manner, the same imaging formulae hold as for thin lenses. That is, the image distance is given by:

$$d_o = \frac{d_o f}{d_o - f} \qquad (\text{cm}) \qquad\qquad (2\text{-}8)$$

and the image magnification is given by:

$$m = \frac{f}{f - d_o} \qquad (\text{N.D.}) \qquad\qquad (2\text{-}9)$$

The focal length of a thick lens is given by the equation:

$$f = \left(\frac{1}{n-1}\right) \left[\frac{r_1 r_2}{r_2 - r_1 + \left(\frac{n-1}{n}\right) t}\right] \qquad (\text{cm}) \qquad (2\text{-}10)$$

and the principal points are located as shown in Figure 8.2.11, in which:

$$h_1 = \left(\frac{n-1}{n}\right) \left(\frac{t}{r_2}\right) f \qquad (\text{cm}) \qquad\qquad (2\text{-}11)$$

$$h_2 = \left(\frac{n-1}{n}\right) \left(\frac{t}{r_1}\right) f \qquad (\text{cm}) \qquad\qquad (2\text{-}12)$$
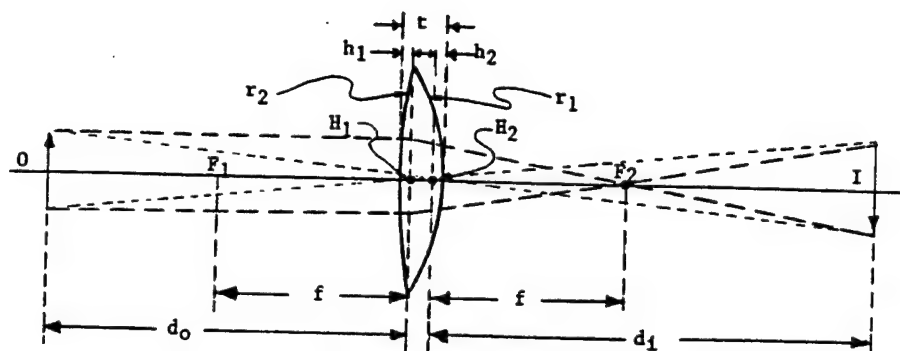
Figure 8.2.11. The Thick Lens

where: d_i = Image Distance

d_o = Object Distance

f = Lens Focal Length

m = Image Magnification

n = Lens Index of Refraction

r_1 = Radius of Curvature of Surface No. 1

r_2 = Radius of Curvature of Surface No. 2

t = Thickness of Lens

3.1.7 <u>Lens Aberrations</u>. Aberrations are those characteristics of optical
elements, other than those associated with diffraction, which prevent the lens
from imaging a point source as a point in the image plane. Both surface
geometry and index of refraction variations contribute to aberration.
Aberrations which are the result of more than one wavelength being present in
the radiation are termed chromatic aberrations. All other aberrations are
monochromatic aberrations. Aberrations cause an optical system to image a
point source as a finite spot known as a blur circle or circle of confusion.
As previously indicated, the effect of aberrations is a function of lens
diameter, the size of the blur circle increasing rapidly with increasing
numerical aperture.

The principal monochromatic aberrations are listed and defined below.

Spherical Aberrations: Rays from a point on the optical axis are not brought to a common focus.

Coma: The image of a point off the optical axis is an egg-shaped spot of finite size.

Distortion: Straight lines are imaged as curved lines.

Curvature of Field: The image of an object in a plane lies on a curved surface.

These monochromatic aberrations are a result of the inability of a lens with spherically ground surfaces to image an object perfectly. They are not due to imperfections in the manufacture of the lens. (In airborne systems, imperfections are generally held within limits which make their effects negligible.) Monochromatic aberrations can be corrected to any desired degree by utilizing non-spherical lenses or by multiple-lens systems as shown in Figure 8.2.12.
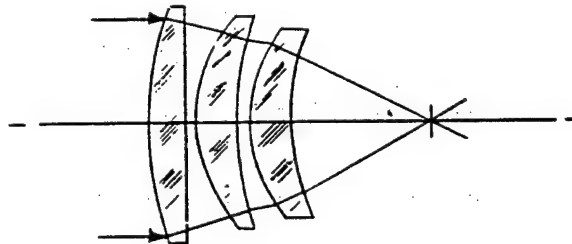
Figure 8.2.12. Correction of Lens Aberrations by the Use of Multiple-Lens Systems

Chromatic aberrations are a result of the variation of the index of refraction of the lens material with the frequency or wavelength of the radiation. When more than one wavelength is present in the radiation from the object, the various frequency components are not refracted identically. Chromatic aberrations are of two kinds, defined below.

Longitudinal Aberration: Different wavelengths are not imaged in the same plane.

Lateral Aberration: The size of the image of an object varies with the wavelength of the radiation.

Chromatic aberrations can be corrected by utilizing multiple-element lenses with different indices of refraction as shown in Figure 8.2.13.
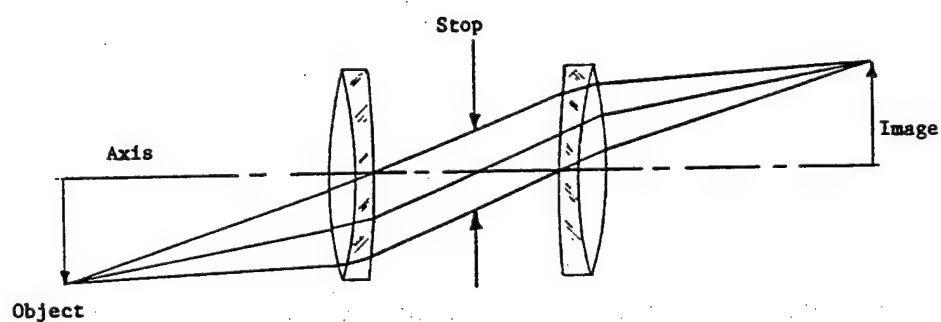
Figure 8.2.13. Correction of Lens Aberrations by the Use of Multiple Lenses of Different Refractive Index

3.1.8 <u>Types of Lenses</u>. The nomenclature and use of various types of lenses is indicated in Figure 8.2.14.
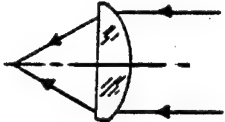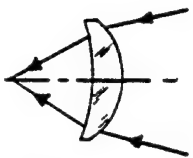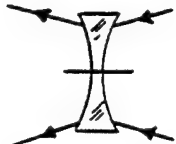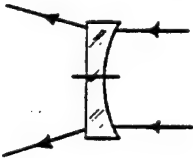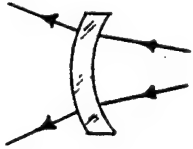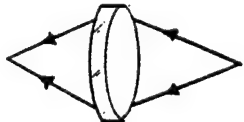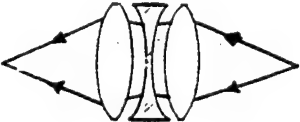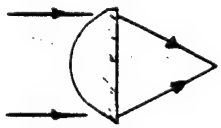
<u>Lens</u>	<u>Type</u>	<u>Characteristics and Application</u>
	Convex	Converging: General Use, Magnification
	Plano Convex	Converging: Used Often in Opposed Doubles to Reduce Spherical Aberration
	Menisus	Converging: Reduced Spherical Aberration
	Concave	Diverging: General Use, Demagnification
	Plano Concave	Diverging: Used in Multi-Element Combinations
	Menisus	Diverging: Reduced Spherical Aberration
	Doublet	Corrected for Chromatic Aberration
	Multi-Element	High Order of Aberrations Correction: Used in Complex Systems
	Aspheric	Corrected for Spherical Aberrations: Used in Condenser Systems

Figure 8.2.14. Types of Lenses

3.1.9 **Multiple-Lens System.** The lens system of a simple non-imaging radiation detector is shown in Figure 8.2.15. The objective lens gathers radiant flux and delivers it to the field lens. The field lens delivers the radiant flux to the detector. Note that the flux is not focused to a point on the detector but irradiates the detector over its entire surface, thereby maximizing the signal-to-noise ratio.
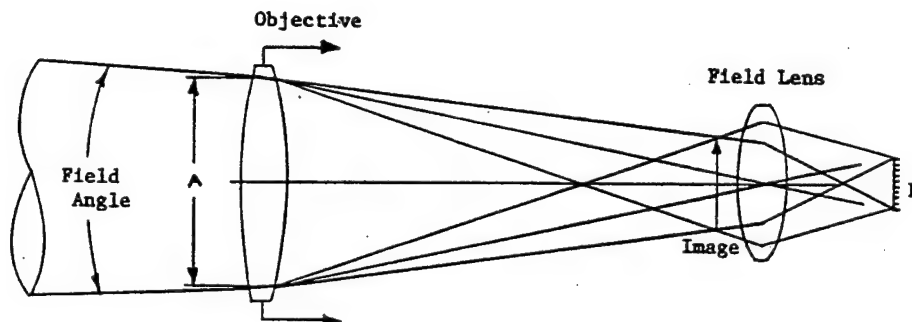
Figure 8.2.15.   Lens System for a Non-Imaging Radiation Detector

A relay lens system is shown in Figure 8.2.16. A relay lens system is used to transmit an image over an extended, narrow path without altering the size of the image or the field-of-view. A typical application is the periscope.

R = Relay Lens
F = Field Lens
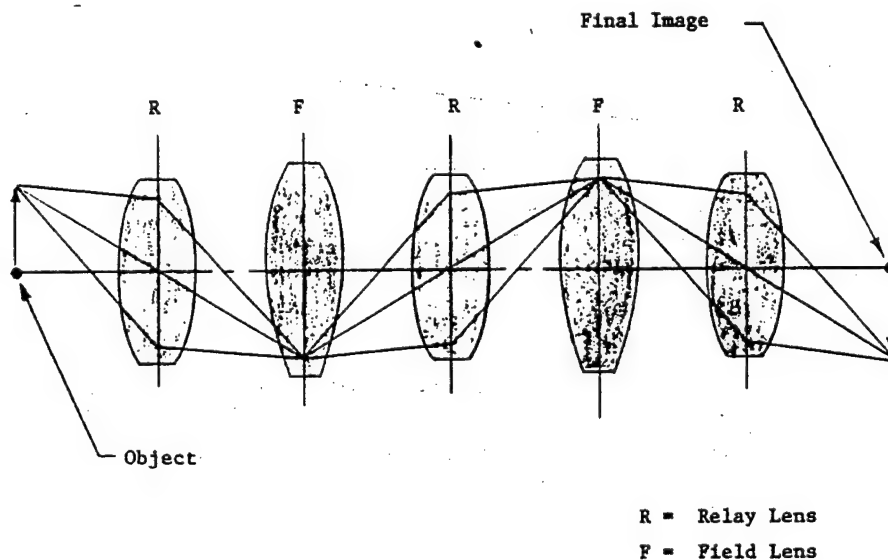
Figure 8.2.16.   Relay Lens System

An afocal lens system focuses the final image at infinity for ease of viewing by the human eye. Two types of afocal lens systems commonly used in telescopes are shown in Figure 8.2.17.

Astronomical Telescope

(inverting)

Gallilean Telescope

(Non-Inverting)
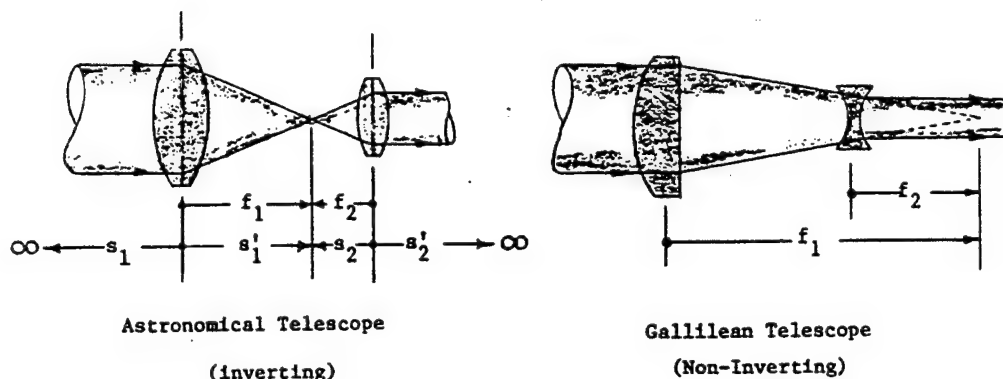
Figure 8.2.17.   Afocal Lens Systems

A typical imaging sensor optical system is shown in Figure 8.2.18. In addition to a multiple-element objective and a field lens, shown are a field stop (physical aperture), that determines the field of view, and an aperture stop, that determines the radiation-admitting area (aperature) of the system. As indicated by this example, field and aperture stops can be located at various points in the path of an optical system.
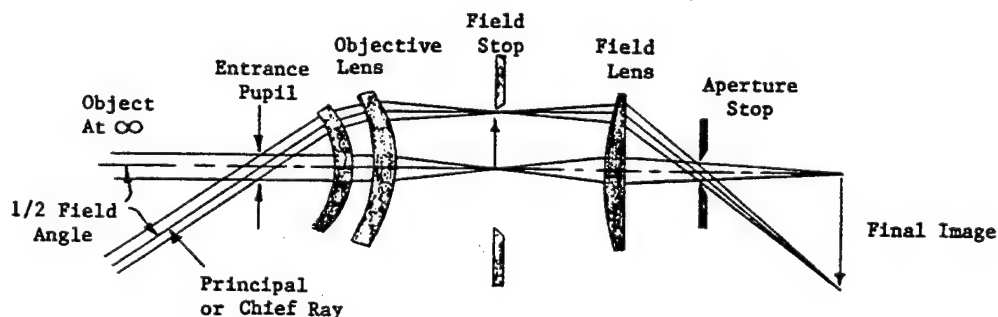
Figure 8.2.18.   Optical System for a Typical Imaging Sensor

3.2   The Mirror

The mirror is an optical element that utilizes the phenomenon of
reflection to collect, concentrate, redirect, and focus electromagnetic
wave radiation. As an optical element, the mirror has many of the same
characteristics and serves many of the same purposes as does the lens. The
reflecting surfaces of a mirror may be curved or planar and may be partially
or totally reflective. Mirrors possess one distinct advantage in comparison
with lenses: They do not suffer from chromatic aberrations when
"front-silvered". (There is no radiation path through a refracting medium
and, hence, no variation of refractive index with frequency.)

As with lenses, most mirrors are sperically ground. The focal point,
(F), of a spherical mirror is located midway between the reflecting surface
and the center of curvature, (c), as shown in Figure 8.2.19. Neglecting
sperical aberrations, incident rays parallel to the optical axis are reflected
(or appear to be reflected) through the focal point. Conversely, rays
emanating from the focal point of a positive (concave) mirror are reflected
parallel to the optical axis.
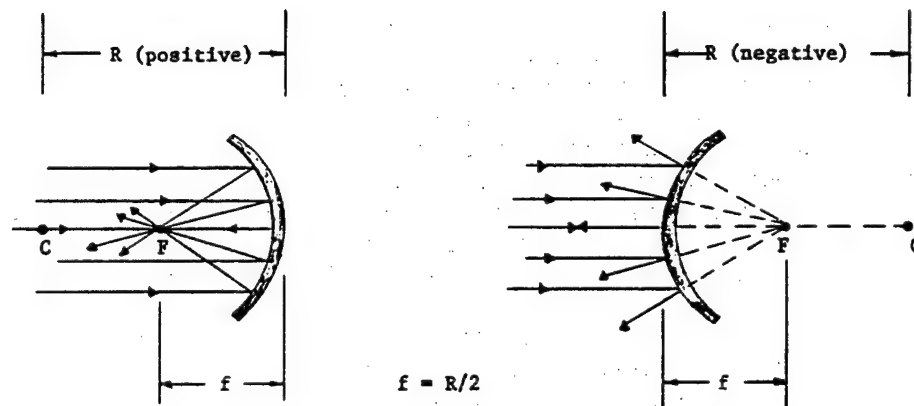
Figure 8.2.19.   The Spherical Mirror

The image produced by a spherical mirror may be geometrically determined
from the object by utilizing the following ray tracing rules.

a.   An incident ray parallel to the optical axis of the mirror passes
     through the focal point after reflection.

b.   An incident ray passing through the center of focus is reflected back
     upon itself.

Rays illustrating these rules are shown in Figure 8.2.20 emanating from the head of an arrow (the object) and converging on the head in the image of. the arrow. Using this method, each point in an object can be traced to the corresponding point in its image. Figure 8.2.21 shows the virtual image produced by a negative (convex) mirror. Also shown are the construction lines corresponding to the following rules for the geometric method of constructing the image of an object produced by a negative lens (f < 0).

a. An incident ray parallel to the optical axis of the mirror is reflected so as to appear to emanate from the focal point on the far side of the mirror.

b. An incident ray directed toward the focus on the far side of the lens is reflected parallel to the optical axis.

c. An incident ray directed toward the center of curvature is reflected back upon itself.
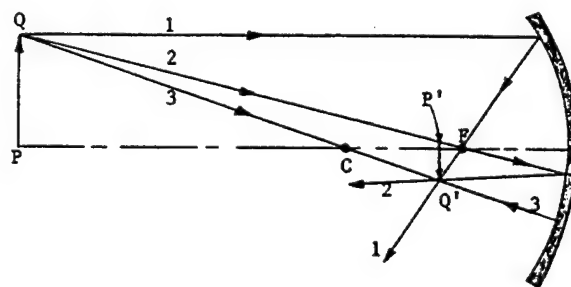
Figure 8.2.20.   Object/Image Geometric Construction
                 for a Spherical Mirror
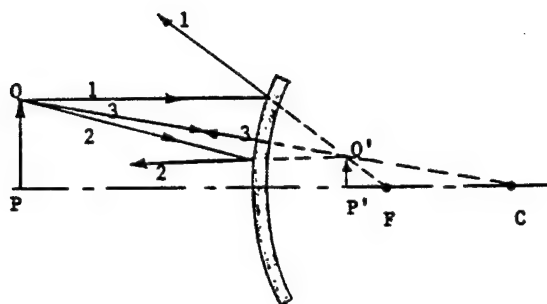
Figure 8.2.21.   The Virtual Image Produced by a Negative
                 (Convex) Mirror

3.2.1 Mirror Imaging Characteristics

The position and magnification of the image produced by a spherical mirror depend only upon the focal length of the mirror and the positon of the object with respect to the mirror, as shown in Figure 8.2.22. Specifically:

$$d_i = \frac{d_o\, f}{d_o - f} \quad (cm) \tag{2-13}$$

$$m = \frac{h_i}{h_o} = \frac{f}{f - d_o} \quad (N.D.) \tag{2-14}$$

where: d_i = Image Distance

d_o = Object Distance

f = Focal Length of Mirror

h_i = Height (size) of Image

h_o = Height (Size) of Object

m = Magnification

If $d_i > 0$, the image is real.

If $d_i > 0^-$ the image is virtual.

$$d_i = \frac{d_o\ f}{d_o - f} \quad \text{(cm)} \qquad\qquad m = \frac{h_i}{h_o} = \frac{f}{f - d_o} \quad \text{(ND)}$$
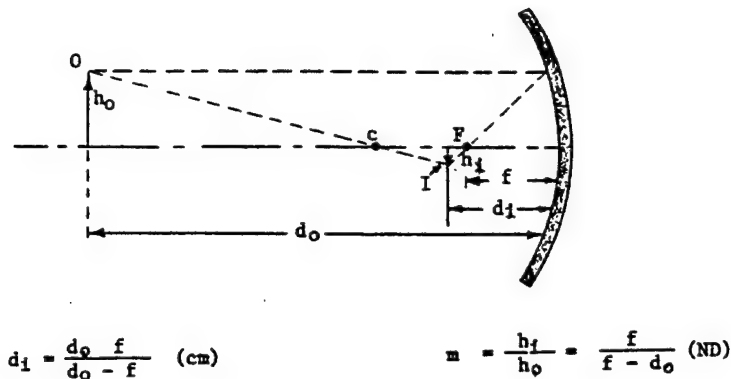
When $d_i > 0$, the image is real
When $d_i < 0$, the image is virtual

Figure 8.2.22. The Imaging Characteristics of the Spherical Mirror

As can be seen by comparison with the equations in Sections 3.1.5 and 3.1.6 of this text, the above equations for a mirror are identical to those for a lens. The rules for assigning the signs of the above dimensions also are identical to those given for the lens in Sections 3.1.5 and 3.1.6.

3.2.2 Mirror f-Number (f_N) and Numerical Aperture (NA)

The f-number and numerical aperture of a spherical mirror have the same meanings and forms as those for a lens. That is:

$$f_N = f/D \quad \text{(cm)} \tag{2-15}$$

and:

$$NA = \frac{f}{2f_N} \quad \text{(1/cm)} \tag{2-16}$$

where: D = Mirror diameter (Aperture)
          f = Mirror Focal Length

The depth of field for a spherical mirror also is identical to that presented for a lens.

3.2.3 Mirror Aberrations

The monochromatic aberrations of a spherical mirror are the same as those for a spherically-ground lens. As previously indicated, there are no chromatic aberrations for a front-silvered mirror. That is, there are no

chromatic aberrations associated with the reflective process. As for the spherically-ground lens, the monochromatic aberrations defined earlier are caused not by imperfections in manufacture of a spherically-ground mirror, but by the inherent inability of a spherically-ground mirror to image perfectly. Mirror aberrations can be corrected by specially ground (non-spherical) surfaces or by the use of specially ground lenses as shown in Figure 8.2.23.

(a) Schmidt

(b) Maksutov
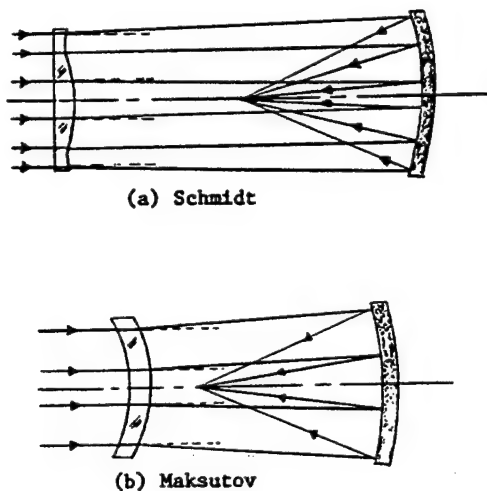
Figure 8.2.23.   Correction of Mirror Aberrations by Means of Lenses

3.2.4   The Ellipsoidal Mirror

The ellipsoidal mirror, consisting of a portion of the surface of an ellipsoid of revolution, possesses two focal points as shown in figure 8.2.24. A point source placed at one focal point is perfectly imaged at the other. Planar, spherical, and parabolioidal mirrors are in fact special cases of the ellipsoidal mirror.
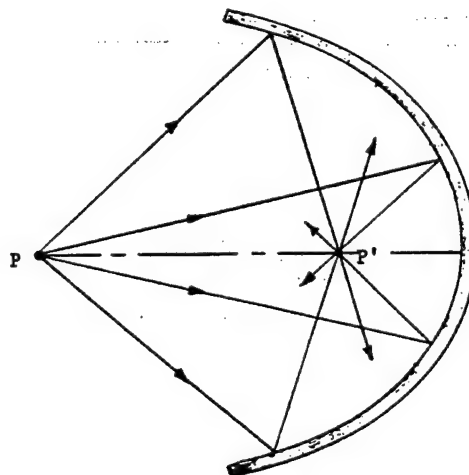
Figure 8.2.24.   The Ellipsoidal Mirror

3.2.5   The Paraboloidal Mirror

The paraboloidal mirror is a portion of a paraboloid of revolution. It is also an ellipsoidal mirror with one focal point at infinite distance. Thus, a paraboloidal mirror perfectly images, at its focal point, an object at infinite distance, as shown in figure 8.2.25(a). Conversely, a point source placed at the focal point produces reflected rays parallel to the optical axis, as shown in Figure 8.2.25(b). (Note that a paraboloidal mirror has no spherical aberration.) Paraboloidal mirrors are widely employed in optical systems for which the object or target of interest is at a great distance in comparison with the dimensions of the system (most airborne applications).

(a) Object at Infinity   (b) Image at Infinity
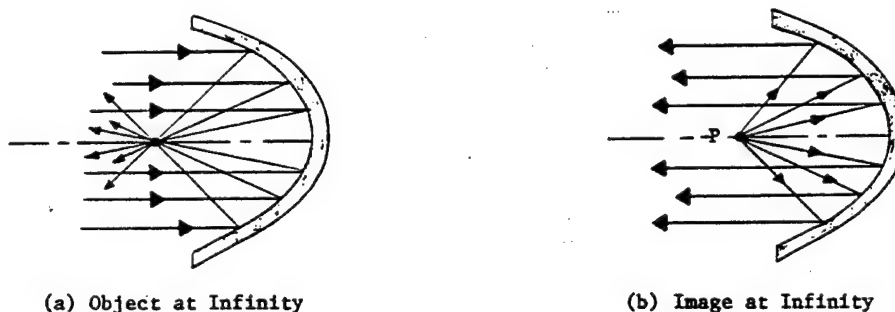
Figure 8.2.25. The Paraboloidal Mirror

3.2.6   The Planar Mirror

The planar mirror is, in effect, an ellipsoidal mirror with both focal points at infinite distance. It perfectly images a point source as a point, but produces only a virtual image (no real image and no focusing effect). The object/image geometry is simple ($d_i = d_o$), as shown in Figure 8.2.26, and the magnification is unity. The principal use of the planar mirror is the redirection of the path of radiation.

$$d_i = d_o$$

$$m = \frac{h_i}{h_o} = 1$$
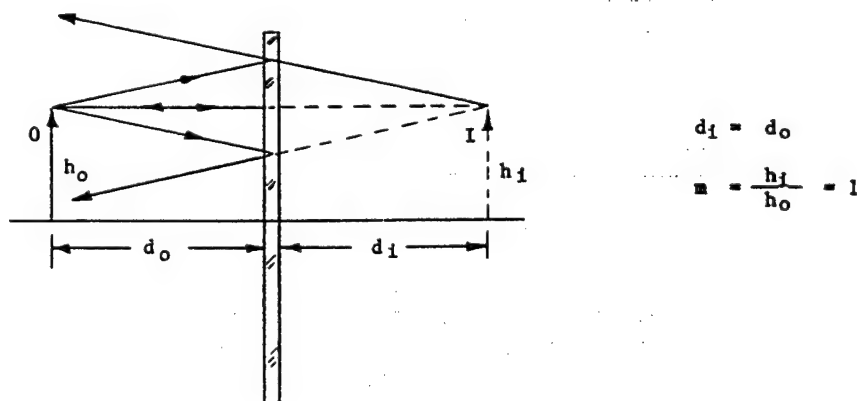
Figure 8.2.26. The Planar Mirror

3.2.7 Types of Mirrors

The nomenclature and use of various types of mirrors is indicated in Figure 8.2.27.
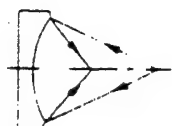
Concave Spherical   Converging: General Use

Convex Spherical   Diverging: General Use

Paraboloidal   Accurately Focuses a Parallel Beam or
                         Produces a Parallel Beam from a Point
                         Source

Conic: Refocuses a Diverging Bundle at Another
Ellipsoidal   Point (P) Displaced from the Point of
                         Origin (O)

General   Used Mostly in Combination Systems of
Aspheric   Two or More Components

Plane   —   Change Direction of Beam

Figure 8.2.27. Types of Mirrors

3.2.8 Multiple-Mirror Systems

Figure 8.2.28 shows several reflective optical systems using primary and secondary mirrors. Such systems are employed in airborne infrared target detection systems to avoid the problem caused by the poor transmittance of many materials used in refractive optical systems.

(A) SIMPLE MIRROR

(B) NEWTONIAN TELESCOPE

(C) OFF-AXIS PARABOLOID

(D) FOLDED
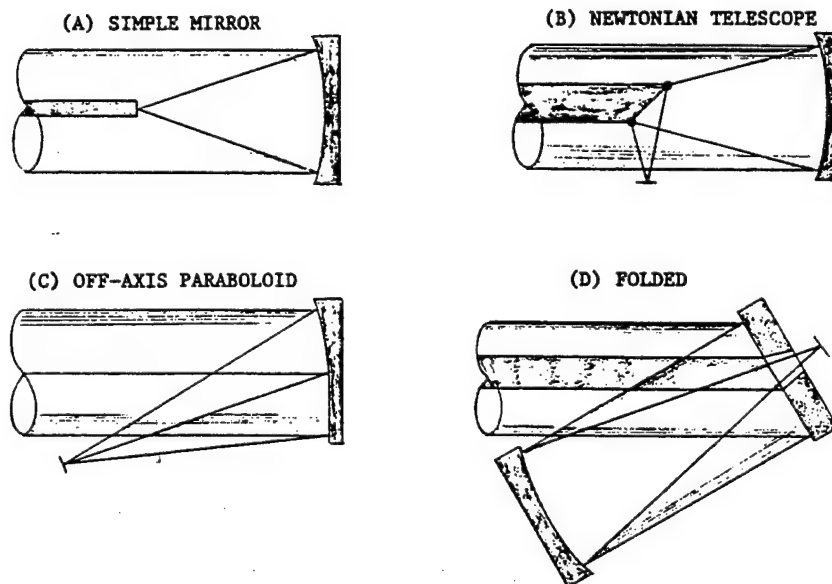
Figure 8.2.28. Multi-Mirror Optical Systems

3.3 The Prism

The prism, or prismatic lens, can utilize both refraction and reflection to alter the propagation path of electromagnetic wave radiation. A prism is characterized by planar surfaces in contrast to the curved surfaces normally associated with a "lens". The principal applications of prisms in electro-optical systems are listed below and discussed in the following paragraphs.

    Beam Angular Deflection (Reflection)
    Beam Retro-Reflection
    Beam Splitting (Partial Reflection)
    Beam Deviation (Refraction)
    Beam Lateral Displacement
    Beam Polarization (Birefringence)
    Beam Chromatic Dispersion
    Beam Inversion and Reversion
    Image Rotation

3.3.1 Beam Angular Deflection

Beam angular deflection entails alteration of the direction of propagation of a beam by internal reflection. Total reflection can be achieved by keeping the angle of incidence at the faces greater than the critical angle. The right angle prism shown in Figure 8.2.29(a) is used to deflect the beam path by 90°. The penta-prism shown in Figure 8.2.29(b) is used to deflect the beam path by twice the angle between the reflecting faces. The porro-prism shown in Figure 8.2.29(c) is used to deflect the beam by 180°.

(a) Right-Angle Prism   (b) Penta-Prism   (c) Porro-Prism
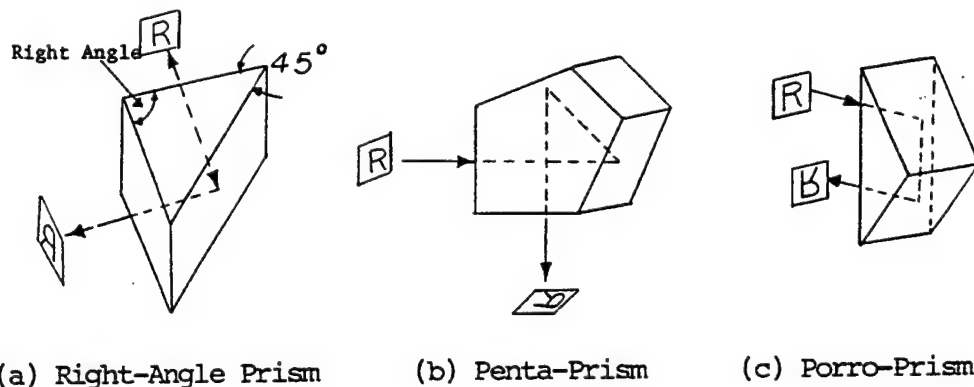
Figure 8.2.29. Beam Angular Deflection

3.3.2 Beam Retro-Reflection

Retro-reflection changes the direction of propagation of a beam by 180° regardless of the angle of incidence. The corner reflector shown in Figure 8.2.30, so called because it's faces form the corner of a cube, provides retro-reflection.
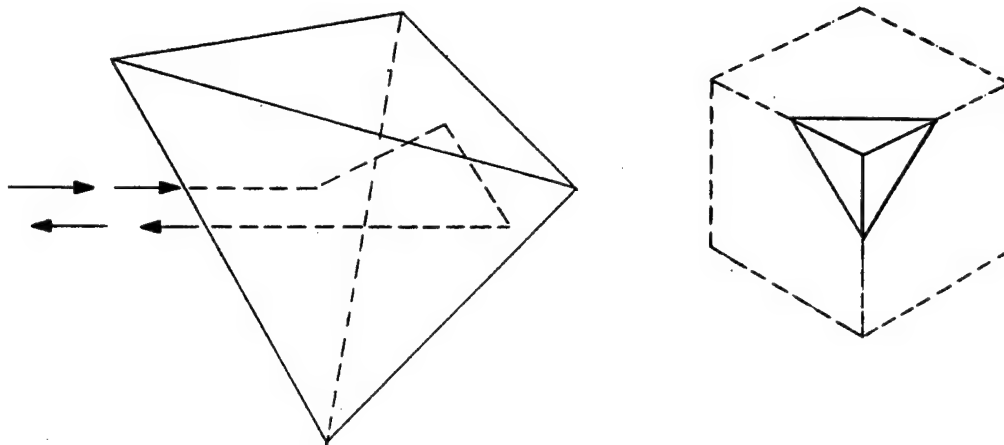
Corner Reflector

Figure 8.2.30.   Beam Retro-Reflection

3.3.3 Beam Splitting

In a beam splitter, an internal, partially-silvered face is employed to "split" the beam into two beams as shown in Figure 8.2.31. A beam splitter is used to obtain two coherent beams.
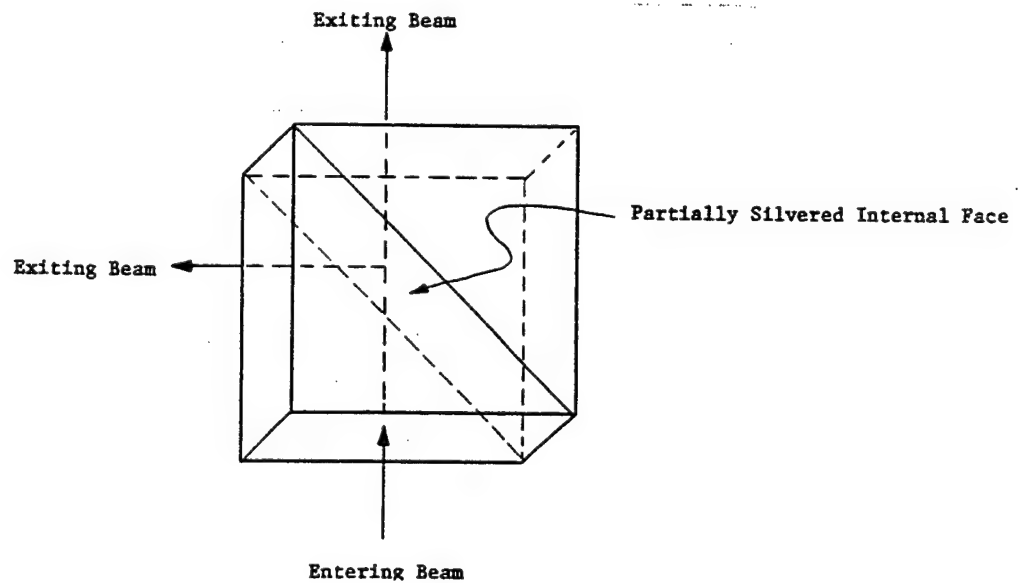
Beam Splitting Prism

Figure 8.2.31.   Beam Splitting

3.3.4 Beam Deviation

Beam deviation effects alteration of the path of propagation of the beam by refraction. The wedge prism shown in Figure 8.2.32 deflects the beam through an angle δ given by the equation:

$$\delta = (n-1)\alpha \qquad \text{(Degrees)} \tag{2-17}$$

where

n = Index of Refraction of Prism

α = Included Angle of Prism (Degrees)

Wedge Prism
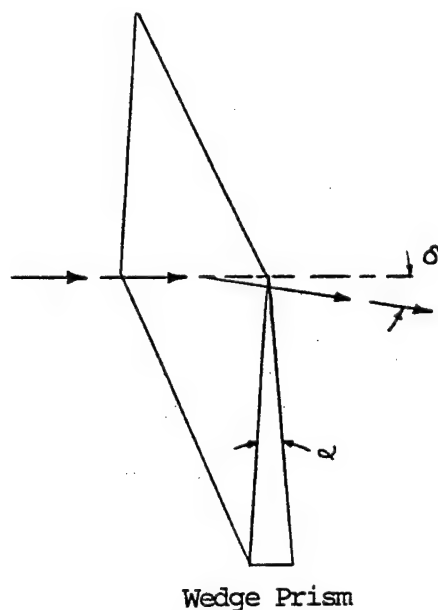
Figure 8.2.32. Beam Deviation

3.3.5 Beam Lateral Displacement

In beam lateral displacement, the path of propagation of the beam is shifted parallel to itself without changing the direction of propagation. The parallel prism shown in Figure 8.2.33 produces a beam lateral displacement, (d), given by the equation:

$$d = W\theta_1 \left(\frac{n-1}{n}\right) \qquad \text{(cm)} \tag{2-18}$$

where

w = Width of Prism

θ_1 = Beam Angle of Incidence

n = Index of Refraction of Prism

Parallel Prism

$$d = \left(\frac{n-1}{n}\right) W \alpha_1$$
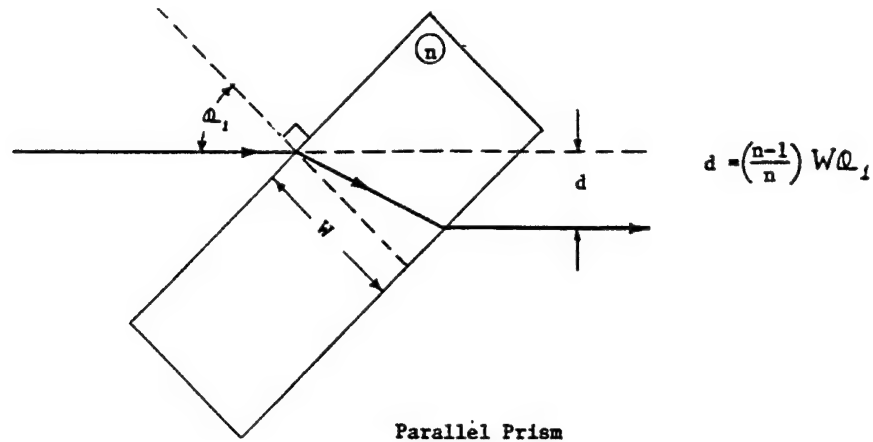
Figure 8.2.33. Beam lateral Displacement

3.3.6 Beam Polarization

In a beam polarizing prism, the beam is resolved into two components with polarization at right angles. The Nicol Prism shown in Figure 8.2.34 employs a calcite crystal, sliced and reattached with Canada Balsam cement. The calcite is birefringent; that is, it exhibits different indices of refraction to the components of the beam with polarization parallel to and transverse to its "optical axis". Because of the difference in index of refraction, the two components of the beam are refracted differently and reflected differently from the internal crystal/cement interface. One component is totally transmitted and the other is totally reflected by the interface, thereby effecting an angular separation between the two cross-polarized beams.
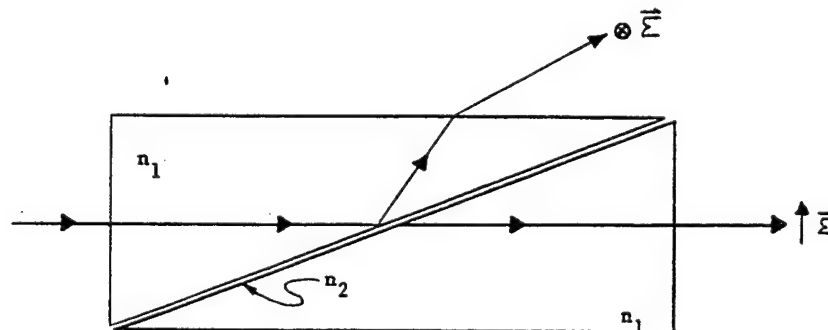
Nicol Prism

Figure 8.2.34. Beam Polarization

3.3.7 Beam Chromatic Dispersion

In chromatic dispersion, the incident beam is dispersed (resolved into its component frequencies) by means of differential refraction, as shown in Figure 8.2.35. Also each frequency component is refracted differently. The

angular deflection, δ_λ, of a component of wavelength, λ, is given by the equation:

$$\delta_\lambda = [n(\lambda) - 1]\alpha \qquad (\text{Degrees}) \qquad\qquad (2-19)$$

where $n(\lambda)$ is the (frequency dependent) index of refraction and α is the included angle of the prism. Since $n(\lambda)$ increases with frequency, the higher frequency components are deflected more than the lower frequency components.
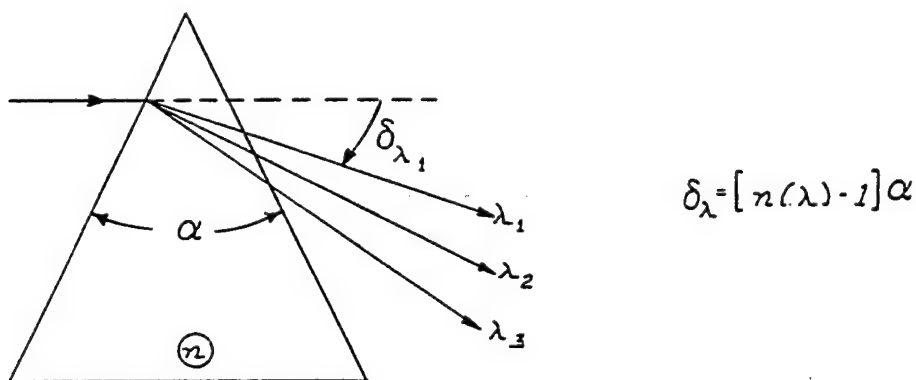
Figure 8.2.35.   Beam Dispersion

3.3.8 Image Inversion and Reversion

The roof prism shown in Figure 8.2.36 reverses and inverts the image produced by radiation reflected from its inner surfaces.
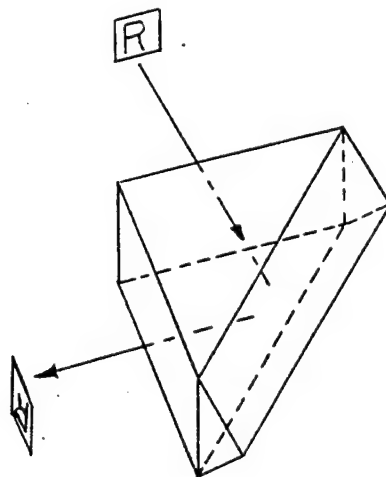
Roof Prism

Figure 8.2.36.   Image Inversion and Reversion

3.3.9   Image Rotation

The Pechan prism consists of two prisms cemented together as shown in Figure 8.2.37. The image of radiation reflected by the prism is rotated through twice the angle through which the prism is rotated about the beam axis.
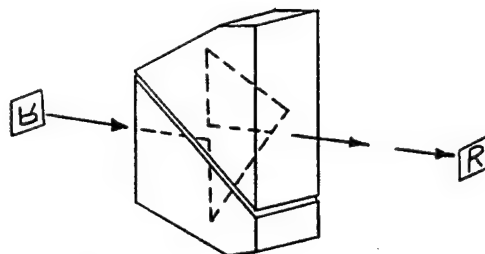
Pechan Prism

Figure 8.2.37.   Image Rotation

3.3.10   Beam Scanning Systems

As previously indicated, a parallel prism produces a lateral displacement of the transmitted beam. The multi-faceted, rotating prism shown in Figure 8.2.38 produces a unidirection-linearly-scanned beam.

PRISM   FILM
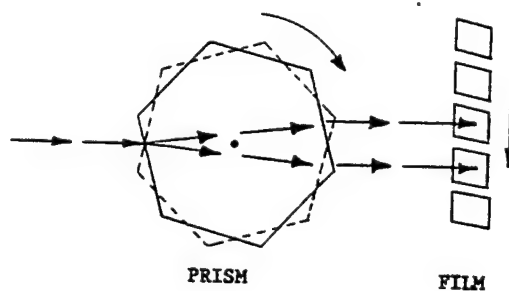
Figure 8.2.38.   Parallel Prism Beam Scanner

3.3.11   Wedge Prism

The rotating wedge prisms shown in Figure 8.2.39 produce varied scans depending upon the relative rotation rates (ω_1 and ω_2) of the two prisms.

Axis of prism
rotation

ω_1 ω_2

Rotating prisms   Optical system

Linear scan   Rosette scan   Circular scan   Spiral scan

$\omega_2 = -\omega_1$ $n\omega_2 = -\omega_1$ $\omega_2 = \omega_1$ $n\omega_2 = \omega_1$
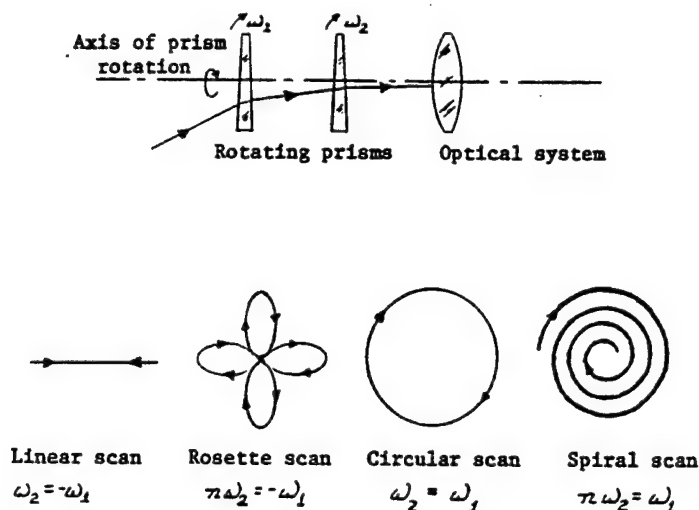
Figure 8.2.39.   Wedge Prism Beam Scanner

3.4 Physical Optics

3.4.1 Chromatic Filtering

Chromatic (color) filtering is the selective alteration of the target/
background clutter radiation spectrum. The selective alteration is dependent
upon the temporal frequency (rather than spatial frequency) characteristics of
the signal. The primary purpose of chromatic filtering is to discriminate
between the target and clutter (noise) radiation on the basis of spectral
differences. Chromatic filtering also can be used to reduce chromatic
aberrations by reducing the spectral bandwidth.

The usual method of chromatic filtering is the interposition, into the
optical path, of elements with temporal-frequency-dependent transmission
characteristics. As with all such frequency filtering, there is some loss of
target signal; but, if the spectral differences between the target and the
clutter signals are sufficient, the frequency discrimination will result in an
increased signal-to-noise ratio.

There are two principal types of chromatic filter: the absorption filter
and the interference filter. The absorption filter removes certain
wavelengths from the incident radiation by selectively converting radiant
energy to thermal energy. The thermal energy must then be dissipated,
possibly creating a cooling problem.

The interference filter removes specific wavelengths from the incident
radiation by selective reflection. Selective reflection is achieved by
utilizing wave interference between the transmitted beam and the radiation
reflected by internal interfaces within the filter. (The filter consists of
multiple layers of thickness equal to an integral odd number of quarter-
wavelengths of the radiation component to be removed.) Since the interference
filter reflects, rather than absorbs the rejected radiation, it does not

create the heat-dissipation problem created by the absorption filter. In addition, the slope (sharpness) of the interference filter is much greater than that of the absorption filter.

The transmission characteristics of a number of chromatic filters are shown in Figure 8.2.40.

The conventional definitions for various chromatic filter parameters are given below.

> Bandpass Filter: A filter that transmits a band of wavelengths sharply bounded by extended regions of low transmittance.
>
> Bandwidth: The wavelength interval over which transmittance is 50% or more.
>
> Center Wavelength: The wavelength at the center of the pass band.
>
> Cut-on and Cut-off Wavelengths: The wavelengths at which transmittance is 5% of the peak value.
>
> Longwave-Pass Filter: A filter that transmits all wavelengths greater than a specified cut-on value.
>
> Shortwave-Pass Filter: A filter that transmits all wavelengths smaller than a specified cut-off value.
>
> Slope: The ratio of the wavelength difference between the 5% and 80% of peak transmittance points to the center wavelengths.

An example of chromatic filtering is the application illustrated in Figure 8.2.41. Shown in the figure are the approximate spectra for a sunlit cloud and a 1000°K Blackbody. (The spectrum of a jet exhaust is similar to that of a 1000°K Blackbody.) As indicated, the radiation from the cloud could obscure a distant target, thereby degrading the performance of a heat-seeking missile or other infrared detector. If, however, a chromatic filter is employed, with a pass band as shown in the figure, the target-to-clutter signal ratio will be greatly improved.

3.4.2 Fourier Optics

The temporal frequency of a time function is defined as the number of times events occur per unit time. The number of pulses per second in a pulse train is a familiar example. In an analogous manner, the spatial frequency of an image is defined as the number of times similar shapes occur per unit distance. The number of pickets per foot in a picket fence is a familiar example. There exists many well known mathematical techniques for dealing with time functions (time averaging, time integration, time differentation, frequency filtering, frequency-response analysis, Fourier analysis and synthesis, Fourier and Laplace transforms, transfer functions, etc.). For every process applied in the time domain, there exists an analogous process in the space domain. The application of these space techniques to optical imagery (a spatial process) is known as Fourier optics. The methods of Fourier optics are identical to the analogous time-domain techniques except
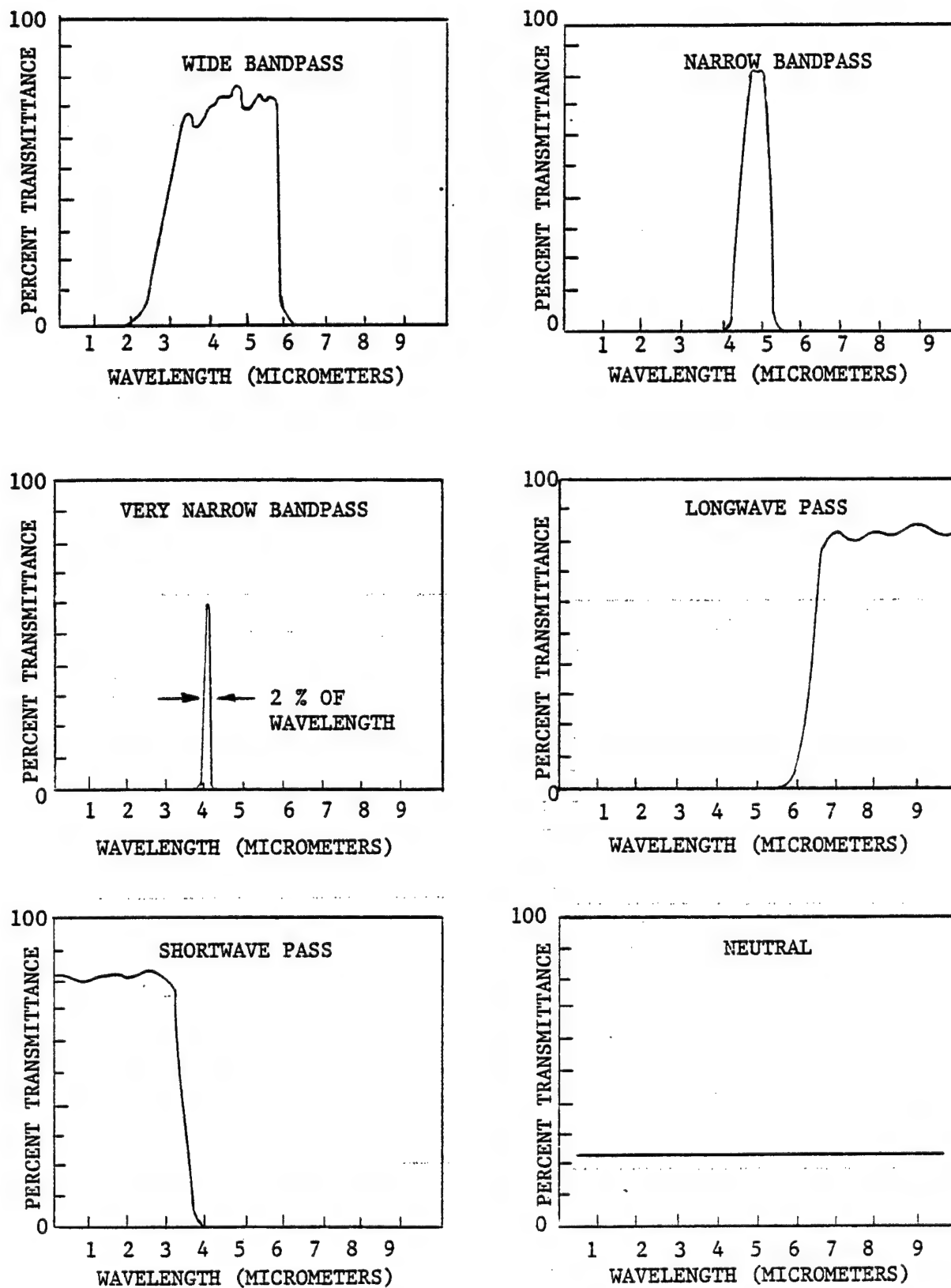
Figure 8.2.40.   Typical Chromatic Filter Transmission
                 Characteristics
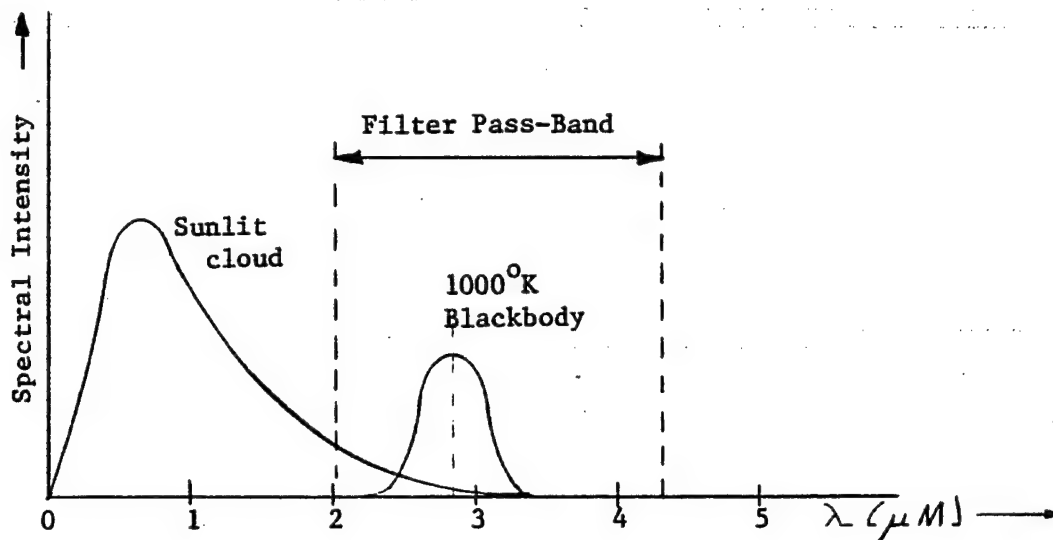
Figure 8.2.41. Example of Chromatic Filtering

for one significant difference -- images are two-dimensional in space; time
functions are one-dimensional in time. For that reason, the implementation of
the spatial techniques is somewhat more complex than that for the temporal
techniques.

3.4.3 The Optical Transfer Function

A commonly applied technique for determining the response of a dynamic
system to a time function is the use of the transfer function, based upon
Fourier of Laplace transforms. The advantage of the transfer function
approach is that the transfer function of a complex system can be derived as
the product of the transfer functions of the system components. The spatial
equivalent of the time-domain transfer function is called an optical transfer
function (OTF). The optical transfer function incorporates information as to
the effect of the system on both the amplitude and the phase of the intensity
distribution of the optical image.

3.4.4 The Point Spread Function

Still another method of time-domain system analysis utilizes the response
of the system to an impulse (pulse of very short time duration). The response
of the system to any other input waveform then can be determined by breaking
the input into a series of very narrow pulses (impulses) and summing the
responses to the individual impulses. The spatial domain equivalent of the
time-domain impulse function is the point spread function (PSF).

3.4.5 The Modulation Transfer Function

In order to determine the time response of a dynamic system to a complex
time function, it is common practice to break the time function into its
frequency components (determine the equivalent Fourier series for the time
function). The response of the system is then determined from steady-state

frequency response data for the system, and the principle of linear super-
position is applied to determine the response of the system to the original
complex waveform (signal amplitude time distribution) by summing the system
responses to the individual frequency components. The spatial response
(imaging performance) of an optical system to a complex space function (object
radiation intensity distribution) can be determined by employing the spatial
equivalent of the above time-domain technique. The spatial-domain equivalent
of the time-domain amplitude (frequency) response is called a modulation
transfer function (MTF). As with its time-domain counterpart, the MFT of a
multi-element optical system is equal to the product of the MTFs of the
individual elements.

3.4.6 Spatial Filtering

As indicated earlier, optical components can be employed to modify the
imaging characteristics of an optical system in the space domain just as
electronic components can be used to modify the waveform shaping
characteristics of an electronic system in the time domain. The purpose of
such spatial filtering is to improve the signal-to-noise ratio of the optical
signal (target image). That is, spatial filtering is employed to discriminate
between target and clutter on the basis of size and shape.

In the time domain, it is impossible to separate the characteristics of a
signal as a function of time from its characteristics as a function of
frequency. That is, the time history of a signal and the spectrum of that
signal are equally valid descriptions of the same phenomenon. Similarly, the
spatial characteristics (size and shape) of an image are inseparable from the
spatial frequency characteristics of that image. Nevertheless, it is possible
to distinguish two methods of implementing spatial filtering: filtering in
the space (image) domain and filtering in the spatial frequency (spectrum)
domain.

3.4.7 Filtering in the Space Domain

Examples of filtering in the space domain are pattern recognition, map
matching, target profile recognition, and the use of field stops to limit the
field-of-view of an optical sensor. The filtering performed in these examples
is accomplished by masks or reticles in the image plane. An example of space
domain filter is the field stop employed in the folliwng example to
discriminate between background radiation and a target of known area. As
indicated in Figure 8.2.42, the sensor has two apertures. The area of the
field-of-view, A_A, of the large aperture is equal to four times the area of
the target, shown as A_T. The area of the field-of-view of the small aperture
is equal to that of the target. It is assumed that the radiance of the target
is twice that of the background. The (normalized) irradiance at the sensor
detector (and hence the sensor response) is shown as a function of scan
position for case (a) where $A_A = 4A_T$ and case (b) where $A_A = A_T$. As can be
seen in the figure, the percentage increase in sensor output as the sensor
scans the target is four times as large for $A_A = A_T$ than for $A_A = 4A_T$. Thus,
the signal-to-noise ratio is improved by a factor of four by limiting the
sensor field-of-view to the known area of the target.
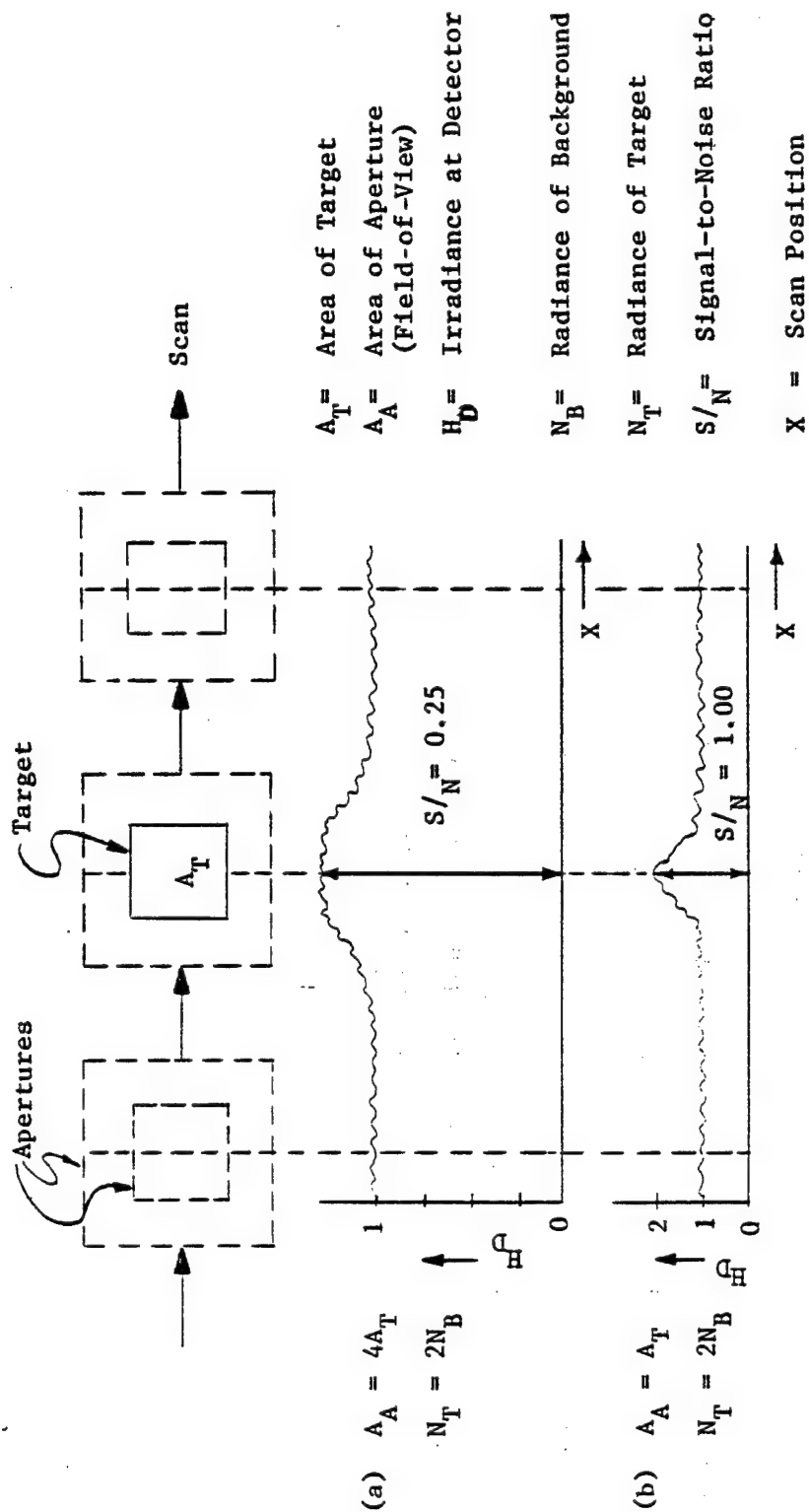
Figure 8.2.42 -- Filtering in the Space Domain

3.4.8 Filtering in the Spatial Frequency Domain

The optical Fourier transform of a (space domain) object represents the (spatial frequency domain) spectrum of that object. Filtering in the spatial frequency domain is accomplished by Fourier transforming the object in question into the spatial frequency domain, altering the resulting spectrum as desired, and transforming back into the space domain. The process of optical Fourier transformation can be implemented for an object delineated by coherent radiation by the apparatus depicted in Figure 8.2.43. The apparatus consists of a positive lens so positioned that the object, (a grid in the illustration), is imaged as shown. The distribution of the density of the radiant flux in the focal plane of the lens corresponds to the two-dimensional Fourier transform (spectrum) of the object with horizontal spatial frequency, k_x, in the horizontal direction and vertical spatial frequency, k_y, in the vertical direction. The irradiance in the focal plane is proportional to the spectral density at the frequencies represented by that point in the plane. The spectrum and corresponding image are shown in Figure 8.2.44. Spatial frequency filtering can be implemented simply by inserting a mask or reticle in the focal plane to block the radiation at those spatial frequencies to be attenuated or deleted in the desired image. Such as optical spectral filter can be fabricated by exposing a photographic negative to the focal plane (Fourier spectrum) image of the space domain pattern to be deleted. For example, the horizontal lines (which create spatial frequencies in the vertical direction) can be eliminated from the image by employing a mask which masks out all vertical frequencies except zero frequency. The resulting spectrum and image are shown in Figure 8.2.45.

3.4.9 Optical Time Modulation

Optical time modulation is time dependent amplitude modulation of the radiant flux in an optical system. The process is a time-domain technique (rather than a space-domain technique) and is intended to "time-color" the radiant "signal" in such a way as to distinguish it from other signals.

The radiant flux emitted by an active target sensor can be time modulated in order to distinguish the radiant flux emitted at one instant from the flux emitted at other instants of time, thereby providing an active ranging capability. Such time-coloring also allows the sensor to discriminate against noise from other emitters.

3.4.10 The Rotating Reticle

A commonly encountered electro-optical system component is the rotating, segmented reticle. As shown in Figure 8.2.46, the reticle is positioned in an image plane in the optical path of the system so that the image of the radiation distribution within the sensor field-of-view is scanned by the rotating reticle. The reticle performs one or more of the following functions: optical time modulation, image scanning, spatial filtering, and chromatic filtering. A rotating reticle application exemplifying all four functions is illustrated in Figure 8.2.47. The optical time modulation function is performed by the difference in transmissivity of the alternating segments of the reticle and serves to differentiate the signal due to incoming radiation from that due to internal noise sources. The image scanning function is performed by the movement of the leading edge of the opaque

portion of the reticle across the field-of-view and provides the scan phase information required to determine the angular position of the target about the reticle spin axis. The spatial filtering action is a result of the relative aperture size of a reticle segment in comparison with the image size of the target (essentially a point source) and the background clutter (the cloud). The detector output signal (after space-to-time and radiation-to-electrical voltage conversion), is shown in the figure, as the reticle is scanned from left to right. The relatively high temporal frequency content of the signal due to the (small) target, compared to that due to the (large) cloud, is a direct consequence of the relatively high (spatial) frequency content of the target image compared with that of the cloud. A high pass filter following the detector would then distinguish the target signal from that of the background clutter (cloud). The chromatic filtering function of the reticle is affected by the frequency (color) - selective transmissivity characteristics of the transmitting segments of the reticle, which discriminate between target and background on the basis of spectral differences.

Object

y_0

x_0

Lens

Spatial Spectrum

k_y

k_x

Focal Plane of Lens

Image

y_1

x_1

x_o, y_o = Object Spatial Distribution

x_i, y_i = Image Spatial Distribution

k_x = Spatial Frequency in x Direction

k_y = Spatial Frequency in y Direction
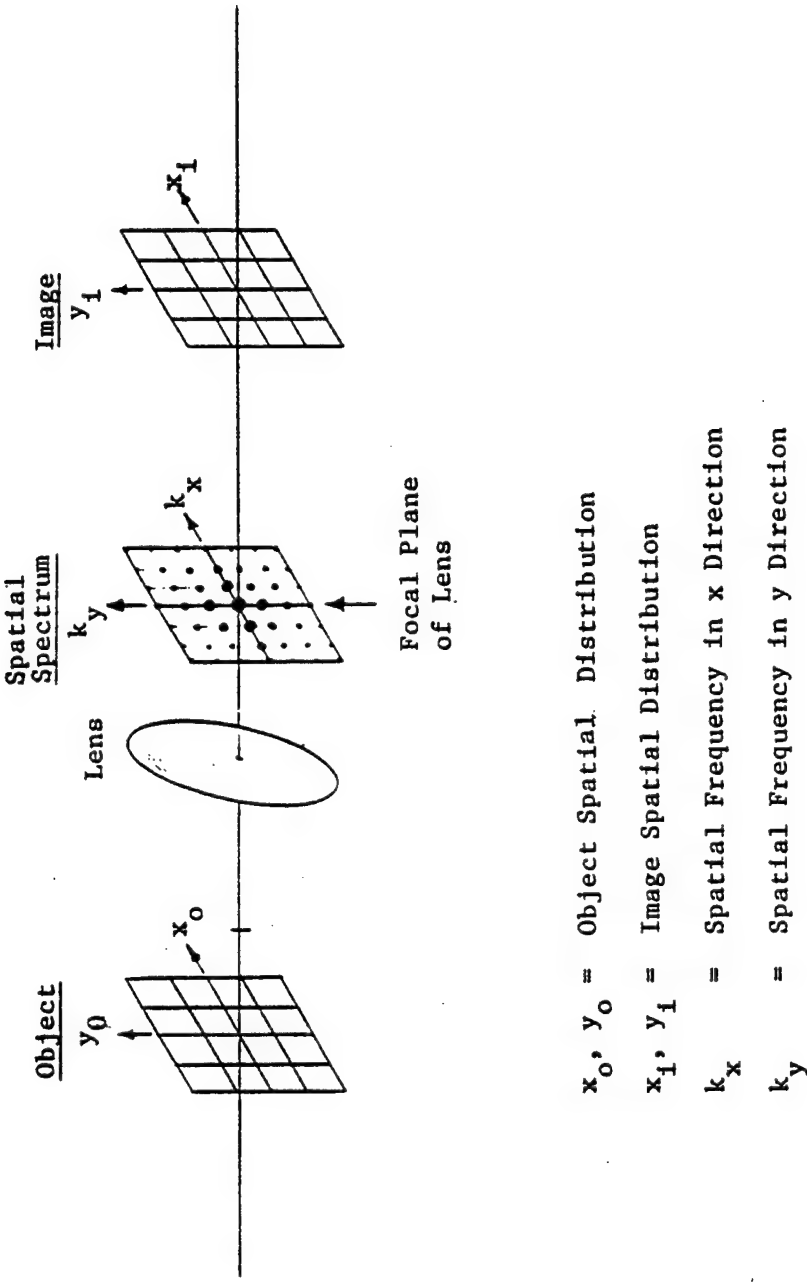
Figure 8.2.43 -- Optical Fourier Transformation
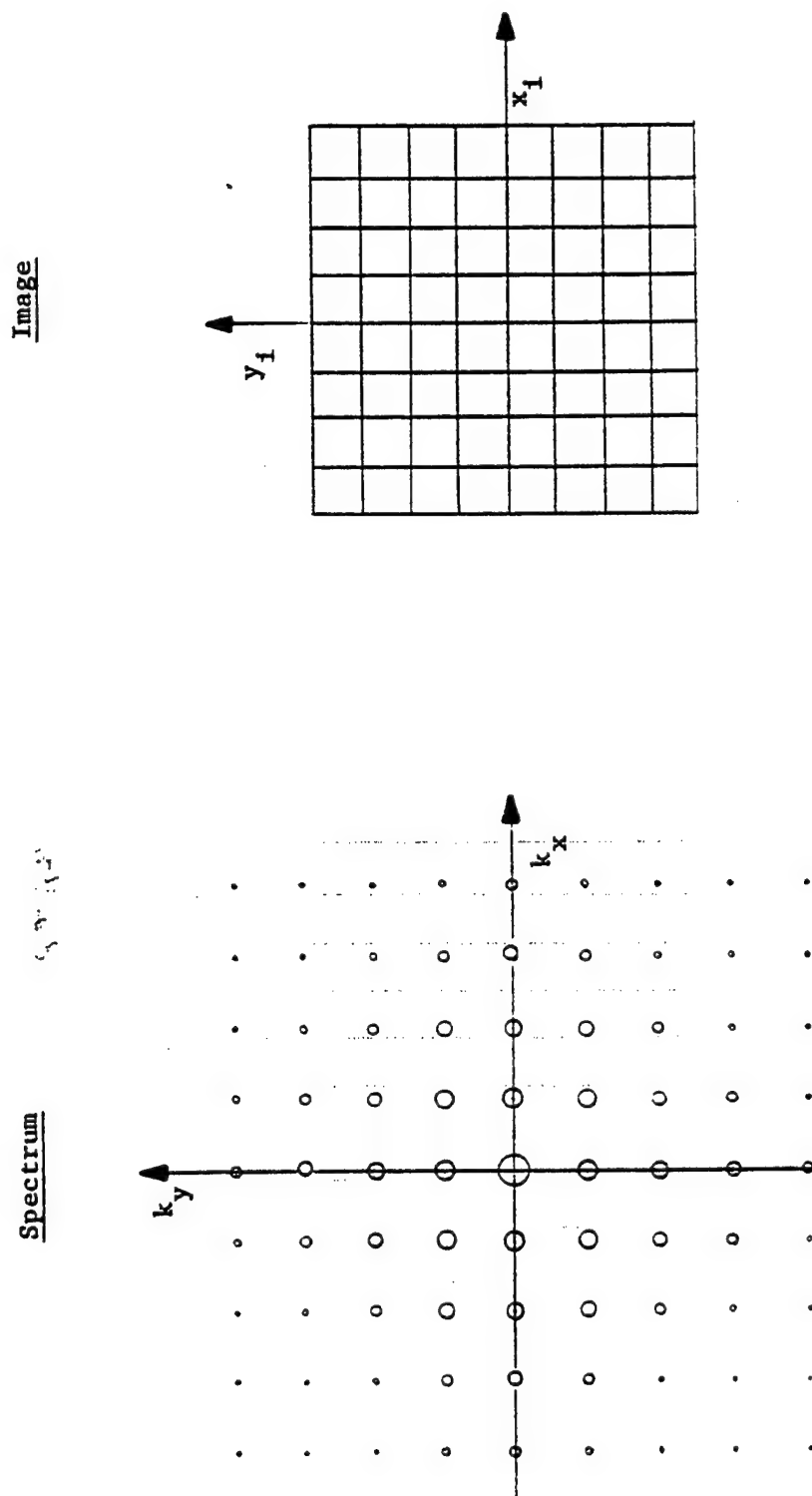
Image

Spectrum

Figure 8.2.44   -- Fourier Transform (Spectrum) and Corresponding Image of Grid

Image

x_1

y_1

Spectrum

k_x

k_y
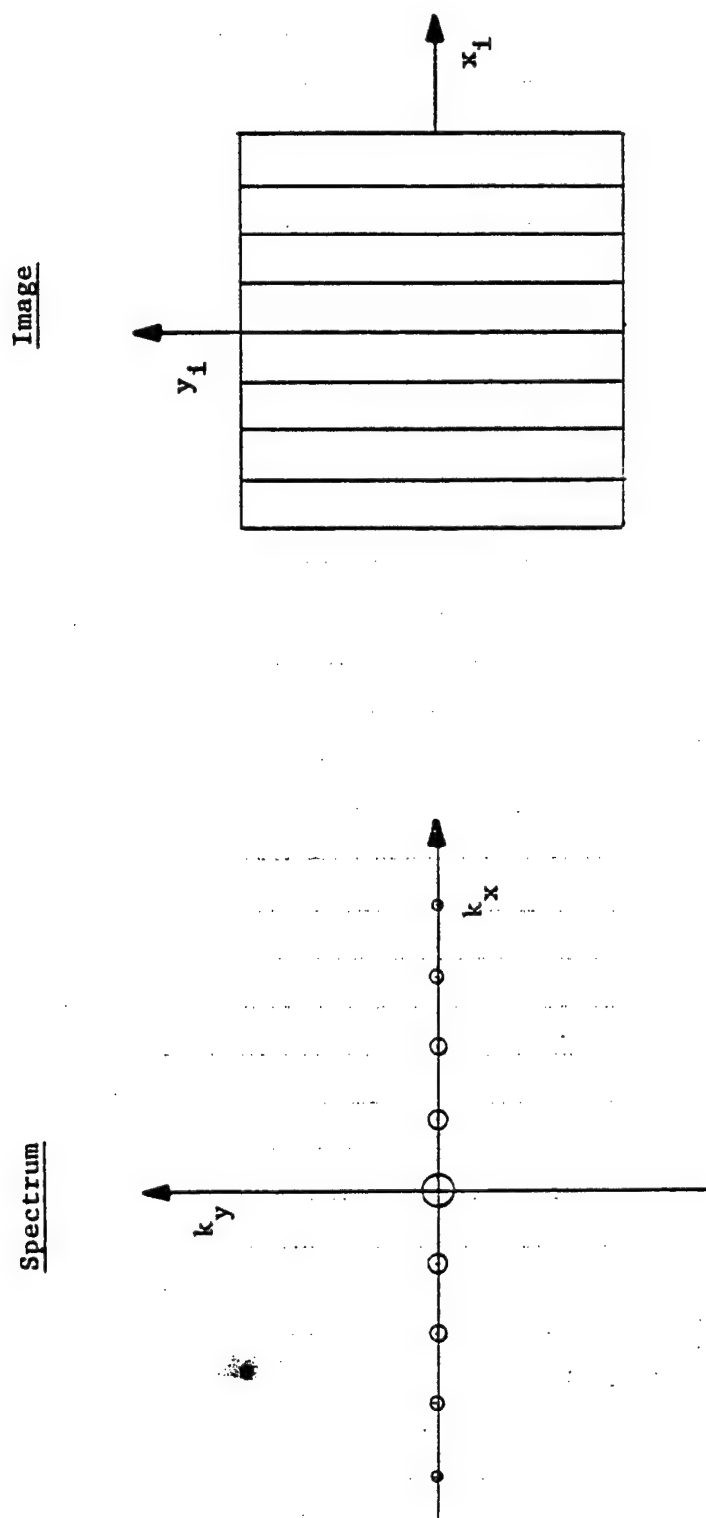
Figure 8.2.45 -- Fourier Transform (Spectrum) and Corresponding Image of Grid with Vertical Frequencies (Horizontal Lines) Deleted
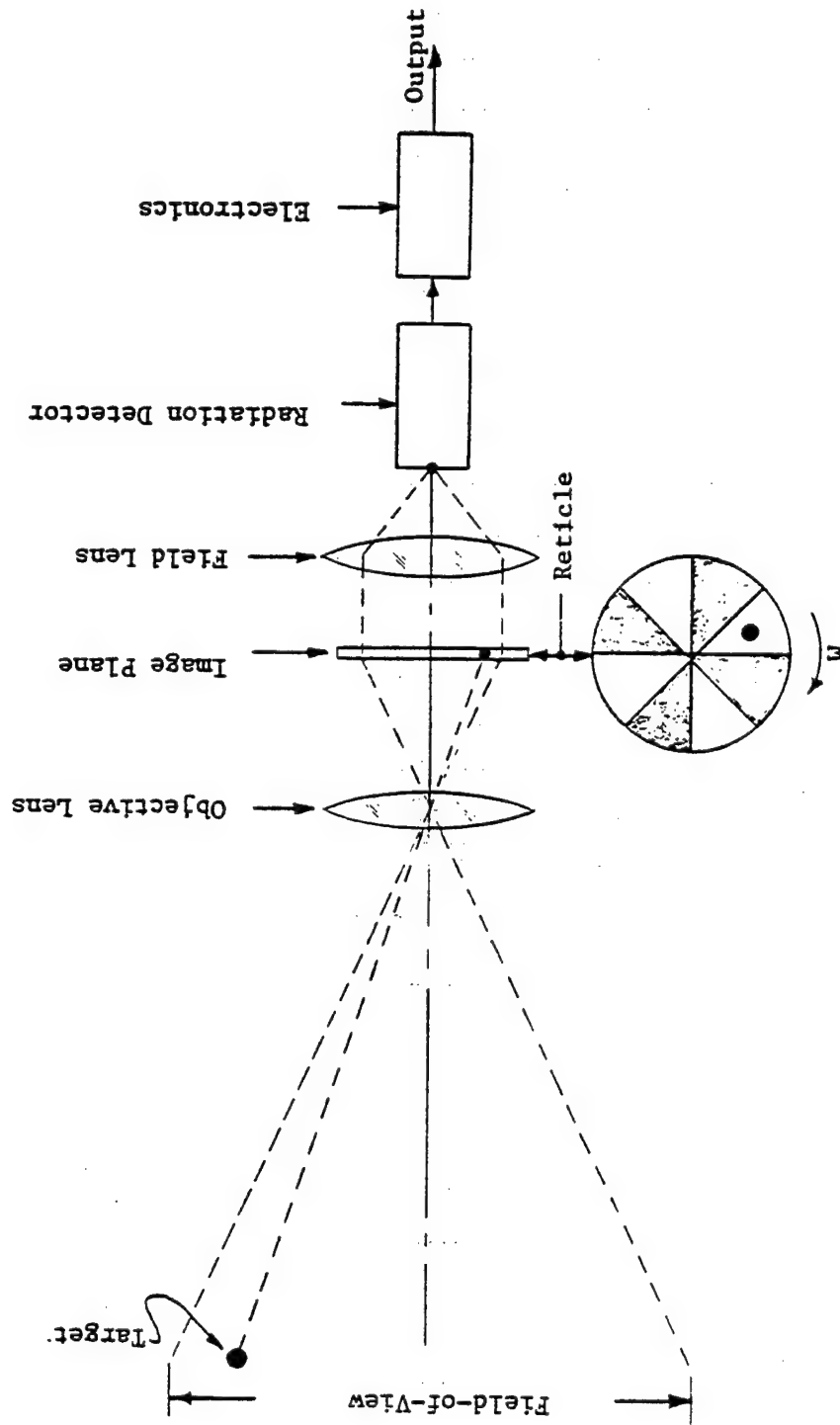
Figure 8.2.46 .- The Rotating Reticle

Cloud Image

Target Image

Rotating Reticle

Scan Direction

Amplitude

From Target

Output Of Detector

From Cloud

Time
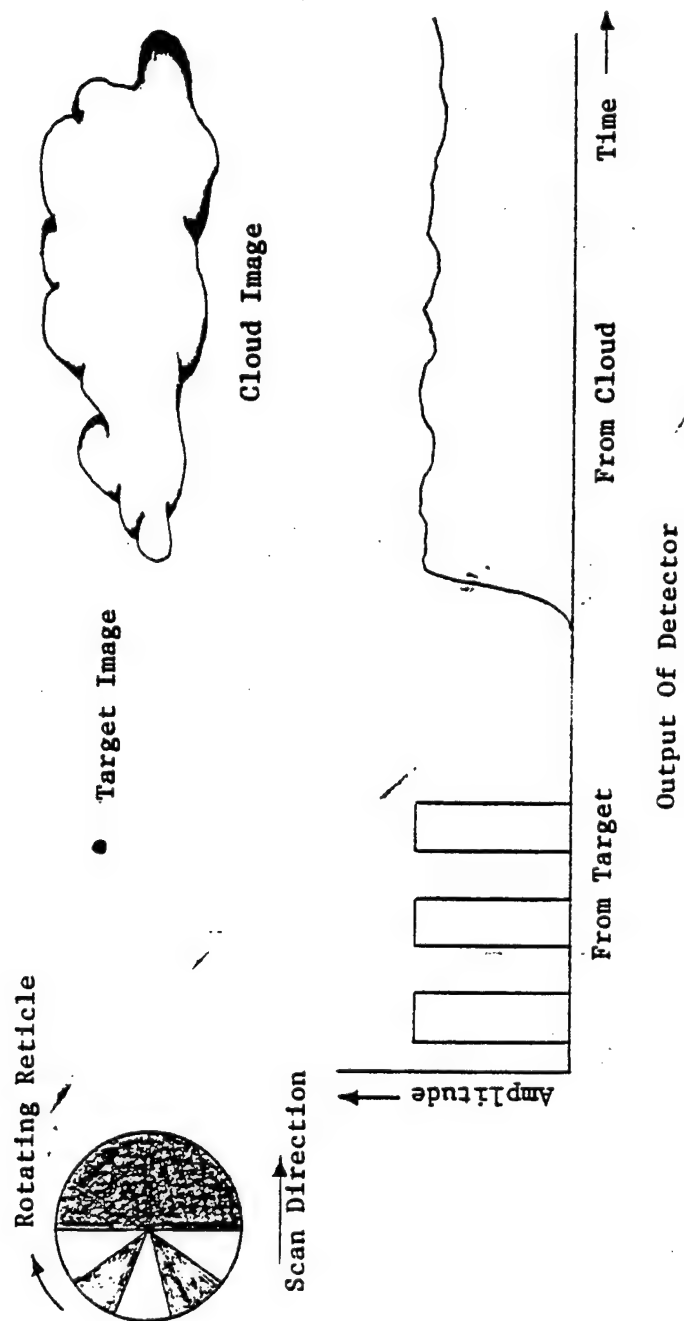
Figure 8.2.47 -- Rotating Reticle Application

(THIS PAGE INTENTIONALLY LEFT BLANK)

SECTION IV

LASER FUNDAMENTALS AND SYSTEMS

4.1 INTRODUCTION. LASER is an acronym for Light Amplification through Stimulated Emission of Radiation. The word stimulated is the key to the principle of the lasers operation and is the basis for the unique characteristics that distinguish the laser from other sources of radiation.

The process of stimulated emission of laser radiation was first described, theoretically, be Albert Einstein in 1917. It is a process whereby a light beam of a specific color or wavelength can interact with an atom in such a way that the atom will emit additional light that moves in the same direction and has the same wavelength as the original beam. If a beam were fed into a suitable laser amplifier, the amplifier would preserve the original direction and wave length of the input beam and the intensity of the light would increase.   An oscillator can be produced by placing mirrors at the ends of the amplifier forcing the light to bounce back and forth between the mirrors. The intensity of the light in such an oscillator can build up to many orders of magnitude greater than the intensity of the original light signal, producing a highly directional laser beam of an extremely pure color. The light is extracted from the laser through one of the mirrors, which is designed to transmit a small percentage of the light.

Common requirements of all lasers are a power source, an optical cavity resonator, a population inversion of the active medium, a pumping technique, and an output coupling technique. Lasers can be designed to operate with a continuous output (CW) or a series of high energy pulses. The average output power can vary from a few milliwatts to over 50 kilowatts. Pulsed outputs in the megawatt range are obtainable with Q - switching techniques.

4.2 THEORY OF OPERATION. All lasers operate in the same basic manner. Laser photon energy is furnished by an active medium with a population inversion. Population inversion means that more atoms are in a state of higher energy (upper lasing level) than in the lower energy state (lower lasing level).

All lasers also contain an optical cavity resonator which provides a low impedance path for the stimulated photon beam to travel within the active medium. The cavity reflects the photon beam back through the active medium several times in order to increase the intensity of the beam. The beam is normally coupled outside the cavity (output coupling) through a partially reflecting mirror, a beam splitter, or fringe coupling.

The details of operation are shown in Figures 4.1 thru 4.3. Figure 4.1 shows an atom with two different energy levels. The electron is excited to the upper lasing level through a process called pumping. Once the atom is in an excited state it can return to the lower energy state through either spontaneous or stimulated emission. Non-radiative process such as collisions with other atoms are possible but the specific material is picked such that the transition to the lower level is always a radiative process. The material is also picked such that the upper lasing level is characterized by a relatively long life time. This means the probability of a spontaneous transition is low and stimulated emission is most probable.

PHOTON

ELECTRON

UPPER LASING LEVEL

LOWER LASING LEVEL

ATOMIC NUCLEI

INNER ELECTRON CLOUD
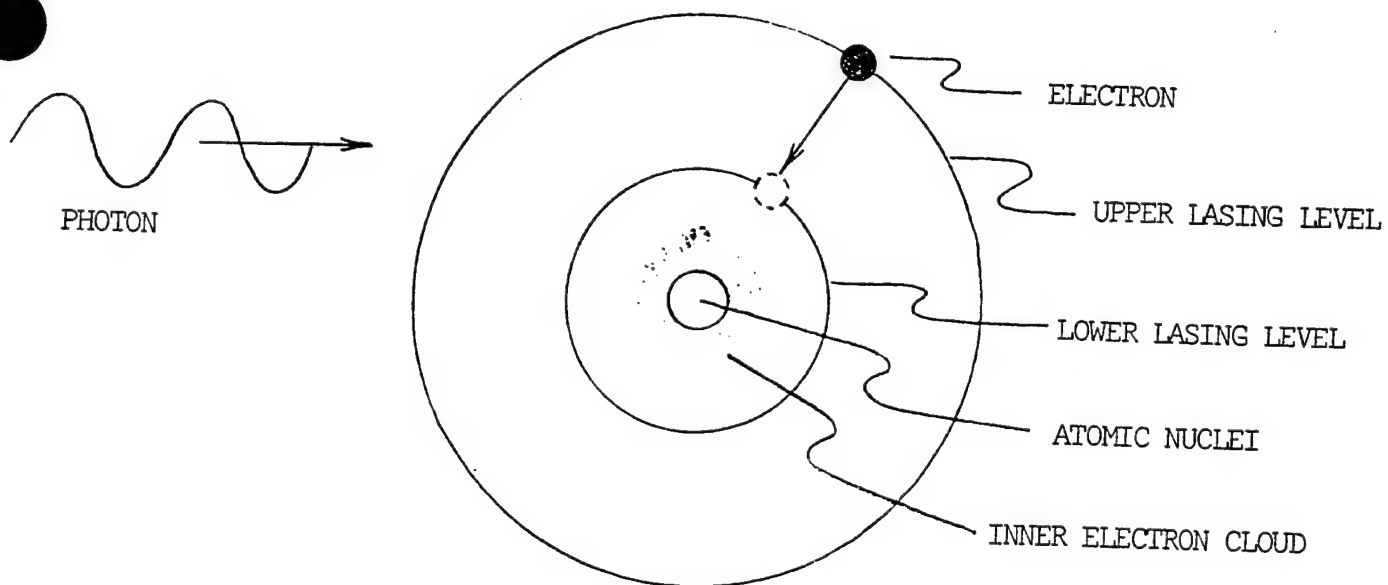
FIG 4.1 DETAILS OF THE LASING PRINCIPLE (The photon induces the excited atom to emit a second photon exactly identical to the original photon. The atom then returns to the lower energy level. The two photons are identical in energy, frequency, phase, and direction.)

In spontaneous emission, the transition the electron makes is from a higher energy level to a lower on, and the difference in energy between the initial and final states of the particle is converted into electromagnetic energy in the form of a single photon. This process forms the basis of operation of the ordinary fluorescent light bulb. Since there is no constraint on the phase or direction of the photons resulting from spontaneous emission, the radiation is non-coherent and isotropic. The spectral output is narrow compared to the thermal radiation sources since the process involves transitions between discreet energy levels; however, it is, in general, not as monochromatic as laser radiation, in which only a very small number of levels is involved.

Stimulated emission results from an important property of virtually all known physical laws: invariance under time reversal. If a microscopic process, such as the collision of two molecules, is recorded by a video camera, it is impossible to tell whether a playback is being run in the forward or the reverse direction. (Macroscopic events do not display this invariance because of the statistical behavior of systems containing many particles.)

In particular, consider an atom that can inhabit one of two distinct energy states (see Fig 4.2). There is no way to distinguish between a sequence of events in which the atom absorbs a photon from the surrounding radiation field and jumps into its excited state and the time-reversed interaction in which it adds a photon to the field and jumps to the lower state. Both events obey conservation of energy; both are in principle equally likely.

Both absorption and stimulated emission require an almost perfect match between the photon frequency and the velocity and energy levels of the interacting atom. As a result, the photon that a stimulated atom gives off is a twin of the one that caused the emission. Within a gas cloud whose particles are moving at nearly the same velocity, one photon with a particular frequency and direction can thus become two, two can become four and so on. The shower of photons therefore maintains close coherence of frequency and direction.

ABSORPTION →

ATOM IN LOWER-ENERGY STATE	ATOM IN HIGHER-ENERGY STATE

← **STIMULATED EMISSION**
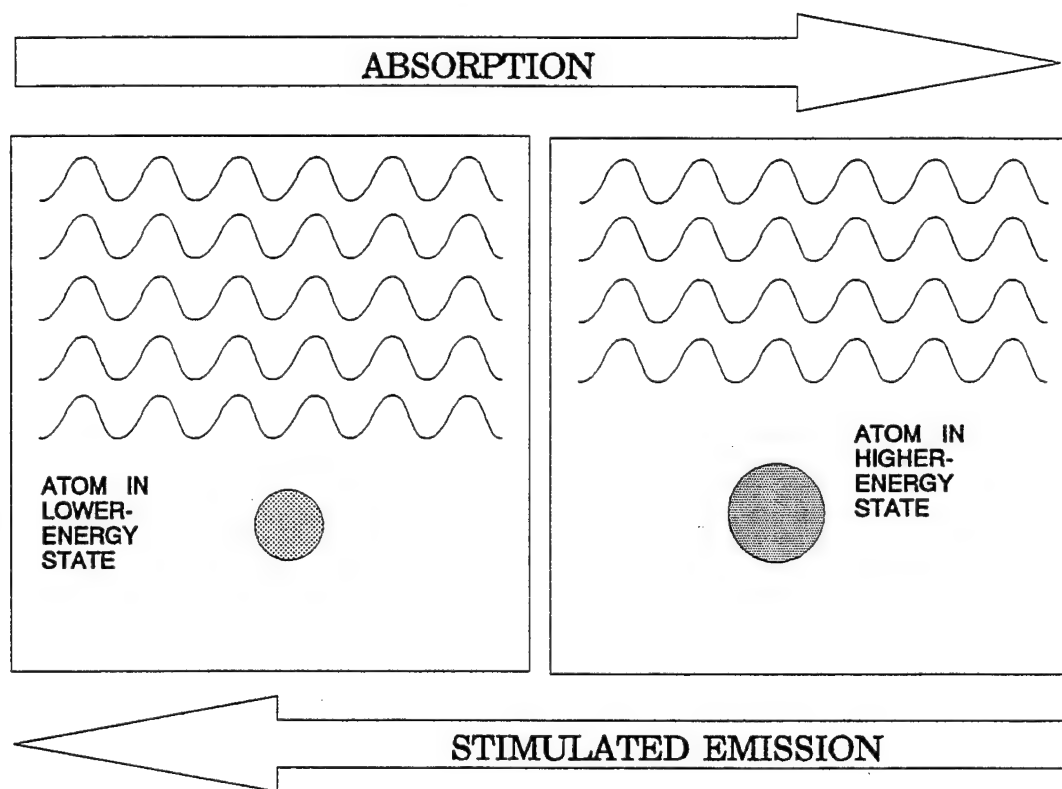
FIG 4.2 Physics of Stimulated Emission

Since the active medium contains billions of excited atoms, once the stimulate process begins a chain reaction quickly follows. Figure 4.3 shows the process in which the lasing action begins and how it is sustained. The optical cavity consists of two circular mirrors placed at the ends of the lasing material. Once the population inversion has been obtained, a spontaneous emission along the axis of the cavity will eventually occur. This emission will be reflected by one of the mirrors back through the active medium stimulating other emissions. These photons induce other emissions until a state of equilibrium is reached.
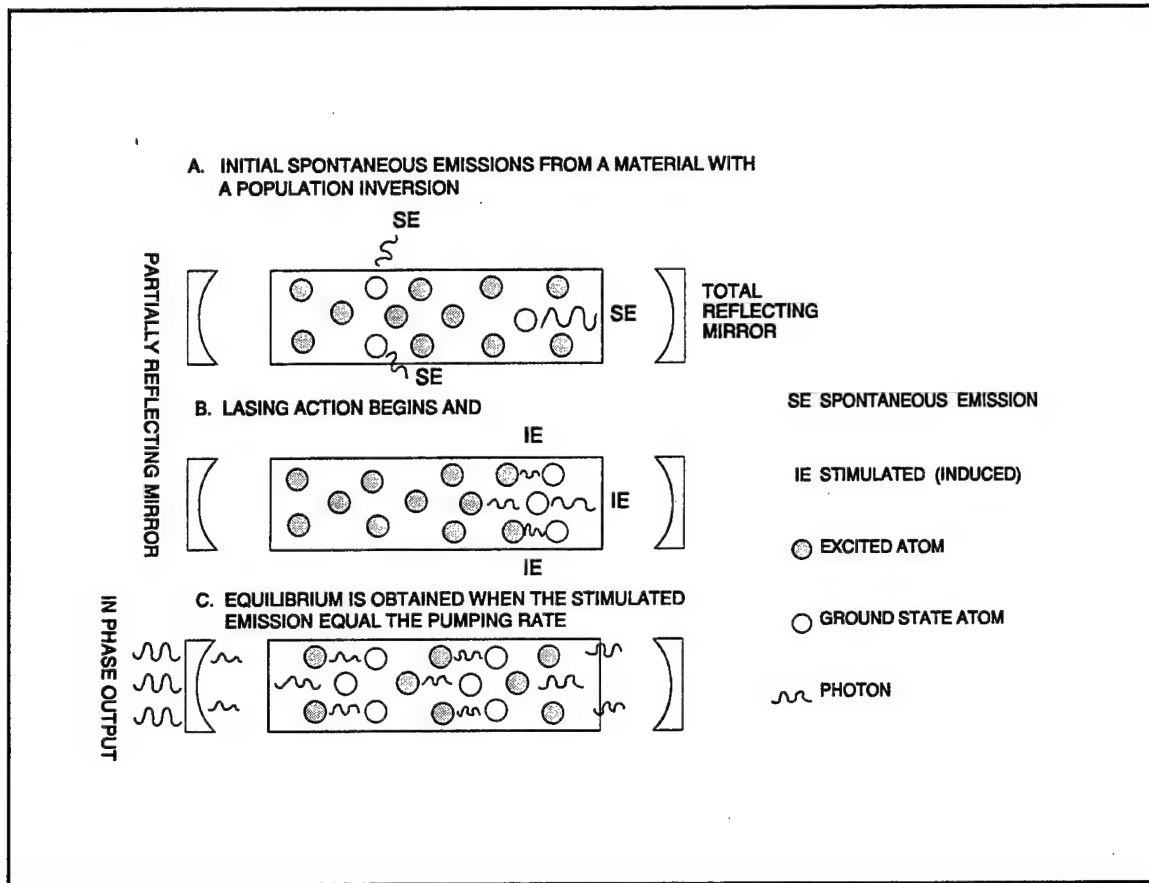
FIG 4.3 OPERATION OF A CONTINUOUS WAVE LASER

A spontaneous emission off the resonator axis is not reflected back into the medium. Consequently there will be very little amplification of this beam and for all practical purpose the effect can be neglected. A stray spontaneous emissions manifest itself as noise in the output beam. However, the number of such emissions sufficiently close to the resonator axis is so small that the overall output is essentially coherent.

The intensity of the output beam is a function of the number of excited atoms which are continually re-excited through pumping. In the equilibrium condition the number of stimulated emissions are equal to the rate at which the atoms are returned to the upper lasing level.

The operation of a specific laser is generally shown on an energy level diagram. The partial energy level diagram of Ruby is shown in Figure 4.4. Ruby is a crystalline material (Al_2O_3) with chromium impurities which give rise to the red color. The population inversion is obtained by a flash lamp which excites the atoms to the 4_{F1} and 4_{F2} levels. The atoms then decay via non radiative processes to the R_1 and R_2 levels which have long lifetimes. Laser action occurs between the two R levels to the 4_{A2} ground state level. The output is characterized by two co-axial beams of slightly different frequency. The R_1 transition yields a wavelength of .6943 microns and the R_2, .6930 microns.
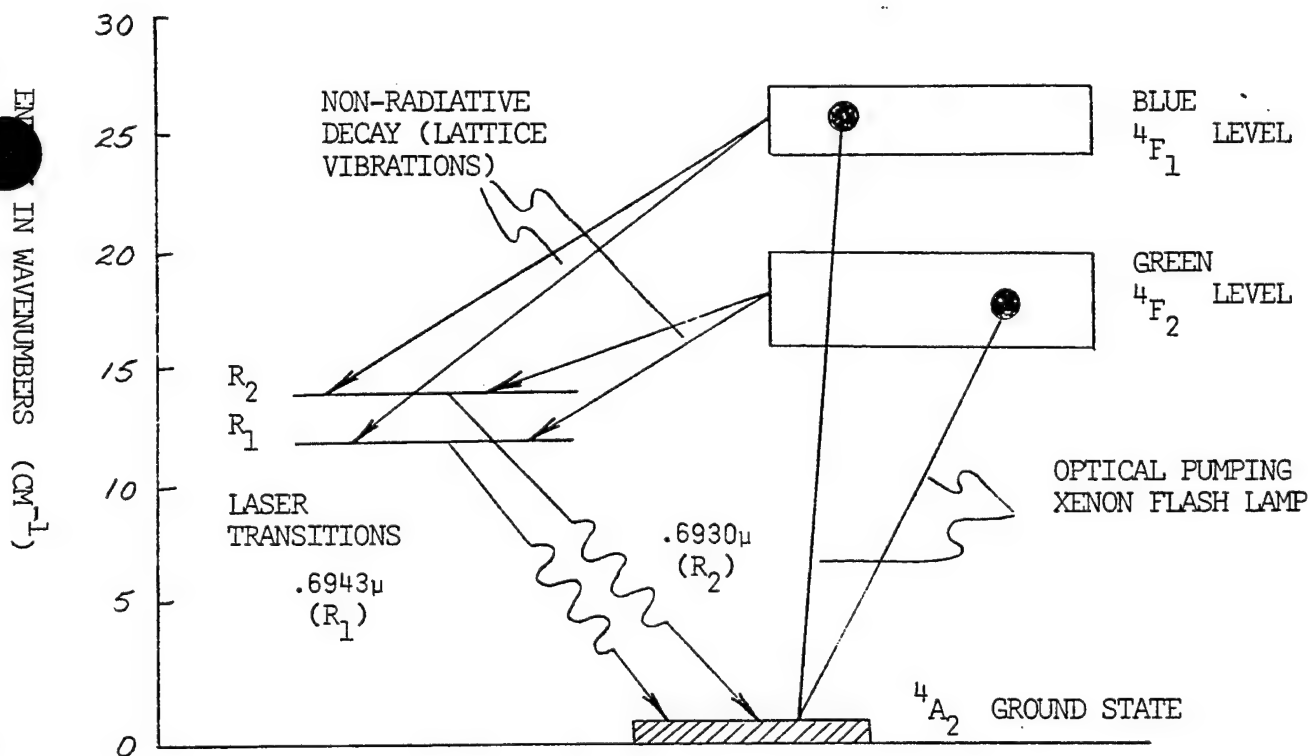
FIGURE 4.4 SIGNIFICANT ENERGY LEVELS FOR RUBY

4.2.1 OPTICAL CAVITY RESONATORS. The divergence characteristics of the beam and the mode structure are determined primarily by the optical cavity. The most commonly used cavity consists of two circular mirrors with radius of curvature R, separated by a distance L. All combinations of R's and L do not yield stable cavity configurations. In an unstable cavity a beam reflected at one mirror will not be reflected along the axis of the cavity. Consequently, the beam cannot be maintained within the cavity, i.e., non-resonant. An optical cavity stability diagram is shown in Figure 4.5 for a resonator with circular mirrors. The characteristics for several of the more important resonator types is shown in Figure 4.6.
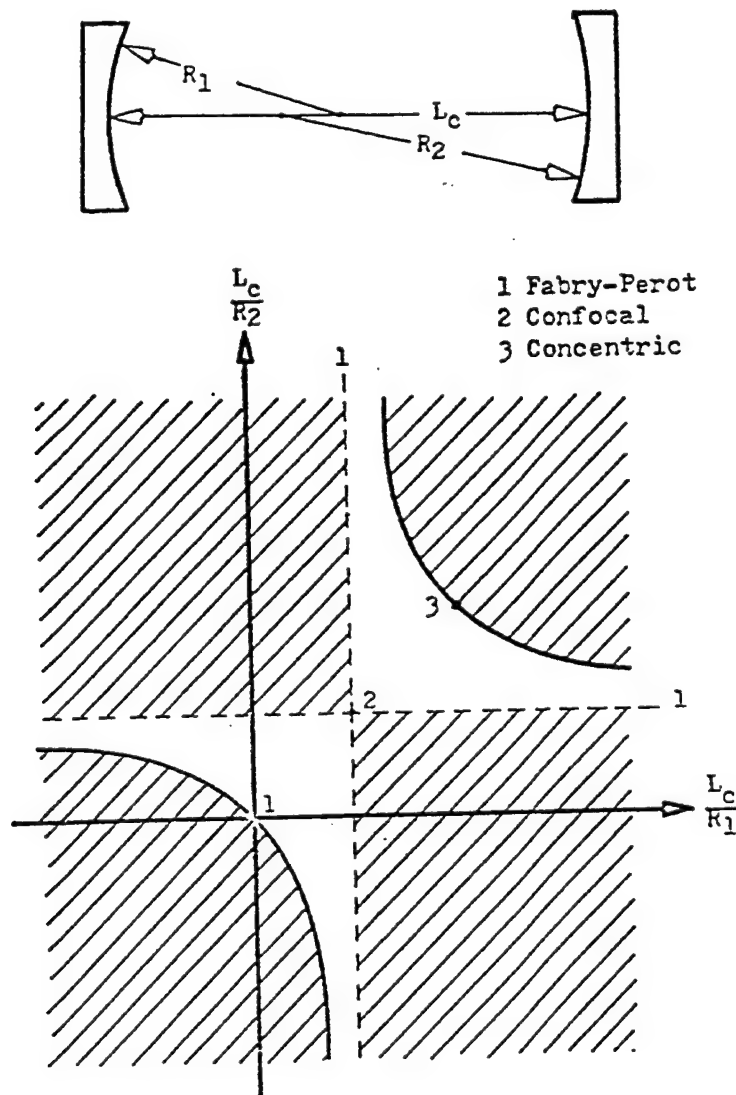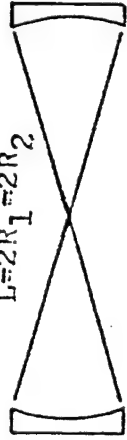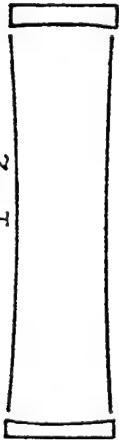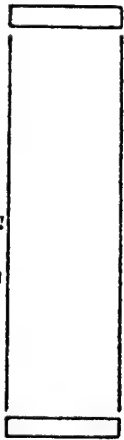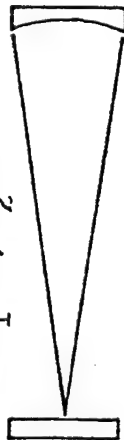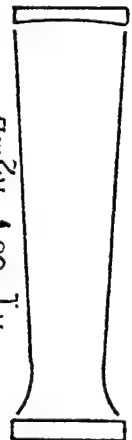
FIGURE 4.5   STABILITY DIAGRAM FOR OPTICAL CAVITY RESONATORS WITH CIRCULAR MIRRORS. SHADED REGION REPRESENTS UNSTABLE CONFIGURATIONS.

FIGURE 4.6　Comparison of several resonator cavity configurations

NOMENCLATURE	MIRROR CONFIGURATION AND RELATIVE MODE VOLUME	MODE VOLUME	DIFFRACTION LOSSES	EASE OF ALIGNMENT	STABILITY
CONCENTRIC (SPHERICAL)	$L=2R_1=2R_2$	Pinched in middle	High	Easy	Marginal
SYMMETRIC CONFOCAL	$L=R_1=R_2$	Down by $1/\sqrt{2}$ in middle	Lowest	Easiest	Marginal
FABRY-PEROT	$R_1=R_2=\infty$	Uniform and maximum	Highest	Very difficult	Marginal
HEMI-CONCENTRIC	$R_1=\infty$, $R_2=L$	Pinched at flat mirror	Moderately high	Not difficult	Stable
HEMI-CONFOCAL	$R_1=\infty$, $R_2=L$	Moderately full	Moderately low	Not difficult	Stable

The mode volume is an important consideration in cavity selection as it determines the percent of the active medium which is actually involved in the lasing process. The dispersion of the beam (increase in beam cross section with distance) increases as the radius of curvature of the mirrors are decreased. If transmission over a long distance is required then a cavity approaching a Fabry-Perot would be employed. In many applications a hemi-confocal cavity is used as a good compromise of the various characteristics.

4.2.1.1   Q - Switching.   The peak output power of most lasers can be increased by allowing the inverted population to build to a maximum number before the system is allowed to lase. This is achieved by the technique termed Q - switching, where Q refers to the quality of the optical resonator. A low Q (poor optical resonator) allows the population inversion to build up, then when a high Q optical cavity is restored, the stored energy is dumped extremely rapidly as a high energy laser pulse. This technique produces output pulse widths on the order of nanoseconds as opposed to hundreds of microseconds or milliseconds for non Q-switched operations.

The first Q-switches used rotating mirrors or prisms in place of one of the resonator mirrors to achieve the variable Q effect. More recently, practically all optically pumped Q-switched lasers use some form of Pockels cell device. The Pockels cell works on the principle that certain crystals exhibit bifringence when placed in an electric field. This effect can be used to cause an electronically controlled change in the polarization state of a light ray passing through the cell. When used in combination with a polarizing element in the resonator, the Pockels cell Q-switch can produce extremely fast Q transition times. When properly designed, this type of Q-switch can provide very high peak power laser operation at the same efficiency of an equivalent long pulse laser.

The Q-switched output is shown in Figure 4.7 compared to a conventional pulsed output.

A) TYPICAL PULSED OUTPUT

0.1 JOULE INPUT YIELDS
100 KILOWATT OUTPUT

ENERGY

1 MICROSECOND   TIME

B) Q-SWITCHED OPERATION

0.1 JOULE INPUT YIELDS
2 MEGAWATT OUTPUT

ENERGY

50 NANOSECONDS   TIME
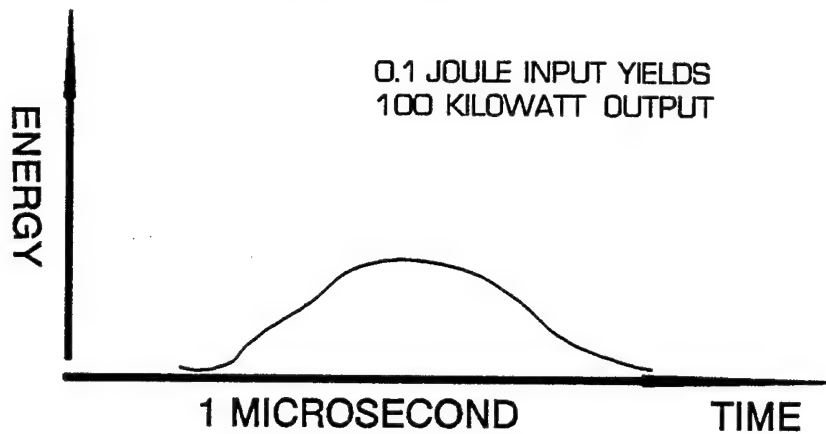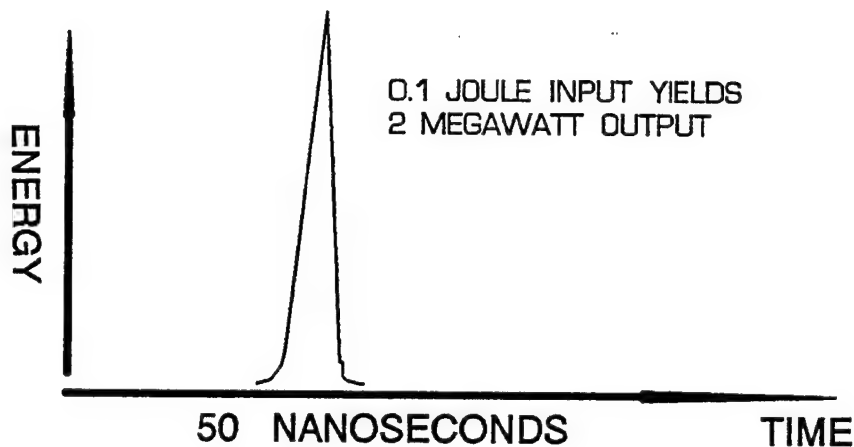
FIGURE 4.7 COMPARISON OF THE CONVENTIONAL PULSED LASER OUTPUT
            WITH THE Q-SWITCHED LASER.

4.2.2 PUMPING TECHNIQUES.   The most common technique for obtaining a
population inversion is an optical flash lamp or an electric discharge (both DC and
RF). Population inversion can also be obtained by direct electron injection as in a
semiconductor laser or a chemical reaction.   Figure 4.8 shows two common
mechanizations for optical and electrical pumping.   Optical pumping is more
commonly employed in crystalline laser in which efficiencies less than one percent are
typical. Efficiencies over 25 percent are possible with electrical pumping but the
technique is in general applicable to only gas lasers.

A) OPTICAL

ELLIPTICAL CYLINDER
WITH POLISHED
INNER SURFACE

XENON
FLASHLAMP

LASING ROD

FLASH RAY

B) ELECTRICAL

GLASS TUBE

IONIZED GAS

GAS IN (+)   GAS OUT (-)

MIRROR   MIRROR

DC OR RF POWER
SUPPLY
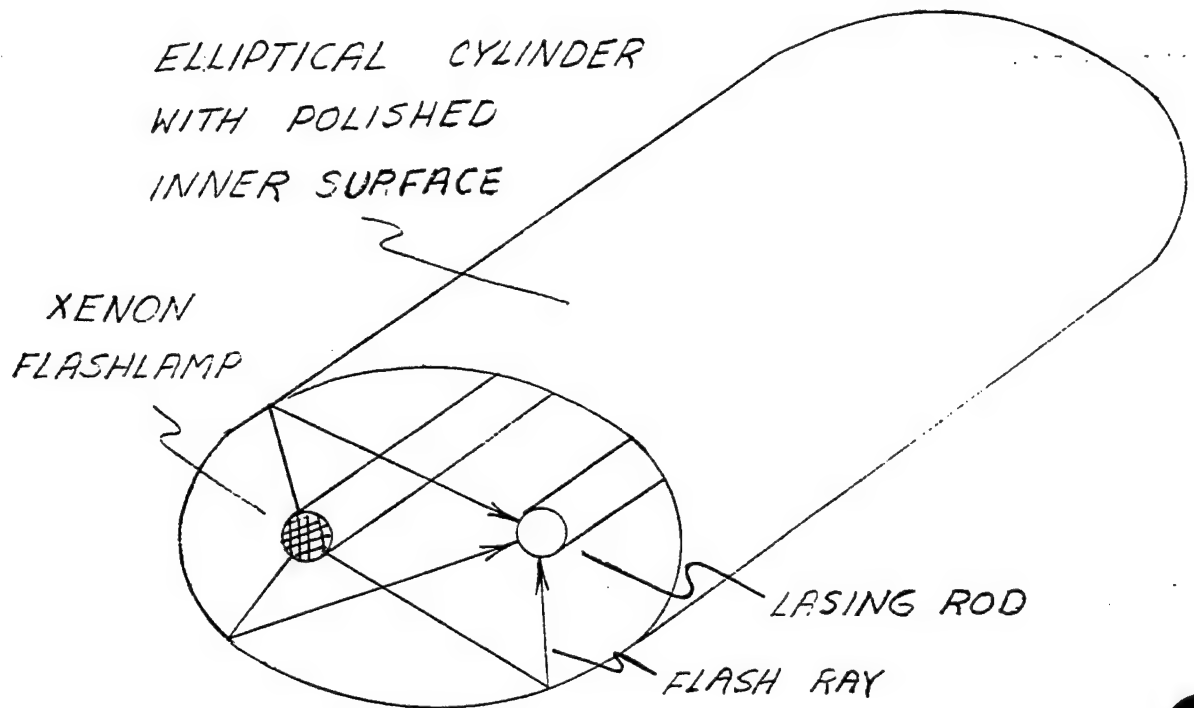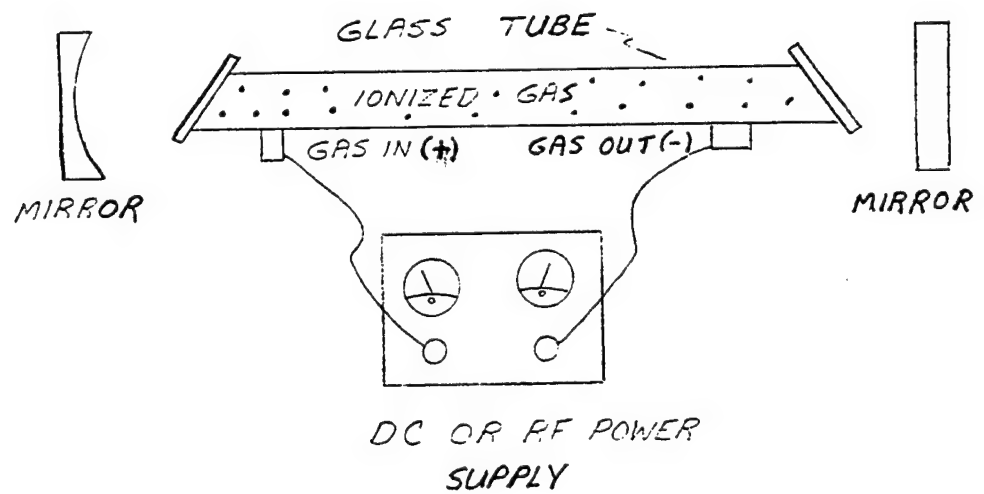
FIGURE 4.8 PUMPING TECHNIQUES FOR OBTAINING A POPULATION
INVERSION.

4.3   CHARACTERISTICS OF LASER RADIATION. The characteristics which differentiates the laser from other sources of radiation are collimatability, monochromaticity, high spectral radiance, and short-pulse capability. Not all of these characteristics are exploited in any particular application but in many cases the system would not be feasible if it were not for one of the special attributes. Now, let's look at each of these characteristics.

4.3.1   COLLIMATABILITY. Laser beams can be collimated to approximately the diffraction limit. That is, the rays are nearly parallel to one another and diverge only slightly as they travel. In fact, a plane-wave laser source radiates a beam which is almost constant in width for a distance (D) given by the following relationship:

$$D = \frac{d^2}{4\lambda}$$

where d = diameter of the source

λ = wavelength of the radiation

The first laser used a ruby crystal which was 4 cm long and 0.5 cm in diameter. The radiated wavelength was 6943 angstroms (Å). Thus no appreciable spreading would occur until the beam had traveled 9 meters. If a ruby crystal 5 centimeters in diameter were used, D would be 900 meters. A laser beam one foot in diameter that was directed at the moon in 1962 illuminated an area two miles in diameter on the moon's surface. In contrast, a beam of ordinary light traveling the same 240,000 mile path would illuminate an area 25,000 miles in diameter. The laser collimation is one half to one order of magnitude better than other optical or infrared devices and equivalent to radars. However compared to radar, the aperture required to produce a specified beam divergence is decreased by a factor of 10^{-6} for laser systems due to the shorter wavelength.

4.3.2 MONOCHROMATICITY. Laser radiation exhibits both temporal and spatial coherence. This relates to the degree in which the radiation can be written as a pure sinusoid in terms of the frequency, v (temporal), and wave number k (spatial). Temporal coherence implies monochromaticity or in simple terms, a single color or wavelength. The characteristic of monochromaticity is also referred to as spectral coherence.

Almost all conventional light sources emit light that is a mixture of wavelengths, or colors, and as a result the light appears white. A few conventional light sources, such as mercury-vapor lamps and neon lights, emit nearly monochromatic light, but their

light is neither coherent no inherently collimated. A laser assembled with sufficient care to operate at all, operates at Q's in excess of 10^4, where Q is a measure of the power distribution or efficiency and is calculated from the following:

$$Q = \frac{f}{BW}$$

Where

> f = central radiation frequency (hertz)
>
> BW = Bandwidth of radiation (hertz)

With careful design and assembly, to minimize the number of modes to the so-called "single mode" of operation, Q's of the order of 10^8 are achieved. Thus, although usual bandwidths are great compared to radars, the fractional or normalized bandwidths can be extremely small.

Spatial coherence relates to the direction of propagation. All photons in the beam have the same direction or same wave vector and are all in phase directionally. The high degree of spatial coherence results in the excellent collimatability characteristics.

4.3.3 HIGH SPECTRAL RADIANCE.   Perhaps the most important limitation of ordinary light sources is their inherent low brightness. No matter how high their temperature, they cannot emit more energy than a perfect radiator. The theoretical output of a perfect radiator, a black body, is given by the black-body radiation curve first derived by Planck. The visible surface of the sun, for example, behaves much like a black body with a temperature of about 6,000 degrees C. The sun's total radiation, at all wavelengths, is 7 Kw per square centimeter of its surface, and no matter how we collect and concentrate sunlight it is impossible to achieve any greater radiation density. Although 7 Kw may seem a substantial amount of energy, it is really not very much considering the tremendous bandwidth of the solar spectrum. In short bursts the ruby laser's power output reaches 10,000 watts for a beam measuring less than a square centimeter in cross section. If desired, the laser's power can be focused to produce intense heating. For instance, a lens with a focal length of one centimeter will focus the beam to a spot only a hundredth of a centimeter in diameter, corresponding to an area of one ten-thousandth of a square centimeter. In this spot the laser beam will deliver power at a density of 100 million watts per square centimeter. Brief though the flash is, its power is thousands of times greater than could be obtained by focusing sun light and is enough to melt or vaporize a spot on the surface of even the most refractory material.

4.3.4 SHORT PULSE CAPABILITY. The energy within the lasing medium can be stored by destroying the Q of the optical cavity. The energy can then be released in one short pulse by restoring the cavity Q. Because the triggering mechanism for energy release in a laser is the passage of photons rather than transport of mass particles, stored energy can be released rapidly to provide short-duration, high-energy pulses as compared to microwave or other visible or infrared pulsed power sources.

4.4 LASER TYPES. Laser action has been achieved in gasses, liquids, crystallin solids, glasses, and semiconductors. Each has its own special excitation process but the basic principles are as previously described. Several representative type lasers are shown in Table 4.1.

TABLE 4.1
REPRESENTATIVE LASER TYPES

TYPE	WAVELENGTH	POWER	APPLICATION

GAS
  CO_2
  ARGON
  H_e - N_e
	10.6 MICRONS
	0.500
	0.6328
		50 KW CW
		5 W CW
		0.1 W CW
			RADAR
			CAMERA
			ALIGNMENT

CRYSTAL
  RUBY
  NEODYMIUM
	0.6943
	1.06
		10 W P
		10 W P
			RANGING
			ILLUMINATING

SOLID STATE Ga As	0.8400	1 W P	ILLUMINATING

CHEMICAL
  DF
  HF
	3.8
	2.7
		20 KW CW	RADAR

4.4.1   GAS LASERS.   Gas lasers fall into three general categories: neutral gas, ionized gas, and molecular gas. Some examples of these types are listed in Table 4.2. Gas lasers are the most powerful type developed thus far.

The major drawback in gas lasers is the low photon energy (IR wavelengths) which tends to decrease the destructive value of the system. Remember the photon energy $E = h\nu$; since the frequency ν is much lower in the infrared than visible regions of the spectrum, the photon energy is also lower.

TABLE 4.2

GAS LASER SYSTEMS

LASER	TYPE	WAVELENGTH (Microns)	AVE POWER (W)
Helium-Neon	Neutral	0.6328	10^{-3}
Xenon	Neutral	2.02	10^{-3}
Argon 11	Ionized	0.4880	5
Krypton 11	Ionized	0.6471	1
CO_2	Molecular	10.6	10^4
DF	Molecular	3.8	10^3

4.4.1.1 CO_2 Laser.   The CO_2 laser is the most important gas laser today and probably will be for some time to come. It is characterized by a very high energy continuous output approaching 100,000 Watts with an efficiency over 25%. (Typical solid state laser exhibit efficiency around 1%). The CO_2 laser has application potential in communications and as a "death ray"! (note 10.6 microns falls within an atmospheric transmission window)

The operation of this laser can be understood by studying the energy level diagram shown in Figures 4.9 and the mechanization shown in Figure 4.10. CO_2, N_2 and Helium are mixed then pumped through the lasing tube under partial vacuum. Helium is used only for cooling via molecular collisions. An electrical discharge across the tube excites the N_2 molecules to higher vibrational energy levels. Since the molecule is symmetric, the dipole moment vanishes meaning a radiative transition to the ground state is forbidden. (A dipole is an oscillating + and - charge pair; a dipole when oscillating yields an electromagnetic field according to Maxwell's equations which leads to radiative processes). Consequently, once the nitrogen molecule is excited it tends to remain excited until some non-radiative process occurs, molecular collisions being the most important. In other words the excited state has a long lifetime.

The energy of the first excited N_2 vibrational state is almost identical to the first excited asymmetric vibrational state of the CO_2 molecule. Consequently in a collision between an excited N_2 molecule and an unexcited CO_2 molecule, there is a very high probability that the excitation energy will be transferred to the CO_2 molecule. Our population inversion is now complete.
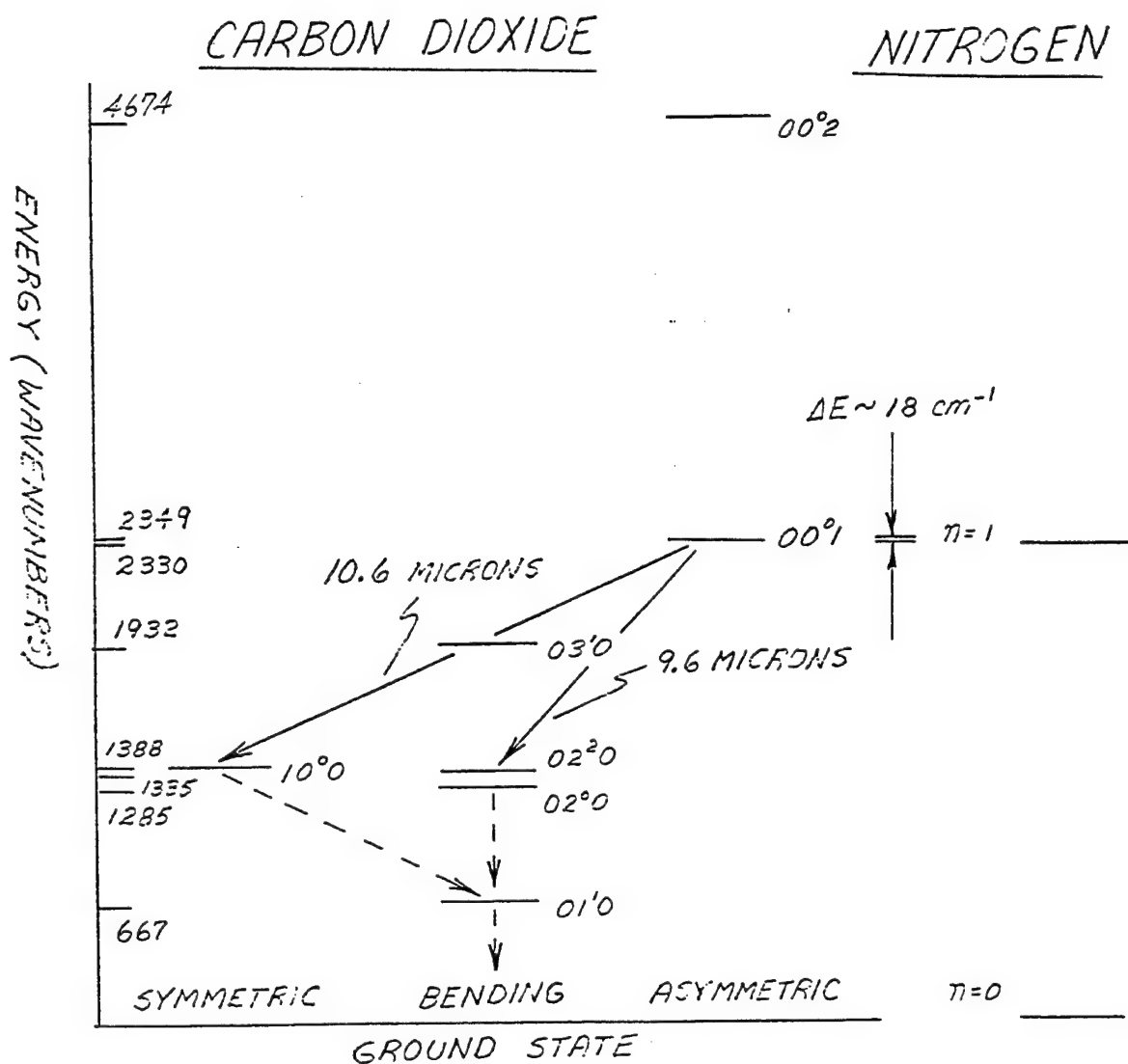
FIGURE 4.9 VIBRATIONAL ENERGY LEVEL DIAGRAM FOR
CO_2 AND N_2 SHOWING SIGNIFICANT LASING TRANSITIONS
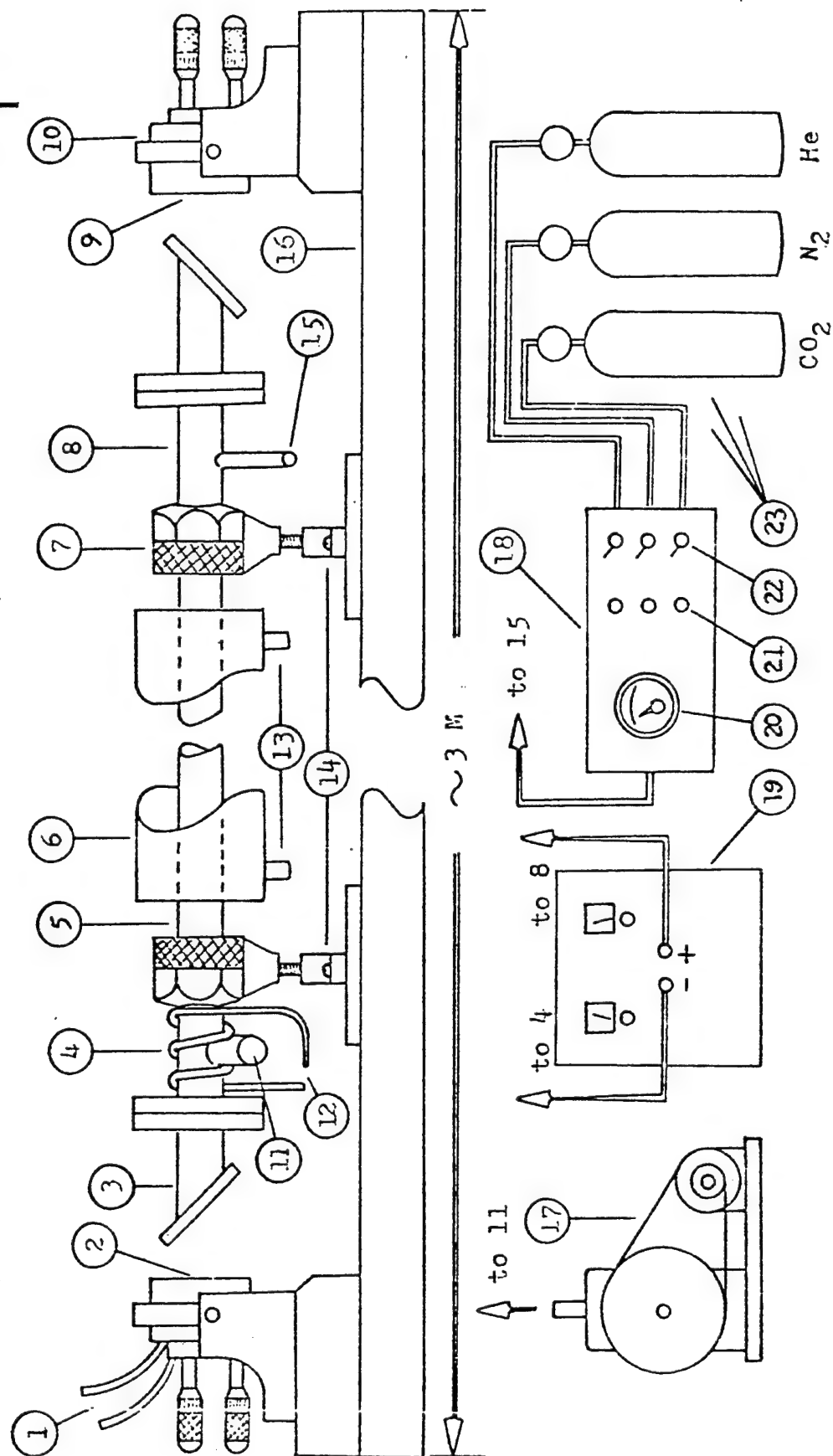
FIGURE 4.10 A COMPLETE 100 WATT CW CO_2-N_2-He LASER SYSTEM

EXPLANATION FOR FIGURE 4.10

1.   Cooling jacket for output mirror
2.   Germanium output mirror with ARC, flat
3.   NaCl Brewster window assembly
4.   Negative electrode; in line brass
5.   Discharge tube: 96 in length with 3/4 in bore, pyrex
6.   Cooling jacket for discharge tube: 1.75 in ID acrylic
7.   Glass to metal quick-disconnect coupling
8.   Positive electrode (no cooling necessary)
9.   Dielectric coated silicon mirror, R = 10 M
10.   Lansing 10.253 mirror mount with variable iris diaphragm
11.   Gas exhaust port: 1 inch OD
12.   Cooling coils for negative electrode
13.   Water inlet and outlet ports for cooling jacket
14.   Adjustable insulating supports
15.   Gas inlet port from mixing tank: 0.25 inch OD
16.   Optical channel: HD 10 inch aluminum
17.   Vacuum pump: 15 cfm Welch Duo-Seal 1397
18.   Mixing and regulatory assembly
19.   Regulated power supply: β model 2010-100R
20.   Vacuum gauge- Heraeus Diavac
21.   Gas inlet needlevalve: Hoke 2355F4Y, 1° included angle stem
22.   Quick disconnect valve: Whitey 1GS4-316SS
23.   Gas tank and regulator assemblies

The lifetime of the asymmetric state is very short due to a strong radiative decay (spontaneous) directly to the ground state. However, once the laser action starts between this state and the first symmetric state, the spontaneous decay quickly drops to an insignificant level. In the steady state condition the number of stimulated photon emissions are equal to the rate at which the asymmetric state is repopulated.

The CO_2 molecules in the first symmetric state decay to the ground state through both spontaneous emissions and non-radiative processes such as in collisions with helium molecules. A medium strong radiative decay takes place between the first symmetric state and first bending state. A very strong radiative decay occurs between this state

and the ground state. The gases may be expended at this point, cooled and recycled, or as in some low power systems, sealed under vacuum in the lasing tube.

4.4.2 LIQUID LASERS. Liquid lasers use certain dye solvent combinations that can be pumped by either a flashlamp or a second shorter wavelength laser. Principal applications are in a field of spectroscopy. The original expectations of the liquid laser to surpass the solid lasers in high average power has not been realized due to low efficiencies and high threshold properties. The output is in the form of pulses with energies up to two joules and peak energies of several mega-watts.

4.4.3 CRYSTALLING LASERS. The crystalling laser is most often used in military applications. The ruby laser (0.6943 μ) and YAG laser (1.06 μ) have the most widespread use. Ruby was the first material in which laser action was achieved. It is commonly used in ranging systems where low pulse repetition frequencies (PRF) are acceptable. The YAG laser is used for high PRF application as less energy is required for population inversion. Both lasers are capable of operating in the Q - switched mode at peak powers in excess of 10 mega-watts with pulse widths on the order of 10 nanoseconds.

4.4.4 GLASS LASERS. The properties of glass lasers are similar to crystalling laser but have the advantage that large laser rods are much easier to fabricate. However, the glass lasers generally exhibit a higher threshold and poorer thermal properties (stability). These lasers are very powerful with output peak powers in the tens of gigawatts. Most of the glass laser development has centered around the use of N_d^{3+} as the active laser ion, yielding an emission wavelength of 1.06 microns. Much effort is being expended in using this laser for controlled thermonuclear fusion.

4.4.5 SEMICONDUCTOR LASERS. The semiconductor or injection laser achieves population inversion by direct injection of electrons into the junction region of a suitable semiconductor. Gallium arsenide (GaAs) was the first and is the most important laser of this type. The output wavelength is a strong function of temperature varying from 0.9 microns at room temperature to 0.86 microns at liquid nitrogen (77°K.). The output power of the injection laser is low, typically less then 10 milliwatts. This is a consequence of the small size of the semiconductor junction. Arrays of GaAs lasers with total power output up to 60 watts have been used as an illumination source for range gated active television systems.

4.5 RANGE EQUATION

4.5.1 RANGE SQUARED VERSION. To foster an understanding of the many laser applications we will derive a form of the range equation. Consider the case in which the "target" is the ground or something on the ground and the laser is in an aircraft. This implies that the full transmitter beam is intercepted. The derivation proceeds as follows. A list of symbols and definitions is included as Table 4.3 and the elements of the problem in Figure 4.11.

The laser transmits energy E_T. This factor divided by the pulse width, τ, is the peak power transmitted. This power is beamed at the ground but is attenuated by the atmosphere. The transmission factor is,

$$\frac{E_T \epsilon^{-\alpha R}}{\tau} \tag{4.1}$$

The ground and/or a target then reflects this power in accordance with the laws of physics. Thus, if the reflecting surface is that of a diffuse reflector, the reflective factor is $\dfrac{\rho \cos \theta}{\pi}$ where ρ is the reflectivity and θ is the incidence angle measured to the normal (Section 4.4.1). Thus, the power reflected by the ground is,

$$\frac{E_T \epsilon^{-\alpha R}}{\tau} \left(\frac{\rho \cos \theta}{\pi} \right) \tag{4.2}$$

Now this power is scattered over a hemisphere and the laser receiver intercepts only a small portion of this. In addition, the atmosphere again limits the transmission as it did to the transmitted power. These combined factors can be expressed as

$$e^{-\alpha R} \frac{\pi d^2}{4 R^2} \qquad \text{where} \quad d \quad \text{is the diameter of the}$$

receiving optics. $\hspace{9cm}$ (4.3)

TABLE 4.3

TERMS USED IN RANGE EQUATION

SYMBOL	DEFINITION	NOMINAL VALUE
E_T	Transmitted energy	0.1 joules
τ	Pulse width	25 nanoseconds
α	Attenuation and backscatter	2 to 5 db / km
R	Range to target	What we are looking for
ρ	Reflectivity	.05 to .7
θ	Angle of incidence	0 to 90 degrees
d	Diameter receiving optics	5 cm
N_t	Optical efficiency of transmitter	.9
N_r	Optical efficiency of receiver	.5 to .8
N_q	Quantum efficiency of detector	.1 to .25
S	Power at receiving optics	small
$(SIN)_o$	Minimum signal to noise ratio	~ 2
$(NEI)_T$	Noise equivalent irradiance	
A_T	Area of target	
A_B	Area of beam	
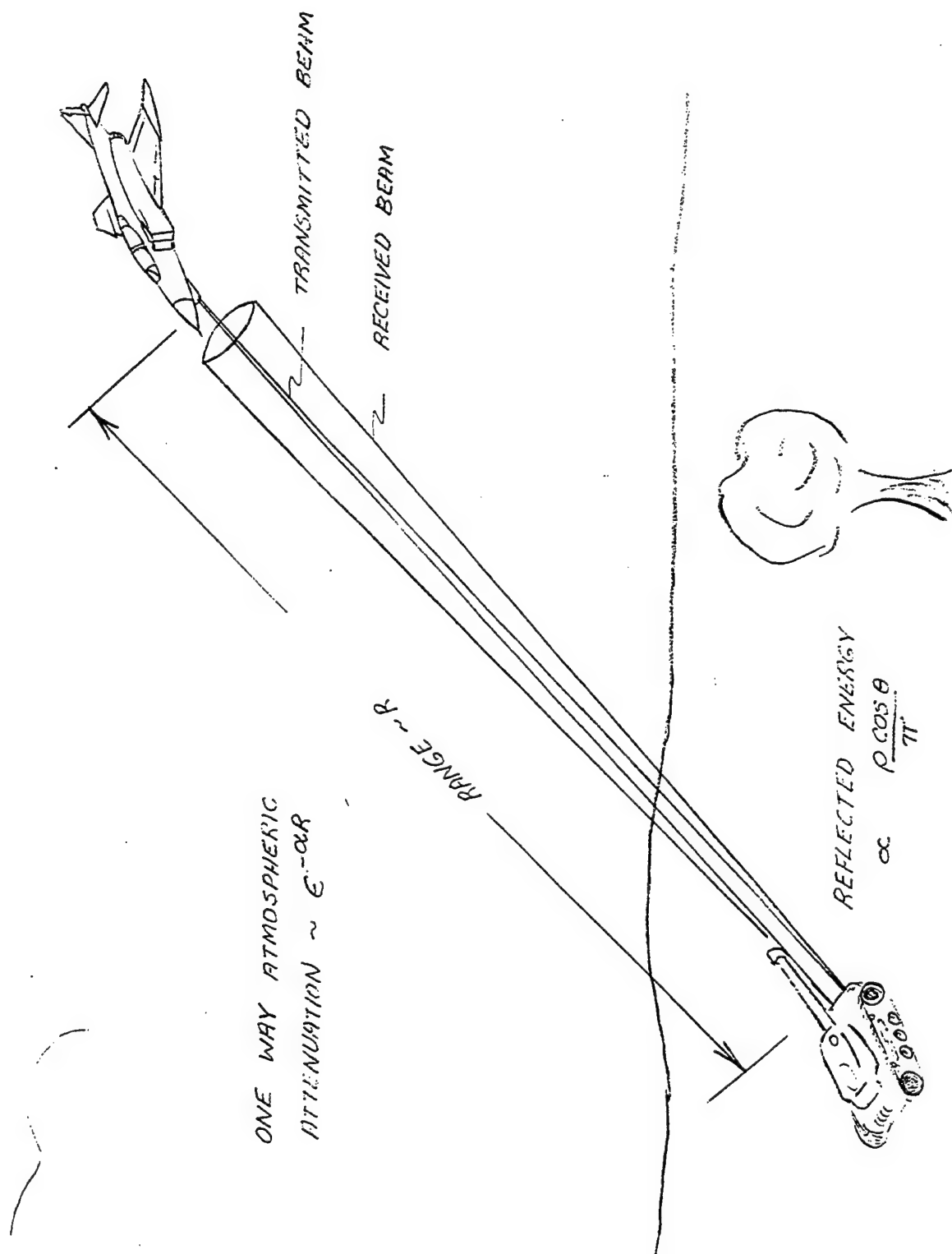
FIGURE 4.11 MODEL FOR DEVELOPMENT OF RADAR RANGE EQUATION

The power at the receiver is then

$$\frac{E_T}{\tau} e^{-2\alpha R} \qquad \frac{\rho \cos \theta}{\pi} \frac{d^2}{4R^2} \qquad (4.4)$$

We must next consider several efficiencies, the optical efficiency of the transmitter η_t, the receiver η_r, the quantum efficiency of the detector $\frac{qe'}{h\upsilon}$, and the signal processing efficiency η_s in the receiver. This then translates the power at the receiving optics to the following signal:

$$S = \frac{E_T}{\tau} e^{-2\alpha R} \eta_t \eta_r \eta_s \frac{qe'}{h\upsilon} \frac{\rho \cos \theta}{\pi} \frac{d^2}{4R^2} \qquad (4.5)$$

Now, for reliable detection of the received signal, a particular minimum signal-to-noise ratio $(S/N)_o$ must be specified. This ratio times the total noise contributions $(NEI)_T$ yields the minimum required signal level. Thus,

$$(S/N)_o (NEI)_T = \frac{E_T}{\tau} e^{-2\alpha R} \eta_t \eta_r \eta_s \frac{qe'}{h\upsilon} \frac{\rho \cos \theta}{\pi} \frac{d^2}{4R^2} \quad (4.6)$$

Rearranging, we have

$$R^2 = \frac{E_t e^{-2\alpha R} \eta_t \eta_r \eta_s \, qeb \cos \theta \, d^2}{4\tau h\upsilon \, (S/N)_o \, (NEI)_T \, \pi}$$

This form of the range equation permits some design decisions. We will examine the nature of the factors in this equation in later sections.

4.5.2   OTHER FORMS.   If we consider an application where the target is smaller than the beam and the background does not return appreciable energy, we must modify te range equation developed above. If the target is smaller in both dimensions than the beam diameter, the right-hand side of the R^2 range equation must be multiplied by-the term:

$$\frac{A_T}{A_B} \tag{4.8}$$

where A_T = area of the target and A_B = area of the beam.

If a target fills one dimension of the beam -- consider a wire
cutting completely across a beamwidth -- then an R^3 equation results. Note also that when the target is smaller than the beam in both dimensions, an R^4 equation results.

4.5.3 ATMOSPHERIC ATTENUATION.   The most authoritative work to date on atmospheric propagation of laser light was performed by T. S. Chu and D. C. Hogg, and D. B. Rensch. A summary of their work appears in the <u>Bell System Technical Journal</u>, May-June 1968, and Ohio State University's Report AFAL TR-69-77, April 1969. Some of the high points are summarized below.

1. Rain attenuates the three wavelengths checked -0.63, 3.5, and 10.6 microns about equally. Over a 2.6-km path, the attenuation is about 14 dB/km for a rainfall rate of 50 mm/hr which is considered heavy.

2. In light fog the 10.6 micron signal is attenuated less than the 3.5 micron signal. The 0.63 micron signal suffers the worst attenuation. The attenuation of the 10.6 micron signal in light fog is about 1 dB/km.

3. A least-squares line to fit measured data at 0.63μ has the equation

$$(\alpha) \; \frac{dB}{km} = 0.155, \; r \; (\frac{mm}{hour}) + 2.66 \tag{4.9}$$

where α is the attenuation coefficient and r is the rainfall rate.

   4. Above 103 mm/hr, all wavelengths checked showed a 10 dB/km loss or more.

   5. In light snow, all attenuations averaged 6 dB/km. The 10.6 micron signal was attenuated more than the others.

4.5.4 REFLECTIVITY. The diffuse reflectance of targets at various wavelengths is an important factor in the range equation.

4.5.5 NOISE. The noise equivalent irradiance term in the range equation is composed of three major noise sources: background noise, detector noise, and back-scatter noise. Examination of the terms in the range equation shows that the signal(s) is in amperes; consequently, noise must also be expressed in RMS current values.

4.5.5.1 BACKGROUND NOISE. Background noise results from black body emissions and solar reflections. If the background noise is NB then the number of photons per unit area at the receiving optics per steradian (unit solid angle) in one second is $N_B \Delta \lambda / h\upsilon = N_B'$ where $\Delta \lambda$ is the bandwidth of the receiver. The number of noise electrons detected per second is then

$$\eta_B = N_B' \; \Omega_r \; \frac{(\pi d^2)}{4} \; \eta_r \; q \qquad\qquad (4.10)$$

where Ω_r is solid angle seen by the receiver optics $\frac{(\pi d^2)}{r}$ and is the area of the optics. The factor $\eta_r q$ converts the photons incident at the aperture to photoelectrons. The noise current entering the receiver is thus

$$I_B = \eta_B e' \qquad\qquad amperers \qquad\qquad (4.11)$$

where e' is the unit of electronic charge 1.602 x 10^{-19} coulombs/electron (amperers = coulombs/second).

A forest produces some of the most intense solar illuminated background radiances in the near infrared. Actual data shows in this case that N_B is typically 100 watts^2/meter^2/micron/steradian at 1.06 microns. Using the nominal values for the other parameters, listed in Table 4.4, the background photoelectron current corresponds to 1.45 microamps.

The corresponding background fluctuation current is,

$$i_B = \sqrt{2\,I_B e' B_N} \qquad\qquad (4.12)$$

where B_N is the receiver noise bandwidth. This yields a background noise equivalent inadiance of

$$(NEI)_B = i_B h\nu / A_r \eta_r q e' \eta_s \qquad\qquad (4.13)$$

TABLE 4.4

PARAMETERS USED IN NOISE DISCUSSION

SYMBOL	DEFINITIONS	NOMINAL VALUE
N_B	Radiant intensity	$100W^2/M^2$ ∘st∘µ
$\Delta\lambda$	Receiver bandwidth	$40\overset{o}{A}$
Ω_r	Solid angle of receiver field of view	
r	Receiver optical efficiency	0.5
q	Quantum efficiency	0.6 (1.06 microns)
i_B	Background fluctuation current	
A_r	Area of receiver optical aperture	20 cm^2
s	Pulse processing efficiency	0.7
i_D	Leakage fluctuation current	
I_D	Detector leakage current	1.0 microamps
F_N	Receiver noise figure	2
$k_B T$	Thermal noise energy	
r	Load resistance seen by detector	
C	Equivalent capacitance of rC filter	10 pf
B_N	Receiver bandwidth	10 Mhz

If, however, noise events occur more frequently, Poisson statistics must be used to determine $(NEI)_B$.

If this sounds like a lot of noise, just read on!

4.5.5.2 DETECTOR AND AMPLIFIER NOISE.   Shot noise due to detector leakage current and Johnson noise associated with the amplifier input impedance give rise to an equivalent noise current given by

and an equivalent noise irradiance of

$$i_D = \sqrt{2 I_D e' B_N + F_N (4 k_B T B_N / r)} \qquad (4.14)$$

$$(NEI)_D = i_D h\nu / A_r \eta_r q e' \eta_s \qquad (4.14)$$

An rC filter is best matched to the pulse shape by taking

$$B_N \tau_r = 0.4 \qquad (4.15)$$

so that a 25-nanosecond pulse implies a noise bandwidth of about 16 Mhz. Then, since this is equal to 1/(4rC), r is only 1560 ohms for a practical capacitance value of 10 picofarads associated with a quadrant detector.

This being the case, the Johnson noise dominates. At 290°K, the Johnson current is about 64 microamps compared with 1.45 microamps for the back-ground photoelectron current and 1.0 microamp for the detector leakage current in the example of Table 4.4 discussed above.

4.5.5.3 Backscattering.   Scattering at 1.06 microns is chiefly due to atmospheric aerosols. Even under good visibility conditions, it is realistic to ignore the Rayleight (molecular) components. As an example, a scattering coefficient of 0.048/km for 1.04

microns has been reported when the transmission at 0.67 microns was 0.95 per km (about 80-km visibility); at that time the Rayleigh component of the coefficient at 1.04 microns was only 0.001 per km, or only 2% of the total.

Aerosol scattering does not have a simple description and a complicated theory first advanced by Mie must be used. General statements can only be qualitative, but in recent years a number of authors have used high-speed computers to obtain theoretical results for specified, but nonetheless fairly realistic, cloud and haze models. In general, as the visibility drops and particle sizes increase, the fraction of light scattered into the back hemisphere increases.

While a precise backscatter calculation would require considerable work for any specified field condition, a conservative estimate of what may be expected is obtained easily. Advantage is taken of the fact that when the receiver and transmitter beams are noncolinear, only scattering from the region close to the target where the beams intersect need be considered. The result is that the backscattering can be expressed in terms of a noise current in which yields a total noise equivalent current of

$$(NEI)_T = \sqrt{i_B^2 + i_D^2 + i_\beta^2} \qquad (4.16)$$

4.5.6 OTHER FACTORS.   A number of other factors must be covered in order to complete the discussion of the range equation and lay the groundwork for laser system design. They are: efficiency of the optics, quantum efficiencies of detectors, types of receivers, mechanical and electrical interfaces, and constraints such as weight, volume, and power drain.

4.5.6.1 EFFICIENCIES.   The efficiency of the optics can approach unity, but costs and environmental factors usually drive this factor to lower values. Optical efficiencies in the visible region are more often about 0.5 to 0.8 total.

The quantum efficiencies of detectors is a strong function of what detector is used. This in turn is usually dictated by the wavelength. Table 4.5 lists typical quantum efficiencies of various detectors at different wavelengths.

TABLE 4.5

QUANTUM EFFICIENCIES OF DETECTORS

DETECTOR	WAVELENGTH (MICRONS)	QUANTUM EFFICIENCY (PERCENT)	COMMENTS
S-20	0.5	15-20	
S-20	0.7	2-3	
S-1	1.0	0.1	
Ge:Hg	10.0	25	Must be cooled to 20 - 40°K

4.6 LASER APPLICATIONS.

Laser applications result from exploiting the unique characteristics of the radiation discussed in Section 4.3 and are summarized in Table 4.6. Most sensor applications exploit collimatability and narrow band monochromaticity. Single mode monochromaticity, short pulse width, and low noise are used in only two functions each. This does not mean that these properties are designed out of other systems but rather that these properties have not been uniquely exploited by these applications.

Few applications to date has taken advantage of the lasers high spectral radiance. The laser stores wide band energy and converts this to narrow band energy. Because of this, the spectral radiance (watts per meter^2 per micron per solid angle per mouth full) is very large compared to any plankian radiator. Considering the number of characteristics that have yet to be exploited, such as the spectral radiance, the laser will play a dominant role in new systems for years to come.

TABLE 4.6

APPLICATION OF LASER CHARACTERISTICS

FUNCTION	COLLIMAT-ABILITY	MONOCHROMATIC		SHORT PULSE	LOW NOISE
		NARROW BAND	SINGLE MODE		
IMAGING (NIGHT USE)	X				X
AMPLITUDE MEASUREMENT		X			X
RANGING HI ACCURACY LOW ACCURACY	X X	X X		X	
ANGLE MEASUREMENT	X	X			
RANGE RATE MEASUREMENT HI ACCURACY LOW ACCURACY	X X	X	X	X X	
ANGLE RATE MEASUREMENT	X		X		

4.7 EYE DAMAGE. Research at a number of institutions, notably Stanford University, has yielded results which are supposed to be applicable to humans. Table 4.7 shows some results obtained in the visible region. Irreversible eye damage is defined as damage to tissue that does not heal without a scar or worse.

It is worth noting that other lasers with wavelengths higher than those indicated in Table 4.7 are less damaging to the eye because of the opacity of the eye at higher wavelengths. Thus, at 10.6 microns, the eye suffers only surface burns and, it were not such a sensitive area, the damage would be akin to a surface burn on the skin for the energies indicated in Table 4.7.

TABLE 4.7

EYE DAMAGE FROM LASERS

TYPE OF ENERGY	DURATION SECTIONS	WAVELENGTH $\overset{o}{A}$	ENERGY DENSITY FOR IRREVERSIBLE EYE DAMAGE JOULES/CM^2
CW	30	6328	2×10^{-6}
One giant pulse	3×10^{-7}	6943	10^{-7}
Several Q switched pulses - until subject blinked?	2×10^{-8} per/pulse	6943	10^{-8}

(THIS PAGE INTENTIONALLY LEFT BLANK)

SECTION V

OPTICAL DETECTORS

5.0   INTRODUCTION. The detector is the heart of an optical sensor and the success of modern IR systems is largely due to the development of greatly improved detectors capable of sensing IR radiation beyond 3 microns. Radiation collected by optics and focused on the detector's focal plane is transformed from an optical signal to an electrical signal. From this point on the system sensitivity and signal-to-noise ratio are primarily governed by the functions for the detector and its immediate processing electronics. The first prerequisite to understanding the design of optical sensors is, therefore, a knowledge of detector operation.

An optical detector transforms an optical signal into an electrical signal. The purpose of this conversion is to provide a signal suitable for electronic processing. There are two basic types of radiation detectors: thermal detectors and photon detectors.

Thermal detectors absorb radiant energy, thereby increasing in temperature. The increase in temperature produces changes in the bulk physical properties of the detector material. These changes are then measured as indications of the amount of radiant energy absorbed.

Photon detectors exhibit measurable effects produced by the direct action of individual photons of radiant energy on atomic electrons within the detector material (the photoelectric effect). The principal types of radiation detectors in each category are listed below.

Thermal Detectors	Photon Detectors
Calorimetric	Photoemissive
Fluid Expansion	Photoconductive
Evaporographic	Photovoltaic
Thermocouple	Photoelectromagnetic
Bolometric	Photographic

The physical principles of operation and operating characteristics of the two basic types of radiation detectors are discussed in the following paragraphs.

5.1   DETECTOR SIGNALS. Depending on the application, the output for an IR detector will be an electrical signal which may be a steady (dc) or varying (ac) quantity. To avoid having to handle a dc output, a steady beam of input radiation may be varied periodically or "chopped", to produce an alternating signal. The chopper is commonly a rotating disc with alternating clear and opaque sectors (sometimes called a reticle) so placed as to periodically interrupt the radiation incident on the detector. The benefits of ac signal handling over dc are as follows:

a.   The rejection of unwanted radiation falling on the detector from its immediate surroundings.

b.   AC signals are much easier to handle electrically.

c.   Any drift with time of the reference level of the detecting system is rejected.

d.   For certain types of detector, noise may be reduced by working at a reasonably high chopping frequency.

e.   The dc level may be restored as convenient at a reduced level to expand the available contrast, which is inherently low in IR systems.

5.2   DETECTOR CHARACTERISTICS. The performance of IR detectors depends on the following characteristics:

a.   Time constant

b.   Spectral response

c.   Responsivity

d.   Frequency response

e.   Noise equivalent power

f.   Detectivity

g.   Normalized detectivity (d-star)

h.   Dynamic range

i.   Stability

j.   Dimensions

5.2.1   TIME CONSTANT. The time constant (t) of any infrared detector is a measure of the time required for the detector to respond to radiation on its surface. There are several definitions of time constants which are in current use. For example, the time constant could be defined as the time required for the response which is 63% of its final value after a sudden change in the irradiance.

5.2.2   SPECTRAL (WAVELENGTH) RESPONSE. Since the response of a thermal detector is proportional to the energy absorbed, the relative response for a constant radiant flux input at all wavelengths would be a horizontal straight line as shown in Figure 5.1 (provided the detector were a blackbody); however, with photon detectors the situation is quite different. Photon detectors respond to the total number of photons absorbed and if the input radiant flux is to be constant over all wavelengths, more photons must be supplied at the longer wavelengths since the energy of the photons is given by

$$E = h\nu \qquad\qquad (5.2)$$

where h is constant and ν is frequency. Accordingly, the relative response of a photon detector for a constant radiant flux input per unit wavelength interval increases with wavelengths until a cut off wavelength is reached. This occurs when the photon energy given by the above equation is insufficient to raise the energy of an electron to a level where it is free to act as a carrier of electrical current. The band of energies which it has vacated is called the valence band (Figure 5.2). In practice the theoretical sharpness of the cut off wavelength in Figure 5.1 is modified by the presence of impurities and effects in the detector material. In addition, the presence of impurities and defects in the detector material. In addition, no detector is a perfect absorber of radiation so the relative response is an indication of the extent to which the detector departs from the concept of a blackbody. The response curve of a practical photon detector resembles that of the broken line in Figure 5.1.
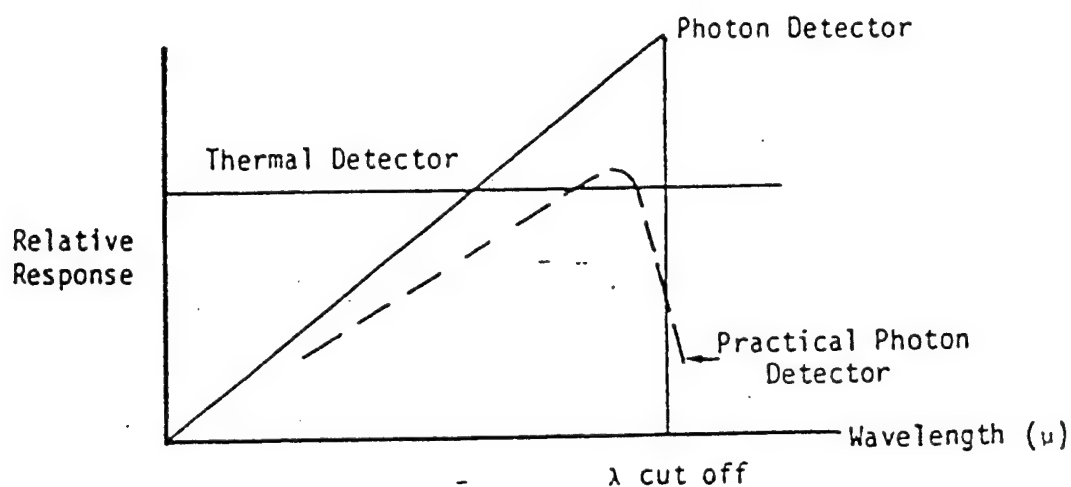
Figure 5.1   Idealized Response Curves of Thermal and Photon
              Detectors With Constant Radiant Flux Input Per
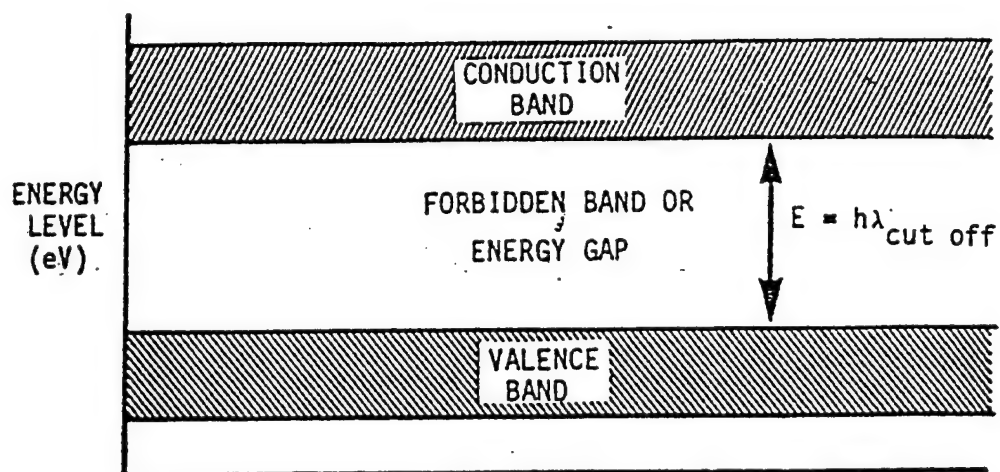   Unit Wavelength Interval

Figure 5.2. Simplified Energy Level Diagram for a Semi-Conductor

5.2.3   RESPONSIVITY (R). The responsivity (R) in an infrared detector is the plot of the output response as a function of the input radiation. In general, most of the detectors are linear, that is, a change in input radiation of a given amount will produce a predictable change in amplitude response of the detector.

5.2.4   FREQUENCY RESPONSE (R_f). The frequency response (R_f) of an infrared detector is the change which occurs in the amplitude of the response when the incident radiation is interrupted at varying frequencies. In general, when the radiation of a source is interrupted at a frequency which is small, with respect to the physical time constant of the detector, the frequency response will be flat (constant). As the frequency at which the incoming radiation is interrupted approaches a value in the order of the time constant, the relative response will decrease until it reaches a minimum useful value which is determined by the time constant of the detector.

5.2.5   NOISE EQUIVALENT POWER (NEP). The noise equivalent power (NEP) of an infrared detector is the amount of electromagnetic radiation which must be put on the detector to get an output response which is equal to the noise of the detector. Noise equivalent power can be defined by the equation

$$NEP = \frac{JA}{V/N} \qquad (5.3)$$

where: J is the root mean square value of the fundamental heat signal.
                          A is the area of the sensitive surface of the detector.
                          N is the root mean square detector noise output.
                          V is the root mean square detector output signals.

5.2.6   DETECTIVITY (D). The detectivity (D) is simply the reciprocal of the noise equivalent power of the detector. This is a more convenient measure of detector performance because large values of detectivity are compatible with high "sensitivity". If NEP were used as a criterion, small values of NEP would be associated with high sensitivity. The detectivity (D) is then given by

$$D = 1/NEP \qquad (5.4)$$

5.2.7   D* (D-STAR). As defined, detectivity is a figure of merit comparable with the noise factor (NF) of electronic amplifiers. However, for perfect detectors NEP varies as $(A)^{1/2}$ and $(\Delta f)^{1/2}$. - where A is detector area and Δf is the bandwidth over which the noise is measured.   Therefore, unless the detector specimen sizes and noise

bandwidths were identical, D would not give a true comparison between different detectors. Hence a better measure of detectivity is given by D*, which is defined as follows:

$$D* = D \ (A\Delta f)^{1/2} \hspace{3cm} (5.5)$$

Thus, D* is a normalized detectivity that is particularly convenient in comparing the performance of detectors of different area when used in circuits having different bandwidths. Since the conditions of measurement can affect the value of D*, these conditions are normally quoted in parenthesis with any statement of D* as follows: D* $(77°K \ 3.7\mu \ 1000 \ Hz)$. This would mean that the value of D* quoted was obtained at an operating temperature of 77°K, at a wavelength of 3.7μ and using a chopper frequency of 1000 Hz.

5.2.8 DYNAMIC RANGE. The dynamic range of an IR device is the ratio of the specified maximum signal level capability of a system component to its noise level. It is not usually limited by the dynamic range of the detector, but is limited by the succeeding amplification apparatus.

5.2.9 STABILITY. The ability to keep a calibration and maintain stability are familiar desirable properties of any component or system and are self-explanatory.

5.2.10 DIMENSIONS. The characteristic size and shape which a detector takes may sometimes influence other characteristics, such as NEP and response time. Many detectors, particularly those with chemically deposited or evaporated sensitive surfaces, and semiconductor types, require as small a sensitive area as possible to minimize cell noise. Thermal detectors are frequently limited in this way because their response times depend upon heat capacity and conductance, which are shape and size dependent.

5.3 THERMAL DETECTORS. A thermal detector transforms incident thermal energy into an electrical signal by means of a temperature sensitive element. Thermal energy heats this sensitive element and produces a signal proportional to the temperature rise of the element. Because of this property, a thermal detector can respond to energy of all wavelengths.

An equilibrium temperature between the sensitive element and its environment will be established under dark conditions. The temperature of the sensitive element will increase when the element is irradiated until another equilibrium condition between absorbed and radiated thermal energy (including heat conduction and heat radiation) is established.

The temperature change of the sensitive element (ΔT) can be obtained as a function of the incident radiant power (P), the heat capacity of the sensitive element (C_h), and the thermal conductance (K_t) of that element:

$$\Delta T = f(P, C_h, K_t) \tag{5.6}$$

The heat capacity (C_h) is defined as the heat energy required to increase the temperature of the sensitive element by one degree. The value of C_h changes with the operating temperature of the sensitive element and the temperature of the environment.

5.3.1   THERMAL DETECTOR CHARACTERISTICS. The general characteristics of thermal type radiation detectors are listed below and discussed in the following paragraphs.

> Response Time Large
> Detectivity Low
> Output Independent of Wavelength
> Heat Dissipation Required
> Cryogenic Cooling Not Required

The relative slow response of the thermal type radiation detector is a result of the time required to raise the temperature of the thermal mass. The long response time (in the order of milliseconds) can be restrictive in a scanning sensor where target dwell times may be in the microsecond range.

The relatively low detectivity of the thermal detectivity of the thermal detector results in a signal-to-noise ratio generally lower than that for a photon type detector.

The most important advantage of the thermal type detector is the fact that it responds to all wavelengths. Photon type detectors do not respond beyond a certain wavelength.

The radiant energy absorbed by a thermal detector must be dissipated continuously in order for the detector to respond to a decreasing flux rate. Eventually, of course, all of the absorbed radiant energy must be dissipated. In situations involving continuing exposure to high level radiation, heat dissipation can be a problem. Unlike photon detectors, however, cryogenic cooling is not usually required.

5.3.2   TYPES OF THERMAL DETECTORS.

Thermocouple

A thermocouple consists of one hot and one cold junction. The hot junction (thermo-electric junction), generates a voltage in response to incident radiation. The cold junction is always in thermal equilibrium with the environment. The voltage (v) generated across the two junctions is related to their temperature differences by the equation:

$$v = C_t \ (T_h - T_c) \tag{5.7}$$

where: T_h is the temperature of the hot function in K,

T_c is the temperature of the cold junction in K, and

C_t is the coefficient called thermoelectric power in volts per K.

Bolometer

The bolometer is the thermal detector most frequently employed in airborne systems. A bolometer senses the change in resistance of a sensitive element caused by the temperature change. The sensitive element may be a metal, a semiconductor, or a superconductor, metallic and semiconductor bolometers are the most widely used. Super conductor bolometers are mostly laboratory devices.

The resistance change in a metallic bolometer is linearly dependent on changes in temperature. The resistance change in a semiconductor bolometer is an exponential rather than a linear function of temperature. For small temperature variations, however, the resistance change can be assumed linearly dependent upon temperature changes.

Superconductor bolometers exhibit a sharp change in resistivity when they are cooled down to near absolute zero. Certain materials (such as tin, lead or tantalum) exhibit

a sharp resistivity change in a small temperature region near their transition temperature (T_O). This transition temperature is usually near absolute zero.

The Calorimeter

The calorimeter consists of a radiation absorbing mass the temperature rise of which is measured, directly, as an indication of total radiant energy absorbed.

The Fluid-Expansion Thermometer

The fluid-expansion thermometer consists of a radiation absorbing liquid or gaseous mass the temperature rise of which is determined indirectly by measuring the change in volume of the fluid.

The Evaporograph

The evaporograph consists of a radiation absorbing screen the temperature rise of which is indicated indirectly by the rate of evaporation of a thin film of volatile substance. By focusing an image of the sensor field-of-view upon the screen, a thermal image is obtained.

5.4   PHOTON DETECTORS. Photon detectors operated according to the Photoelectric Effect and they are the most sensitive and widely used optical detectors.

5.4.1 THE PHOTOELECTRIC EFFECT. All electromagnetic radiation occurs in discrete quanta called photons. Each photon contains an amount of energy (E_γ) ‡ determined solely by the frequency of the radiation, according to the equation:

$$E_\gamma = hf = \frac{hc}{\lambda} \qquad\qquad (5.8)$$

where: h = Planck's Constant = 6.63 x $10^{-3/4}$ 8 (Watt-Sec^2)
                   c = Velocity of Propagation = 3 x 10 (Meters/Sec)
                   f = Frequency of Radiation (Hertz)
                   λ = Wavelength of Radiation (Meters)

The incident radiant flux (P) is related to the photon rate (Φ_γ) by the equation:

$$P = \Phi_\gamma E_\gamma \qquad \text{(Watts)} \qquad (5.9)$$

or:

$$P = \frac{hc}{\lambda}\Phi \qquad \text{(Watts)} \qquad (5.10)$$

The electrons surrounding the nucleus of an atom exist in energy bands as illustrated in Figure 5.3. Electrons in the lower energy state, Eo throughout En, are bound to the atom in sharply defined energy levels and take no part in electrical conduction. Electrons in the nondiscretized energy band (continuum) above En but below that required to escape the material, (En + Φ), are not bound to the atom and are, therefore, free to take part in electrical conduction. Electrons that have energies above the escape level take part in emission (escape from the surface of the material). The work function (Φ) is the minimum incremental energy required to cause a bound electron to be emitted from the material.

An incident photon of radiation can interact directly with an atom to raise the energy level of a bound electron to the conduction band or even to the point of emission. Both of these events are termed the photoelectric effect. When the freed electron remains within the material, the process is called photoconduction. When the freed electron is emitted from the surface of the material, the process is called photoemission. In either case, the photon of radiation is annihilated.
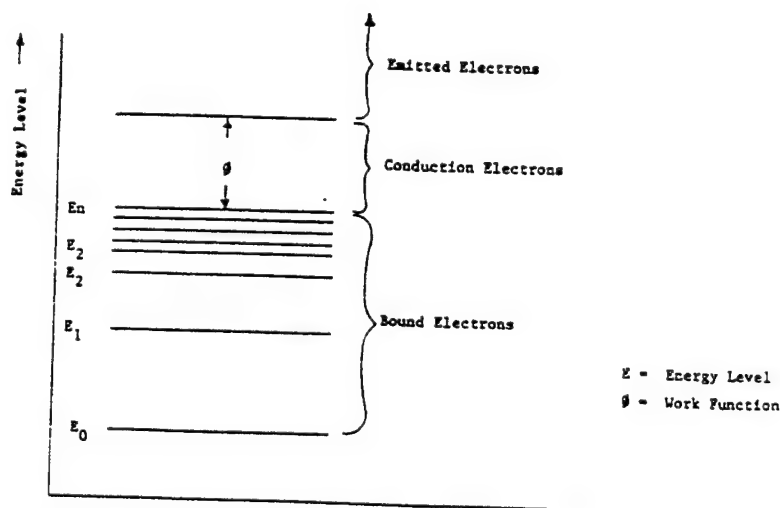
Figure 5.3.   Energy Levels of Atomic Electrons

As previously indicated, the energy contained in a photon of radiation is proportional to the frequency of the radiation. In order for photoconduction to occur, the incident photon must possess enough energy (the radiation must be of high enough frequency) to raise the energy level of a bound electron into the conduction band. In order for photoemission to occur, the incident photon energy must be even higher as indicated in Figure 5.4. Thus photon type radiation detectors exhibit a cut off wavelength beyond which they do not respond. There is a corresponding cut off frequency below which they do not respond.

Figure 5.4   The Photoelectric Effect

5.4.2 PHOTON DETECTOR CHARACTERISTICS. The general characteristics of photon type radiation detectors are listed below and discussed in the following paragraphs.

>   Response Time Small
>   Detectivity High
>   Output Dependent Upon Wavelength
>   Cryogenic Cooling Required

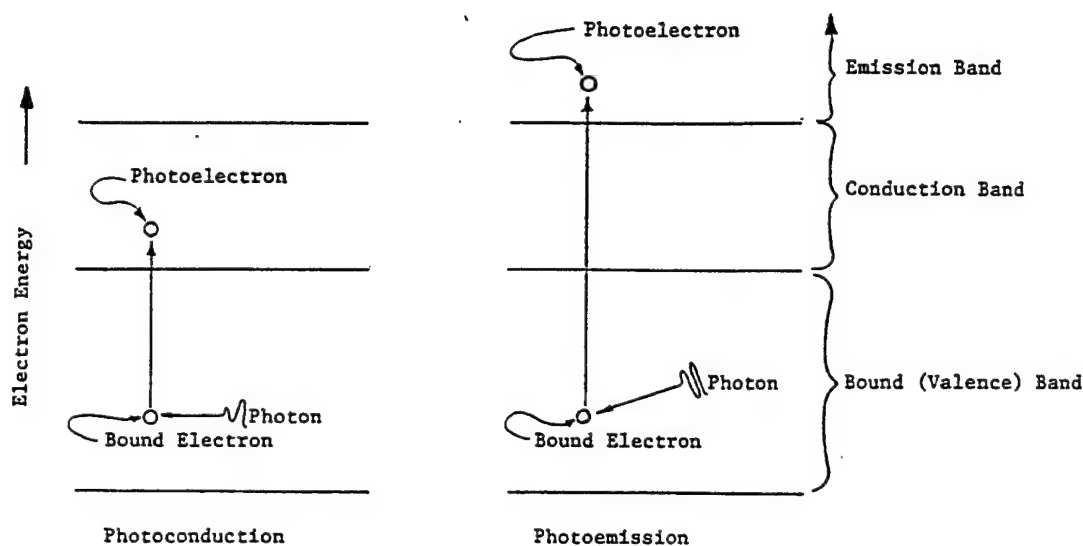The interaction between an absorbed photon and the absorbing atom (the photoelectric effect) is essentially instantaneous. Photon detectors are therefore characterized by a relatively fast response (in order of microseconds). This characteristic generally makes photon detectors more suitable for rapid scan sensors than are the much slower thermal detectors.

The signal-to-noise ratio at the output of a photon type radiation detector is, generally, larger than the for a thermal type detector. Thus, the detectivity (a direct measure of signal-to-noise ratio) is, in general, higher.

The most unfortunate characteristic of photon detectors is the existence of a cut off wavelength beyond which the detector will not respond. (The cut off wavelength is, as previously indicated, a result of the minimum photon energy (frequency) required to produce the photoelectric effect). Unfortunately, many targets of military significance are at temperatures so low (infrared radiation wavelength so large) that photon detectors do not respond well to their radiations.

Most photon type detectors perform well only at extremely low (cryogenic) temperatures. Since detectivity generally decreases rapidly with increasing temperature, most radiation sensors utilizing photon type detectors must incorporate relatively elaborate cryogenic cooling mechanisms.

5.4.3 TYPES OF PHOTON DETECTORS

The Photoemissive Radiation Detector
A photoemissive radiation detector usually takes a form similar to that shown in Figure 5.5. It consists of an evacuated vessel in which two electrodes are located.

One for the electrodes, the cathode, is coated with a photoemissive material. The external circuit consists of a voltage supply (the battery) and an electrical current
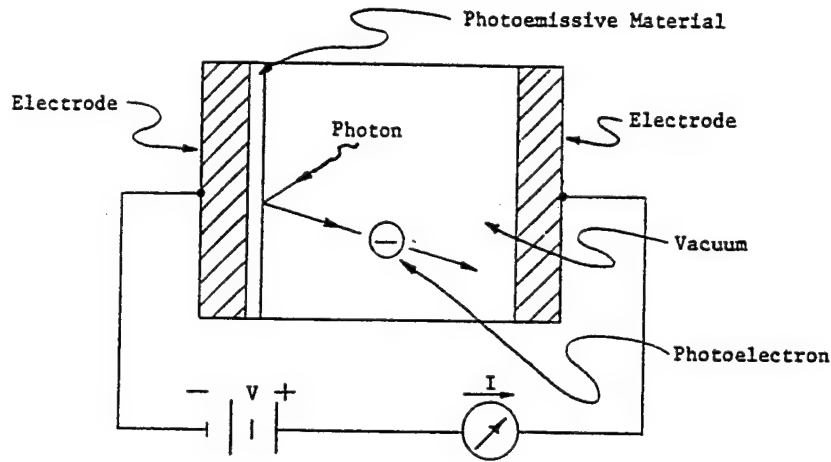
Figure 5.5   Photoemissive Radiation Detector

measuring device (the ammeter). Photons of sufficient energy striking the surface of the coated electrode produce photoemissive photoelectrons which flow to the positive electrode (anode), thus causing an electrical current in the external circuit, indicated by the ammeter. Photoemissive detectors include vacuum phototubes, photomultipliers, channeltrons, and others. In order for an electron to escape from a photoemissive surface, the absorbed photo energy (E) must exceed the work function of the material. The excess energy is converted to kinetic energy of the emitted electron according to the equation:

$$E_v - \Phi = 1/2 \ M_e V_e^2 \qquad (Joules) \qquad (5.11)$$

In order for an electron just to escape (Ve = 0), the photon energy must be:

$$E_\gamma = \frac{hc}{\lambda} = \phi \qquad (Joules) \qquad (5.12)$$

Thus, the cut off wavelength of a material is given by the equation:

where: h = Planck's Constant = 6.63 x 10$^{-3/4}$ (Watts-Sec 2)

$$\lambda_{cut\ off} = \frac{hc}{\Phi} \qquad\qquad \text{(Meters)} \qquad (5.13)$$

c = Velocity of Light = 3 x 108 (Meters/Sec)

M_e = Mass of Electron (Grams)

Ve = Escape Velocity of Electron (Meters/Sec)

λ = Radiation Wavelength (Meters)

Φ = Work Function of Material

5.4.4 THE PHOTOCONDUCTIVE RADIATION DETECTOR. A photoconductive radiation detector consists of a piece of semiconductor material with two electrodes attached as shown in Figure 5.6. The external circuit consists of a voltage source (the battery) and a current measuring device (the ammeter). Photons entering the semiconductor material produce photoconductive photoelectrons within the semiconductor material (and corresponding "holes" in the bound states of the atoms). Under the influence of the externally applied electric field, the photoelectrons move toward the positive electrode and the "holes" move toward the negative electrode thus causing a measurable electrical current to flow in the external circuit. Since the energy required to induce photoconduction is less than that required to induce photoemission, photoconductive detectors can respond to longer wavelength radiation.
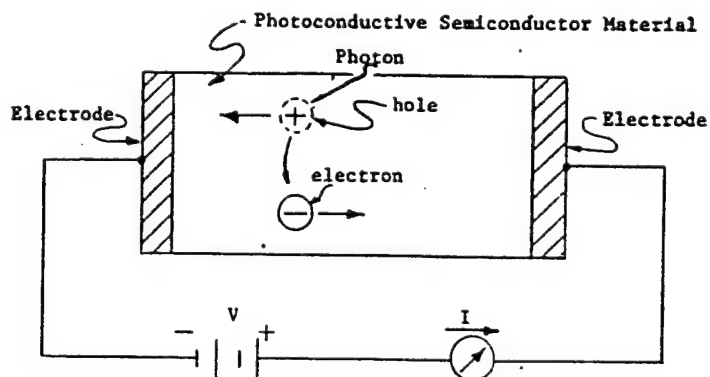
FIG 5.6   Photoconductive Radiation Detector

5.4.5   THE PHOTOVOLTAIC RADIATION DETECTOR.   A photovoltaic radiation detector consists of a semiconductor diode as shown in Figure 5.7.   The external circuit consists of an electrical voltage measuring device (the voltmeter).   Photons entering the semiconductor material produce photoelectrons and corresponding "holes".   As a result of the difference in energy levels in P-type material, thus producing an electric potential (voltage) across the P-N junction.   This voltage is measured by the external voltmeter.   The photon energy required for photovoltaic detection is essentially the same as that for photoconduction.   Therefore, the cut off wavelengths are approximately the same.
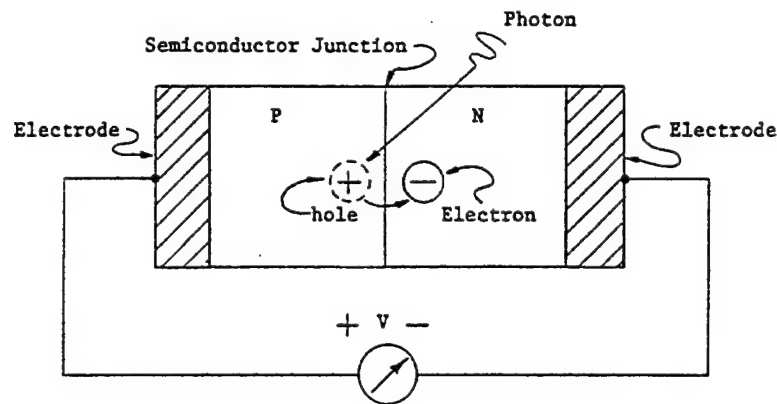
FIG 5.7   Photovoltaic Radiation Detector

5.4.6 THE PHOTOELECTROMAGNETIC RADIATION DETECTOR. A photoelectromagnetic radiation detector is constructed as shown in Figure 5.8. Two pair of electrodes are attached to a photoconductive semiconductor bare, at right angles, as shown. The power electrodes are connected to an external voltage source (the battery). The output electrodes are connected to a voltage measuring device (the voltmeter). A magnetic field is impressed as sown (perpendicular to the plane of the drawing).

Photons entering the semiconductor bar produce photoelectrons (and holes) which move under the combined effects of the electric and magnetic fields. The photoelectrons (and holes) move in curved paths with the result that an excess of electron is accumulated at one output electrode and a scarcity of electrons at the other. Thus, a voltage is generated across the output electrodes.
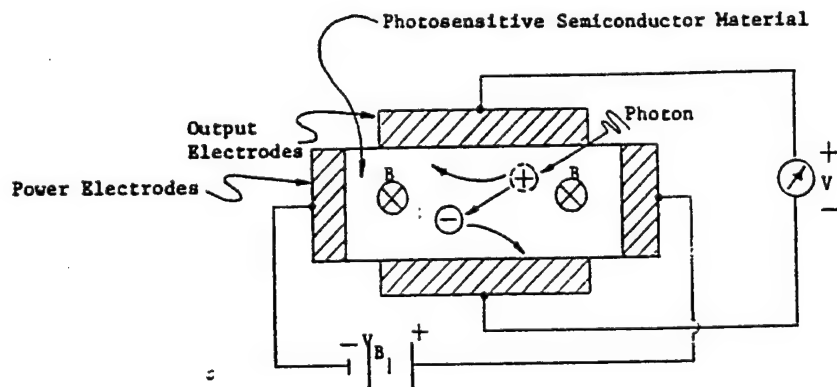

FIG 5.8   Photoelectromagnetic Radiation Detector

5.4.7   THE PHOTOGRAPHIC RADIATION DETECTOR. The photographic radiation detector consists of a thin film of a photosensitive material. The photosensitive material undergoes a chemical change when exposed to radiation of sufficient energy (of sufficiently high frequency) to release electrons from atoms within the substance. When the radiation incident upon the photosensitive film represents an image (focused on the film), that image can be made evident by further chemical processing.

5.5   SEMICONDUCTORS. Photoconductive detectors are most commonly used in IR systems since they are capable of operating out into the far IR region. Two kinds of semiconductors are available--intrinsic semiconductors and extrinsic semiconductors.

5.5.1   INTRINSIC SEMICONDUCTORS. Intrinsic semiconductors are obtained by refining the material to a high degree of purity. They are insulators at absolute zero since the valence band is full and the conduction band is empty. As the temperature is increased, an increasing number of electrons obtain sufficient energy to cross the energy gap between the valence and conduction bands. If the semiconductor is irradiated with photons of the correct energy, electrons can again be excited into the conduction band and this is the photoconductive process. The thermally excited electrons are a prime source of detector noise and this effect can be reduced by cooling the detector to very low temperatures. The characteristics of common intrinsic detectors are given in Table 4.

5.5.2   EXTRINSIC SEMICONDUCTORS. Efforts to exploit materials with smaller intrinsic energy gaps for operation at longer · wavelengths have so far been unsuccessful. Progress towards operation at longer wavelengths has been based mainly on the exploitation of the small energies required to ionize impurity atoms in the pure host material. The deliberate introduction of impurity atoms into the host material is known as doping and quite small concentrations of impurity substantially increase the conductivity of the material which results from irradiation. This process is called extrinsic detection. It will be appreciated that the smaller the ionization energy the lower must be the detector's operating temperature if thermal ionization (noise) is to be kept acceptably low. The characteristics of common extrinsic detectors are given in Table 5.

Detector Material (Operating Mode)	Approx Cut Off Wavelength (μ)	Operating Temp (°K)	Typical Time Constant (sec)	D* (1000 Hz) cm Hz$^{1/2}$watt^{-1}
Lead Sulphide (PbS) (pc)	4	77	3×10^{-3}	2×10^{11}
Indium Arsenide (InAs) (pv)	4	77	5×10^{-7}	4×10^{11}
Lead Selenide (PbSc) (pc)	6	77	4×10^{-5}	3×10^{10}
Indium Antimonide (InSb) (pc)	5.5	77	6×10^{-6}	8×10^{10}
	7.5	295	1×10^{-6}	2×10^{8}

Table 4.   Characteristics of Common Intrinsic Detectors

Detector Material (Operating Mode)	Approx Cut Off Wavelength (μ)	Operating Temp (°K)	Typical Time Constant (sec)	D* (1000 Hz) cm Hz$^{1/2}$watt^{-1}
Mercury doped Germanium (Ge:Hg) (pc)	14	27	2×10^{-7}	2×10^{10}
Mercury Cadmium Telluride ((Hg:Cd)Te) (pv)	13	77	$<1 \times 10^{-8}$	5×10^{9}
Cadmium doped Germanium (Ge:Cd) (pc)	20	4.2	1×10^{-7}	2×10^{10}
Antimony doped Silicon (Si:Sb) (pc)	23	4.2	1×10^{-7}	1×10^{10}
Copper doped Germanium (Ge:Cu) (pc)	27	4.2	5×10^{-7}	3×10^{10}
Zinc doped Germanium (Ge:Zn) (pc)	40	4.2	2×10^{-8}	1.5×10^{10}

Table 5.   Characteristics of Common Extrinsic Detectors

Finally, Figure 5.9 shows the parameter D* against wavelength for some of the previously mentioned IR detectors. The curves are for a particular material operating at a specified temperature. The two dark curves are for the (currently) most preferred detectors: InSo and HgCdTe (or MCT). Note that these matter very sharp cut off frequency.
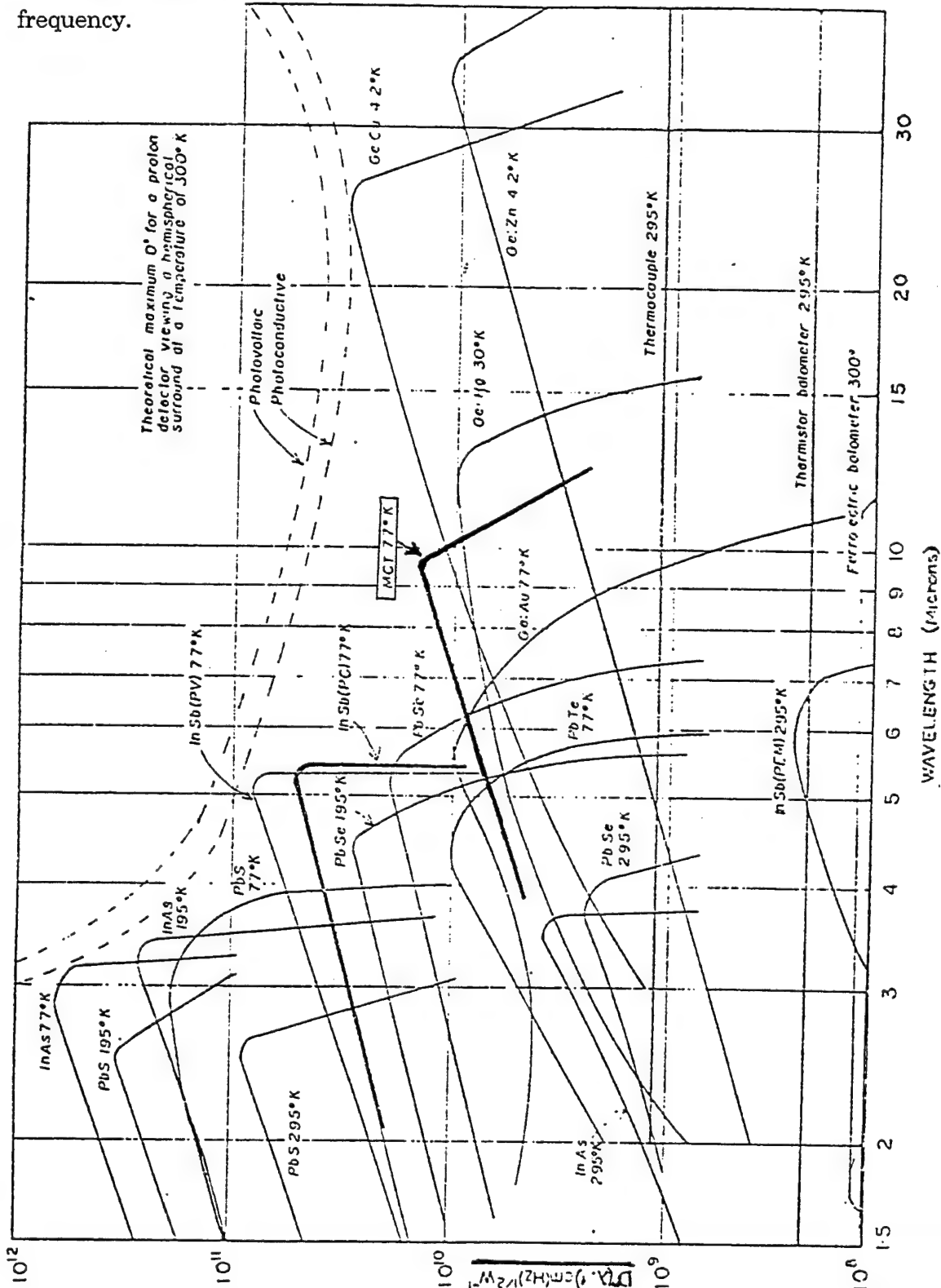

Figure 8.3.10.   D* Versus Wavelength for Various Detectors

5.6   RADIATION DETECTOR NOISE.

As previously indicated, signal-to-noise ratio, (rather than signal alone), generally determines system performance. For that reason, noise assumes an importance equal to that of the signal itself. In a radiation sensor, two fundamentally different types of noise are evident: externally generated noise (produced by background clutter in the sensor field-of-view) and internally generated noise (produced by the sensor system itself).

5.6.1   EXTERNALLY GENERATED NOISE.

Externally generated noise, which is dominated by background radiation noise, can be reduced only by limiting the response of the sensor system. Sensor response characteristics that often can be limited to increase the signal-to-noise ratio include: field-of-view-, spectral response (bandwidth), spatial response (spatial frequency response or angular resolution), time response, and threshold sensitivity.

Field-of-View Limiting. The sensor field-of-view can be reduced by means of appropriate optical design, including the use of field stops. Limiting the field-of-view discriminates against clutter of spatial extent greater than that of the intended target.

Spectral Response Limiting. Limiting the spectral response of the system can be accomplished by selection of the radiation detector or by the use of chromatic filters. In either case, the result is to discriminate against the clutter on the basis of frequency (wavelength).

Spatial Response Limiting. The spatial response of the system can be limited by spatial filtering, generally achieved by the use of reticles or by controlling the shape and size of the radiation detector. Spatial filtering discriminates against clutter on the basis of size and shape.

Time Response Limiting. The time response of the sensor is limited by frequency filtering of the signal after conversion from the space domain to the time domain. A typical example is the use of an electronic low pass (smoothing) filter to attenuate the time response of a scanning system to a flare (very strong point source).

Threshold Sensitivity Limiting. The threshold sensitivity of a radiation sensor can be adjusted to discriminate against low level clutter.

Limiting the response of the radiation sensor by any of these methods degrades the performance of the system to some extent. The use of these techniques is, therefore, restricted by the required performance of the system.

5.6.2 INTERNALLY GENERATED NOISE. Internal noise, usually referred to as system noise, is the noise generated in the preprocessing components such as the detector, preamplifier, transmitter, etc. The major sources of internally generated noise are radiation effects, thermal effects, and electronic effects. Radiation effects are caused by extraneous radiation reaching the radiation detector. Thermal effects are short term effects due to thermal noise and long term effects due to component heating. Electronic effects are caused by inadvertent electric and magnetic coupling and by the discrete nature of electronic phenomena. The dominant source of noise in a radiation source of noise in a radiation sensor is the radiation detector itself. Radiation detector noise is the vector sum of the six types of noise discussed in the following paragraphs.

Thermal (Johnson) Noise. Thermal noise is caused by the thermal motion of the electrons in a resistive component. The power amplitude of thermal noise is proportional to the absolute temperature of the component. The RMS value of the thermal (Johnson) noise voltage is given by the equation:

$$V_J = [4kR\ (\Delta f)\ T]^{1/2} \qquad (5.14)$$

where: k = Boltzmann's Constant
                          R = Resistance (Ohms)
                          T = Component Absolute Temperature (Deg., K)
                          (Δf) = Noise Bandwidth of Measuring System (Hertz)

Note that thermal noise is white (i.e., not a function of frequency). Since the other major types of detector noise decrease with frequency, thermal noise generally dominates at high frequencies. As suggested by the above equation, thermal noise can be reduced by lowering the temperature of the detector or reducing the bandwidth of the system.

Contact Noise. Contact noise is caused by fluctuations in the contact resistance at discontinuities and interfaces between materials of differing electrical properties. Because the power varies inversely with frequency, contact noise is sometimes called "1/f" (one-over-f) noise. It also is sometimes called "excess noise" and "current noise".

The RMS value of the contact noise voltage is given by the equation:

$$V_c = C_n \, R \, I \left[\frac{\Delta f}{f}\right]^{1/2} \qquad\qquad (5.15)$$

where: Cn = Constant Characteristic of Material (N.D.)
                      I = Average Detector Current (Amps)
                      R = Detector Resistance (Ohms)

Because of its (1/f) characteristic, contact noise generally dominates at very low frequencies in a radiation detector. For the same reason, it is usually negligible above a few hundred hertz and therefore can be eliminated by optical modulation above that frequency.

Generation/Recombination Noise.   Generation/recombination noise is caused by fluctuations in the rates at which charge carriers (electrons and holes) are generated and destroyed within a semiconductor.   Such carriers are created by photon absorption and by the motion and by the motion of electrons in the semiconductor material. The RMP amplitude of the generation/recombination noise voltage is given by the equation:

$$V_{GR} = I \, R \left[\frac{4\tau \, (\Delta f)}{n(1 \, + \, 4 \, \pi^2 \, \tau^2 \, f^2)}\right]^{1/2} \quad (Volts, RMS) \qquad (5.16)$$

where: f = Frequency (Hertz)
                      I = Average Detector Current (Amps)
                      n = Carrier Charge Population (N.D.)
                      R = Detector Resistance (Ohms)
                      (Δf) = System Noise Bandwidth (Hertz)
                      τ = Carrier Charge Lifetime (Secs)

Generation/noise is generally dominant at midfrequencies in photon detectors and can be reduced by "doping" of the semiconductor material and by limiting the system bandwidth.

Shot Noise. Shot noise is caused by random fluctuations in the rate of arrival of electrons at an internal junction in an electrical circuit. (It is called "shot" noise

because, at low current levels, it sounds like shotgun pellets (shot) sprinkled on a tin roof). The RMS amplitude of the shot noise voltage is given by the equation:

$$V_s = R\,[2q_e\,I\,(\Delta f)]^{1/2} \qquad \text{(Volts, RMS)} \qquad (5.17)$$

where: I = Average Detector Current due to Photon Absorption (Amps)
                          qe = Electronic Charge (Coulombs)
                          R = Detector Resistance (Ohms)
                          (Δf) = System Noise Bandwidth (Hertz)

Shot noise is generally dominated by other noise processes though it can be significant in photon detectors. Shot noise can be reduced by limiting system bandwidth.

$$V_p = R\left[2q_e\,\overline{I_r}\,(\Delta f)\right]^{1/2} \qquad (Volts, RMS) \qquad (5.19)$$

where: $\overline{I_r}$ = Average Detector Current due to Photon Absorption (Amsp)

               q_e = Electronic Charge (Coulombs)

               R   = Detector Resistance (Ohms)

               (Δf) = System Noise Bandwidth (Hertz)

Although photon noise is caused by photons originating external to the sensor, it is considered internal noise because it arises as the result of an internal process (photon absorption). Although photon noise is usually dominated by other noise processes, it can be significant in background limited detectors. Photon noise can be reduced by limiting the bandwidth of the system.

Temperature Noise. Temperature noise is caused by fluctuations in the rate at which heat is absorbed and dissipated by the detector. It is not thermal (Johnson) noise, however, but is caused by variations in the electrical properties of the detector with temperature (temperature coefficients). Temperature noise is generally significant only in thermal type radiation detectors and is usually dominated by other noise processes. Temperature noise can be minimized by proper cooling and thermal isolation of the detector.

Total Internally Generated Noise. The combined effects of the dominant internal noise sources in a radiation detector are shown in Figure 5.10. The individual noise voltages are assumed to be statistically independent and are, therefore, root-sum-

squared according to the equation:

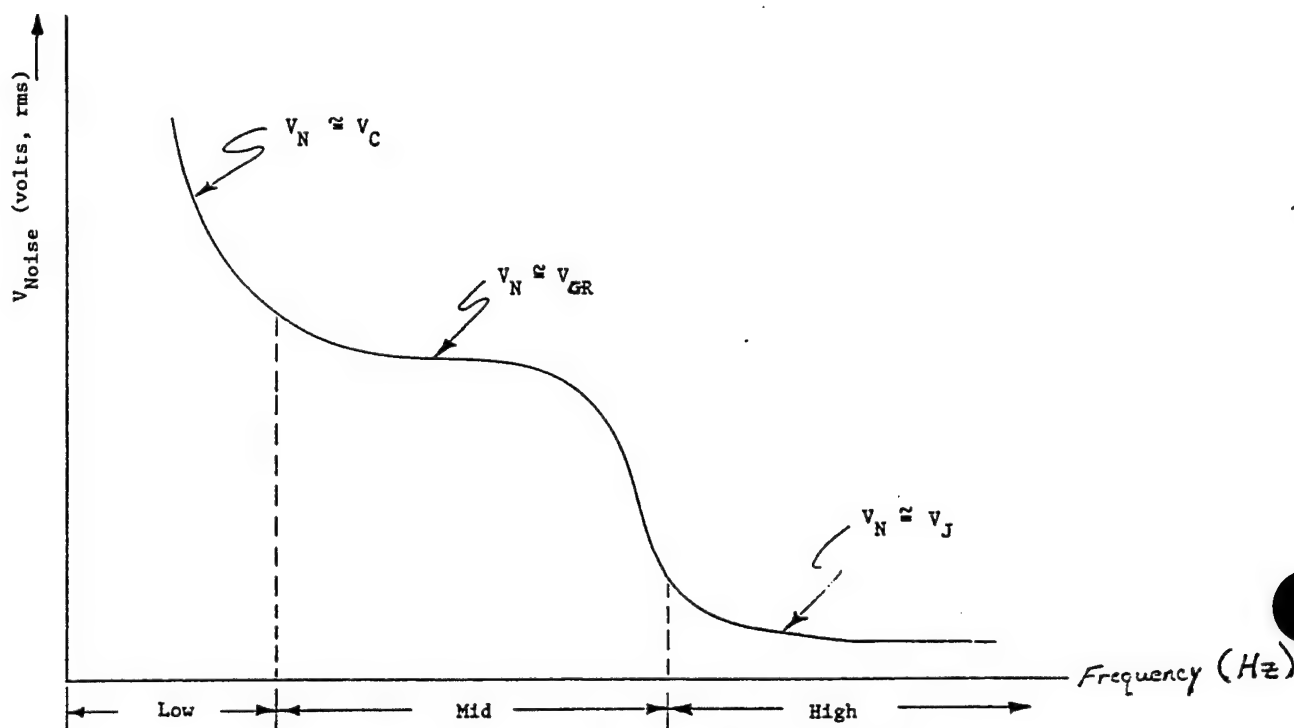$$V_{Noise} = [V_C^2 + V_{GR}^2 + V_S^2]^{1/2} \quad (Volts, \ RMS) \qquad (5.19)$$

Figure 5.10   Radiation Detector Noise

Note that, in the low frequency range, contact (1/f) noise dominates; in the midfrequency range, generation/recombination noise dominates; and in the high frequency range, thermal (Johnson) noise dominates.

<u>Background Limited Infrared Photodetection (BLIP)</u>. The goal of radiation sensor design is to reduce the internally generated noise to the level where the external (target background) noise is dominant. Such a sensor is said to be in BLIP operation. Further increase in signal-to-noise ratio can be obtained by employing temporal,

chromatic, or spatial filtering to discriminate between target and clutter. A theoretical limit exists in the specific detectivity (D*) that can be achieved for a given detector field-of-view and target background temperature (background radiation level). The theoretical limit on specific detectivity is given by the equation:

$$D^*_{LIMIT} = \left[\frac{\lambda}{2hc}\right]\left[\frac{\eta}{Q_b}\right]^{1/2} \qquad (5.20)$$

where: c = Velocity of Propagation (cm/Sec)

h = Planck's Constant

Q_b = Background Photon Flux (Photons/Sec)

η = Responsive Quantum Efficiency (N.D.)

λ = Wavelength (cm)

5.7 MERCURY CADIUM TELLURIDE. The Mercury Cadium Telluride
(MCT) detectors provide outstanding performance in the 8 to 14 micrometer region with a spectral response that extends as low as 2 µm. MCT detectors are presently being employed in Infrared Detecting Systems. The MCT detector requires an operating temperature of 77°K or -196°C for operation which allows a choice in the type of cool down system to be sued.

5.8 DETECTOR COOLING SYSTEMS. The proper operating temperature
for an electro-optical detector is determined by studying the effect of temperature on the detector parameters, and selecting the temperature that provides the optimum results for the detector under consideration. The major requirements of a detector cooling system are: long operating time, stable temperatures, light weight, small size, and maximum reliability. Baths of liquefied gases are the most frequently used method of providing low temperatures because of their simplicity of design and compactness. Dewar flasks are used to house the coolant which reduces the detector temperature.

5.9 CRYOGENIC COOLER/DEWAR. Recently manufactured Infrared
Detecting Systems use a combination cooler/dewar assembly to cool the IR detectors. Since the detectors must be cooled to an extremely cold temperature, it is necessary that they be mounted in a vacuum to minimize the transfer of heat from the outside environment. A dewar assembly is used to provide this thermal isolation with the detectors being mounted on the inside of the vacuum chamber. Infrared radiation

which has passed through the system's optics enters the dewar assembly through a special IR window and is absorbed by active area of the detectors. When the dewar assembly is mounted on a cooler, the detector mounting plate makes contact with a cold finger which extends from the cooler. Since MCT detectors are normally used. The Dewar assembly may be removed from the cooler for servicing, or may even be moved from cooler to cooler, without disturbing the vacuum integrity. (Figure 5.11).
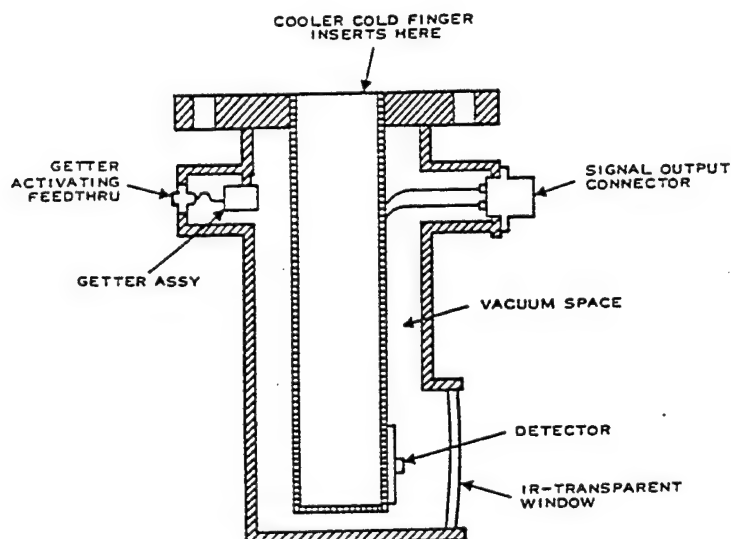
Figure 5.11   Dewar Assembly

The Stirling cycle cryogenic coolers' principle of operation is as follows (refer to Figure 5.12). This type of cooler uses two pistons; one alternately compresses and expands the refrigerant and a second shuttles between two operational positions. The shuttle piston is phased relative to the main compressor piston so that the working fluid is kept in contact with the area to be cooled during the time the compressor piston is allowing the refrigerant gas to expand and cool. During the compression and warming cycle, the shuttle moves to its other extreme position. A regenerator is located in the fluid path between the cold and hot stations and alternately removes heat from and returns heat to the fluid as it is passed from the cold to the hot station. Excess heat generated in the compression cycle is dissipated through an external heat exchanger.
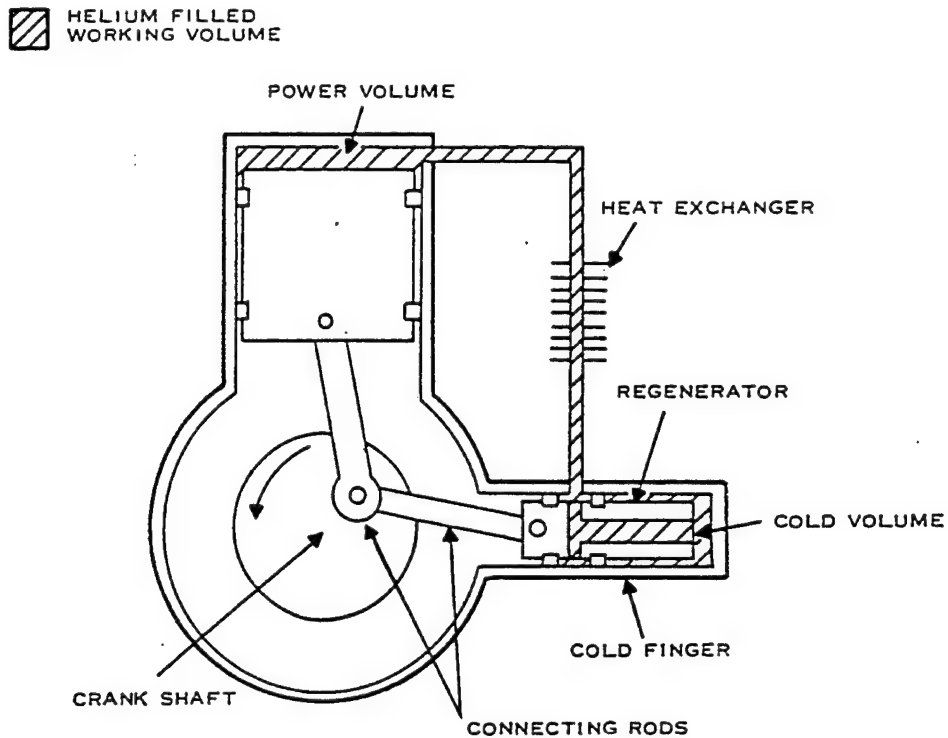
HELIUM FILLED
WORKING VOLUME

POWER VOLUME

HEAT EXCHANGER

REGENERATOR

COLD VOLUME

COLD FINGER

CRANK SHAFT

CONNECTING RODS

Figure 5.12   Stirling Cycle Cooler Schematic Diagram

5.10 SIGNAL PROCESSING - FROM IR TO VIDEO. Infrared radiation from the scanned scene enters the system's optics through the IR window. It passes through the IR optics and is focused onto the detector array. This infrared energy is absorbed by the detectors and transformed into a minute electrical signal. This minute signal is then used as the input signal for the preamplifiers. There is one preamplifier channel for each detector.

The signals generated by the detectors are unusable as a composite video signal because of their low level. For this reason, several stages of amplification are required to produce a usable signal. The signal to noise ratio is very critical when working with such a minute signal. With a signal of only a few microvolts, noise from

the detectors, the interconnecting wiring, or the early stages of amplification could mask the signal to the point that no intelligence is detectable in the output. Therefore, proper shielding is essential for the detectors, wiring, and preamplifiers and special care must be taken to limit the distance between the detectors and preamplifiers.

The detector signal is normally amplified from 70 to 1,500 times in the preamplifier. In all except the latest model Infrared Detecting Systems, a gain of approximately 1,000 would be considered normal. In the latest model systems the preamplifier gain may be as low as 70, therefore, more amplification is required in succeeding circuits. A gain adjustment is located either in the preamplifier or postamplifier to allow balancing of the video output.

The output from the preamplifiers provides the input for the postamplifiers which is sometimes referred to as the video processor or video control. There is a separate postamplifier channel for each preamplifier channel. In the postamplifier the video signal is amplified to the level necessary to drive the LED's. The postamplifier circuit also contains the summing circuitry for video gating, gain control, level control, and video polarity (white hot/black hot).

Video on/off time is determined by the gating circuits located in the auxiliary electronics section of the system. As the scan mirror moves across the scene, IR energy will be reflected onto the detectors. At certain points in scan cycle the mirror will be in a position where IR energy passing through the optics will not be reflected onto the detectors. This part of the scan is referred to as the inactive part of the scan cycle, and that part of the cycle where video is reflected on the detectors is called the active part. The gating circuit gates the video off during the inactive part of the scan. The width of the video gate will determine how much of the active video time is actually used for recording or viewing. Full active time is referred to gating the entire active part of the scan cycle "ON".

On many of the infrared systems, the operator can select either white hot or black hot by utilizing a polarity with which is located on the control panel. This switch activates an additional inverter stage on each of the postamplifiers and reverses the polarity of the video signal. Thus, hot infrared targets can be made to appear as either black or white targets on the display.

The IR Level (brightness), Video gate, video polarity, and gain control circuits are all located in auxiliary electronics. These signals are mixed with the video signal in the postamplifiers to produce a composite video output signal. This composite signal is used to control the brightness and contrast of the LEDs during the active part of the scan cycle. The LED output is used to reproduce the image of the scanned scene.

TV SYSTEMS

5.11 TV SYSTEMS. TV has been applied to a wide variety of uses in avionics systems ranging from aerial reconnaissance cameras to missile homing devices. The airborne TV versions differ in size and ruggedness from their commercial counterparts, but their principles of operation are identical.

TV is accomplished by scanning different parts of a scene with a camera tube which converts the incident light into photo-electric energy--a voltage proportional to the light intensity of the scene under examination. The varying voltage resulting from this scanning is amplified and can either be passed directly to a display, or it can be modulated upon a radio frequency carrier wave that is radiated to another area.

The display, or TV receiver, synthesizes the original fluorescent scene of a CRT by causing a cathode ray spot to trace over successive portions of the reproduced scene in accordance with the scanning of the original scene. At the same time, the CRT varies the brightness of the spot in accordance with the envelope amplitude of the received signal. As the scanning process is carried out with sufficient rapidity, an illusion of continuous, nonflickering motion is achieved.

5.11.1 TV CAMERA TUBES. As stated previously, a TV camera receives light energy from a scene and converts it into photo-electric energy. The TV camera is more sensitive than the human eye since it has higher quantum efficiency and a larger light sensitive area. There are two processes by which the conversion of light energy into electrical energy is obtained--photo-emission and photo-emission and photo-conduction.

Figure 5.13 shows the relationship between energy (eV) and wavelength (microns) for the EO part of the EM spectrum. For visible wavelengths ranging from .4μ to .7μ, the corresponding energy ranges from 3.3eV to 1.63eV.
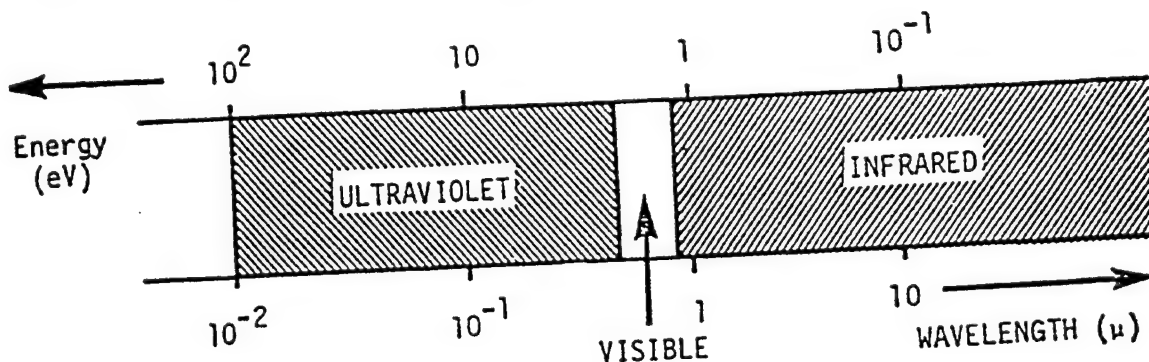

Figure 5.13 Wavelength/Energy Diagram

These energies are sufficient to cause the ejection of electrons from the surface of materials such as sodium, cesium, and potassium. The process is called photoemission and the number of electrons emitted is directly proportional to the incident light level.

If electrons are not ejected, but are moved to a higher energy level that corresponds to a conduction band, then the process is photoconduction. This process takes place in materials such as selenium, arsenic trisulphide, or lead monoxide, and conductivity increases with increasing light level.

There are two main types of TV camera tubes which have been generally used. They are the Vidicon, in which the optical/electrical conversion occurs by a photoconductive process, and the Orthicon, where the process is photoemissive. The Vidicon is widely used in many general and military applications, and the Orthicon was, until the advent of color, the standard broadcast tube.

5.11.2 THE VIDICON. The vidicon television camera tube, shown in Figure 5.14 is an electronbeam--scanning imaging sensor which scans the overall field-of-view by deflecting an internal electron beam. In the vidicon, the incoming radiation is focused onto an internal screen composed of photoconductive material. An conductivity. A narrow beam of electrons is deflected in such a way as to scan the back of the photoconductive screen as shown in the figure. When the electron beam impinges upon an irradiated area of the screen, the electrons are conducted through the screen to a transparent, conductive signal plate and into an external circuit. The resulting current in the external circuit constitutes the output signal from the sensor. Beam electrons not conducted through the photoconductive screen are collected by a grid (mesh), also shown in Figure 5.14. Suitable photoconductive materials are available which respond to radiation up to about 13 micrometers (μ) in wavelength.

An electron-multiplying target screen can be employed in a vidicon to increase the output of the sensor. A camera tube employing such a device called SEC (secondary electron conduction) vidicon, is illustrated in Figure 5.15. In a SEC vidicon, a photoemissive screen is eradicated by the incoming radiation, thus producing a photoemissive stream "image" as in the image converter/intensifier. The photoelectrons are accelerated toward, and focused upon, an internal screen called the "target". When the accelerated electrons strike the target, electrons within the target are ejected, (due to secondary emission) thereby leaving areas deficient in electrons on the target screen. The target screen is then scanned from behind by a narrow

electron beam. When the electron beam impinges upon an area of the screen deficient in electrons, electrons from the beam flow into the target and out into the external circuit, thus producing an output signal.
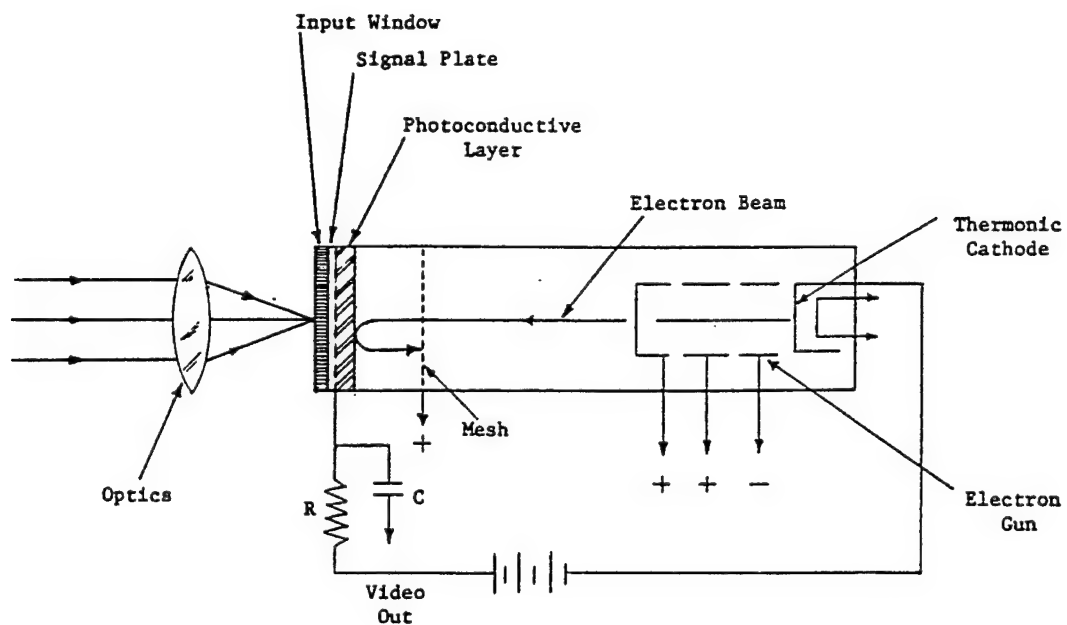
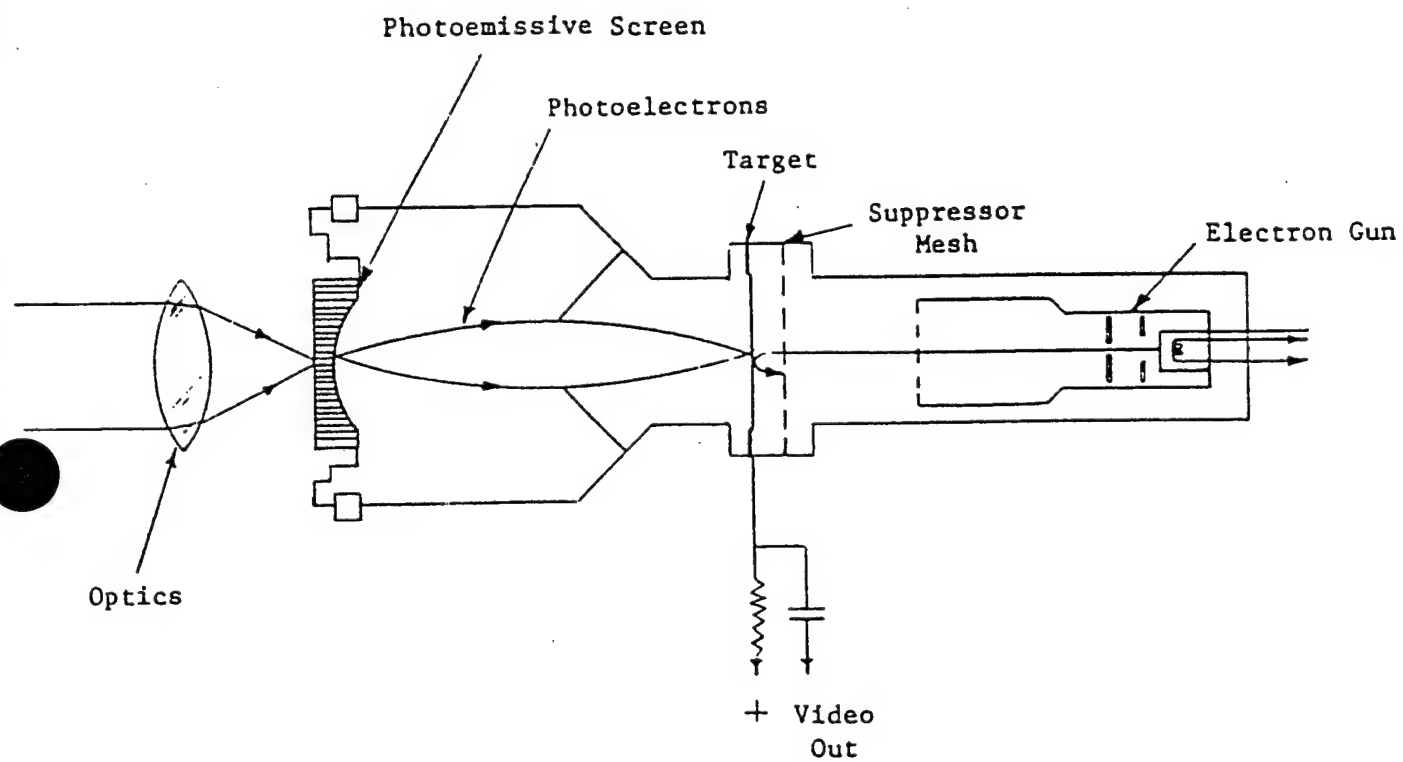Figure 5.14 The Vidicon Television Camera Tube

Figure *5.15*   The SEC Vidicon Television Camera Tube

5.11.3 LIMITATIONS OF THE SEC VIDICON. One limitation of the SEC vidicon that must be emphasized is its tendency to smear moving images. This is an example of the effect known as lag. Lag occurs in all TV tubes to some extent, and becomes worse at low light levels, and it can represent the real limit to tube performance in airborne applications. The causes of lag vary considerably from tube to tube. In the vidicon, the main lag effect is target element capacitance.

As a rule of thumb, if the human eye can discriminate a specific target or contrast feature, the EO weapon vidicon will also be able to define and display that particular feature. However, notable exception occurs when we deal with variations of the same basic color groups. Since EO vidicons delay only in black, white, and shades of gray, certain camouflage schemes when viewed against a similar background will be discernible by color contrasts to the human eye. The same color contrasts, however, may be converted to the same shade of gray and be indistinguishable on a TV display. A more dramatic example may be a day-glo orange practice target on a brown background. Here the color contrast is discernible for a great distance, but when converted to black, white, and gray contrast and resulting target definition are lacking.

Low ambient light conditions present special problems for an EO weapon. The vidicon system normally lacks the low light level TV systems filter wheels, and iris type devices used to operate over a wide range of lighting conditions. The photoconductive material used by the vidicon needs a minimum level of light intensity to function. Under low ambient light conditions, normally around sunrise or sunset, the signal-to-noise ratio between the light and dark contrast areas becomes too close for the video processor to resolve. The result is insufficient video contrast for video identification processor to resolve. The result is insufficient video contrast for video identification and target tracking.

Extremely bright light conditions (the sun in particular) also cause special problems for the vidicon system. A direct view of the sun, focused by the lens system onto the signal plate, will actually burn the photosensitive material. This damage shows up as a "scar" on the video and will severely degrade weapon performance if the scar covers any part of the tracking gate. Another problem encountered is illuminating targets at night. Bright night targets would be seemingly ideal EO targets. In face, however, the contrast is too great and a phenomenon called target bleed occurs. The target spreads out over nonilluminated areas and creates an indistinct target image.

A combination of target bleed and processor logic, which identifies the contrast as noise, degrades tracker performance.

5.11.4 THE ORTHICON. Another type of electron-beam-scanned TV camera tube is the image orthicon shown in Figure 5.16. The orthicon is the basic photoemissive tube. In an image orthicon, the incoming radiation is focused upon a photocathode, thus producing an electron-cloud "image" of the field-of-view. These photoelectrons are accelerated toward a target screen as shown in the figure. The accelerated electrons strike the target screen producing secondary emission and leave areas of the screen deficient in electrons. The screen is then scanned from behind by a narrow beam of electrons. Where the scanning beam impinges upon an electron-deficient area of the target screen, the beam loses electrons to the screen. The electrons remaining in the beam (not absorbed by the target) constitute the output signal and are returned to an electron multiplier in the base of the camera tube. The electron multiplier, a device which amplifies current by cascading secondary emission, greatly increases the output current. The image orthicon is, therefore, much more sensitive than a vidicon. However, it has limitations as a low light tube because of its poor noise performance at low light levels.
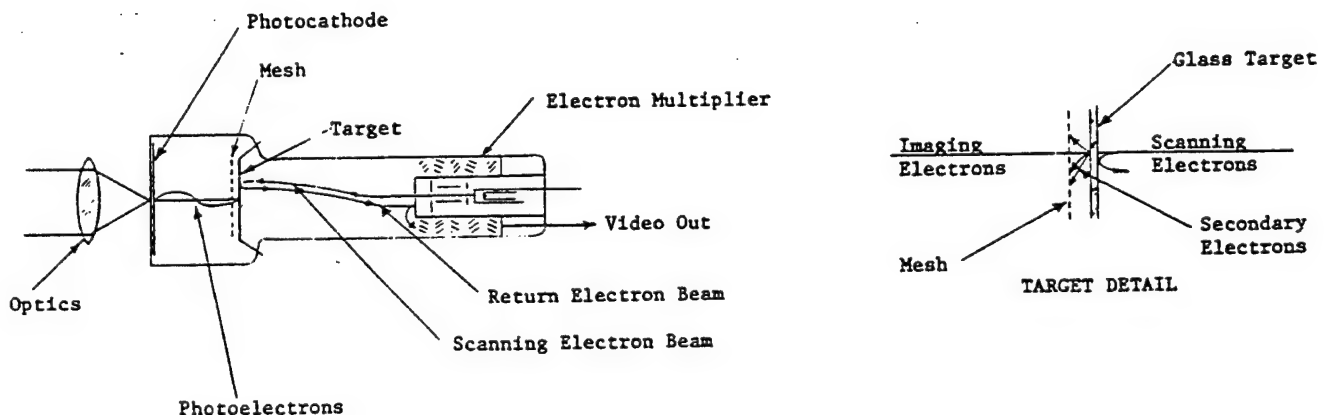
Figure 5.16   The Image Orthicon Television Camera Tube

5.11.5 OPTICALLY SCANNED IMAGING SENSORS.

Optically scanned imaging sensors employ point source radiation detectors and scan the field-of-view by deflecting the incoming radiation or by moving the radiation detector elements. The scanning motion can be effected by moving components in the optical system, moving the detectors only, or moving the entire sensor. Scanning of the two dimensional field-of-view can be performed by scanning a point source detector in two dimensions or by scanning a linear array (line) of detectors in a single dimension. An example of the later (one dimensional scanning of a linear detector array) is the airborne I/R ground mapping arrangement showing in Figure 5.17. The linear array of detectors is mounted on the underside of an aircraft so as to view a narrow strip of ground track. Thus, the forward motion of the aircraft provides the required one dimensional scanning motion for the sensor, the detectors viewing a "swatch" of terrain parallel to the ground track. The individual outputs of the detectors are amplified and used to drive light emitting diodes mounted in a linear array similar to that of the detectors. Photosensitive film is transported past the LED array in a direction transverse to the array thus irradiating a "swath" of film and reproducing the ground I/R radiation pattern viewed by the detector array. In order to reproduce the radiation pattern without distortion, the rate at which the film is transported pas the LED array must be proportional to the ground speed of the aircraft. The need for synchronization between sensor field-of-view scanning and display implementation is common to all scanned imaging sensors and is shown explicitly in the figure.

A two dimensional scanning mechanism for an airborne ground mapper is shown in Figure 5.18. With such a mechanism a single detector element is used with the cross-track scanning being provided by the rotating mirror. Along-track scanning is provided by the motion of the aircraft. Unless measures are taken to remove distortion in this type of system, distortion will be present due to geometry (for large angles off the vertical) and due to lateral motion (drift) of the aircraft.
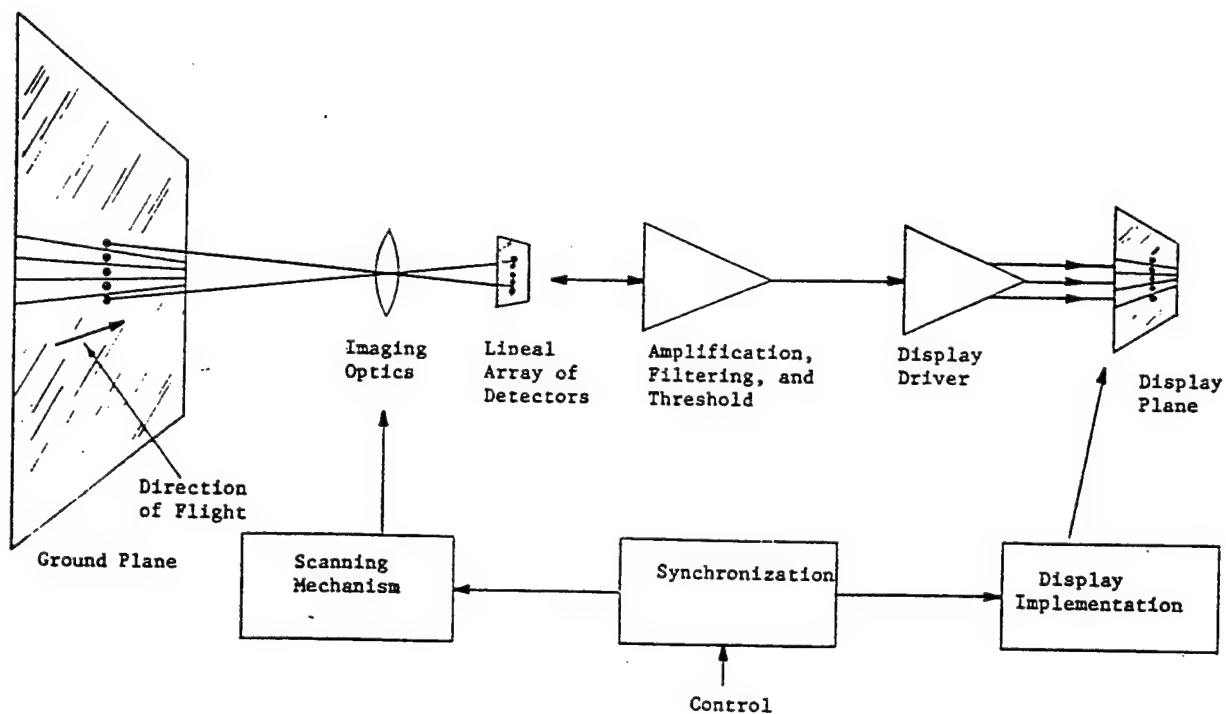
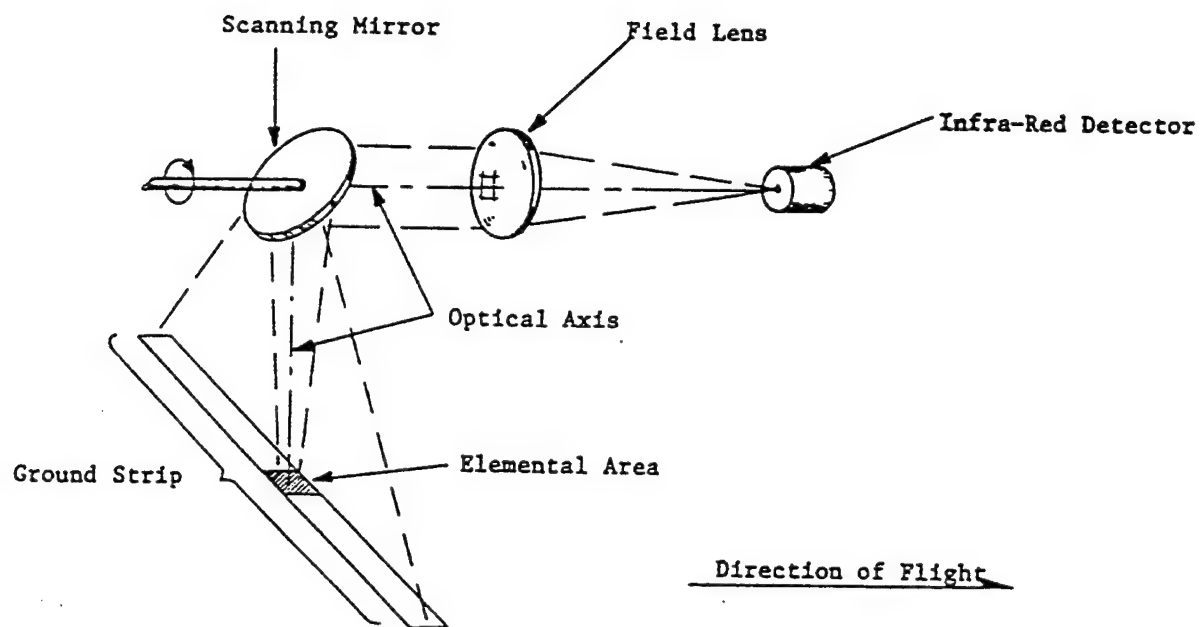Figure 5.17   One-Dimensionally Scanned Ground Mapper

Figure   5.18   Two-Dimensionally-Scanned Ground Mapper

5.11.6 COLOR TELEVISION CAMERAS. After light passes through the reticle, color cameras split the light into three primary colors. Then three individual camera tubes generate electrical signals from each of these primary colors. In some color cameras, a forth tube is used to provide an improved monochrome picture and better details for the color picture.

Except for the number of camera tubes, the distinguishing feature of the color camera is its optical system. The color cameras optical system divides or splits all light entering the camera's lens into separate color beams: one beam for each camera tube. This beam-splitting is accomplished by mirrors, prisms, and lenses arranged in a unit called a beam-splitter.

Figure 5.18.A shows a simplified diagram of a 4-way beam-splitter used in a typical 4-tube camera. Incident light from the scene being televised is divided into two parts. One part of the split beam is focused onto the fourth camera tube to provide the monochromatic video signal or luminance channel. The other part of the beam is reflected by a front-surface mirror through a relay lens into a system of dichroic mirrors. These mirrors are designed to reflect light of only one particular color and to allow light of all the other colors to pass through. In the figure, the first dichroic mirror(1) reflects only the red light from the scene onto the red-channel tube to provide the R voltage of the video signal. Likewise, the second mirror reflects blue light and the remaining green light is directed to the green-channel tube. The final color video signal is composed of the red, blue, green and luminance channels.

FIGURE 5.18A
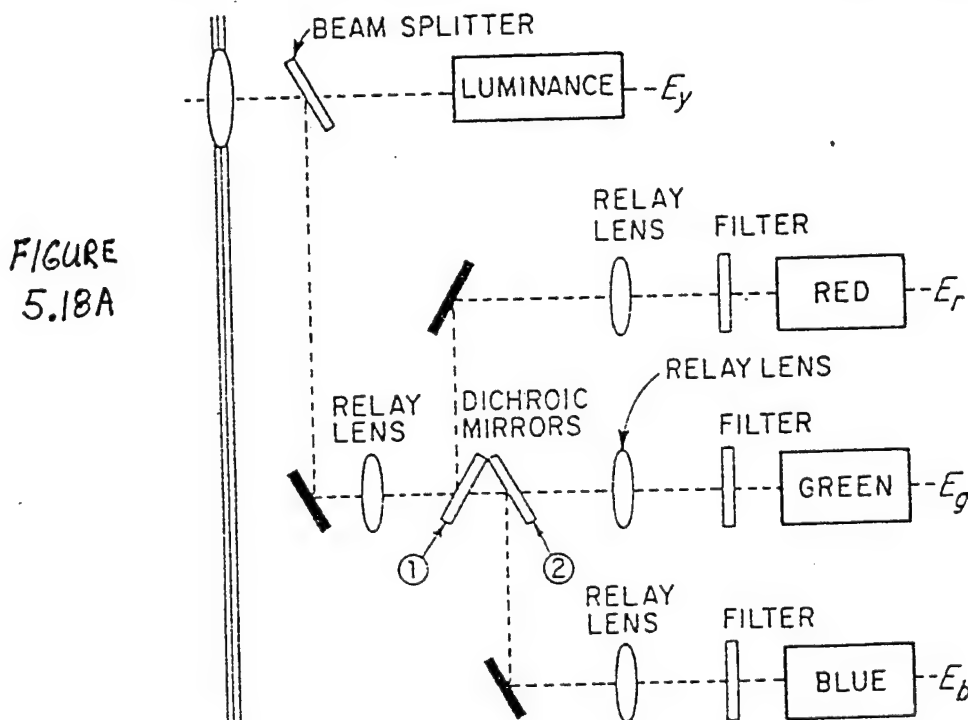
5.11.7 CHARGE COUPLED DEVICE (CCD). A Charge Coupled Device (CCD) is the solid-state equivalent of a vidicon tube. The CCD is a staring focal plane assembly (two-dimensional detector array) consisting of individual detector chips. Each detector chip creates an element or pixel of the image. Over a short period of time, called the accumulation time, each detector of the CCD array converts incident illumination into a proportional charge or charge packet. Each charge packet is then electronically transferred to a single output. The orderly transfer of the charge packet, or information stored by each detector element, constitutes the main technological problem which the CCD must overcome.
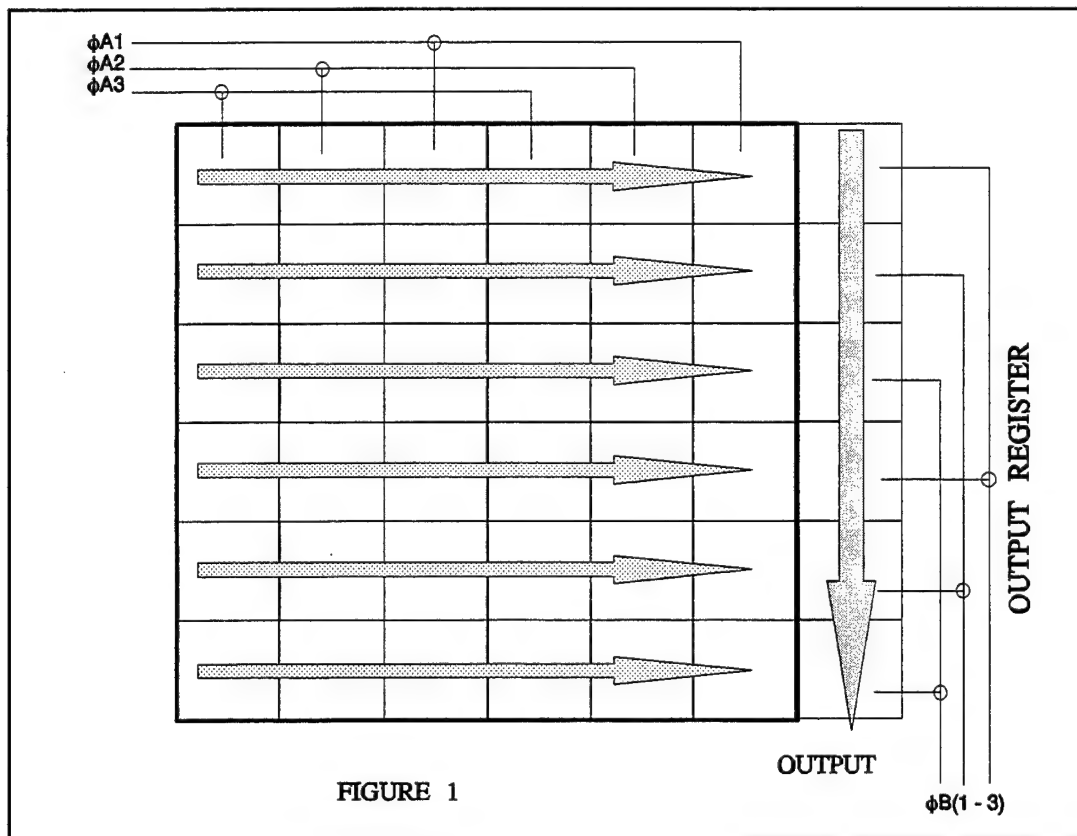

FIGURE 1

Figure 5.18.B shows a simplified example of a CCD device. During the accumulation time each detector builds an electrical charge proportional to the electromagnetic energy that is incident upon it. The charge from each row of the CCD is then transferred serially to the output register. The output register then transfers each charge to a single serial output where, again, each charge represents the output of one detector element.

Figure 5.18.C shows the build up of charge under each detector element during the accumulation time. Figure 5.13.D shows the transfer of that charge(or information from each detector element) toward the output gate or output register. In a charge coupled device, potential "wells" are formed by closely spaced metal oxide silicon (MOS) capacitors. These wells or depletion regions are formed by a multiphase clock voltage. The charge is transferred from one well to another by applying clock signals to the gates. As in the figure 5.13.D example, increasing the negative voltage to the second gate caused the well under the second gate to go deeper. At Time = T(3) in the figure, the voltage to the first gate is decreased as the voltage to the second gate is increase further causing the charge to spill into the well under the second gate.

For the device shown, three of the gates make up a stage in this multistage CCD. When the charge is in the well under the third gate, it can be passed along to the first gate of the next stage.

As the technology evolves, the number of individual detectors on a given area of the detector continues to increase. State-of-the-art provides over 400,000 detectors on a one-half inch chip. As this number of detectors is increased, the camera's resolution is increased or the size of the chip and resulting camera can be decreased.
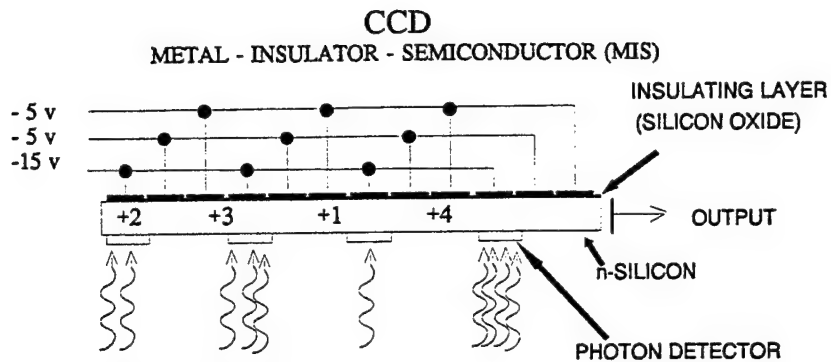
CCD
METAL - INSULATOR - SEMICONDUCTOR (MIS)

- 5 v
- 5 v
-15 v

INSULATING LAYER
(SILICON OXIDE)

+2   +3   +1   +4

OUTPUT

n-SILICON

PHOTON DETECTOR

FIG 5.18 C

- 5 v
- 5 v
-15 v

TIME = T(1)

PHOTO DETECTOR GENERATED (+)
CHARGE IS TRAPPED IN NEGATIVE
CHARGE WELLS

POTENTIAL WELL

- 5 v
-10 v
-10 v

TIME = T(2)

CHARGES MOVING TOWARD OUTPUT

- 5 v
-15 v
- 5 v

TIME = T(3)

(+) CHARGE PACKETS CONTINUE
TOWARD SERIAL OUTPUT

-10 v
-10 v
- 5 v

TIME = T(4)
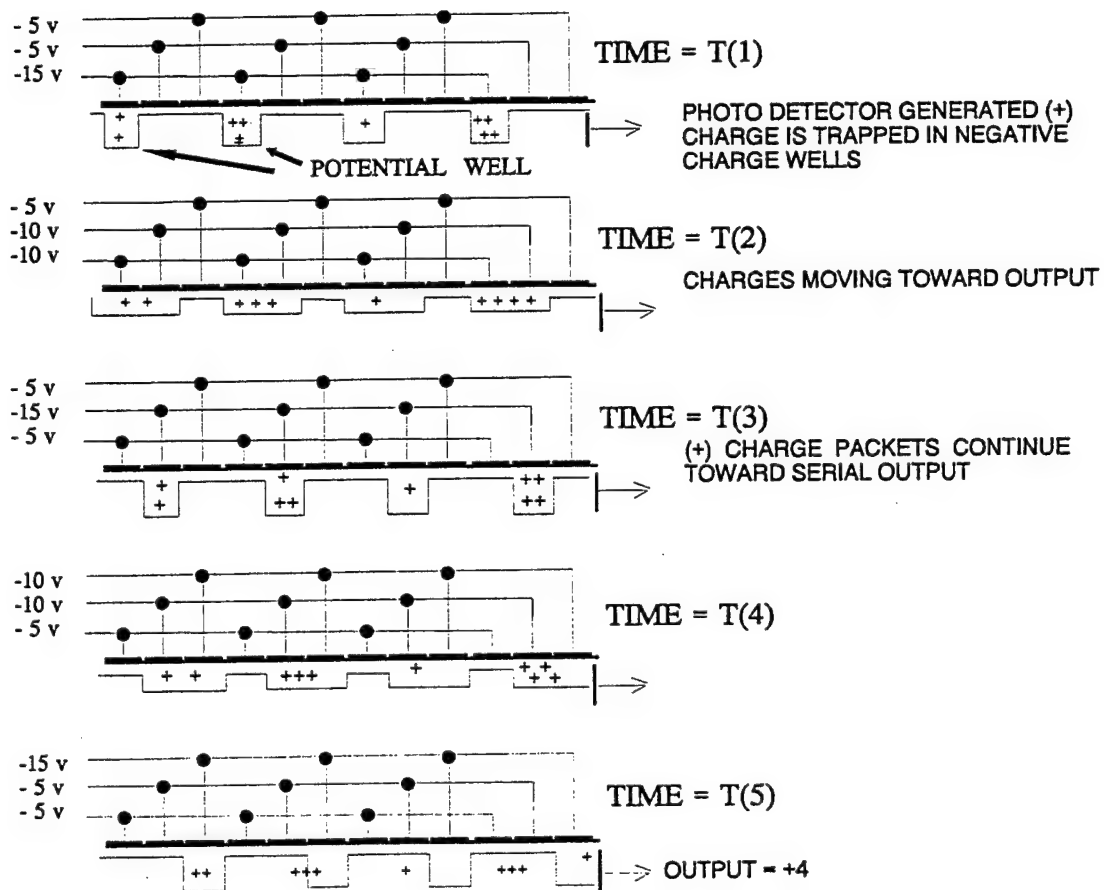
-15 v
- 5 v
- 5 v

TIME = T(5)

OUTPUT = +4

FIG 5.18 D

5.12 LOW LIGHT LEVEL TV (LLTV) SYSTEMS.
Low light level TV systems are light amplification devices which can extend human vision down to very low levels of ambient lighting. By definition, a light amplifier is any electronic device which, when actuate by a light image, can reproduce a similar image of enhanced brightness and which is capable of operating at very low light levels without introducing spurious brightness variations in the reproduced image. The range of illumination levels available to us is shown in Figure 5.19.
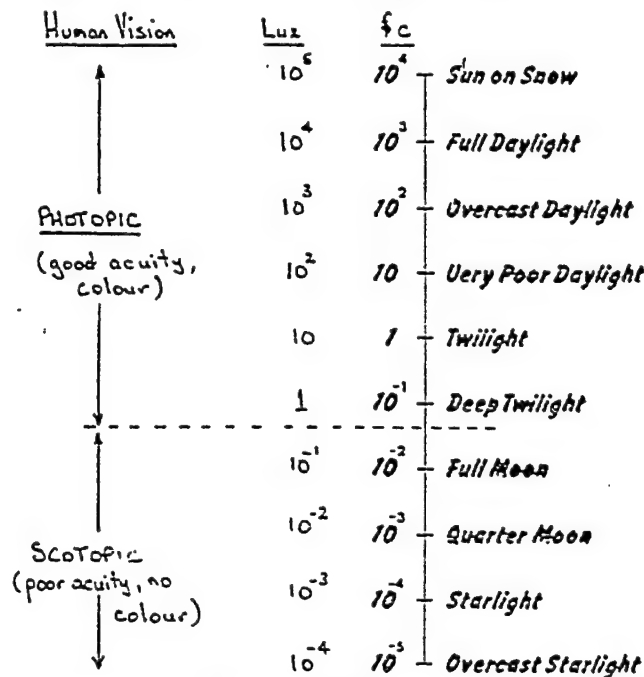

The human eye is at its maximum efficiency in daylight. The eye adjusts to lower illumination levels by pupil dilation, the use of rods in lieu of cones, and by integrating light signals over a longer time interval. The eye can see in conditions of darkness between 10^{-1} and 10^{-2} foot candles; however, no color perception is now available. The acuity (resolving power) of the eye decreases rapidly with decreasing light level, such that at 10^{-5} fc (the lowest occurring natural light level) the eye is only capable of discerning large, high contrast subjects and only after a long period of dark adaptation.

Military aircraft obviously need to operate by day and night and one of the great advantages of LLTV systems is that they provide a bright image in almost completely dark conditions. The operator's eyes can operate at their maximum efficiency as LLTV represents an extension of normal vision in otherwise adverse conditions.

5.12.1 THE ENVIRONMENT. Before attempting to describe television techniques which have been developed for low light use, consider the illumination environment with which the television engineer is faced.

The television camera forms an image of the scene being viewed by utilizing a very small proportion of the radiant energy which is incident upon the scene. The amount of energy which strikes the camera sensor depends mainly on the:

    Incident Radiation Level
    Reflectance of the Subject
    Light Collecting Power of the Optical System

Further, the video signal current obtained from the sensor will be dependent on the:

    Spectral Response of the Sensor
    Spectral Energy Distribution of the Illuminance
    Sensitivity of the Camera Tube

Dealing just with the incident radiation level, these last three parameters will depend on many geographical and meteorological factors such as the time of night, the latitude, the delineation of the sun (i.e., the season), the phase of the moon, and the degree of cloud cover.

Study of measured light levels obtained from worldwide surveys shows that the minimum clear sky winter illumination are practically constant everywhere. A good practical figure for the minimum world wide illumination level is 1×10^{-5} fc. Values below this will be very rare. Figure 5.20 shows the proportion of the time that the light level exceeds a given value at different latitudes and indicates, for example, that in temperature climates the light level will be above 10^{-4} fc for 82% of the time.

Under clear sky, moonless conditions, the incident irradiance contains contributions from a number of separate sources:

    30% of the total is direct or scattered starlight
    15% is of Zodiacal origin
    5% is of galactic origin
    40% is from air glow
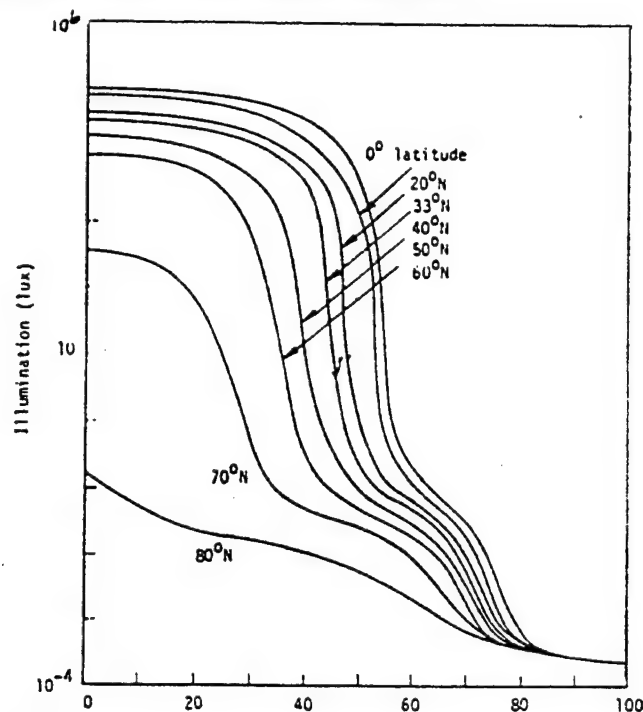
10% is scattered light from these various sources

Figure   5.20 Fraction of Time Illumination Exceeds Particular Values

The air glow (or night sky luminescence) phenomenon contributes nearly half the incident irradiance and originates from the ionization of rare gases in the upper atmosphere due to radiation. Studies show that the natural night sky spectral irradiance contains nearly ten times as many incident photons/units wavelength at 0.8μ as at 0.4μ. To make use of this high energy content, it is desirable that the sensor has the highest possible sensitivity in the red and near infrared parts of the spectrum.

5.12.2   SUBJECT REFLECTIONS AND CONTRAST. To the eye (and therefore to the TV camera since it is ultimately viewed by the eye), the brightness of an object depends not only on the illumination level, but also on how the object reflects the illumination. If all objects reflected an equal amount of light, there would be no contrast between a target and its background, and thus it would probably not be seen. In general, the reflectance of a surface depends on the type of surface, wavelength, and the illuminating and viewing angles. The reflectance (k) of an object is normally defined as the ratio of reflected to incident light. Typical values of reflectance are given in Table 2 below:

Snow	0.7 - 0.86
Clouds	0.5 - 0.75
Limestone	0.63
Dry Sand	0.24
Wet Sand	0.18
Bare Ground	0.03 - 0.2
Water	0.03 - 0.1
Forest	0.03 - 0.15
Grass	0.10 - 0.25
Rock	0.12 - 0.30
Concrete	0.15 - 0.35
Blacktop Roads	0.08 - 0.09

Before the TV tube can sense the scene, the scene must be imaged onto the tube through the sensor head optics. What really matters, therefore, is not so much the scene illumination, but the illumination at the focal plane of the objective lens. A simple analysis shows that:

$e = kE/4f^2$

Where

e = illumination at the focal plane

E = incident illumination

f - relative aperture of lens

k = reflectance

Thus, if k = 20% and f = 1.4

e = 1/40 E, i.e., 0.025 E

Closely tied in with reflectance is subject contrast. Contrast is defined in terms of highlight brightness (M) and is given by:

$$M = B_{max} - B_{min}/B_{max}$$

Where B_{max} is the maximum luminance and B_{min} the minimum luminance in the scene. Performance is often rated using 100% contrast test chart, but in practical airborne applications, contrast may be as low as 10%. The result of a reduction of contrast from 100% to 10% will be a reduction of resolution by a factor of 10, excluding noise effects.

5.12.3   IMAGE INTENSIFICATION. Neither the basic Vidicon nor the Orthicon tubes are inherently capable of low light operation, but variants of these two systems have been developed to enable them to operate as LLTVs, and one of the fundamental requirements in this development is the use of image intensifiers. Indeed, the fiber optically coupled image intensifier is a useful building block for any LLTV system.

5.12.3.1 FIBER OPTICS. A fiber optic plate, shown in Figure 5.21 is made up of a complex of minute glass tubes clad with another type of glass of lower refractive index. These tubes form "light guides" in which light entering at one end of the tube is trapped until it emerges at the other end. The cladding glass often includes a dark material known as dark cladding, which prevents crosstalk between adjacent fibers. These fiber optic plates have the useful property that they can transform the flat image plane of a conventional optical lens to the curved image plane of the simple electrostatic lens in an image intensifier.
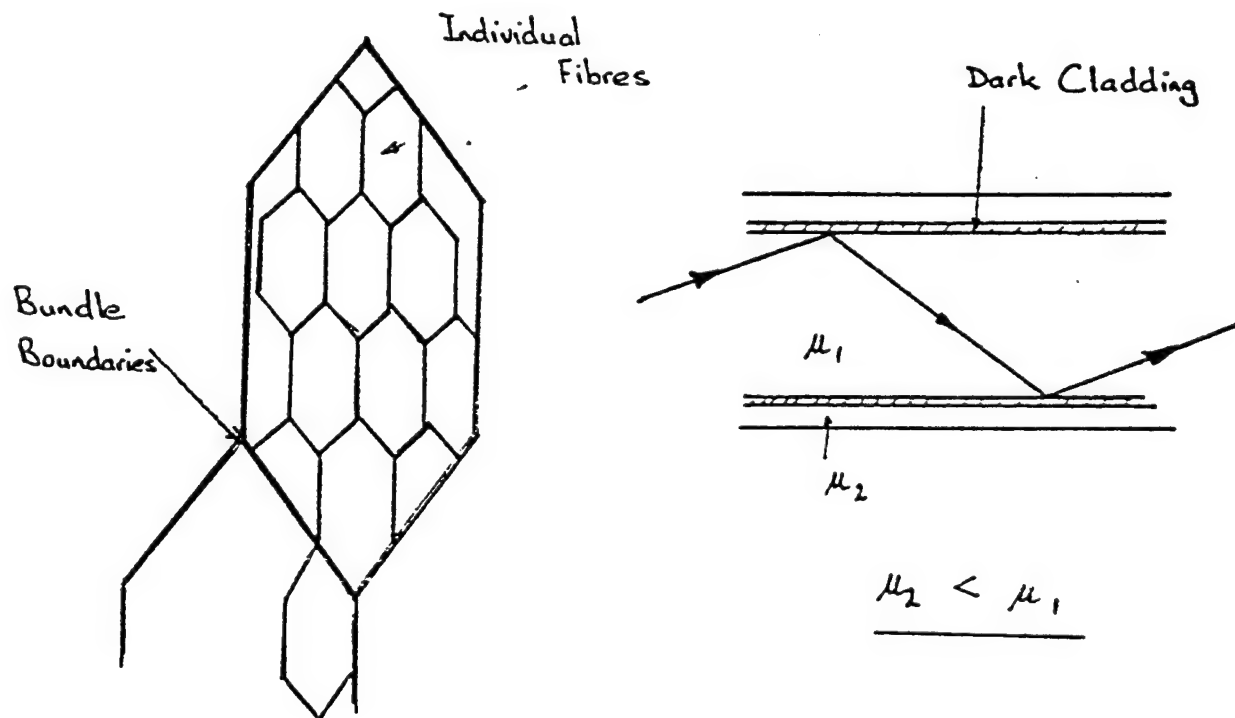

Figure   5.21 Fiber Optics

5.12.3.2 BASIC IMAGE INTENSIFIER. A basic image intensifier, also called an image tube or image converter tube, is an electron device that reproduces an image of the radiation pattern focused on its photosensitive surface onto its fluorescent screen. Figure 5.22 shows a typical intensifier with fiber optic plates as input and output surfaces, the former coated with a photocathode material and the latter with a phosphor. When light falls upon the photocathode, electrons are generated, and these are accelerated toward the phosphor by the 15kV field across the device. The increased energy acquired by the electrons is expended in exciting the phosphor and the image formed can be 40 to 50 times brighter than the original scene.

A careful selection of the photocathode material used will provide a greater quantum efficiency and a substantial improvement in spectral sensitivity over the dark adapted human eye, extending the observer's visual range into the near infrared region.
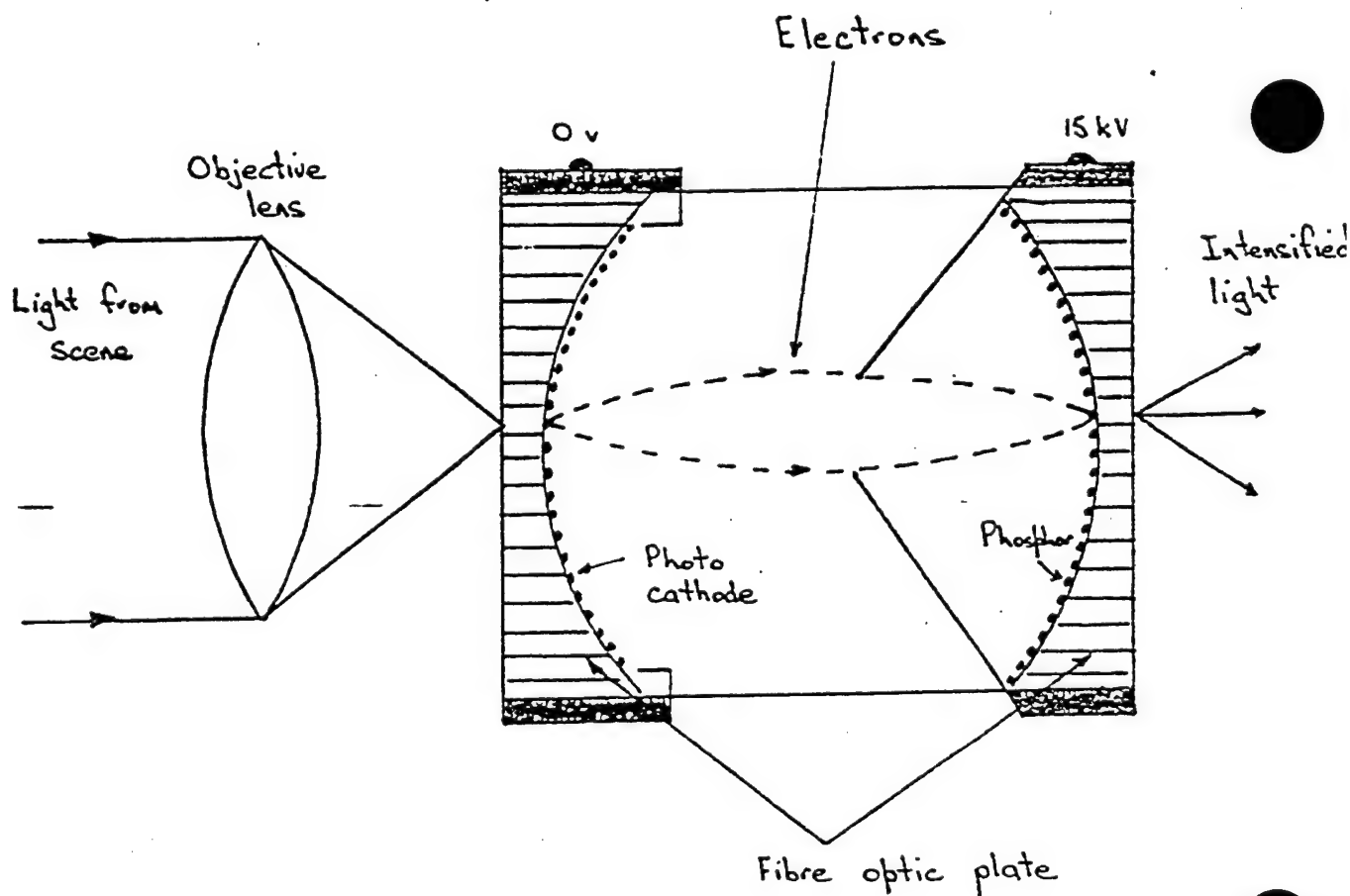
Figure   5.22 Basic Image Intensifier

5.12.3.3 MULTISTAGE IMAGE INTENSIFIER. An obvious extension of the basic intensifier just described is to stack two or three tubes together in cascade (hence, cascade intensifier). This can result in gains up to 50,000 times at .4μm. This approach would be sufficient to convert a simple vidicon into a LLTV tube. The three stage cascade device has been applied in the many direct view, hand held image intensifiers now in service with many countries; an example of this employment is shown in Figure 5.23.
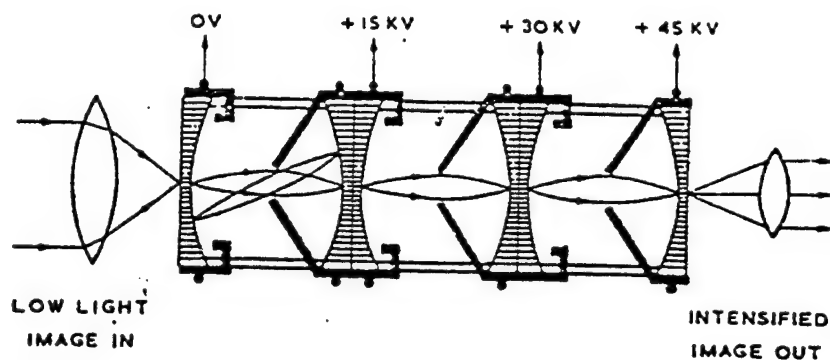

Figure   5.23 Cascade Image Intensifier

5.12.3.4 MOTION COMPENSATED INTENSIFIER.

If a LLTV system is used in a moving vehicle, there is likely to be some angular vibration of the system which will degrade resolution to some extent. It is possible to compensate for this vibration with a special image intensifier which has been designed to allow for magnetic deflection of the output image, and it is shown in Figure 5.24. The photocathode and front end of the intensifier are similar to the basic intensifier, but the output end has a relatively long field free section where the electron beams are moving essentially parallel to each other. A transverse magnetic field produced by saddle coils will deflect the output image as a whole. Consequently, if one can sense the angular motion of the LLTV system with, for example, position gyros, one can then produce the appropriate signals to feed to the saddle coils around the intensifier. The magnetic field thus produced will deflect the output image so as to compensate precisely for the angular movement of the system. The intensifier must have extremely good geometry in the image reproduction. Otherwise, the deflected image will not register accurately with the underdeflected image and severe loss of resolution will result. However, these problems are capable of being solved.
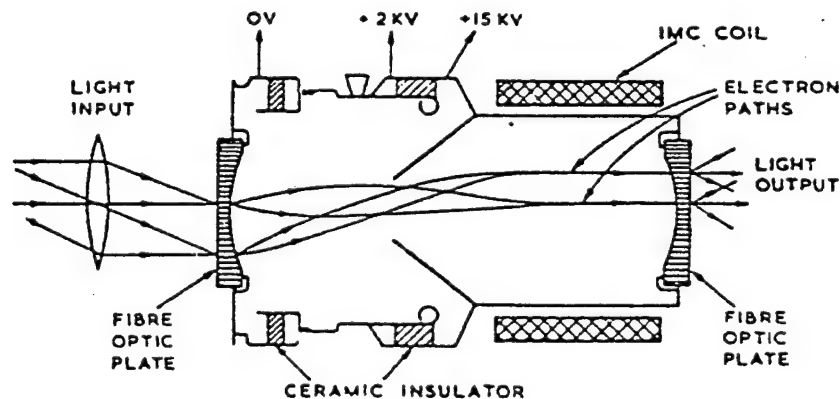

Figure   5.24 Motion Compensated Intensifier with Gating

5.12.3.5 MICROCHANNEL PLATE INTENSIFIERS (MCP). MCPs are second generation image tubes making use of microchannel plates to obtain luminance gains of up to 10^5. The channel plate is a thin plate of special glass with a matrix of fine holes (channels) through it (the holes are from 10-20 m in diameter and about one mm or lesson length). Primary electrons from the input fiber optics or photocathode strike the inside walls near the entrance end and cause secondary electrons to be emitted from the specially coated lining as shown in Figure 5.25. Thus, the MCP is essentially a thin secondary emission current amplifier located between the photocathode and the phosphor screen.
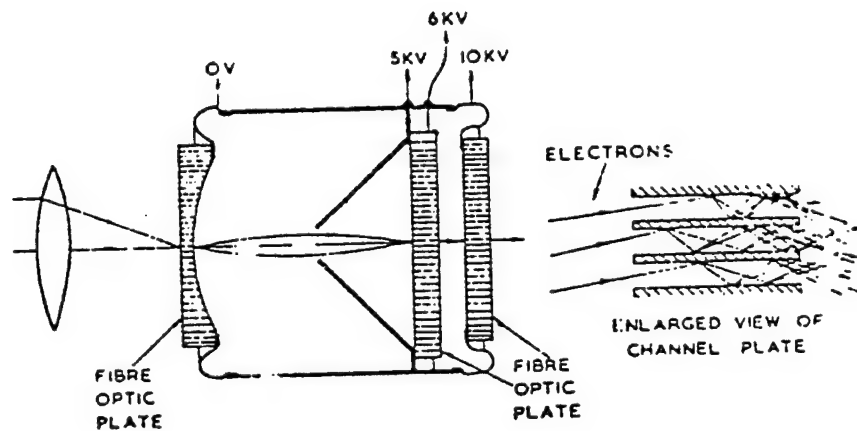
Figure   5.25 Inverter Channel Plate Intensifier

5.12.4   ATTRIBUTES AND COMPARISON OF LLTV SYSTEMS. The performance of LLTV systems is based on the following parameters:

Resolution - static and dynamic
Sensitivity
Dynamic Range
Lag
Overload Performance
Ruggedness

5.12.4.1   RESOLUTION.   LLTV (or TV for that matter) resolution is usually expressed as number of TV lines resolved normal to the scan lines in a distance equal to the picture height (i.e., TV lines per picture height) with a high contrast target. A general classification for resolution is as follows:

TV Lines/Picture Height	Description	Rating
>800	Very Good	4
600 to 800	Good	3
400 to 600	Fair	2
<400	Poor	1

5.12.4.2 SENSITIVITY. Sensitivity is a measure of how low in light level a system will continue to give useful results. It is an arbitrary choice as to what constitutes "useful" results, so for comparison purposes, this will be deemed to be the minimum light for which a system will give 400 TV lines resolution. A rating system for LLTV sensitivity for light at the photocathode to be independent of input optics is as follows:

Light Level	Rating
below 10^{-4} lux	4
10^{-4} to 10^{-3} lux	3
10^{-3} to 10^{-2} lux	2
10^{-2} lux and above	1

5.12.4.3 DYNAMIC RANGE. Dynamic range is the ability of a LLTV tube to cope with both high and low light levels without loss of picture quality or damage to the tube. In general, Isocon variants are greatly superior to vidicons in this respect.

5.12.4.4 LAG. All LLTV systems suffer to some extent from lag due to the high energy tail of the thermonic electron distribution which ultimately completes the target recharging process--complete recharge takes time, meaning several frames of TV readout and thus lag or the smearing of moving objects occurs on the screen. The lag rating performance for the light level necessary to give 300 TV lines on a target crossing rate of ten seconds per picture width is as follows:

Light Level	Rating
below 10^{-4} lux	4
10^{-4} to 10^{-3} lux	3
10^{-3} to 10^{-2} lux	2
10^{-2} lux and above	1

5.12.4.5 OVERLOAD PERFORMANCE.   Overload performance stems from the dynamic range of the system. The range of light levels can vary from overcast starlight to intense light sources such as shell bursts, fires, or headlights all at the same time. Such overloads can have two effects on the system:

(1)   Temporary or permanent damage to the system in the form of burn marks on the tube target or perhaps on an image intensifier phosphor.

(2)   Degradation of the picture due to spreading of the bright light image (sometimes called blooming) and veiling glare producing an all over masking effect on the unlit parts of the scene. On these aspects, the rating is not accurately quantified for all systems, but the marks given are based on experience with the various systems.

5.12.4.6 RUGGEDNESS. This refers to the mechanical ruggedness of the system, and like overload performance, it is not accurately quantified, but is based on laboratory testing and field trials.

5.12.5 GATED ACTIVE TELEVISION.   One solution to the extreme low light quantum limited performance is to use active illumination in conjunction with the LLTV system.   To overcome the problems of close range back scatter from the atmosphere, it is highly desirable to use a short pulse of illumination, usually obtained from a laser and to gate the TV system to respond only when the light scattered back from the target is anticipated. By varying the "on" time of the TV system, range gating can be achieved to search at different ranges in the field of view. The intensifier has provision for gating and is gated on during the line blanking period of the TV system. The laser is pulsed at some time delay after line blanking so that the effective range illuminated is determined by the time interval to the next line blanking period.

(THIS PAGE INTENTIONALLY LEFT BLANK)

SECTION VI

DISPLAYS

6.1   TV DISPLAYS. The construction and principles of operation of a typical TV display are the same as those associated with any CRT. A raster scan is used for imaging detail, whereby the spot formed by the electron gun is moved over the whole area of the screen in a regular series of parallel horizontal lines. The image is built up by varying the brightness of the spot in synchronization with the raster. The process is repeated at a sufficient refresh rate and usually involving an interlace method so as to produce an apparently continuous and dynamic image.

The TV raster used for EO weapons is produced by deflecting an electron gun in the aircraft television picture tube in a series of horizontal scans and vertical deflections (Figure 6.1). The aircraft electron gun and the weapon electron gun are aligned or synchronized by the master oscillator sync signals. Current USAF EO systems use a horizontal scanning by the master oscillator sync signals. Current USAF EO systems use a horizontal scanning frequency of 15,750 hertz and a vertical deflection period of 60 Hz. The product of these parameters is a TV picture or field consisting of 262 1/2 line of video. An entire field is generated every 1/60th of a second.
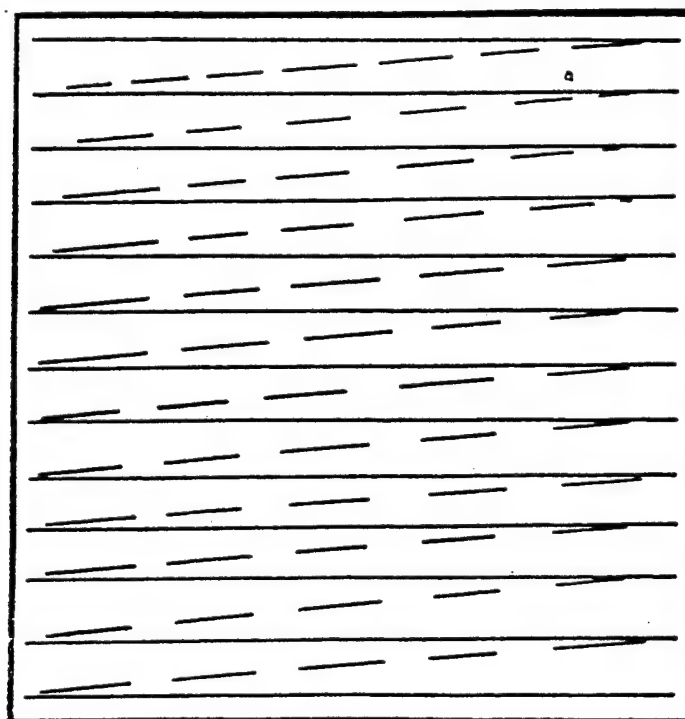

Figure   *6.1*   TV Raster

Apparent resolution of the displayed TV presentation is improved by using a technique called a 2:1 interlace. The lines of each successive field are interlaced by scanning first the odd lines of the display ant then filling in the even lines when the following field is generated (Figure 6.2). Two interlaced fields comprise one frame consisting of 525 lines of video whose repetition rate is 60/2 or 30 times a second. The frame constitutes a complete TV picture element, but its relatively low repetition rate does not generate flicker because of the two vertical scans required to produce it. The result is an improved apparent video resolution. The human eye then uses the property of image retention to tie successive frames together and create apparent motion in the same manner as a motion picture.
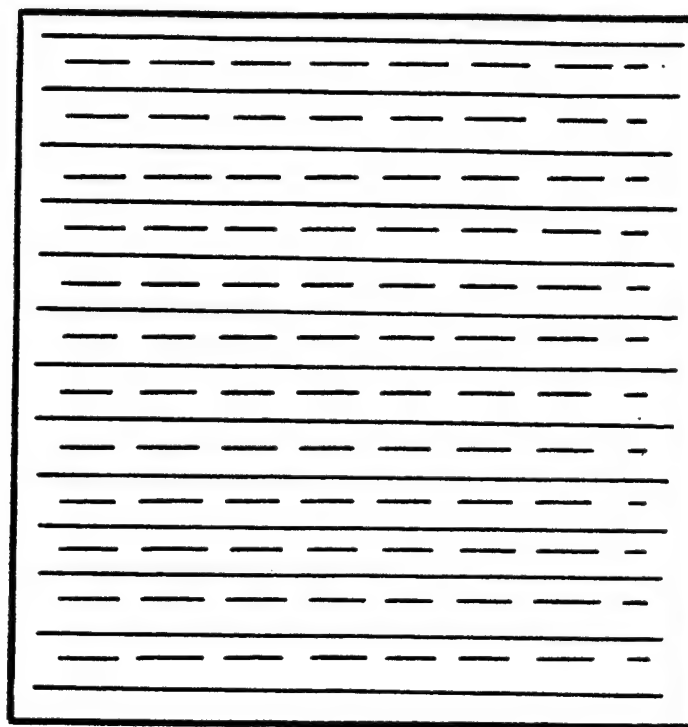

FIG 6.2   2:1 Interlace

6.1.1 TV FREQUENCY AND DISPLAY RESOLUTION. The detail of a TV picture in the vertical direction is determined by the number of scanning lines, since gradations in the light intensity of the image in the vertical direction that takes place

in a distance less than the width of a line obviously cannot be reproduced. Resolution in the horizontal is similarly determined by the speed with which the TV system is able to respond to abrupt changes; i.e., by the frequency band that the TV system transmits. Using the US domestic TV system as an example and assuming that in scanning a horizontal line the transition from black to white is accomplished in a distance along the line equal to the spacing between and adjacent lines, then:

485 active lines with a width-to-height ratio of 4:3, the distance is:

$1/485 \times 1.33 = 0.00155$ of active length of one line

The spot moves from left to right across the scope in 53.5 μ secs, hence the time interval for resolution is:

$0.00155 \times 53.5 = 0.08$ μ sec

In situations where the overshoot is less than 5%, the relationship between rise time and bandwidth (B) is given by:

Risetime = $.35/B$

Hence, a video system which will permit the response to rise from a minimum to a maximum in this length of time without overshoot must have a bandwidth of not less than:

$.35/.08 = 4/375$ MHz

A larger bandwidth than this will give greater horizontal resolution, while a reduced bandwidth degrades the horizontal resolution.

6.1.2 BRIGHTNESS DISTORTION AND GAMMA (γ). The relationship between the brightness of an element of the reproduced image and the brightness of the corresponding element of the original scene, termed the transfer characteristic of the RV system, is normally shown as in Figure 6.3. (Note the log-log scale employed). The slope of the transfer characteristic is called the gamma (γ) of the system. A straight line where $\gamma = 1$ corresponds to linear system completely free of brightness of amplitude distortion. A straight line where $\gamma > 1$ has uniform brightness of amplitude distortion. A straight line appears to the eye to be independent of the brightness. When γ is curved, the apparent brightness distortion will depend upon the brightness of the area under observation.

Image
Brightness
(log scale)

$\gamma = 1.5$

UNIFORM
BRIGHTNESS
DISTORTION

$\gamma = 1$

NO DISTORTION

HIGHLIGHT CONTRAST
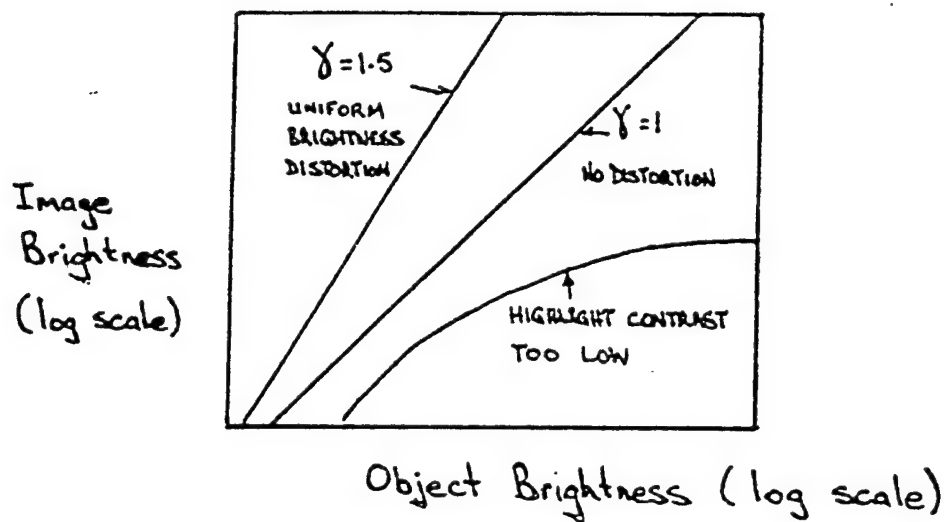TOO LOW

Object Brightness (log scale)

Figure 6.3   Image/Object Brightness

6.2 COLOR CATHODE RAY TUBE (CRT). Most color CRTs employ a tri-color, tri-gun picture tube. The tri-gun portion of the name indicates that the tube possesses three electron guns, instead of only one electron gun as found in black-and-white CRTs. The tri-color portion of the name reveals that the viewing screen of the tube possesses three different color-emitting phosphors. This, of course is basic to the entire color television system which employs the three primary colors -red, green, and blue- to synthesize the wide range of hues and tints required for the satisfactory presentation of a color picture.

The tie-in between the three electron guns and the three different types of screen phosphors now becomes evident. Each gun is concerned with one type of phosphor. Thus, one of the electron guns develops an electron beam which strikes, for example, the phosphor which emits red light. This gun is labeled the "red gun".   The second and third guns direct their beams at green and blue dots. In each case, the color of the phosphor refers to the light which this phosphor gives off when struck by an electron beam, not the actual color of the phosphor. The actual color of the substance and the color of the phosphorescent light it emits do not necessarily bear any

relationship to each other.

The overall color that is seen on the screen is determined by two general factors: (1) the phosphors which are being bombarded by the three guns, and (2) the number of electrons which are contained in each beam. For example if we turned off the green gun, leaving only the red and blue guns in operation, the screen color would fall somewhere in the purplish range. If the blue gun were stronger than the red gun, the color would appear closer to blue, say bluish purple.

If all three guns are operating you generally see the lighter or pastel shades. This is because red, green and blue combine in some measure to form white, and although white may not be predominant, it will mix with whatever colors are present and serve to lighten, or desaturate them.

The phosphorescent dots which produce the colored light are arranged on the screen in an orderly array of small triangular groups, called triads (Figure 6.4). The actual number of dots for a 21 inch TV screen is on the order of 1,071,000; making up 357,000 triads.

B = BLUE
G = GREEN
R = RED

FIG 6.4
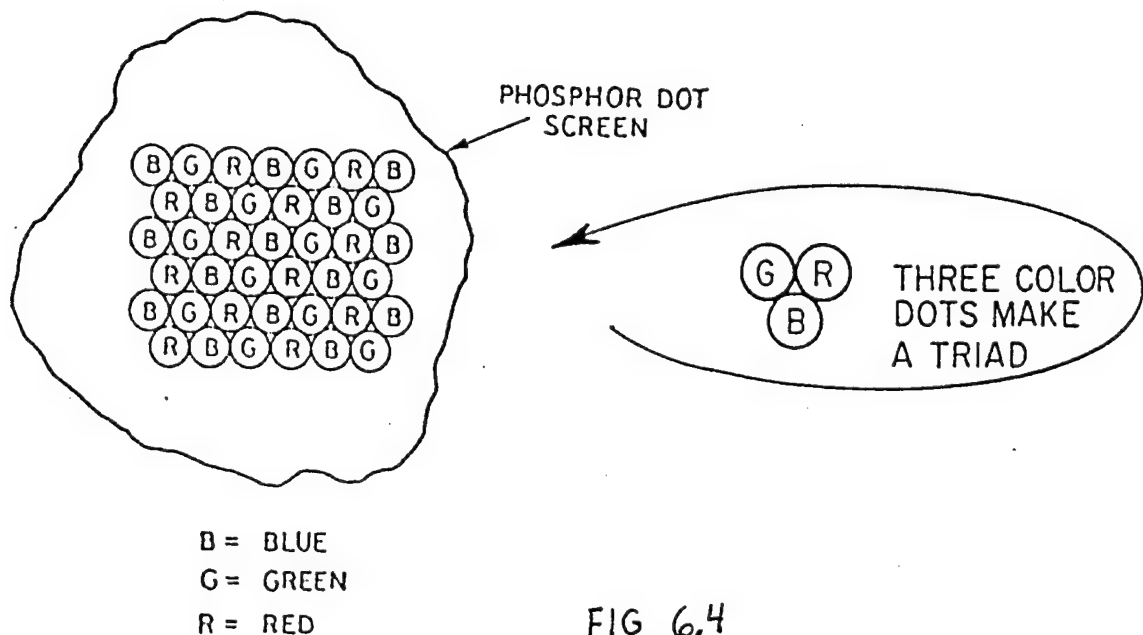
In a color CRT, magnetic fields force the electrons from the three electron guns to converge, so that each beam will strike the proper phosphor dot of a triad at any one instant of time; that is, one beam will strike the red dot, a second beam will strike the green dot, and the third beam will strike the blue dot. The three dots are bunched close together so the light they produce combines and appears to the eye as a single color.

Proper beam convergence is an important aspect of tri-gun picture-tube operation. To insure each beam strikes only one type of phosphor dot as the beams scan, a mask, called a shadow or aperture mask, is inserted between the electron guns and the phosphor dot screen (Figure 6.5).
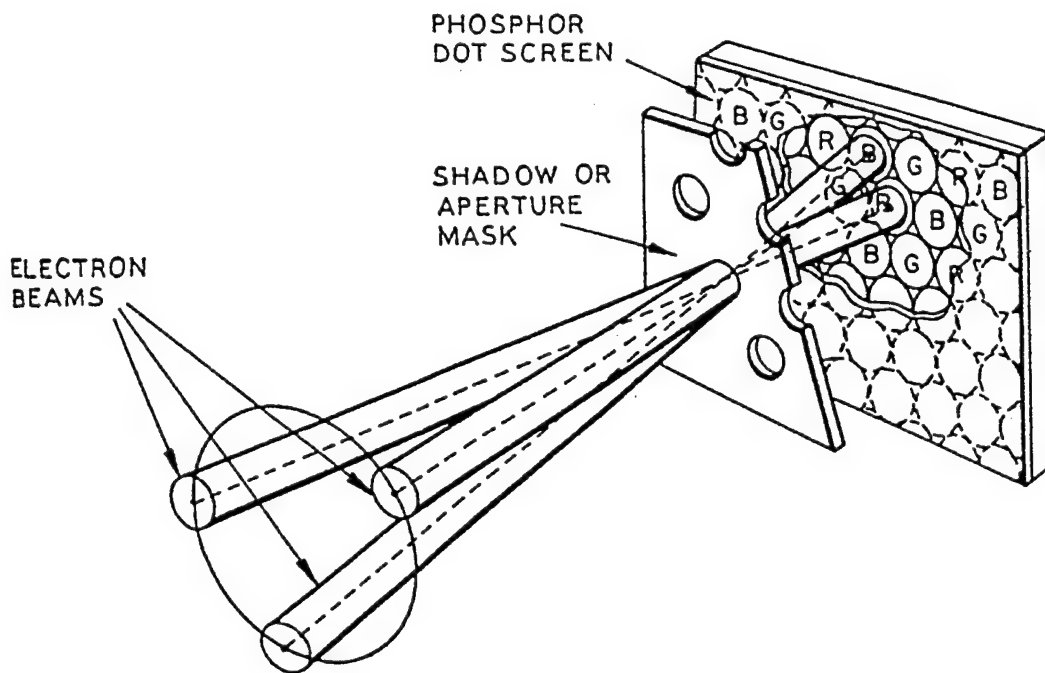

FIG 6.5

The mask contains circular holes, equal to the number of dot triads. Each hole is so aligned with respect to its group that any one of the approaching beams can strike only one phosphor dot. The remaining two dots are hidden by the mask; that is, the two other dots are in the "shadow" of the mask opening-hence the name shadow mask.

6.3   RESOLUTION OF SCENE DETAIL.

All photon sensors are characterized by some form of limiting resolution; i.e., the smallest detail that can be seen will be limited by some sensor parameter. An optically perfect lens will create a divergent beam; thus once a lens size has been chosen for a system, the maximum angular resolution is then determined and system resolution can never be better than the diffraction limitation of that lens. (This aspect is more applicable to IR rather than visual systems). In the case of film the limit is due to the photosensitive particles which are of finite size. With TV, as already covered, vertical resolution is set by the number of horizontal lines employed and horizontal resolution is determined by the video bandwidth and the size of the electron beam affects both horizontal and vertical resolution.

When the TV camera itself has a resolution limit, greater scene detail can be viewed at a given rage only by increasing the lens focal length (F). However, such an increase in F without a corresponding increase in lens diameter may result in a decrease in lens resolution and a loss of image light level resulting in a less than hoped for scene resolution. In low light level conditions, this method of increased focal length will probably result in a loss of scene resolution. Therefore, when designing a system, the required scene resolution must be determined first and then size the particular elements to meet this required performance.

6.4   JOHNSON'S CRITERIA.

To a human observer, a scene object at very long range will appear only as a "blob". By moving closer, the observer will, in turn, begin to discern its shape, classify it, and finally, positively identify it. Johnson arbitrarily divided these levels of object discrimination in four categories as follows:

CLASSIFICATION OR DISCRIMINATION LEVEL	MEANING
Detection	An object is present.
Orientation	The object is approximately symmetrical (or unsymmetrical) and its orientation may be discerned.
Recognition	The class to which an object belongs may be discerned (e.g., tank, truck, man).
Identification	The target can be described to the limit of the observer's knowledge (e.g., T34 tank, friendly jeep).

And, after a series of experiments with EO sensors, Johnson determined his criteria for the "resolution required per minimum object dimension for various levels of discrimination," which are shown in the following table:

DISCRIMINATION LEVEL	RESOLUTION/MINIMUM TARGET DIMENSION (TV LINES)
Detection	2
Orientation	3
Recognition	8
Identification	13

SECTION VII

HUDS

7.1 HUDS. The following information is a reprint of two articles titled Holographic HUDS De-mystified and a non-published paper/briefing on head-up and helmet mounted display technology.

HOLOGRAPHIC HUDS DE-MYSTIFIED

Jerold H. Gard

Kaiser Electronics, San Jose, CA 95134

ABSTRACT

Recently, so-called holographic Head Up Displays (HUDs) have burst on the fighter and attack cockpit scene, supposedly offering revolutionary advantages over any previously available techniques. Although frequently described as a nearly miraculous technological breakthrough by their promoters, there has been, unfortunately, little information provided as to what these devices are, how they work and, more importantly, what are their advantages and the disadvantages. Thus, the user community has been provided with little knowledge with which to make the required tradeoffs or, for that matter, upon which to base intelligent questions.

This paper attempts to provide, without tedious mathematical treatment, a physical understanding of the optical principles involved in such a HUD and a readily grasped understanding of what holographic optical elements are and how they contribute to the performance.

REFRACTIVE (ORDINARY) HUDS REVIEWED

"Collimating optics" cause a portion of the rays emanating from a point source to form a parallel beam, or bundle, while all other rays are usually ignored or occluded by a housing. A comparison between collimated and uncollimated point sources is shown in Figure 1. Here the observer on the left notices that three visual effects are apparent when viewing the uncollimated point source: 1) his eyes must cross (convergent parallax), to allow his brain to merge the images appearing on each retina; 2) his lens must be squeezed by their surrounding sphincter muscles to thicken them to the point where they will focus the close object on his retinas; and, 3) if he moves his head from side to side he must change his viewing angle by rotating either his eyeballs or his head to keep the source centered in his view. The same observer viewing the collimated source to the right sees that his eyes aligned to parallel, the sphincter muscles are relaxed, and, most important, he can move from side to side or up and down and the point source appears to be at the same angle. That is, no eye or head rotation is required to view the point directly. Passing these three tests means that

as far as the observer can detect, the point source appears to be located an infinite distance away. To provide an aiming device, the point source is viewed as reflected in a partial reflector (the combiner) so that both the point source and the outside world can be seen. Essentially parallel rays from both sources may then be observed simultaneously regardless of the eye position, provided the eye does not move out of the circular bundle emanating from the lens.
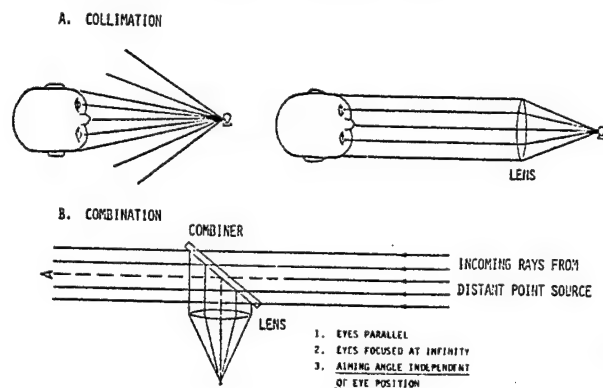

Figure 1
What Is Collimation and How Does It Help?

In HUDs, the CRT is substituted for the point source, giving an image plane on which flexible symbology formats may be placed (See Figure 2). Each point puts out its own bundle at an angle determined by the optics design, so that not only aiming points but larger arbitrary symbol shapes including alphanumerics, tapes, scales, etc., can be shown for simultaneous real world viewing. In Figure 2, two points at the edge of the available area (the ends of the arrow) are shown along with the rays which emanate from them and which are collimated into "bundles" by the simplified "perfect" lens. The eye position 1 is within both bundles and can view both points, and by symmetry the total CRT face, and thus the total field, with only an eyeball rotation. The eye at position 2, however, can not see either the head or tail of the arrow but only a portion of the shaft, giving rise to an "instantaneous" field (seen instantly with the eye in one position only) which, it turns out, is the solid angle subtended at the eye by the clear aperture of the optic. Since two eyes can view the optic

"Instantly" without head motion, we usually deal with the "binocular Instantaneous field of view" or the sum of the two solid angles subtended at each eye by the aperture. By moving the head about, the eye at distance may peer through the lens at various angles and ultimately see the total field. Akin to peering through a knot hole, the name sometimes given to this effect, It is In this position which most cockpit designs place the pilot. As long as the head motion requirements are not excessive (an inch or so in any direction, which means also that the HUD Is properly placed to begin with) then this solution gives acceptable results. An example of practical optics (4" clear aperture) used to handle this task Is shown In Figure 3.
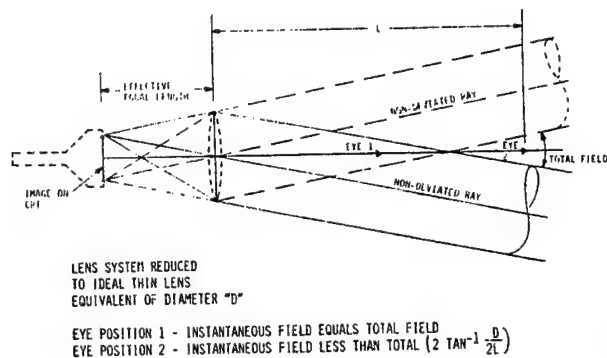
LENS SYSTEM REDUCED
TO IDEAL THIN LENS
EQUIVALENT OF DIAMETER "D"

EYE POSITION 1 - INSTANTANEOUS FIELD EQUALS TOTAL FIELD
EYE POSITION 2 - INSTANTANEOUS FIELD LESS THAN TOTAL $\left(2 \; TAN^{-1} \frac{D}{2L}\right)$

Figure 2
Refractive Collimating Optics Schematic

JAN 12, 1981   SPACE SHUTTLE HUD
KAI-HUD-OSCD,   101 DEGREE FOLD

CRT FACEPLATE

NITE FILTER
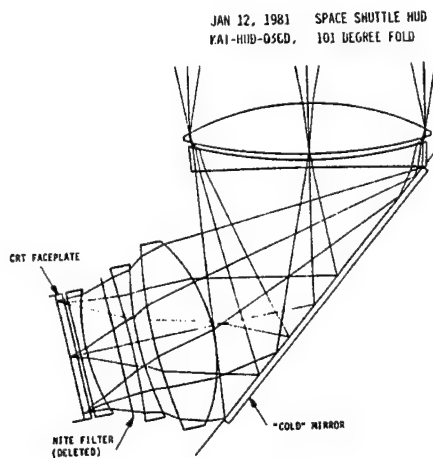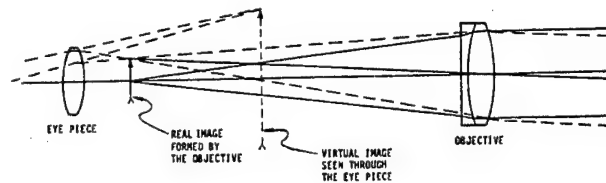(DELETED)   "COLD" MIRROR

Figure 3
A Practical Collimating Optic

DEVELOPMENT OF THE REFLECTIVE HUD

The refractive telescope shown In Figure 4 Is related to the HUD optics In that parallel rays entering from a distant object are focussed by the color corrected doublet objective Into a real Image which Is then viewed through a magnifying
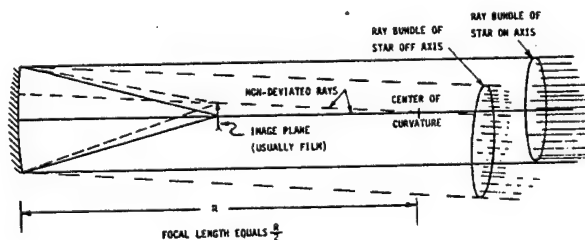
EYE PIECE   REAL IMAGE
                 FORMED BY   VIRTUAL IMAGE
                 THE OBJECTIVE   SEEN THROUGH   OBJECTIVE
                                  THE EYE PIECE

AGAIN, AN ILLUMINATED IMAGE AT THE PLANE OF THE REAL IMAGE
WILL PRODUCE COLLIMATED BUNDLES OUT OF THE TELESCOPE

Figure 4
A Related Optical System

glass. However, If a CRT were placed at the real Image plane and Illuminated, rays opposite to those shown would come out collimated just as In a HUD, according to an optical reversal principle known as reciprocity. Refractive telescopes In large sizes are rare because of the cost of the four precision surfaces In the objective; large aperture telescopes use a mirror reflector focussing the Image (see Figure 5) since only one precision surface Is needed (mirrors do not require color correction). Again, reciprocity states that an Illuminated object at the Image plane will be collimated, albeit over a very narrow field. If, as some clever Inventor undoubtedly reasoned, we apply this reflective collimator Idea to the cockpit, first Increasing the curvature to shorten the focal length, we find we can place a large collimator much closer to the pilot (giving a large Instantaneous field), In previously unused space above the glare shield (see Figure 6). The location of the Image plane would put the CRT In the pilot's face, but this Is corrected with a turning mirror and a lens set called a relay lens. This acts somewhat like a slide projector, placing an Image of the CRT up near the turning mirror where It Is needed by the curved collimator, which (with a partially reflecting coating) also doubles as the combiner.

ANOTHER RELATED OPTICAL SYSTEM: THE NARROW-FIELD,
REFLECTIVE ASTRONOMICAL TELESCOPE

                                    RAY BUNDLE OF   RAY BUNDLE OF
                                    STAR OFF AXIS   STAR ON AXIS
                     NON-DEVIATED RAYS   CENTER OF
                                          CURVATURE
                     IMAGE PLANE
                     (USUALLY FILM)

FOCAL LENGTH EQUALS $\frac{R}{2}$

NOTE: RECIPROCITY SAYS THAT IF AN ILLUMINATED IMAGE IS PLACED
         AT THE IMAGE PLANE, COLLIMATED BUNDLES WILL EMERGE FROM
         THE MIRROR

Figure 5
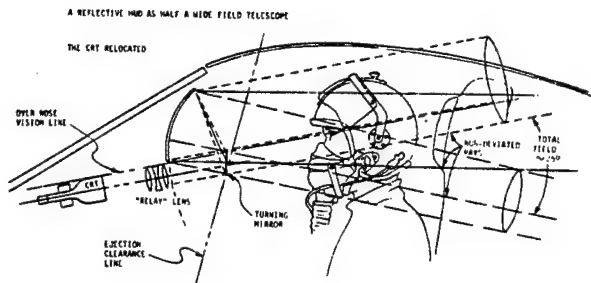**The Reflective Astronomical Telescope**

Figure 6
A Reflective HUD

All peaches and cream? Not quite, and Figure 7 enumerates some of the difficulties, which start with the poor collimating performance of the strongly curved mirror when forced to operate over a wide field. Because parallel rays sent in focus into a very poor, fuzzy image, reciprocity says to get parallel rays _out_, the image must be in precisely this same poor focus (and also somewhat tipped). The relay lens must then take the flat CRT (which is tilted to get the image tipped) and precisely defocus it into the exact fuzzy three dimensional cloud needed to produce good collimation. Even with this, to get equal angles in the field, unequal distances are required on the CRT, creating the need for a highly distorted image. These problems, not

cockpit. Because of this and the complicated optical geometry, reflective HUD designs will rarely transfer from one cockpit design to another (as some have discovered the hard way) but almost always must be designed uniquely for the particular application. These factors will greatly extend the lead time required for new designs over the current experience with all-refractive systems. This is not to say that all of these problems have not been over-come, as shown by this data sheet (Figure 8) published in 1965 by Farrand Optical Company, New York, describing such a reflective HUD with a 25°x 25° instantaneous field. Actually, the first such reflective HUD known to the author was built by Bell Helicopter in the mid-fifties for helicopter application, and it also provided a wide field of view, although the exact figures are buried in the archives.

To summarize, the advantage of the reflective collimating element (or loosely, the reflective HUD) is that it permits the installation a larger collimator closer to the pilot, thus giving a larger (20° - 30°) instantaneous field than refractive HUDs buried in the glare shield (12°-18°). The disadvantages are larger size, weight, complexity and cost, longer and more expensive design cycle, disturbing visual effects because of a constricted head box, complicated CRT distortion correction circuitry, and a nagging problem that there is no place to put a decent gun camera.

Figure 7
Problems Due to Wide Field Off-Axis Rays and Relay Lens

Figure 8

trivial, can nevertheless be overcome but the small "head box", caused by the fact that rays emerge from the relay lens over a very limited set of angles, will plague us forever. Outside the head box, the pilot sees nothing and moving within it can create disturbing visual effects as the picture comes and goes. Therefore, the head box must be very carefully located in the

Not exactly a free lunch, which is probably why operational application of this idea has been limited to just one aircraft type, and that with not altogether satisfactory results. But the point is that none of these wide field of view HUDs employed a single hologram!

HOLOGRAPHIC OPTICAL ELEMENTS (HOE)

A holographic optical element is an element which changes the path of a light ray by means of diffraction (addition of wave fronts) rather than by refraction or reflection. Fine, you say, but you want to know how it works. Well, do you know for instance how refraction works? You just know it works, right? You mean you accept it. But lets have a look at Figure 9. Light moves slower in glass so the plane wavefront is slowed on one side first, and like a crawler tractor with one track slowed down, it bends. On the other side, one side escapes and speeds up first. So it bends toward the normal going from high speed (low index--air) to low speed (high index--glass) and away from the normal in the opposite condition. In fact the index of refraction of a glass is simply the ratio of the speed of light in a vacuum to its speed in the glass.
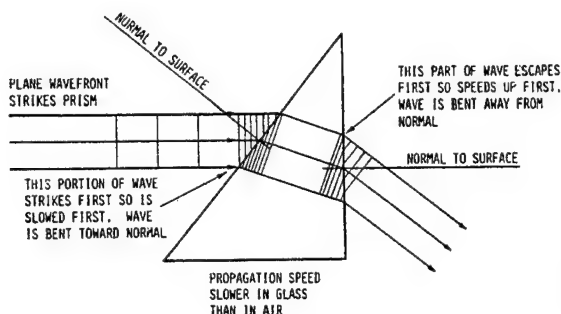

Figure 9
How Does Refraction Work?

A HOE works differently but can have similar effects. Figure 10 shows a cross section of a set of precisely spaced apertures of a geometry or the order of one wave length, and formed in a thin absorptive material. When illuminated by a single wavelength coherent point source the peaks shown radiate spherically and, according to the geometry, strike the apertures in a precise, time related fashion. Then each aperture radiates circular wavefronts in a definite phase relationship one with the other. These radiating wavefronts add, peak to peak and valley to valley, forming a plane wavefront going in a quite different direction. This is an example of altering a wavefront by means of diffraction occuring at a thin film absorptive hologram. It is, unfortunately, not the type of hologram used in HUDs, but it is the easiest to diagram and explain.

A second type, a volume Bragg hologram, was discovered by Bragg when trying to photograph crystal molecular structures using X-rays. In this case, the radiators are planes in a volume (See Figure 11), again spaced on the order of a wavelength. Incoming light is scattered along each plane in all directions, but by each plane

in precisely the same directions and amplitudes as by other planes, and also, as in the thin film case, in a definite and constant phase relationship, one to the other. Again, scattered wavefronts from these planes will add in various directions, causing several altered wavefronts to emerge from the hologram. These holograms are inherently more efficient than thin film absorptive hologram because they have no absorption. This is important to the HUD application, as we shall see.
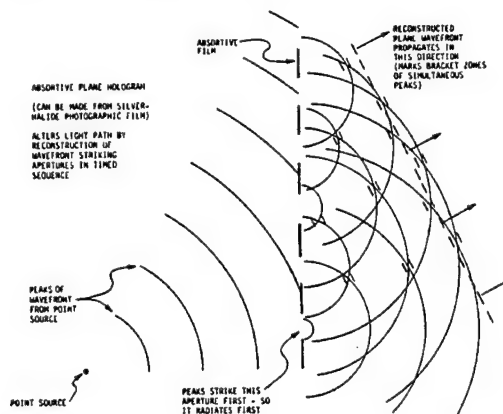

Figure 10
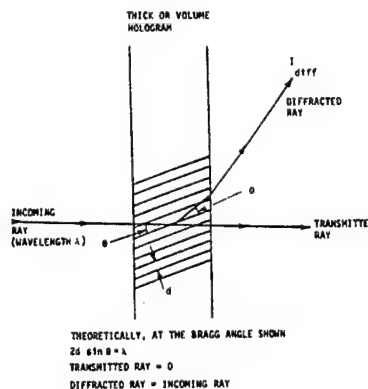How Does A Holographic Optical Element Work?

Figure 11
Bragg Diffraction (Volume Transmission Hologram)

Production (called construction) of such a hologram can be accomplished by recording in a suitable medium the interference pattern formed by two crossing coherent beams of a constant phase relationship as shown in Figure 12. For ease of discussion one beam is arbitrarily termed the reference wave and the other, the construction wave. Very complicated vector mathematics predicts the reconstruction shown below. That is, the fringes so constructed and recorded, if illuminated by the construction wave, will replicate the reference wave. The converse is also true. Also, interestingly, the device also conforms to the laws of reciprocity,

and the opposite of the reference wave will produce the opposite of the construction wave. Again the converse is also true. Unfortunately, this is not the kind of hologram used in HUDs, but we are getting closer.
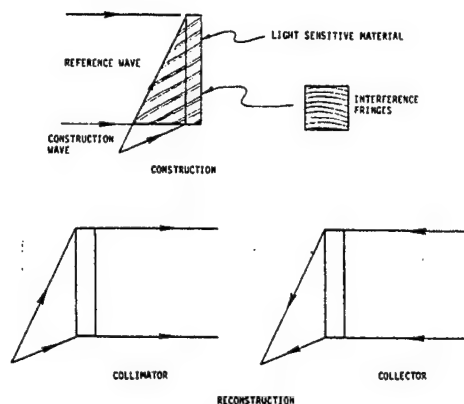

Figure 12
Transmission Bragg Diffraction

Some study of the rules inherent in Figure 12 will show the observant and perspicacious reader that if we want a reflective Bragg hologram the two beams must come from opposite sides as in Figure 13. Now reconstruction by illuminating with the construction wave again replicates the reference wave, but since the latter was going in the opposite direction, this appears for all the world to be a reflection. At last we have the type of hologram which we want to use in the HUD combiner. Of course, those very complicated mathematics we avoided before would have predicted this, and we will avoid them again (and not without reason, believe me). But for those of you who are like me and need a physical reality to envision (a sort of mental security blanket, if you will) then the other portion of Figure 13 shows something to cling to. Imagine multiple reflections from each internal plane, all in the same direction and all adding in phase to produce a highly efficient, almost total reflection at one wavelength. That's the kind of performance we want, and, since HUDs are green anyway, by merely selecting the proper phosphor we can have nearly monochromatic (single wavelength) light, so this type of hologram will reflect nearly all the CRT light toward the pilot. A disadvantage of broadband (gray looking — without color selectivity) combiner reflectors is that as the reflection is increased to increase symbol brightness, the real world is correspondingly darkened. This reflective hologram can reflect a high percentage of a single wavelength yet efficiently and transmit the remainder of the visual spectrum nearly unattenuated. This is a very nice effect in a combiner, offering brighter HUDs and better see-through transmission at the same time. Sounds like that free lunch at last and maybe it will be someday but not yet.
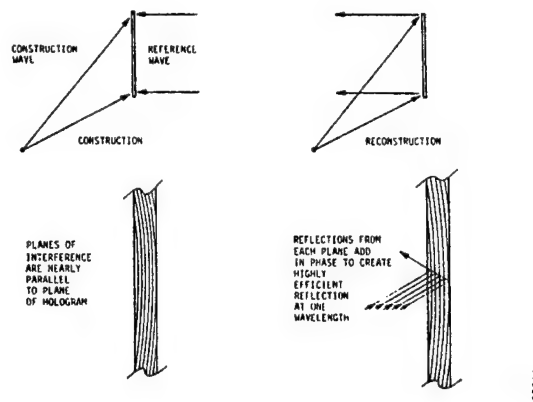

Figure 13
Reflection Holograms (Volume Holograms)

To show why and to also answer the nagging question "but what is really in there" let's look at the fabrication shown in simplified form in Figure 14. Animal protein called gelatin (first cousin to the Knox gelatin in the supermarket and second cousin to your hair and fingernails) is deposited on a suitable substrate, usually glass. It has been known for centuries that gelatin is light sensitive. Both its solubility in water and its hardness can be altered by exposure to light. It has also been known that absorbing dichromate of ammonium or potasium in the gelatin increases this sensitivity. No one has really bothered to find out why, but they mumble about cross links. Dried again, the gelatin is exposed to the two beams, obtained from a single coherent laser to assure constancy of phase in both beams. Even sensitized, this stuff is slow and the laser is not the sun, so exposures can be long. Originally taking hours, these protracted exposures lowered yield nearly to zero, as any vibration in the setup altered the phase relationship and thus the interference pattern in the area of the hologram. This has the same effect as photographing a moving object with a fixed camera with a slow shutterspeed — the photographic equivalent of "garbage in equals garbage out".
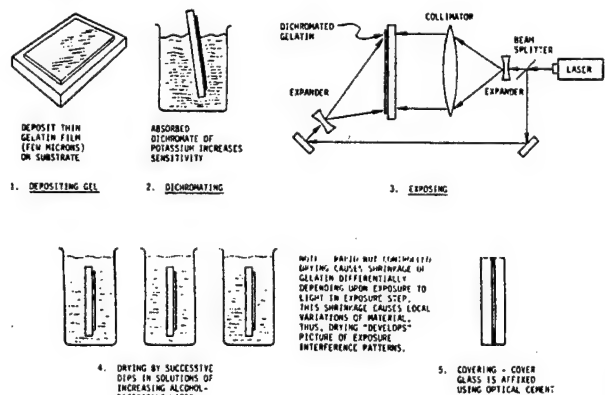

Figure 14
Steps of Fabrication

But what is the form of the recorded image in the gelatin? At this stage the picture is in there, but it must be developed. The process goes like this. By wetting the gelatin it is caused to expand and by rapidly drying it through exposing it to increasing solutions of alcohol in water, this expansion is reversed and it shrinks. This shrinkage is differential, due probably to the local variations in hardness, which in turn depend the variations in upon exposure to light. Some hypothesize that tiny fractures result from these shrinkage planes, others that tiny light scattering bubbles form. My favorite theory is that sudden local changes occur in the refractive index due to the differential shrinkage, and that this records the interference pattern for subsequent playback. Whatever it is, it is beautiful when it works and achieves the desired result. Of course, if re-wetted it re-swells and the hologram is lost or altered. It could only be recovered by a repetition of the same careful drying process. Therefore, the hologram must be sealed away from the humid real world atmosphere or it will quickly absorb moisture from air and be ruined. An organic, the gelatin can also be chemically destroyed by high temperatures, so it must be protected from this exposure also.

Why use such an environmentally delicate material? We would prefer a material good environmental stability, but also with low noise, a high diffraction efficiency at low exposure energies, and high resolution. Since almost all reasonable materials are organics, the diffraction efficiency and signal-to-noise ratio are the ruling factors. Dichromated gelatin exhibits high diffraction efficiency levels (around 90%) at the same exposure levels at which it has a reasonable noise figure (100:1). Other materials exhibit such high diffraction efficiency only at exposure levels which cause them to become uselessly noisy. Thus, dichromated gelatin at present is the most practical known material and we must simply live with its environmental requirements.

THE HOLOGRAPHIC COMBINER IN THE REFLECTIVE HUD

If we combine this holographic reflector with the reflective HUD concept developed previously several advantages accrue. First and foremost, the high reflective efficiency (some 85%) for P-43 contrasts favorably with the 30% or so broadband coating normally used on HUDs employing P-1 phosphor. For stroke written HUDs, this advantage is somewhat offset by the fact that, because of burn considerations, P-43 can only provide some 70% of the brightness of P-1, but the combination still provides a 2:1 improvement in stroke brightness, or, if desired, the same brightness with longer CRT life. For raster HUDs not limited by phosphor burn, a nearly 3:1 improvement can be achieved over P-1 and a 30% reflector. Although this still does not allow viewing of wide field TV or FLIR images in full daylight, it does make them practical in dusk conditions.

A second advantage is that the hologram can have an effective optical shape which is different from the physical shape of the substrate. This is helpful in three ways. It allows some freedom in fitting the physical combiner to the available windscreen space, it allows the combiner's optical effect to be aspherical even though the substrate and cover are of more easily fabricated spherical shapes, and, since the hologram is exposed on the substrate upon which it will be used, minor imperfections are, to a great degree, cancelled. This last occurs because the laws of replication of the reference wave during reconstruction do not depend upon the exact physical shape of the gelatin layer (review Figure 13).

Although aspherizing the combiner through the use of the hologram simplifies to some degree the relay lens requirements, we are nevertheless left more or less with all the difficulties of the reflective HUD concept and in particular, the nagging problem of the small head box with its disturbing visual effects is still with us. The problem of development time is exacerbated, since transfer from one design to another is still low, and design time with aspheric holograms is even more protracted. In addition, the combiner must now be made of two fitted pieces rather than one, so the advantage of easier tolerances is quickly lost. Lastly, we have introduced into a critical element of the aircraft an organic compound with which there is limited environmental experience and we may have much to learn about its delicacy as time goes on.

That the reflective HUD incorporating a holographic combiner is still complex is demonstrated by Figure 15, which is titled: A "Conventional" "Holographic" HUD. The separate quotes are intended, the first set indicating that this is the type of holographic HUD with which most of the readers will be familiar, so I have dubbed it "conventional". The second set indicates that, while most in the trade refer to these as holographic HUDs, they are really reflective HUDs employing a holographic optical element in the combiner. In some of these, the hologram is used only as a high efficiency green
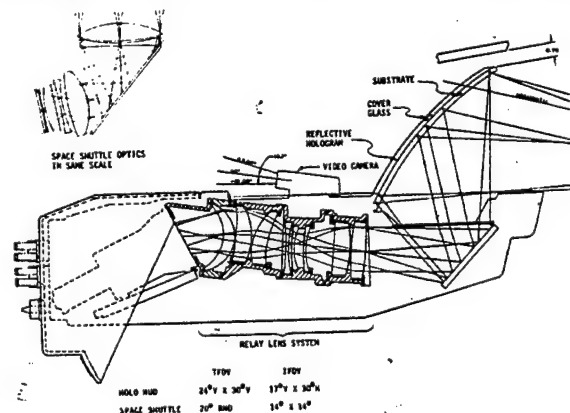

Figure 15
A "Conventional" "Holographic" HUD

reflector and has no optical power other than that which comes from the curved shape of the substrate, making the title "Holographic HUD" even more tenuous, scientifically speaking.

Figure 15 is an optical ray trace of a holographic HUD and shows a comparison of its complexity with a conventional four inch refractive HUD, drawn to about the same scale. The exterior of this HUD, being readied for flight test later this year, is shown in Figure 16. That the instantaneous field increase comes at a considerable price is obvious even to the casual observer.
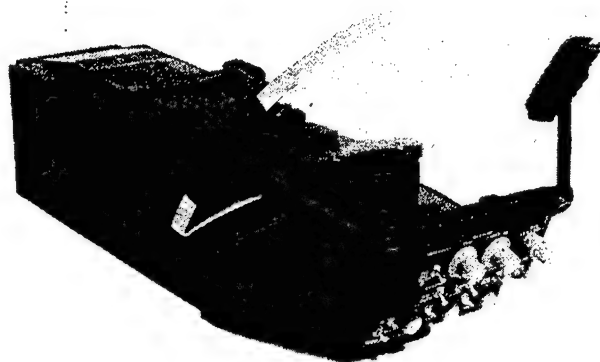

Figure 16
A "Conventional" "Holographic" HUD

Note that because of the way the rays emanate from the combiner in such an optical system, the total field can only be seen from the head box. Thus the gun camera is mounted forward of the combiner where it views only the real world. Therefore, it must be a TV-type camera and HUD symbology must be in or converted (in an electronic scan converter) TV format for subsequent mixing with the TV real-world picture. This mixing invariably gives rise to questions as to the accuracy of the overlay of symbology on the real world, but it is virtually unavoidable in the reflective HUD without mounting a camera on the pilot's forehead.

NON-CONVENTIONAL HOLOGRAPHIC ELEMENTS AND HUDS

Holographic optical elements discussed to this point might be termed conventional elements, in that they have counterparts or near counterparts in conventional refractive elements. Non-conventional elements as defined here are those whose functions can only be realized by diffractive techniques. Some interesting ones are shown in Figure 17. These reflective holograms are designed to have a limited angular bandwidth and as a result reflect rays impinging at a low incidence angle (with respect to a normal to the surface) while transmitting, without optical effect, rays impinging at a higher incidence angle, even though the wavelength is constant.

RAY 1 - TRANSMITTED
RAY 2 - REFLECTED
REASON: ANGULAR BANDWIDTH OF HOLOGRAM INSUFFICIENT TO REFLECT RAY 1 AT HIGH ANGLE OF INCIDENCE

RAY 1, 2, 3 - REFLECTED AT DIFFERENT ANGLES
REASON: REFLECTIVE HOLOGRAM HAS POWER (CONVEX MIRROR)
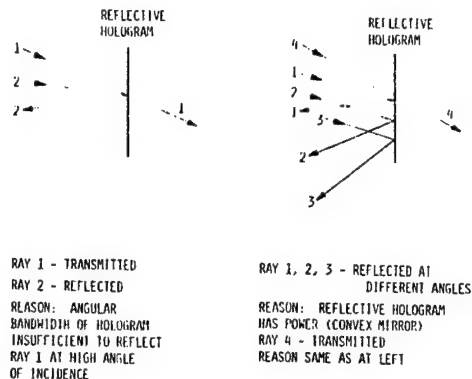RAY 4 - TRANSMITTED
REASON SAME AS AT LEFT

Figure 17
Non-Conventional Holographic Elements

A possible form of "non-conventional" "holographic" HUD formed using these two types of elements is shown in Figure 18. In this design, the turning mirror is a conventional mirror, while the upper three reflectors are holograms. A usual relay lens forms a real image for the collimator at the location of the dotted arrow. The rays from this image are reflected downward from the upper plate which is a conventional holographic reflector. These rays must pass through the curved collimating surface so it must be designed with a limited angular bandwidth. Having come through unaffected, they strike the third (flat) hologram at a low incidence angle and so are reflected back to the curved collimator, where this time they all must strike at a low enough incidence angle to be reflected toward the pilot. In this design (not a Kaiser design, incidentally) the collimation is accomplished by the combination of the curved surface and the positive lens formed by the rear piece of the large collimating element. The holograms themselves have no optical power but are used only for their high transmission and reflection and in the case of the rearward two, their ability to reflect with angular discrimination.
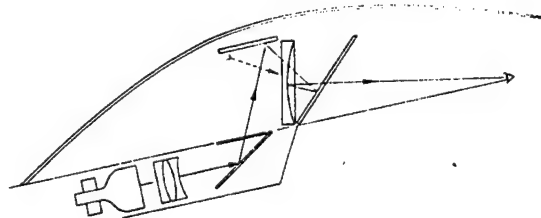
ADVANTAGES
- ABERRATIONS ARE REDUCED
- BELOW GLARESCREEN SIZE REDUCED

DISADVANTAGES
- COMPLEX HOLOGRAMS REDUCE YIELD
- CUSTOM DESIGN FOR EACH SITUATION
- SUN REFLECTIONS ARE DIFFICULT TO CONTROL
- MASSIVE SUPPORT STRUCTURE REQUIRED

Figure 18
A Possible Form of "Non-Conventional" "Holographic" HUD

Why go to all of this trouble? The two advantages are that the below-the-glarescreen size of the HUD is reduced by moving the intermediate image up high in the cockpit, and the collimating element is more nearly on axis than in the "conventional" reflective HUD. This latter condition tends to reduce aberations (optical problems) in the collimator, reducing the "fuzziness" of the intermediate image, and thus making life somewhat easier for the relay lens. However, several new problems are encountered. For starters, controlling the angular bandwidth adds new problems to the fabrication of two of the three holograms. Seemingly, the fit of the layout to a particular cockpit has been made even more unique. From the pilot's point of view, controlling sun and other reflections would seem to be a grave concern and evaluation of this could accurately be accomplished only in the aircraft itself. But the most severe disadvantage is the massive mounting structure required to rigidly support all of these elements up in the windscreen area. When shown this structure in the artist's conception of Figure 19, one can only wonder what
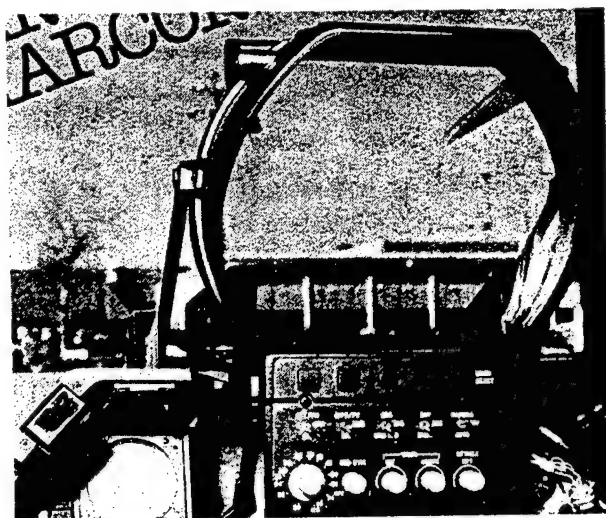
happened to the fighter pilot's old maxim "Lose sight - lose fight".

COMPUTER ORIGINATED HOLOGRAPHIC OPTICAL ELEMENTS (COHOE)

These elements differ from all the holograms previously discussed in that they are not produced by interferences between reference and construction beams which are themselves formed by refractive optical elements. Construction using refractive optical elements (review Figure 14) places severe limitations on the possible forms of diffractive wave front modification which can be effected by a hologram. By generating a hologram point by point by a computer-controlled laser, any arbitrary optical property which can be computer-defined can be produced. Such a hologram provides the HUD designer with much greater freedom in optimizing the design and controlling aberrations and holds promise of eliminating the relay lens and at the same time, linearizing the image plane. Kaiser is directing a heavy research effort in this direction at its Ann Arbor holographic facility (Kaiser Optical Systems, Inc.) and by this means expects to produce a wide field HUD with none of the size, weight, and complexity limitations inherent in the current brute-force approaches. Such a HUD would appear as in Figure 20 and one could truthfully ask "What could be simpler?". Perhaps by 1990 such a HUD will be considered standard.

Figure 19
Example of Massive Support Structure

WHAT COULD BE SIMPLER?
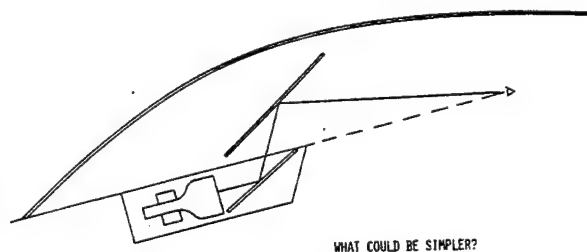
Figure 20
HUD Using Computer Originated Optical Elements (COHOE)

7.9

- BASIC PRINCIPLES

- WIDE FIELD HUDS

- RASTER HUDS

- .SYSTEM CONSIDERATIONS

Parallel light rays reach observer

Light from a distant source

Light from nearby source

Collimating Optics

Light from
nearby source

Light Bundle

Collimating Optics

reflex gun sight

Parallel light rays
from a distant source

Collimating lens

Light bundle
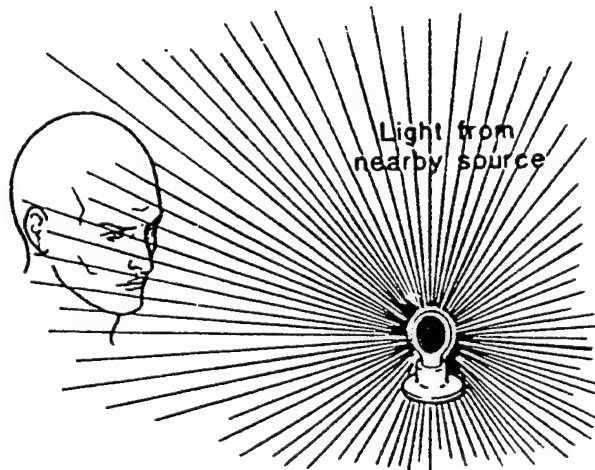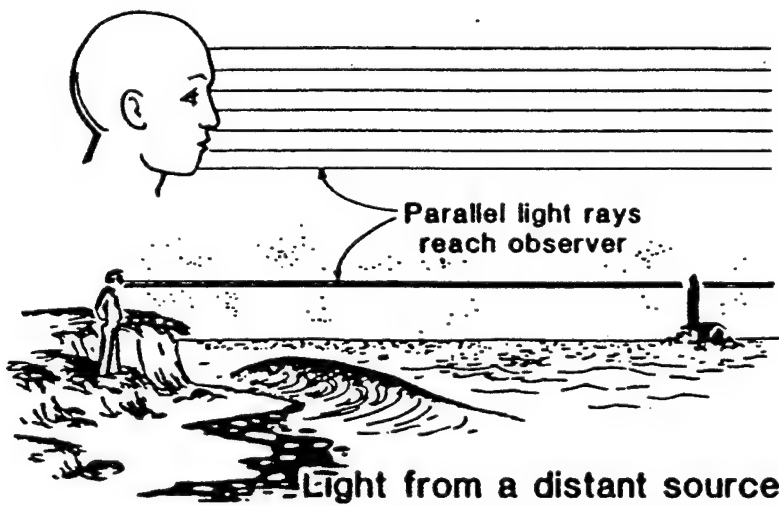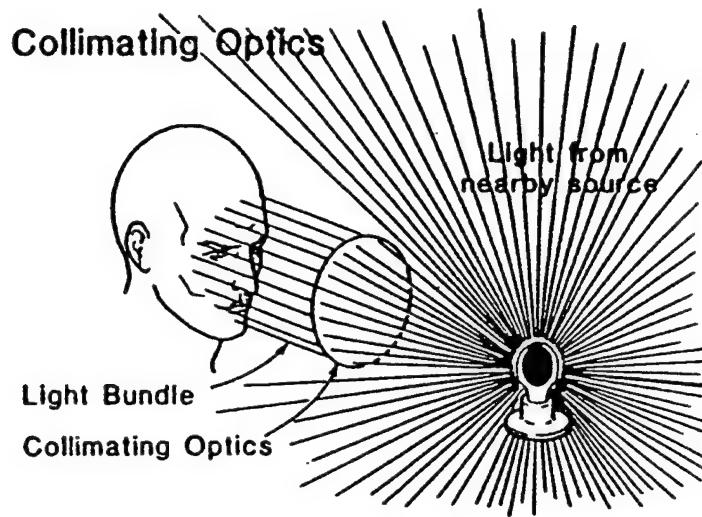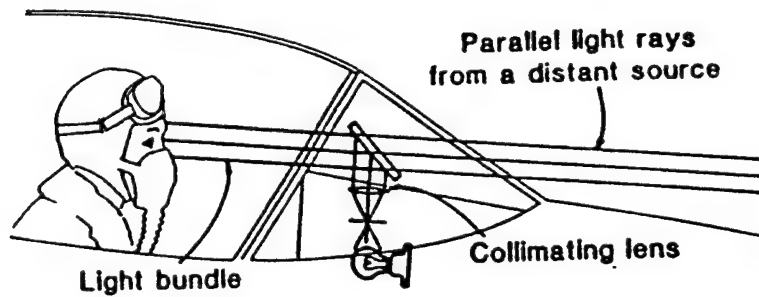
Collimating optics in gun sights

Parallel light rays
from a distant target

Collimating lense

Light bundle

CRT

Aiming symbol
positioned by computer
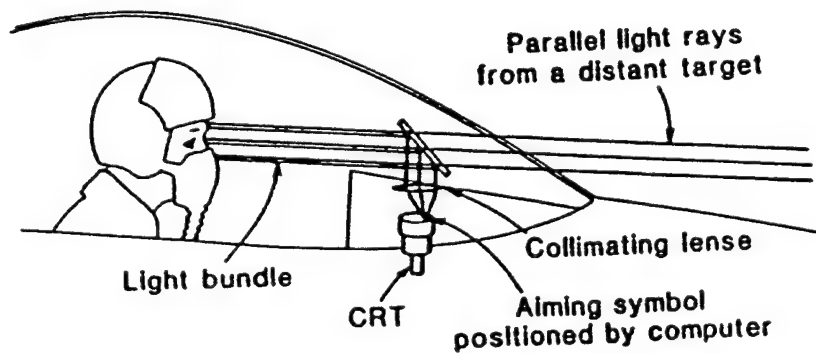
Collimating optics in HUDs

KAISER

Example of refractive HUD
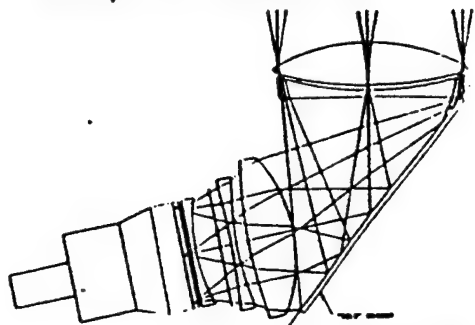
SPACE SHUTTLE HUD OPTICS

requires more lenses to do good job of collimating.

IFOV - can see without moving head around

Total FOV

② unfolded by mirror

①

WHAT IS FIELD OF VIEW?

because of 2 eyes

reason most modern HUDs have 2 glasses
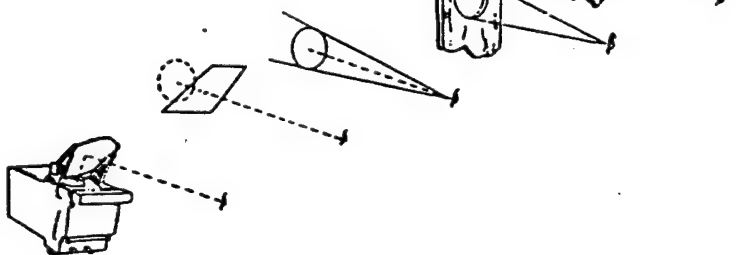
WHY DUAL COMBINERS?

7.12

WHAT ABOUT "WIDE FIELD HUDS"?

A + B = 24° - 30°

3-7 INCHES

3-7 INCHES

16°

16°

12°

20°-26°

30°

30°

17°
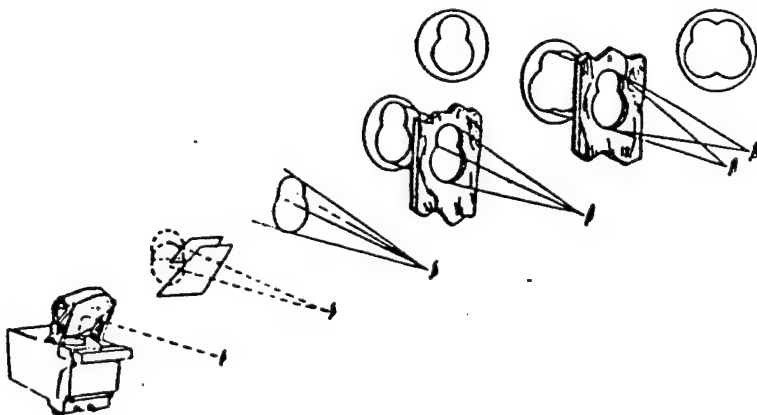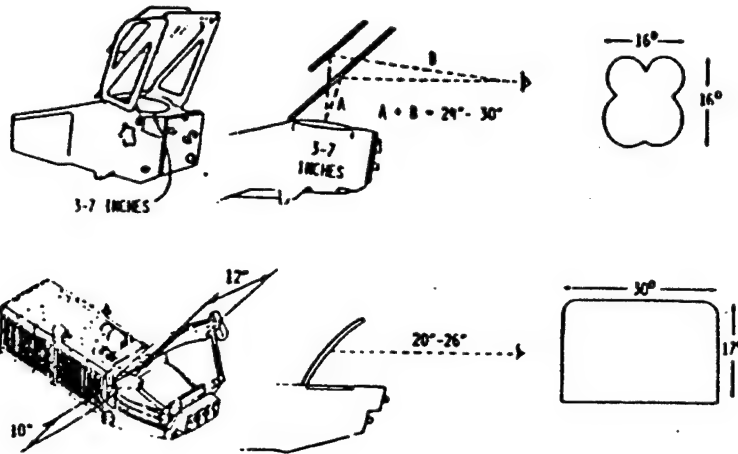
reflective HUDS

FARRAND BULLETIN 1965

Heads-Up Display System

FACTS — FARRAND OPTICAL CO., Inc.

A DEVICE WHICH VASTLY EXTENDS THE OPERATING LIMITS OF BOTH COMMERCIAL AND MILITARY AIRCRAFT THROUGH POSITIVE

- LANDING
- ENROUTE GUIDANCE
- PATH IN HOVER
- ACCURATE TARGET SIGHTING AND WEAPONS DELIVERY

NO HOLOGRAM

SPECIFICATIONS

1. DISPLAY — SUPERIMPOSED ON COCKPIT WINDOW AREA
2. DATA PRESENTATION —
   - AIRCRAFT ATTITUDE (PITCH AND ROLL)
   - HORIZON REFERENCE
   - AZIMUTH-ELEVATION COMMAND INDICATOR
   - FLIGHT PATH
   - HORIZONTAL AND VERTICAL MAP LINES WITH DESTINATION INFORMATION
   - OCTIVLE WITH CONTROLLED-SHARP CAPABILITY
3. FIELD OF VIEW — 25° HORIZONTAL, 25° VERTICAL
4. EXIT PUPIL — 3° HORIZONTAL, 3° VERTICAL
5. ACCURACY — ±1 MIL ACROSS FIELD OF VIEW
6. HEAD MOTION — UP TO 9° LATERAL HEAD MOTION PERMITTED WITHOUT LOSS OF FIELD
7. IMAGE GENERATION — REMOTELY GENERATED, THEN FED INTO DISPLAY HEAD C.R.T.

so pilot gets 70 90 of real world

color coating reflects green

WHAT DOES THE HOLOGRAM BUY YOU?

70% WASTE

1.0   0.7
             0.3
        1.0

TYPICAL HUD

20% WASTE

1.0   0.9
             0.8
        1.0

WIDE FIELD HUD WITH HOLOGRAM

EYE RESPONSE
HOLOGRAM REFLECTS
HUD PHOSPHOR LIGHT

BLUE CYAN GREEN ORANGE RED

Head-Up and Helmet Displays

Gard

KAISER ELECTRONICS

HEAD DOWN A TAD   HEAD UP A TAD   LANTIRN FLIR

WAITING FOR A NEED
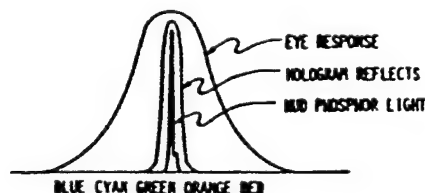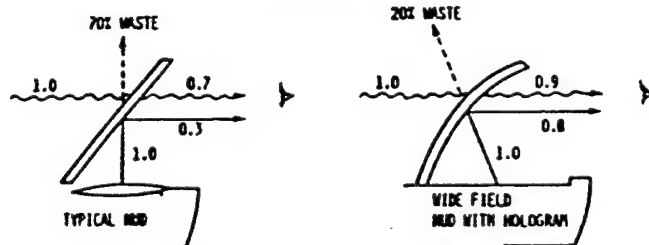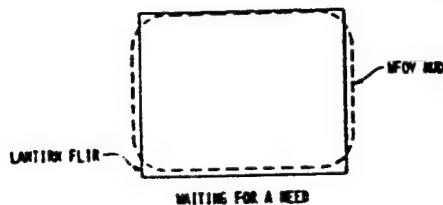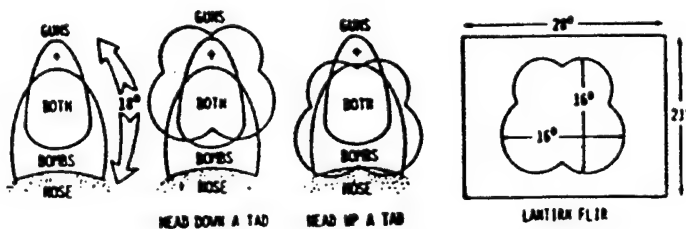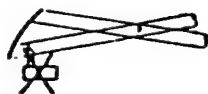
IS THIS A FREE LUNCH?

HEAD BOX AND GUN
CAMERA PROBLEMS
SOLUTION: NEW DESIGN FOR EACH COCKPIT ($)
            AND SCAN CONVERTER + VIDEO RECORDER ($)

OPTICS SIZE, WEIGHT AND $

DISTORTION CORRECTION FOR CRT
SOLUTION: EXOTIC CIRCUITRY ($)

REAFFIRMING: THERE IS NO SUCH THING AS A FREE LUNCH.

"HEAD BOX" LOCATION PROBLEM

REFRACTIVE
SYSTEM
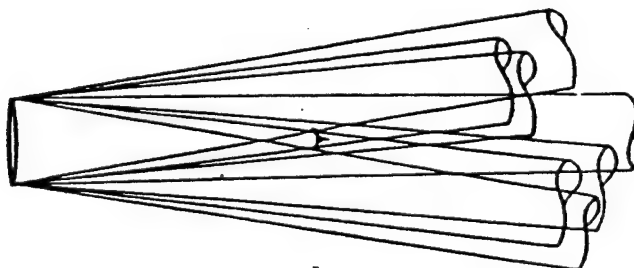
REFLECTIVE
SYSTEM
7.14
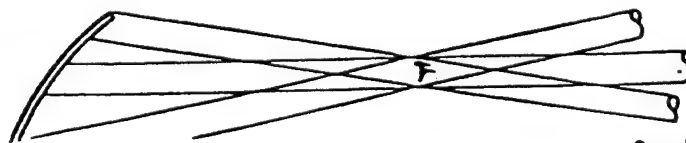
Head Up and Helmet Displays

Gard
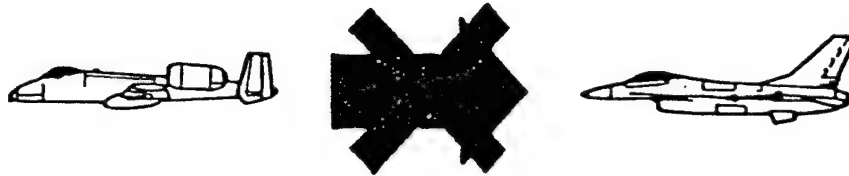
A new design is required for each aircraft
and
we have to know where the pilots really sit

FOV IS THEN EVALUATED BASED
UPON REAL SEATING POSITIONS
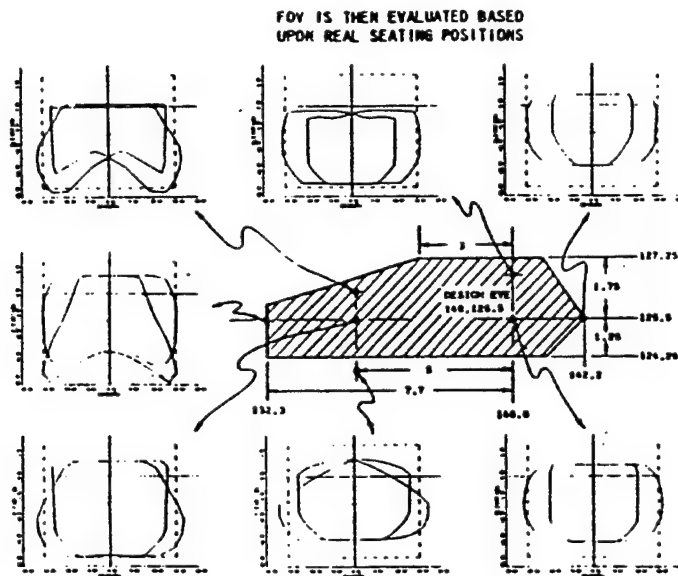
* HEAD BOX LOCATION?

* COLLIMATION/WINDSCREEN CORRECTION?

* REFLECTIONS?

* IS THIS BECAUSE HOLOGRAMS AREN.'T READY?

"HEAD BOX LOCATION"

WFOV HUD AND REFRACTIVE HUD DIFFER

WITH REFRACTIVE
IF IT WAS WRONG,
YOU COULD ALWAYS
MOVE THE COMBINER

BUT IN WFOV HUD

NOT WHEN THE COMBINER IS AN
OPTICAL ELEMENT IN THE SYSTEM

(NOT A HOLOGRAPHIC PROBLEM)
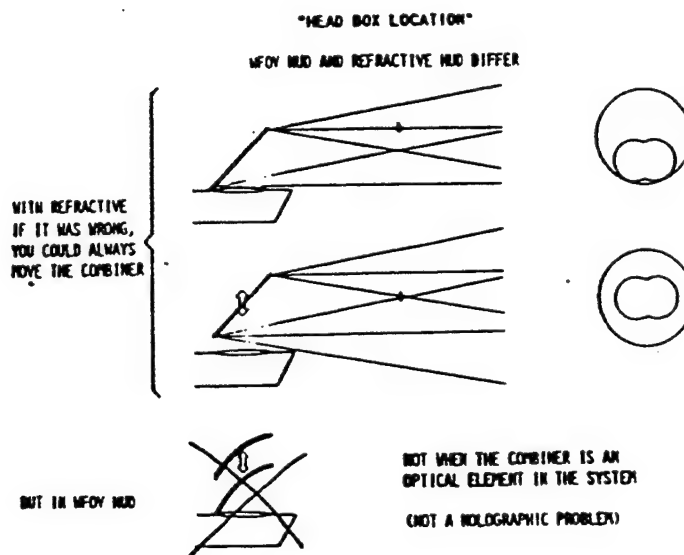
curved windscreen problem

COLLIMATION/WINDSCREEN CORRECTION

F-16 HAS AN OPTICALLY POWERFUL W/S

TARGET AT 300 FT.

HUD @ INFINITY

W/S   LANTIRN HUD
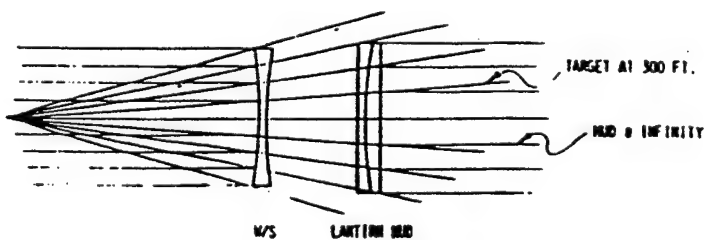
RESULT: LOOK AT PIPPER - SEE TWO TARGETS
LOOK AT TARGET - SEE TWO PIPPERS

7.16

*KAISER
ELECTRONICS*
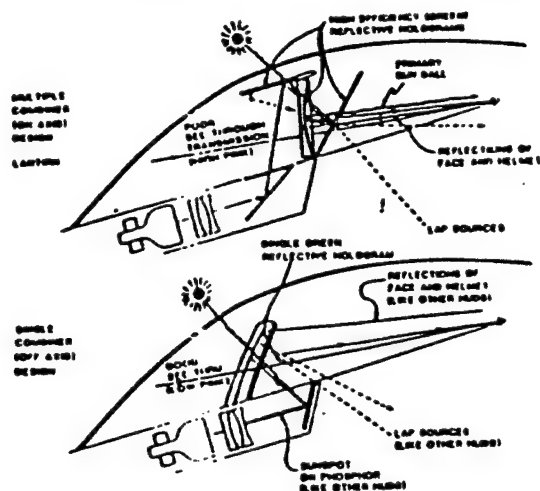
CONCLUSIONS ABOUT LANTIRN PROBLEMS

- THESE ARE NOT HOLOGRAPHIC PROBLEMS

- HEAD BOX AND W/S CORRECTION ARE SPEC PROBLEMS NOT ANTICIPATED

- REFLECTIONS ARE DUE TO PECULIAR LANTIRN OPTICAL IMPLEMENTATION

WFOV HOLOGRAPHIC HUD PROGRAM STATUS

AIRCRAFT	CONTRACTOR	STATUS
F-4E (ISRAEL)	KAISER DESIGN ELBIT ELOP BUILD	IN FLIGHT TEST PROD DEL SEPT '88
LAVI (ISRAEL)	HUGHES OPTICS - ELBIT ELECTRONICS	AIRCRAFT CANCELLED
JAS (SWEDEN) (J-39 GRIPPEN)	HUGHES OPTICS - LM ERICSON ELECTRONICS	FLIGHT TEST
F-15E (USAF)	KAISER	FLIGHT TEST; PROD DEL
LANTIRN (USAF)	MARCONI	PRODUCTION NOW AFTER LONG DELAYS

CONVENTIONAL HUDS PROGRAM STATUS

AIRCRAFT	CONTRACTOR(S)	STATUS
F-16 C/D (USAF)	MARCONI	PRODUCTION DEL
AMX (ITALY/BRAZIL)	OMI (ROME)	PRODUCTION DEL
F-14D/A-6F (USN)	KAISER	FLIGHT TEST
A-10 (USAF)	KAISER	PRODUCTION COMPLETE
AV-8B/GR-5 (USMC/RAF)	SMITHS	PROD/NITE ATTACK UPDATE
F-4EJ (JAPAN)	KAISER/SHIMADZU	PRODUCTION DEL '88
T-4 (JAPAN)	KAISER/SHIMADZU	PRODUCTION DEL '88
FA-18 (USN/USMC)	KAISER	PROD/NITE ATTACK UPDATE
MBB-339 (ITALY)	KAISER	FLT TEST; LTD. PRODUCTION
CASA 101 (SPAIN)	FERRANTI	FLIGHT TEST
F-20 (NORTHROP)	MARCONI	AIRCRAFT CANCELLED

A REVIEW
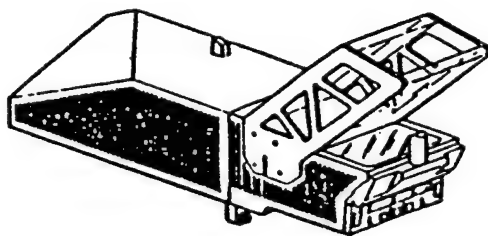
TYPE	NAMES
REFRACTIVE OPTICS	CONVENTIONAL STANDARD

WITH BIGGER OPTICS "WIDE ANGLE"
WITH LOW OPTICS "LOW PROFILE"
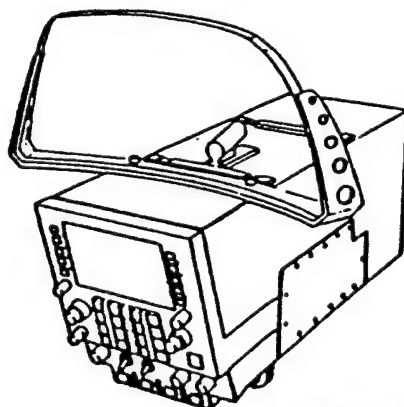
REFLECTIVE OPTICS (PUPIL FORMING) USUALLY WITH HOLOGRAM	WIDE FIELD-OF-VIEW "D" HUD (FOR DIFFRACTIVE) DIFFRACTIVE OPTICS HUD HOLOGRAPHIC HUD

EITHER CAN BE A "RASTER" HUD

KAISER
ELECTRONICS

RASTER

TV

RADAR PPI

PREDETERMINED PATTERN,
INFO IS INTENSITY (Z AXIS),
NO INFO IN PATTERN
EXAMPLES: TV, PPI RADAR, IMAGING FLIR

STROKE OR
CALLIGRAPHIC

STROKE MANAGEMENT

AIR TO AIR
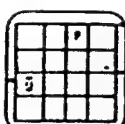
PATTERN CREATED IN SYMBOL SHAPES
ALL INFO IN PATTERN, NONE IN Z
ALMOST ALL HUDS ARE DONE THIS WAY
FOR SEE-THROUGH AND BRIGHTNESS
AGAINST DAYLIGHT BACKGROUNDS

HYBRID
(RASTER/STROKE)

TV + SYMBOLS

RADAR + SYMBOLS
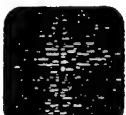
BOTH PREDETERMINED PATTERN WITH INFO
IN Z AXIS PLUS, DURING RETRACE TIME,
STROKE WRITTEN SYMBOLS OVERLAID

THE RASTER REQ's STORY

* ALL STANDARD HUDS WERE STROKE FOR DAYTIME BRIGHTNESS

* LANTIRN ESTABLISHED PLAN TO FLY FLIR ON HUD IN 1:1 OVERLAY - REQ's
  RASTER CAPABILITY

* RASTER BRIGHTNESS INSUFFICIENT FOR GOOD DAYTIME CONTRAST SO STROKE
  STILL REQ'D

* RASTER/STROKE CAPABILITY IS CALLED "HYBRID"

* WFOV HUDS ARE EXPENSIVE, ESPECIALLY TO RETROFIT

* NVG'S CAN GIVE GOOD FIELD-OF-VIEW AND WIDE FIELD-OF-REGARD (F.O.R.)
  FOR "LOOK INTO TURN"

* "CHEAP NITE" EXPLOITS NVG'S FOR F.O.R. AND FLIR ON A RASTERIZED
  CONVENTIONAL HUD FOR RESOLUTION AND EAST OF RETROFIT

* SEEMS LIKE A GOOD COMPROMISE ESPECIALLY FOR RETROFIT

HUD BRIGHTNESS

1.2 good contrast ratio

W/S
T = .9   80/20
WHITE
CLOUD   11000   9900   7520 FL
FL   FL   1600 FL
8000
STROKE: 10000 FL   CR = $\frac{Bo + Ba}{Ba}$ = 1.20
1.20:1 IS SATISFACTORY

W/S
T = .9   80/20
WHITE
CLOUD   11000   9900   7520 FL
FL   FL   160 FL
800
RASTER: 1000 FL   CR = 1.02

too low contrast ratio

THIS IS ALMOST INVISIBLE

shades of grey

RASTER HUD CONTRAST

To solve contrast problem - lower the ambient

VIDEO IN RASTER
(6 SHADES)

6
5 S
4   4
3   3
2   2
1   1

5.66:1

BLACK

CR OF 5.66:1 (6 SQG = $\sqrt{2}$) IS REQUIRED

W/S
(HOLOGRAM)
80/45
DUSK ON   100 FL   90 FL   72 FL
FOREST   360 FL
800
1000 FL   CR = $\frac{432}{68}$ = 6.0:1

GOOD FOR SIX SHADES
AGAINST A 100 FL
BACKGROUND

RASTER/STROKE (HYBRID) REQs

STROKE

CONTRAST   : 1.2:1 AGAINST 10,000 FL

TRANSMISSION : 80% MINIMUM THRU GEN III BAND

LINE WIDTH   : 1.2 MR ± 0.2 MR

RASTER

TRANSMISSION : 80% MIN THRU GEN III BAND

CONTRAST   : 5.66:1 AGAINST 100 FL

RESOUTION   : 20 LINE PAIRS PER DEGREE

- NAVIGATION

    - SIMULATORS SHOWED 25° AZ FOV WAS ADEQUATE

    - LANTIRN FLIGHT TESTS SHOWED 25° AZ X 18° EL IS INSUFFICIENT

    - SNAP LOOK/LOOK INTO TURN WERE PATCHES

- TARGETING

    - NARROW FIELD (2° X 2° - 8° X 8°) IS ESSENTIAL FOR IDENT AT RANGE
      SUFFICIENT TO ALLOW ATTACK

- A-10 SINGLE SEAT NIGHT ATTACK (SSNA) DEMONSTRATOR

    - NAVIGATED WITH THE INS WITH FLIR FOR UPDATE AND TURN SAFETY (BUT
      TURNS WERE RESTRICTED EVEN WITH LANTIRN-SIZE NAV FLIR)

    - SWITCHED TO NARROW FIELD FLIR - 5° X 7° FOR TARGET IDENT AND
      PRESSING GAU-8 ATTACKS (NOT 1:1 SCALED, OF COURSE)

CHEAP NITE APPROACH

- COMBINATION: (A) NVGs (GEN III)

              (B) MED FIELD FLIR DISPLAYED ON RASTER HUD IN 1:1 OVERLAY

- PRINCIPLES

    - NAV - VIA NVGs WHEN ATMOSPHERE PERMITS - WIDE F.O.R. GIVES GOOD
      TURN RATE

    - NAV ON FLIR WHEN ATMOSPHERE BLANKS NVGs

    - TARGET IDENT ON BETTER RESOLUTION OF FLIR

- SHORTCOMINGS:

    - PROBABLY WILL NEED NARROW (2° X 2°) TARGETING FLIR TO PROVIDE LONG
      RANGE IDENT FOR AMPLE MANEUVERING ROOM

    - EJECTION WITH NVGs DICEY AT BEST

- TECHNOLOGY OF HUD, IF NOT TRIVIAL, IS STANDARD

- CAN BE USEFUL FROM ZERO AMBIENT TO BRIGHT DUSK

- SYSTEM EXPERIENCE EXTREMELY LIMITED GIVEN THE COMPLEXITY OF THE PROBLEM

- WE SHOULD BE TALKING LESS AND FLYING MORE (BOTH SIMULATED AND REAL)

RECOGNIZING THAT:

"ABOUT TO DIE IN A SIMULATOR IS NOT THE SAME AS ABOUT TO DIE"
BERT GREEN - TEST PILOT

"THE RECORD FOR FLYING TOO LOW CAN ONLY BE TIED"
A-10 SQUADRON BRIEFING ROOM, NELLIS AFB, NEVADA

7.22

HELMET DISPLAYS IN TACTICAL AIRCRAFT

THE NEED

The need for helmet displays in the modern fighter/attack cockpit arises from several sources. These include: (a) the increasing field of regard of seeking weapons which are becoming available (b) the increasing field of regard necessary to counter tactics employed by ever more agile adversary aircraft and (c) the need for attack aircraft to fly at night at very low levels and employ terrain masking to avoid enemy defenses. The limits of the fixed HUD with its relatively small, forward oriented field of view (and regard, also) are compared graphically in figure 1 with representative sensors (Forward Looking Infrared-FLIR, Laser Spot Tracker-LST and radar) and in the global view of Figure 2 a possible weapon and threat.
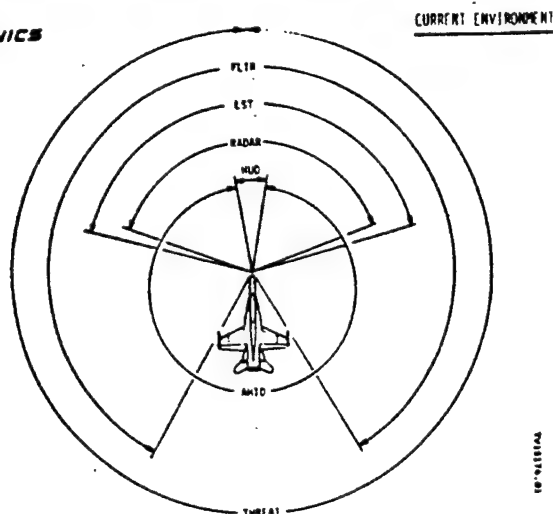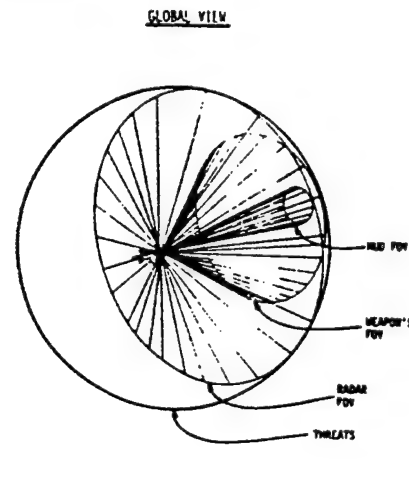
Figure 1

Figure 2

Obviously, the fixed HUD cannot present symbology throughout the set of solid angles one might desire to employ the available sensors and weapons to their fullest capability and without severe limitations on how the pilot employs his aircraft and systems. In the past a HUD was adequate to present symbology needed to use forward firing weapons, i.e. guns, bombs and simple seeking missiles, since the delivery envelopes were by and large contained within the total field of view (TFOV) of the available HUDs. In addition, low level

0034s

7.23

tactics for attack aircraft have only recently been developed, and opinions are forming that these tactics require turns in terrain which are too tight to be safely accomplished with the restricted HUD field, even with so-called Wide Field of View (WFOV) HUDs. One can hypothesize a helmet mounted display which, in combination with a helmet position tracking system, could satisfy the requirement for a large field of regard visual display which would allow off-boresight designation, greater attack flexibility, and selective targeting with weapons such as the AIM-9L/M Sidewinder. In snap-shot visual engagements using such a display, which can fundamentally provide HUD stroke symbology on a moveable but accurately calibrated base, the pilot can positively verify missile lock-on to the proper target before firing. Likewise, ground targets can be identified and designated at almost any aspect angle so the nav-attack system can allow terrain masking to be effectively employed while the pilot manuevers to a successful final attack profile. A handoff from the helmet display to laser ranger or radar can provide simple and accurate ranging for computed solutions which lay either guns or bombs on the target. A further enhancement provides a helmet display which can present video. By coupling a slewable FLIR sensor through to the helmet tracker so the pilot can look with "FLIR eyes" in almost any direction, the attack pilot can successfully fly and turn at night at low altitudes in terrain. At the same time, symbology superimposed on the FLIR display can provide nav data and system failure indications to obviate the need to return to the cockpit in this most difficult of scenarios. Figures 3 through 8 illustrate some of these and other useful functions which can be fulfilled by such a helmet display.

In addition, the possibility that this most useful display could be provided while at the same time reducing the need for precious panel space has further increased the interest of those concerned with modern cockpit design. Most of the high-g cockpits under consideration for such aircraft as the Advanced Tactic Fighter (ATF) recline the pilot and elevate his knees, excacerbating the problem of limited panel area already made difficult by a constantly decreasing fuselage cross section. Thus, despite the fact that such a helmet display must cost more than a fixed HUD because it contains the same basic elements and requires in addition an accurate position tracker, many see it as an item whose cost will be borne because it solves so many problems. And if it could indeed replace a fixed HUD, then the extra cost paid would presumably

0034s

7.24

KAISER ELECTRONICS

AIR-TO-AIR MISSION PROFILE:
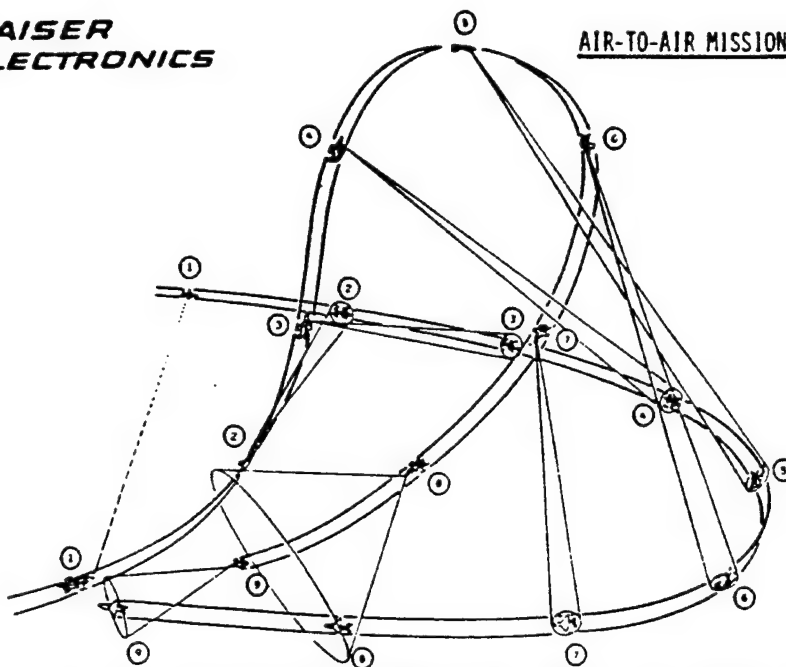
1. BOGEY ACQUIRED AND TRACKING COMMENCED WITH ADVANCED HELMET INTEGRATED DISPLAY (AHID).
2. TARGET IDENTIFIED AS A BANDIT, SYSTEM LOCK-ON MAINTAINED.
3. AHID INFORMATION USED TO DEVELOP BANDIT ENERGY PREDICTIONS.
4. VISUAL CONTACT MOMENTARILY LOST, BANDIT REACQUIRED BY STEERING CUES ON AHID.
5. CONTINUOUS LOCK-ON MAINTAINED WITH AHID, EVEN WHILE INVERTED.
6. PILOT RELIES SOLELY ON AHID FOR CRITICAL SYSTEM INFORMATION.
7. MISSILE LOCK-ON ACHIEVED PRIOR TO RADAR LOCK-ON.
8. RAPID RADAR LOCK-ON ACHIEVED BY TARGET HAND-OFF FROM AHID.
9. MORE EFFICIENT INTERCEPT ACHIEVED THROUGH INTEGRATION OF AHID WITH WEAPONS SYSTEMS.

Figure 3

KAISER ELECTRONICS

QUICK REACTION TIME
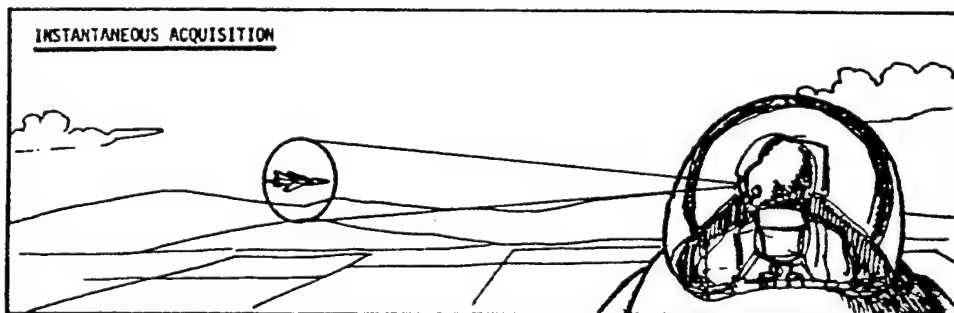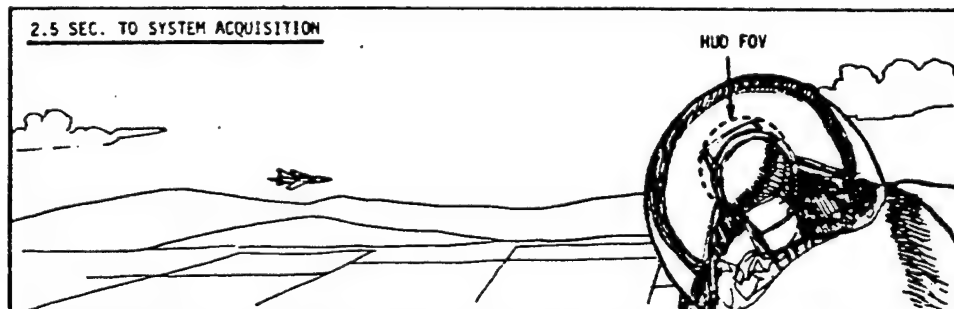
Figure 4
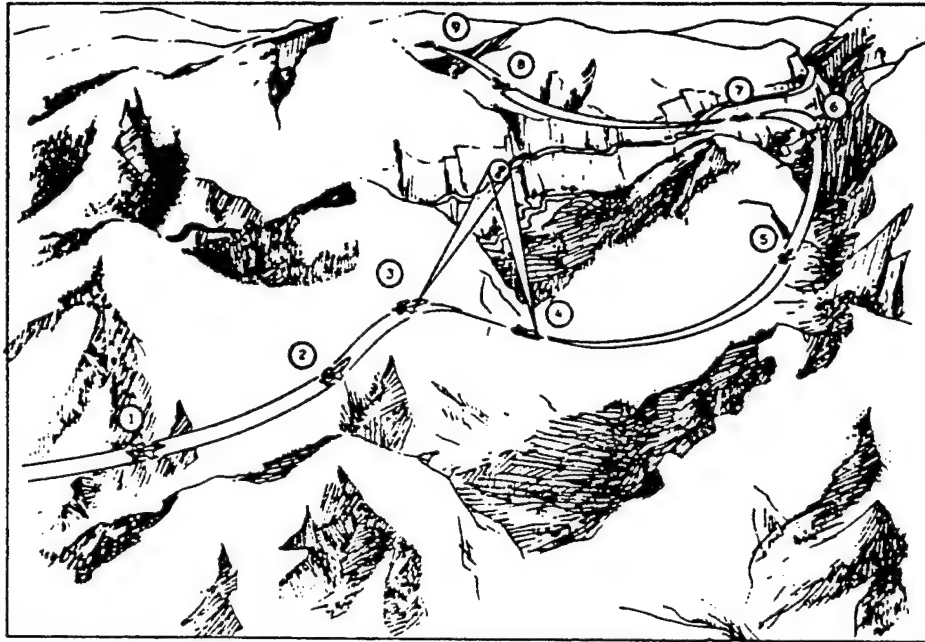
1. LOW LEVEL INGRESS.
2. COMMENCE SEARCH FOR AGGRESSOR COLUMN.
3. TARGET LOCATED AND DESIGNATED WITH AHID.
4. TARGET POSITION FIXED THROUGH TRIANGULATION.
5. RETURN TO LOW PROFILE FOR TERRAIN MASKING.
6. ATTACK PROFILE INITIATED.
7. ATTACK ON AGGRESSOR COLUMN.
8. EGRESS FROM TARGET AREA.
9. RETURN TO LOW LEVEL.

Figure 5

KAISER
ELECTRONICS

COCKPIT VIEW
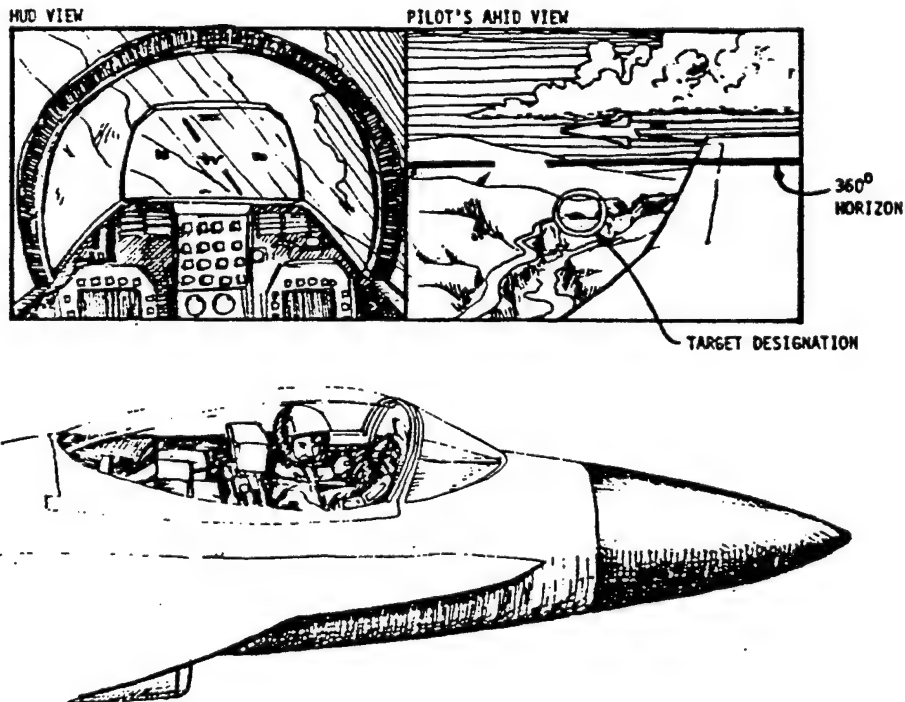
Figure 6

KAISER ELECTRONICS

SEA-AIR-RESCUE (SAR) MISSION PROFILE:

1. DOWNED PILOT HAS DEPLOYED HIS EMERGENCY BEEPER.
2. AIRCRAFT CONDUCTING SEARCH.
3. SEARCH AIRCRAFT PICKS UP EMERGENCY BEEPER.
4. THROUGH TRIANGULATION, DOWNED PILOT LOCATION DISPLAYED ON AHID.
5. SEARCH AIRCRAFT SPOTS RAFT AND MAINTAINS VISUAL CONTACT WITH AID OF AHID.
6. RESCUE HELICOPTER VECTORED TO SCENE THROUGH EFFECTIVE USE OF AHID.
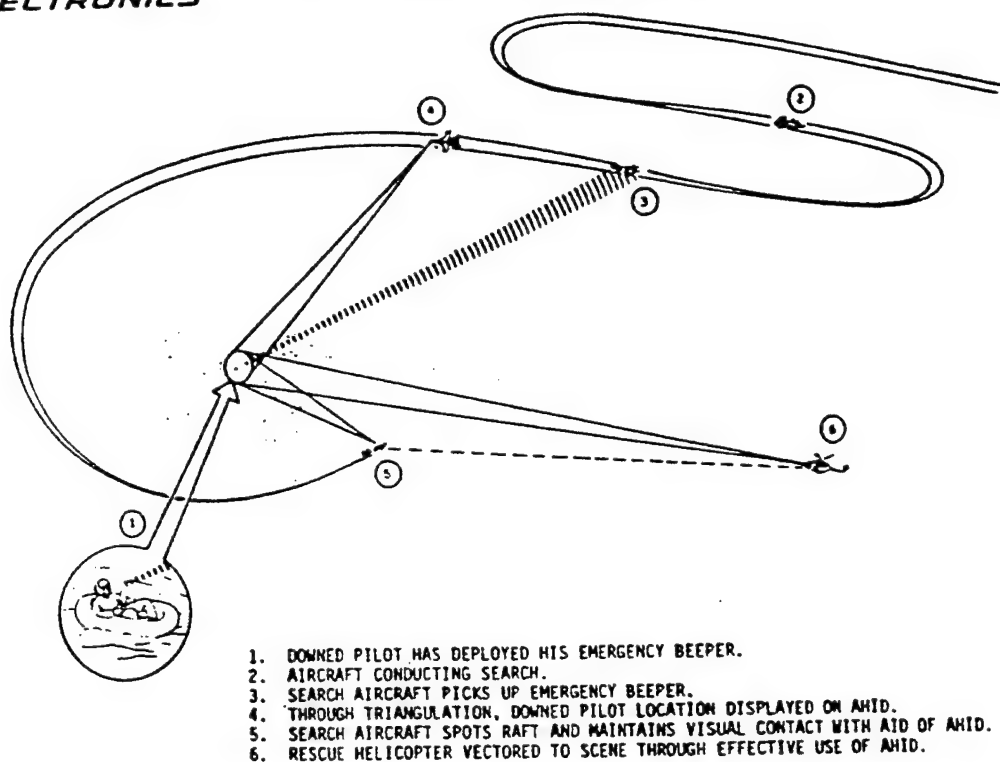
Figure 7

KAISER ELECTRONICS

CARRIER NIGHT LANDING MISSION PROFILE:

1. AIRCRAFT BOLTERS AT NIGHT.
2. TURNING CROSSWIND, PILOT LEVELS AT 800 FEET.
3. FLYING DOWNWIND, PILOT SEES SPN 42 BEAM AND HORIZON ON AHID.
4. AT 90 DEGREE POSITION PILOT BEGINS DESCENT TO INTERCEPT BEAM.
5. NORMAL 90 DEGREE POSITION AT NIGHT WITHOUT USE OF AHID.
6. AT 1-1/2 NAUTICAL MILES, FINAL ADJUSTMENTS MADE TO INTERCEPT GLIDESLOPE AND CENTERLINE.
7. FINAL APPROACH INFORMATION DISPLAYED ON HUD.

Figure 8

7.27

Gard

only be for the helmet tracking system. In the past, the accuracy of available tracking systems has not been adequate to allow the helmet sight to replace the HUD as an air to air gunsight, which function requires a pointing accuracy on the order of 2 to 3 milliradians. However, the development of IFFC (Integrated Flight/Fire Control) relieves this requirement. Demonstrated in 1982, IFFC can function with a 10mil designation accuracy, after which the radar Fire Control System (FCS) coupled to the AFCS (Automatic Flight Control System) automatically directs the attacking aircraft flight path to bring the gun to the proper lead angle to get a hit. In addition to being a better gun solution than the pilot can usually fly manually, a side benefit is to free the helmet tracker from the most stringent of the system accuracy requirements.

THE PROBLEM

With all this promise, there must be another side to the coin. One is reminded that there is no such thing as a free lunch, and the hypothesized helmet is no exception. In fact, the technical problems are extremely difficult to surmount and few would argue that an adequate solution is currently available. Past attempts have failed in part because of limits placed by available component technology. But the major difficulty has been that the displays have been designed as add-ons to existing helmets rather than being designed as an integrated device wherein the whole is designed to satisfy all the needs of the wearer/user simultaneously. As a result they have exhibited excessive bulk and high weight combined with assymetric center of gravity. These characteristics have contributed to wearer discomfort, which Gene Adam has referred to as "man's inhumanity to man". In addition, restriction of normal vision and inadequate optics have caused poor performance. The combination of these have limited acceptable helmet sights to helicopter applications, where low g-levels, larger canopies, and lack of ejection seats simplify the physical problems. Ironically, the high-g environment (sustained 9-gs) contemplated for the ATF, which contributes to the desireability of the helmet in this application, severely compounds the difficulty of satisfying the needed performance with a helmet which can be comfortably worn.

0034s

7.28

Part of the problem is that the helmet is required to simultaneously fulfill a number of diverse requirements for the user, and these requirements continue to expand. The function of protection of the head both within the aircraft and during and after ejection is basic, but the helmet is also used for support of the oxygen mask, the communication system (microphone and earphones) and the visors (clear for night overlaid with dark for daytime use). These functions alone have made the helmet marginally heavy for high-g applications. More recent developments indicate the need to provide additional protection for nuclear, biological and chemical (NBC) defenses, which affect the visor design and seal and dictate the need for a further seal between helmet and flightsuit. These additional functions are currently being developed independently from display needs, but it is obvious that the successful tactical helmet display development will need to consider all of these simultaneously in order to arrive at an optimum solution.

Of course, the addition to the existing helmet of the display function adds mass to an almost unacceptably heavy device. Also, this added mass tends to be off-center, and a high or off-center center of gravity is even more unacceptable than sheer mass. Further, if a display design has attachments to the helmet such as wires or fibre optic bundles, careful attention must be given not only to freedom of movement but also the need for quick disconnects in the ejection sequence. Damage to the helmet and sensitive connections during ordinary ingress and egress and when the helmet is carried outside the aircraft is also an important consideration, since during a scramble in inclement weather the helmet will doubtless receive less than tender treatment.

Because of the difficulty of finding a simultaneous solution to these diverse requirements while providing a helmet display design which fulfills all mission scenarios, it is doubtful if a single design can suffice. It is natural, therefore, to examine the requirements and in this area, some relief can be found. For example, the ATF, which requires the lowest mass helmet because of its sustained high-g capabilities, can use a monocular stroke display with a small field (10-12° round) for its target designation role and hand-offs to missiles and IFFC. Attack aircraft, navigating in terrain, may require a somewhat larger field of view (20° round?) with a raster capability to show FLIR, but the g-levels are somewhat lower and the cockpit can be more spacious in subsonic aircraft. Helicopters, probably require the largest raster FOV of all, but operate in a relatively low-g regime, do not use

ejection seats, and generally have enough space to accommodate the needed additions to the helmet. For these and other reasons, helmet sights are currently operational in the AH-1S Cobra helicopter and a helmet display is used in the AH-64. This latter, termed IHADSS (Integrated Helmet and Display Sight System), provides a 30V by 40°H monocular raster display used by the pilot for low altitude navigation and target designation.

Thus, it would seem that the basic helmet requirements will be split into a minimum of three, i.e., fighter, attack and rotary wing, with further subclasses created by other factors than those mentioned. These other factors include the ever present considerations of economics and politics. For example, economics may dictate that the slewable FLIR is too expensive for a given system solution. In this case, night vision goggles (NVG) may be substituted, with obvious affects on the helmet design. This whole subject of slewable FLIR versus NVG's is currently being intensely debated, and considerably more flying experience will doubtless be needed before capabilities and limitations and of each are quantified to the point where system tradeoffs can be accomplished scientifically. Complicating the controversy, of course, is the continually changing state of the art in FLIRs, NVG's and to a lesser extent, helmet displays themselves.

HELMET POSITION TRACKING

To provide the most useful functions available from a helmet display in tactical aircraft, it is essential to know with reasonable accuracy the angular relationship between the helmet (and therefore, the collimated display rigidly attached to it) and the airframe. For some peculiar applications, it is also necessary to know the spacial position (x; y, and z) of the helmet within the cockpit, but these are too esoteric to be discussed here. It is not necessary, as some at first assume, to know the relationship between the eye ball itself and helmet or the airframe. The display is properly oriented on the combining glass as true angles in space by a computer knowing the angle of the helmet with respect to the airframe. The eyeball is then free to rotate in its socket or translate inside the helmet, and the symbols, being collimated (focused at infinity) will be perceived at the correct angular position in space. Thus, the aiming/target designation functions, et al may be accomplished within the accuracy of the system without knowledge of eye or head position.
0034s

In the aiming function, the accuracy of the angular position measurement of the helmet enters directly as an error, and the aiming can be no better than this measurement. Thus, considerable attention is paid to the accuracy of the tracking system, especially in the range of angles close to the boresight of fixed weapons, where accuracy requirements are most stringent. To a first order, the tracking system selected is independent of the cockpit application although the low-g environment and walk-in cockpit of helicopters allows use of techniques which would clearly be impractical in the fighter/attack aircraft. The AH-1S Cobra, for example, uses rods mechanically attached to the helmet and a system of angular sensors to allow computation of helmet position. Such mechanics are clearly unacceptable in an ejection seat and methods which require no physical connection and cause, therefore, no constraint to head motion are clearly preferred. Methods which have been utilized for this purpose use one of two types of emissions, either magnetics or light of one form or another. While these completely uncouple the helmet from the aircraft, they are not without problems.

The magnetic methods all provide an airframe-mounted radiator which acts as the primary coil of a transformer, filling the cockpit space with an alternating magnetic field of a frequency high enough to be distinguished from other fields already there. A receptor, helmet mounted, has several coils in different orientations, each acting like the secondary coil of the transformer. Depending upon the helmet orientation and the angular relation between the receptor coils themselves, each will generate a different signal voltage. These signals are used to determine the helmet orientation. Unfortunately, the pattern of the radiated magnetic field is locally distorted by metal objects within the cockpit and cannot be predicted with sufficient accuracy. It must be determined emperically by measurements taken throughout the real cockpit using equipment which itself does not distort the field pattern. The computer software must then be adjusted to match the measured data so that the helmet orientation can be accurately determined. These are non-trivial tasks and must be performed again if a significant change occurs in cockpit layout. Nevertheless, the receptor is light and so adds little mass to the helmet and accuracies are reported to be within 5mr in the forward field and within 10mr throughout a 120° FOR (Field of Regard).

0034s

More variety is to be found in systems employing light in the tracker. One of the first developed used rotating fans of non-visible infrared (IR) light wiping across the head area from each side of the cockpit. The time of passage of these fans across the helmet was noted by several small IR detectors embedded in the helmet and these times were used to calculate helmet orientation. In addition to being a fairly expensive solution, it was difficult to locate the emitters in the required position on each side of the seat without interference with other cockpit equipment.

Light emitting diodes (LED's) mounted in patterns on the helmet and viewed by various kinds of fixed electronic cameras viewing the helmet from the side or rear are now the most popular method of using light in tracker systems. it is also possible to use painted patterns on the helmet, detecting these with cameras working on daylight and substituting LED's for the patterns at night. Obviously, systems which use light must take pains that direct light or reflections from the canopy and/or instrument faces are not observable by the aircrew, especially at nite. Also, the light sources cannot be allowed to increase the emission signature of the aircraft so that it becomes easier to detect. Yet with these restraints, the system must also function accurately throughout a wide variety of ambient lighting situations from sunlight glare to total darkness, and on helmets which are covered in random patterns with reflective material. Perhaps the fact that none of these systems based on light (other than the IR fan arrangement, which has been dropped) have been fielded operationally indicates that the solution is non-trivial. On the other hand, the availability of low cost solid state single chip TV cameras has only recently rendered some of these possible systems practicable, and there simply has been insufficient time to bring some of the schemes to fruition.
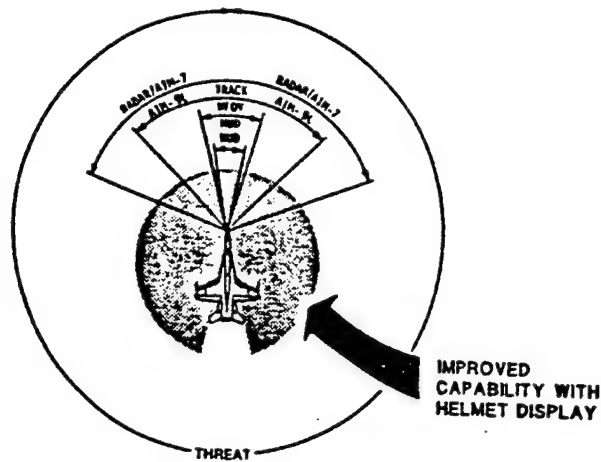
CONCLUSIONS

Given the physical difficulties of the fighter/attack cockpit, it is not surprising to see that the vast majority of helmet sights and all helmet displays are currently confined to rotary wing aircraft, with their low-g environment and walk-in cockpits. But the need is pressing for the lighter, tailored, and ejectable helmet displays required for off-boresight target

0034s

designation in high performance aircraft. The required technologies have also been advancing steadily so that a solution is no longer complete out of reach. The solid state camera mentioned above may simplify the tracking problem and obviate the necessity for tedious magnetic mapping. Improvements in the small CRT's have resulted from development money spent with a view to making this important element more suitable for helmets. Holography, in the form of holographic optical elements, developed primarily for fixed WFOV HUDs, may play an important role in simplifying the optics required to collimate the image and in reducing the weight and bulk of the remaining optics. Coherent fibre optic bundles, which provide a handy means for moving an image from one place to another, are well developed and available. With the need becoming well recognized and the enabling technologies coming into view, serious development efforts are underway which virtually guarantee that the ATF and other tactical aircraft of the 1990's will have a helmet display. The exact form of that display and its tracker system is much more difficult to predict, however. There must first occur a technical and economic shake-out of the different display and tracker system configurations. With the helmet being so intimately coupled with the user and providing him with so many different services, it is difficult to believe that such a shake-out can be accomplished without a considerable amount of flying. Since flying takes time, we can predict that final answers to these very complex questions are still several years away.

0034s

A WFOV HUD CANNOT MATCH THE SYSTEMS
THE HELMET COMPLETES THE COVERAGE

IMPROVED
CAPABILITY WITH
HELMET DISPLAY

THREAT

THE GLOBAL VIEW

HUD FOV

WEAPON'S
FOV

RADAR
FOV

THREATS
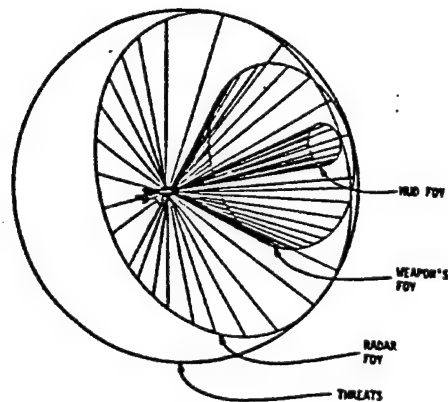
IT'S EVEN MORE DRAMATIC IN THREE DIMENSIONS

CURRENT DISPLAY LIMITATIONS

HEAD-UP DISPLAYS

- INFORMATION FIXED IN FORWARD VIEWING AREA
- NO TARGETING DATA WHERE TARGET NORMALLY OBSERVED
- SMALL FIELD-OF-REGARD

MULTI-FUNCTION DISPLAYS

- REFOCUSING TO INSTRUMENT PANEL WITH SUBSEQUENT LOSS OF EXTERNAL AWARENESS
- INFORMATION NEVER IN TRUE WORLD PERSPECTIVE
- TIME CONSUMING INTERPRETATION OF THREAT LOCATION

KAISER
ELECTRONICS

THE BASIC HELMET DISPLAY IDEA
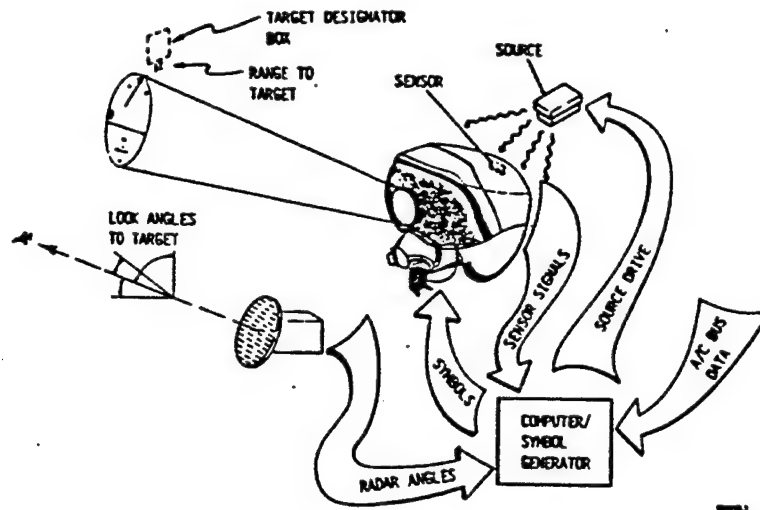
THE BASIC HELMET DISPLAY IDEA
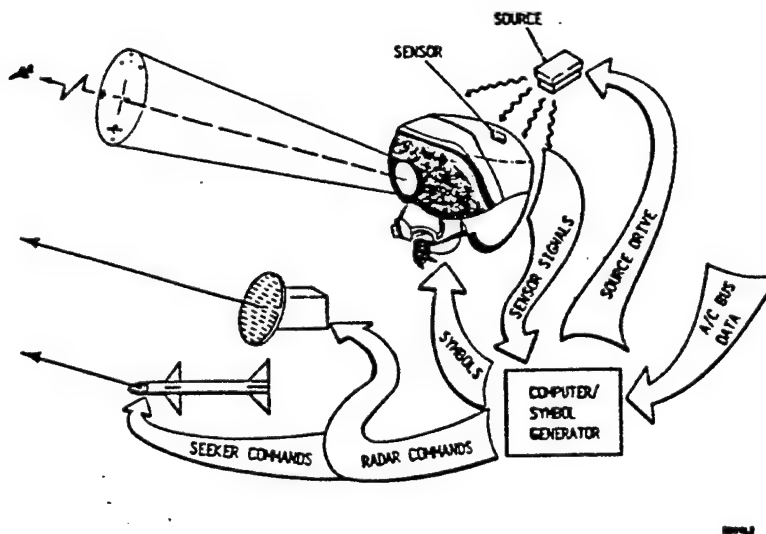
MULTIPLE BENEFITS

VISUAL ACQUISITION
RADAR-TO-EYE HANDOFF

RADAR ACQUISITION
EYE-TO-RADAR HANDOFF

MISSILE ACQUISITION
EYE-TO-SEEKER HANDOFF

GROUND TARGET DESIGNATION
EYE-TO-SYSTEM HANDOFF
(ALSO USEFUL IN AIR-SEA RESCUE)
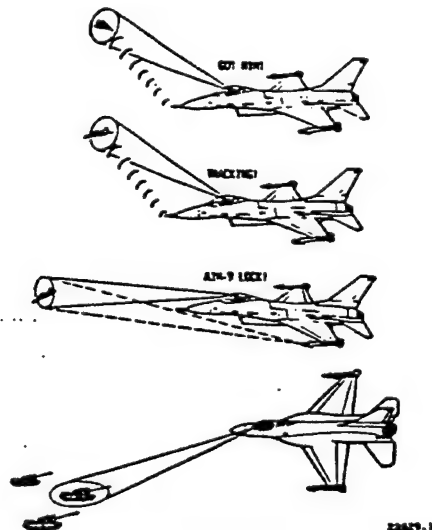
*KAISER
ELECTRONICS*

TACTICAL ADVANTAGES OF HMD

(AS DEMONSTRATED)

- MOAL (MISSILE OFF AXIS LOCK) CAPABILITY
  - GIVES ABILITY TO LOOK'N SHOOT
    VS. POINT'N SHOOT

  - EASIER "SNAP SHOTS" — MORE KILL
    OPPORTUNITIES

  - PILOT FRIENDLY — MUCH EASIER THAN
    PRESENT V-ACQ & MUCH FASTER
    THAN WIDE-ACQ.

RAPID AMRAAM/SPARROW AND SIDEWINDER TARGETING

RADAR LOCK

MISSILE SLEW WITH HMD

AMRAAM SPARROW LOCK-SHOOT

SWITCH - POINT - UNCAGE - SHOOT

AGILE EYE

KAISER ELECTRONICS
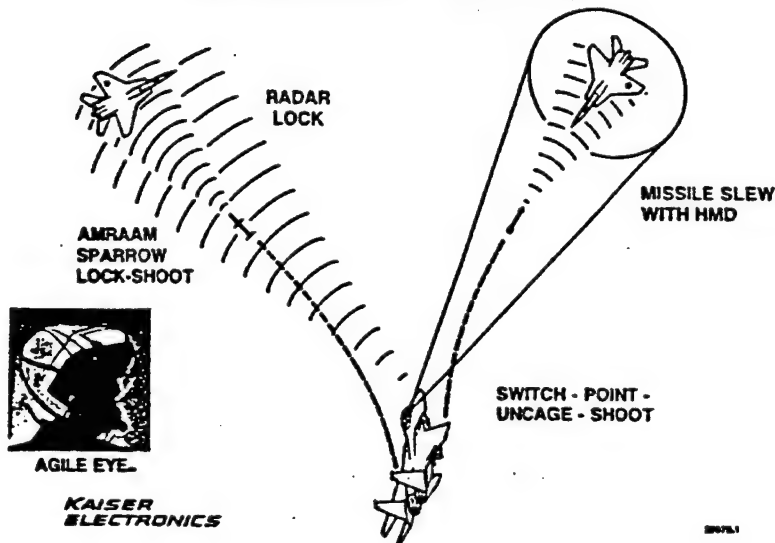
- OFF-BORESIGHT AIM-9 LOCKS W/O RADAR LOCK
  NOW EASY

  - RARELY UTILIZED W/ TODAY'S MECHANIZATION
    UNLESS FORCED

  - MULTIPLE QUICK SHOT CAPABILITY
    DRAMATICALLY ENHANCED

- CROSS LOCKS (RADAR & HEAT) NOW EASY
  - MULTIPLE SHOTS NOW POSSIBLE ON VID/1st PASS
    - BIG ADVANTAGE WHEN YOU'RE OUTNUMBERED

    - WHICH IS ALWAYS.

7.36

HELMET SIGHT

VIEW FIXED RETICLE OVERLAID ON OUTSIDE WORLD

HELMET DISPLAY

VIEW "FULL FUNCTION" DISPLAY OVERLAID ON OUTSIDE WORLD

STROKE ONLY - HUD-LIKE STROKE SYMBOLOGY

RASTER ONLY - SHOWS VIDEO AND SYMBOLS IN RASTER FORMAT

HYBRID - COMBINED RASTER/STROKE CAPABILITY WITH STROKE AVAILABLE IN
RASTER RETRACE

SIMULATOR HELMET DISPLAYS

INTENDED TO SIMULATE THE REAL WORLD VIEW IN FRONT OF THE EYES WHILE
MOUNTED ON THE HEAD

T18144.1

TYPICAL HELMET SIGHT FORMAT

AIMING RETICLE
FOR TARGET
INSERTION

POINTERS FOR
TARGET CUEING
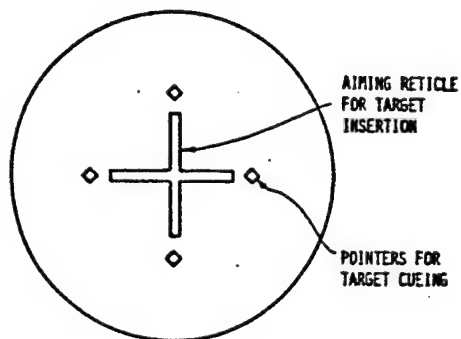
18145.1

A SIGHT IS NOT ENOUGH

TYPICAL SIGHT SYMBOLOGY
ONLY FIXED PATTERNS AVAILABLE (LIKE THE OLD GUNSIGHT)

AIMING
RETICLE
FOR TARGET
INSERTION

POINTERS
FOR TARGET
CUEING
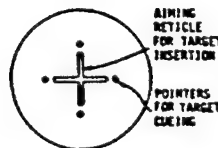
TYPICAL HELMET DISPLAY SYMBOLOGY (THE SAME FLEXIBILITY
AND SOFTWARE PROGRAMMABILITY AS A HUD)

PILOT'S COMMENTS: "ALTITUDE AND AIRSPEED IN HELMET REALLY
HELPED DURING THE ENGAGEMENT"
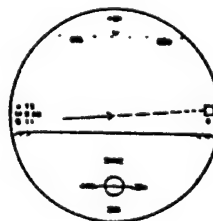
HEAD-UP DISPLAYS DEVELOPED FROM GUNSIGHTS THE SAME WAY - STARTING WITH AN
AIMING RETICLE - THEN SYMBOLOGY WAS NEEDED FOR SITUATION AWARENESS

KAISER
ELECTRONICS

CE7430.18

Head Up and Helmet Displays   36   7.37   Gard

- SA (SITUATIONAL AWARENESS) INCREASED
  - THERE'S NO SUCH THING AS "TOO MUCH SA"
  - HMD ARROW ALWAYS POINTS TO LOCKED TARGET - SUPER!

- AIRSPEED & ALTITUDE ALWAYS IN FOR
  - GREAT FOR "OVER THE TOP" MOVE DECISIONS

(NO LONGER HAVE TO COME BACK INTO COCKPIT - HUD - TO CHECK TO ENSURE THAT YOU HAVE ENOUGH "Q" TO MANEUVER OVER THE TOP. IF YOU DON'T HAVE IT, YOU "GO UNDER", PROVIDED YOU HAVE ENOUGH ALTITUDE ... WHICH IS ALSO DISPLAYED) WHEN YOU FOCUS BACK INTO COCKPIT & THEN ATTEMPT TO REACQUIRE THE BOGEY YOU FREQUENTLY EXPERIENCE DIFFICULTY

HELMET TRACKING

Used in rotary A/C

MECHANICAL

SENSING COILS

MAGNETIC FLUX

TO COMPUTER

RADIATORS
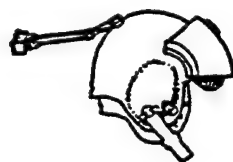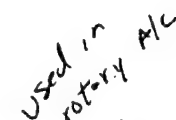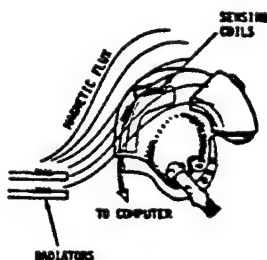
MAGNETIC

KAISER ELECTRONICS

Used in AH-64

LIGHT AS A SENSOR

IR DETECTORS

EMITTER

ROTATING IR BEAMS METHOD

EMITTER

TO COMPUTER FOR TIMING ANALYSIS
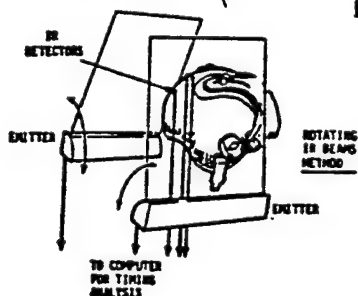
PATTERNS ON HELMET

CCD CHIP CAMERAS

VIDEO ANALYSIS COMPUTER

LED EMITTERS

LED EMITTERS ON HELMET

CCD CHIP CAMERAS
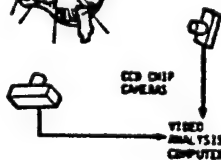
VIDEO ANALYSIS COMPUTER

MECHANICAL -
A LITTLE
TROUBLESOME
DURING EJECTION

RADIATOR
RECEIVER
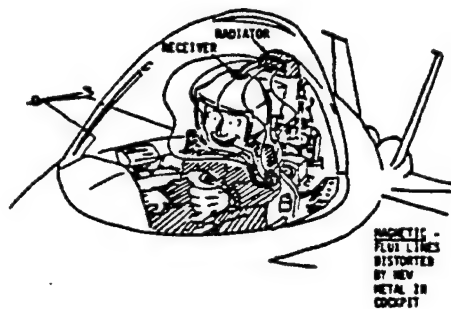
LIGHT SYSTEMS -
TARGET ARE OBSCURED
BY REFLECTIVE TAPE
ON THE HELMET
(TAPE REQ'D TO AID
SEARCH AND RESCUE)

MAGNETIC -
FLUX LINES
DISTORTED
BY NEW
METAL IN
COCKPIT

THE TECHNICAL PROBLEM

MASS

3 LB

13.5 FT LBS

27 LB

SUPPORT

OFF CENTER MASS

5 LB

27 LB

3G

9G

EJECTION
HAZARD

DANGLING WIRES
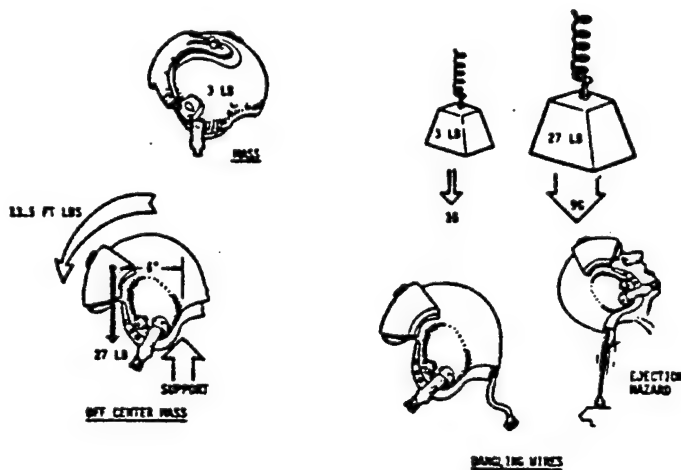
18132.1

COMFORT DEPENDS ON BOTH
HELMET WEIGHT & CENTER OF GRAVITY

HEAD
CG

2 LBS (0.91 kg)

AGILE EYE

HGU-33/P

HEAD
WEIGHT

4 LBS (1.82 kg)

+ GU TOLERANCE

DISTANCE FROM NECK SUPPORT (mm)

NECK
SUPPORT

(EXTRACTED FROM STUDY BY DR. MARK DARRAH, Ph.D., McDONNELL AIRCRAFT CO.)
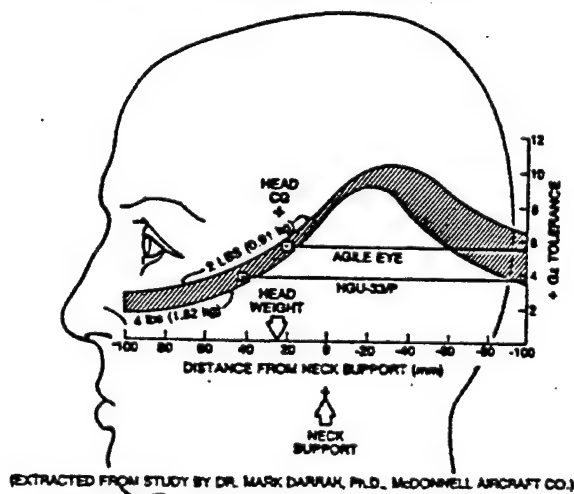
HELMET FUNCTIONS

PRESENT

PROTECTION

SUPPORT
OXY MASK
HEAD SETS

VISOR/FACE PROTECTION
CLEAR - NITE
DARK - DAY

FUTURE

NUCLEAR,
BIOLOGICAL,
CHEMICAL DEFENSE

SUPPORT

LASER PROTECTION

DISPLAYS

VISOR
CLEAR - NITE FACE PROTECTION
DARK - DAY FACE PROTECTION

EXIT PUPIL/EYE
SPACING CONSIDERATIONS (SCALE 2:1)

2.756"

2.5"

0.4" OPTICS
EXIT PUPIL

0.4" OPTICS
EXIT PUPIL

95TH PERCENTILE
NAVAL AVIATOR
(2.756 I.O.D.
4.0 MM PUPILS)

5TH PERCENTILE
AF AVIATOR
(2.244 I.O.D.
4.0 MM PUPILS)

2.244"

EXIT PUPIL: 0.4 INCH
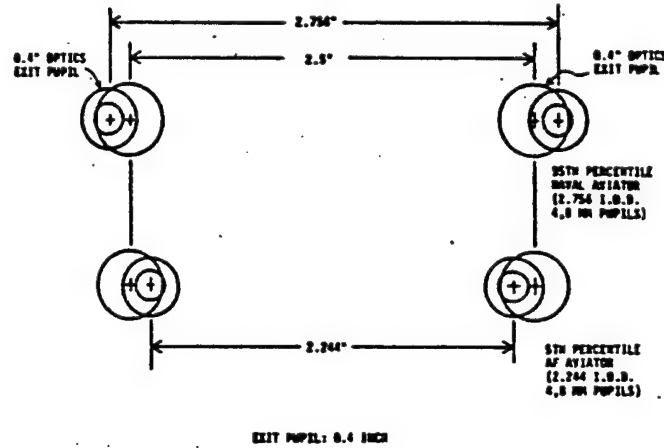
18142.1

EXIT PUPIL/EYE
SPACING CONSIDERATIONS (SCALE 2:1)

2.756"

2.5"

0.75" OPTICS
EXIT PUPIL

0.75" OPTICS
EXIT PUPIL

0.090

0.090

95TH PERCENTILE
NAVAL AVIATOR
(2.756 I.O.D. -
4.0 MM PUPILS)

5TH PERCENTILE
AF AVIATOR
(2.244 I.O.D. -
4.0 MM PUPILS)

2.244"

EXIT PUPIL: 0.75 INCH
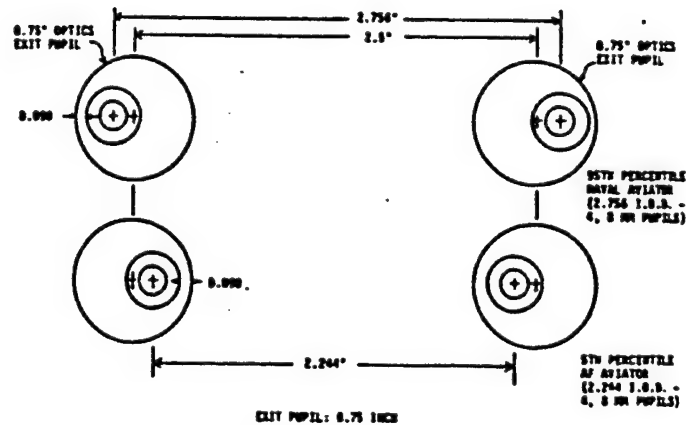
LOCATION OF IMAGE SOURCE

- CRT IN HELMET?

    - HVPS IN HELMET?

- FIBRE OPTICS BUNDLE TO HELMET?

    - NATURE OF DISCONNECT?
      (MUST EXCLUDE DIRT)

    - HOW IS MASS SUPPORTED?

- VISOR OR SEPARATE COMBINER?

    - HOW ARE VISORS RETRACTED?

    - HOW ARE EYE GLASSES ACCOMMODATED?

    - TRANSMISSION/REFLECTION OF COMBINER?

high voltage power supply? eject? disconnect explosive gases?

18148.1

THE PAST: ADD-ONS   **WHERE HAVE THEY BEEN?**
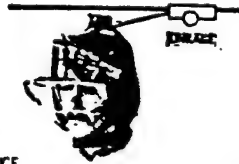
ALL TOO HEAVY, CLUMSY AND OFF BALANCE

NEEDED: A NEW METHOD

- START WITH A CLEAN SHEET OF PAPER

- DESIGN A DISPLAY INTEGRATED INTO A
  NEW HELMET SHELL AND LINER

- CONTROL WEIGHT AND CENTER-OF-GRAVITY
  THROUGHOUT THE DESIGN PROCESS

- INCORPORATE PILOT'S COMMENTS AS YOU GO

- NEVER, NEVER COMPROMISE SAFETY OR COMFORT

helicopter NVG's 4 hour limit due to fatigue moment of inertia

ATF 600 KT EJECTION DESIGN.

ANOTHER EXAMPLE

mock-up *caution* *reality*

LHX 3.95lb design

fiber optic coupled

MOCK UP   PRODUCT

THE RESULT: KAISER'S AGILE EYE
ALL OF THE ADVANTAGES OF AN INTEGRATED APPROACH

- PROTECTION LEVELS OF CURRENT HELMETS
- LIGHTWEIGHT
- LOW PROFILE (REDUCED BULK)
- IMPROVED CENTER OF GRAVITY
- IMPROVED SOUND ATTENUATION
- EJECTION SAFE
- CUSTOM FIT
- HIGH OPTICAL PERFORMANCE
- UNRESTRICTED VIEWABILITY
- DAY/NIGHT COMPATABILITY
- INTEGRAL LIGHTWEIGHT COMM & OXYGEN MASK (OR STANDARD MASK MAY BE USED)
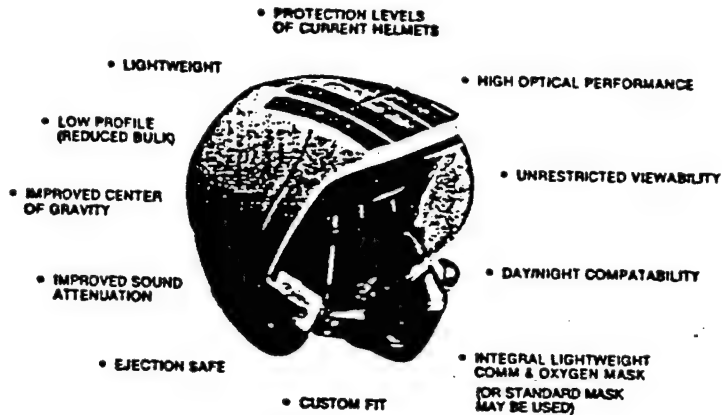
... FOR MAXIMIZED SYSTEM PERFORMANCE
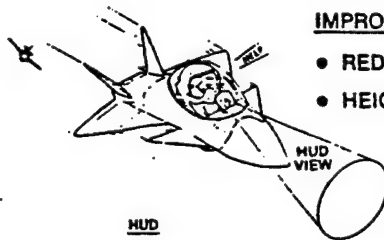
IMPROVE MAN/MACHINE INTERFACE
- REDUCE PILOT WORKLOAD
- HEIGHTEN SITUATION AWARENESS

HUD

HUD VIEW

INCREASE SURVIVABILITY
- CONTINUOUS EYE CONTACT WITH THREAT
- DECREASE LAUNCH TIMES
- EMBEDDED TRAINING

HELMET VIEW

HELMET DISPLAY
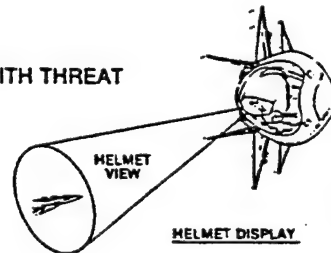
SUCCESS: AGILE EYE WEIGHT
(MEDIUM, SINGLE VISOR)

Chart (POUNDS):

	STANDARD HGU-33/P	KEVLAR HGU-55/P	LIGHTWEIGHT HGU-55/P WITH ADD-ON OPTICS	KE'S INTEGRATED HELMET
Total	3.76 (1.7 kg)	3.24 (1.47 kg)	3.99 (1.81 kg)	2.99 (1.38 kg)
OPTICS	.91	.91	.75	.75
MASK			.91	.57
HELMET	2.85	2.33	2.33	1.57

OPTICS
MASK
HELMET
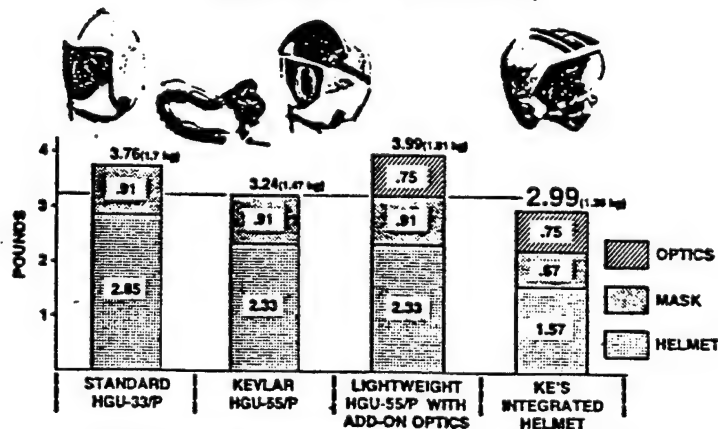
AND THE CENTER-OF-GRAVITY IS A FULL INCH (25 MM)
AFT OF THAT OF THE HGU/33-P

7.42

AGILE EYE. PERFORMANCE

360° FIELD-OF-REGARD

0.75 INCH (19 MM) PUPIL SOLVES HELMET SLIP

3-8 MILLIRADIAN ACCURACY

12° MONOCULAR FIELD-OF-VIEW
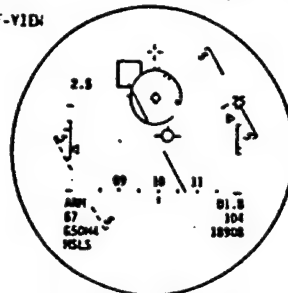
AND 12° WILL
CONTAIN THE
ENTIRE F-16 HUD
SYMBOLOGY!

THE PILOTS JUST SAY "SUPER!"

CUSTOM FORM FIT
5TH TO 95TH PERCENTILE

VISOR
ASSY.
(FITS ALL SHELLS)

MEDIUM
SHELL

LARGE
SHELL

EX-LARGE
SHELL

THIN
CUSTOM LINER

REGULAR
CUSTOM LINER

THICK
CUSTOM LINER

(EACH SHELL SIZE ACCEPTS 3 DIFFERENT CUSTOM LINERS)
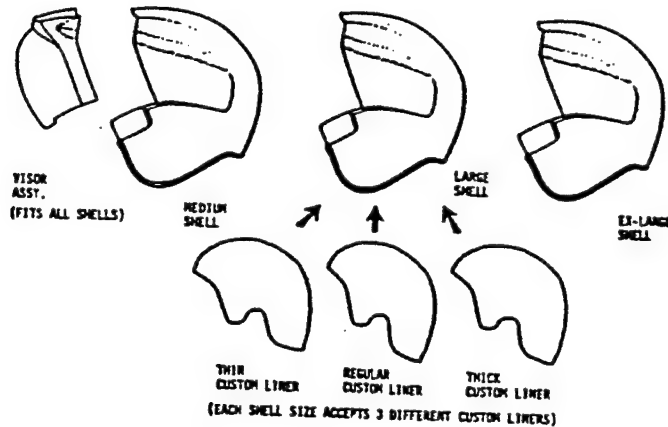
TV18688.81

SAMPLE SYMBOLOGY: AIR-TO-AIR

HELMET HEADING
(A/C HDG + HELMET TO A/C HDG)

HELMET TRUE ELEVATION
(A/C EL + HELMET TO A/C EL)

+01

015   020

CUEING ARROW
(DIRECTION TO T.D. BOX)

ANGLE OF ATTACK   α 1.5
MACH   M 0.98
G 1.1

TARGET
DESIGNATOR BOX

TARGET RANGE

12

NORMAL ACCEL

HORIZON

AIRCRAFT ROLL TABS

SW2

ALTITUDE

440   220

AIRSPEED

335

A/C HEADING
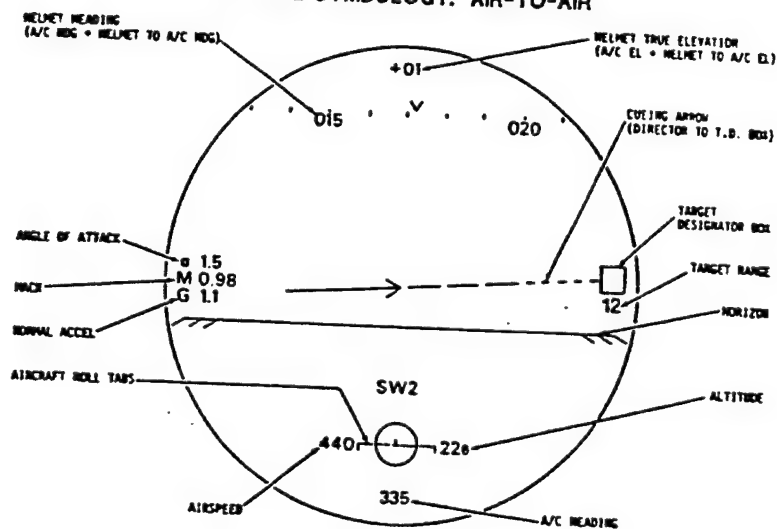
AGILE EYE. SIMULATOR TESTING

THE TEST
- SPONSORED BY U.S. AIR FORCE •
- CONDUCTED AT MCDONNELL DOUGLAS CORP., ST. LOUIS, MISSOURI
- F-15C AGAINST MIG-23,27 AIRCRAFT
- TACTICAL AIR COMMAND (TAC) PILOTS AGAINST AGGRESSOR PILOTS

THE RESULTS
- WHOEVER USED AGILE EYE. WON THE FIGHT
- BECAUSE OF QUICKER RADAR LOCKS AND QUICKER MISSILE LOCKS - MORE SHOTS PER ENGAGEMENT (AND MORE IMPORTANT - QUICKER THAN THE BAD GUYS)
- F-15 EXCHANGE RATIOS DOUBLED USING AGILE EYE.
- (ARMSTRONG AEROMEDICAL RESEARCH LAB, WRIGHT PATTERSON AIR FORCE BASE, OHIO)

AGILE EYE. SYSTEM CONFIGURATION
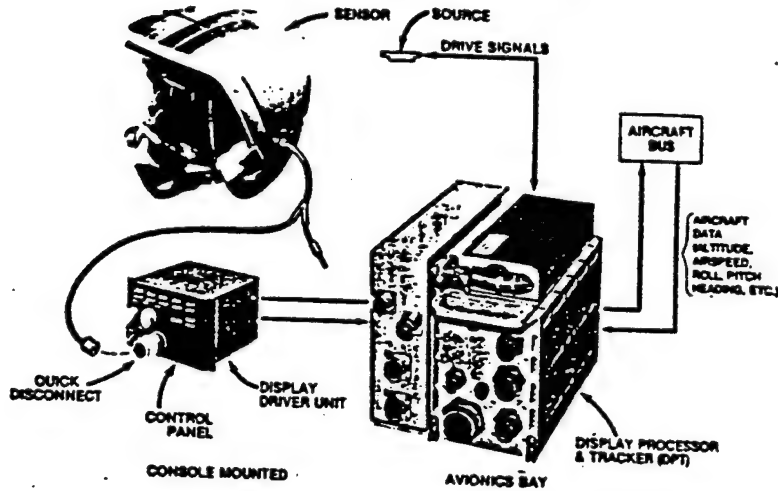
AGILE EYE. FLIGHT TESTING

THE TEST

- SPONSORED BY U.S. NAVY

- FOUR FLIGHTS IN NOVEMBER, 1987 AT NAVAL WEAPONS CENTER, CHINA LAKE, CALIFORNIA

- TESTS WERE FLOWN IN A NAVY F-18 AND SUPPORTED BY MCDONNELL DOUGLAS AND KAISER ELECTRONICS
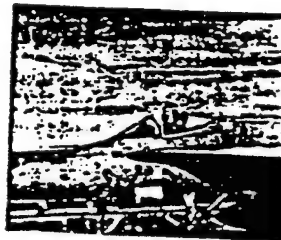
TAXIING WITH AGILE EYE. IN THE F-18

PRELIMINARY RESULTS (MORE FLIGHTS ARE SCHEDULED)

- HELMET CUEING TO GET PILOT TO TARGET IS SUPER

- MAINTAINING SITUATION AWARENESS WAS EASIER USING THE HELMET DISPLAY

- WHEN TARGET IS OFF BORESIGHT, AGILE EYE. IS SUPER

- VISUAL ACQUISITION RANGE MORE THAN DOUBLED (RADAR TO EYE HANDOFF)

7.44

INTENSIFIED NIGHT VISION FOR LOW ALTITUDE NAVIGATION
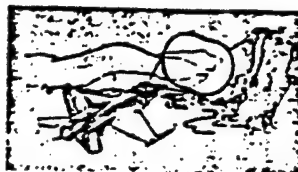
FLIR RASTER WITH SYMBOLS FOR NAV/ATTACK SMOKE PENETRATION

IN-WEATHER NOE NAVIGATION AND ATTACK

AS VISUAL REQUIREMENTS INCREASE G LEVELS COME DOWN
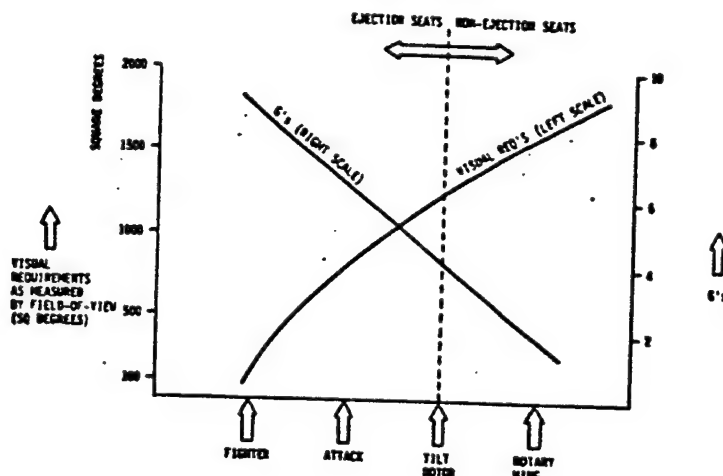
NIGHT VISION - KAISER'S NITE EYE.

- A HELMET WITH TWO INTERNAL IMAGE IN- TENSIFIERS, WITH THE IMAGE SHOWN ON COMBINING GLASSES AND FOCUSED AT IN- FINITY FOR EASY VIEWING

- LIGHTER THAN A STANDARD HELMET, IT IS ALSO AERODYNAMI- CALLY COMPATIBLE WITH EJECTION AND ALSO HAS A CON- TROLLED C.G. LOCATED BEHIND THE HEAD C.G.

- STATUS: IN DEVELOP- MENT NOW. AVAILABLE FOR FLIGHT TESTING IN 1989

KAISER
ELECTRONICS
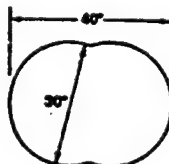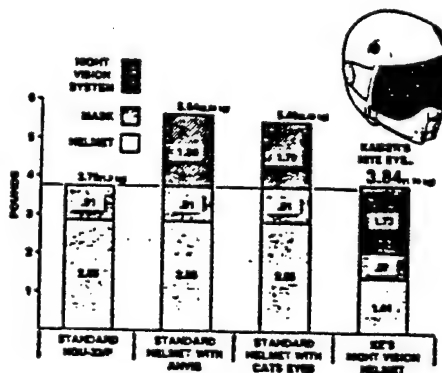
THE BINOCULAR 30° X 40° INSTANTANEOUS FIELD-OF-VIEW.

FLIR DISPLAY/NIGHT VISION PLUS SYMBOLS
KAISER'S STRIKE EYE.

- NIGHT EYE. WITH TWO ADDED CRT'S IS CAPABLE OF DISPLAY OF BOTH STROKE SYMBOLOGY AND RASTER WITH VIDEO FROM A TURRETED FLIR

- IMAGE INTENSIFIERS OR A 24° X 32° RASTER SEEN IN 1:1 OVERLAY WITH THE REAL WORLD PROVIDE FOR LOW ALTITUDE NAVIGATION - A TARGETING FLIR SHOWN MAGNIFIED MAKES THIS HELMET PARTICULARLY SUITED TO ATTACK AIRCRAFT

30° X 60° NIGHT VISION
PLUS 24° X 32° RASTER
AND STROKE SYMBOLOGY

KAISER'S
STRIKE EYE.

NIGHT VISION

FLIR FOR SMOKE
PENETRATION
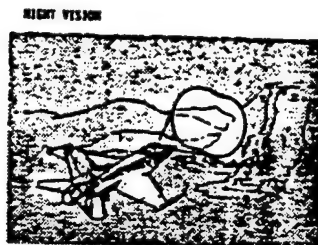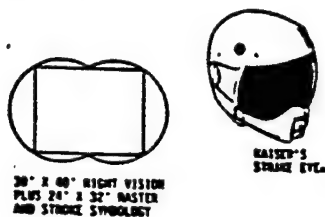
WIDE EYE. PERFORMANCE

360° FIELD-OF-REGARD

12.7 MM H X 15 MM W PUPIL SOLVES
HELMET SLIP

4 - 8 MILLIRADIAN ACCURACY

FLIR COMPATIBLE

40°

60°
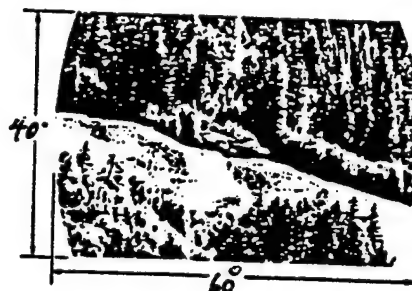
SYMBOLS IN RETRACE
5.2? POUNDS   4.2 # prototype

CENTERED, AFT C.G.

APPLICATIONS AND BENEFITS

MAP OF THE EARTH NAVIGATION USING
TURRETED FLIR WITH OVERLAID
SYMBOLOGY ON VERY-WIDE-FIELD-OF-
VIEW (VWFOV) HELMET DISPLAY

LAUNCH OF AIR-TO-GROUND MISSILE
DIRECTED AND LOCKED USING HELMET
FLIR DISPLAY AND OVERLAYED
SYMBOLOGY

Head Up and Helmet Displays

Gard

APPLICATIONS AND BENEFITS (CONTINUED)

**AIR-TO-AIR DAYTIME USING STROKE
SYMBOLOGY FOR GUNS, STINGERS OR
AIM-9 SIDEWINDERS**
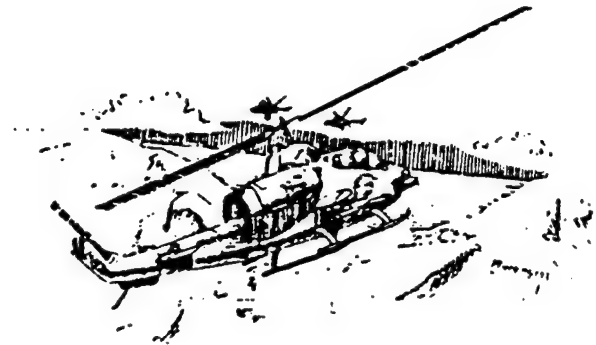
**SEARCH AND RESCUE OPERATIONS
USING HELMET SYMBOLS TO LOCATE
AVIATOR AND FLIR SYSTEM TO
SIGHT HIM AND EFFECT THE RESCUE**

HUD BRIGHTNESS/CONTRAST

10,0000 FL

8,000

1,700 FL

WHITE CLOUD

20%

8,500

CP

21,000

24,000

CRT AT 24,000 FL

$$CR = \frac{9700}{8000} = 1.21:1$$
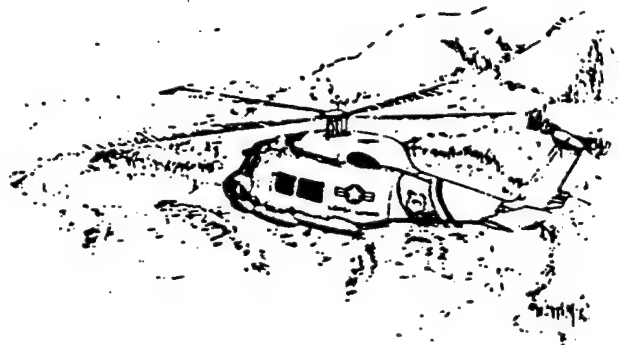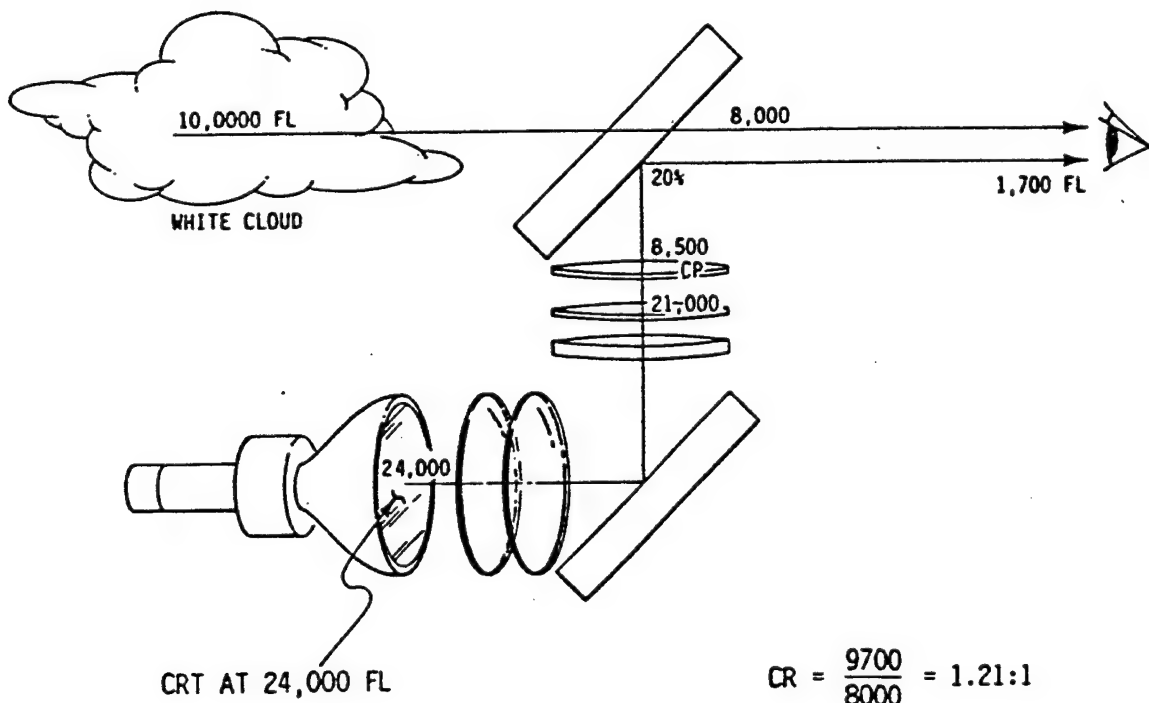
FOR GOOD HUD, CR > 1.2:1

HUD IMAGE PLANE
SIZE/TRANSFER FUNCTION

OPTICS

2.5
INCHES

20°
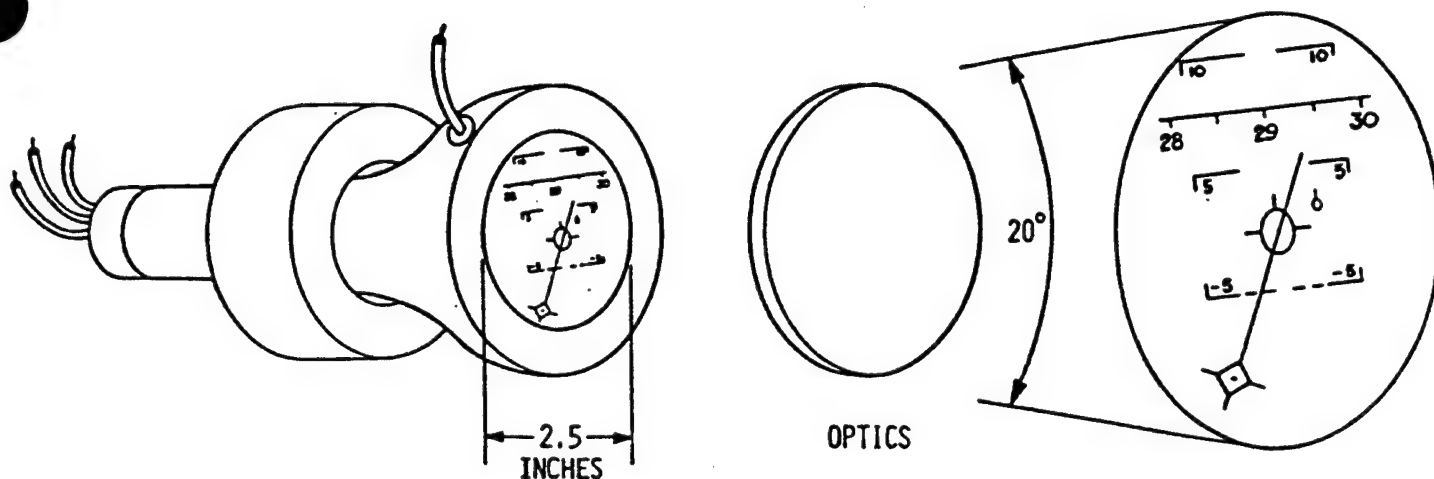
2.5 INCHES = 20 DEGREES

$$20 \text{ DEGREES} \times 17.45 \frac{\text{MILLIRADIAN}}{\text{DEGREE}} = 349 \text{ MR}$$

MILLIRADIANS EXPLAINED

1 RADIAN

r

r

$$\frac{\text{1 RADIAN}}{1000} \qquad \frac{r}{1000} \qquad = 1 \text{ MILLIRADIAN}$$

r

EXAMPLES:

.001 INCH

1 INCH

OR

1 FT

1000 FT

3 1/2 INCHES

1 FOOTBALL FIELD

100 YDS = 300 FT

3 1/2 INCH POST

1 FOOTBALL FIELD

300 FT

Head Up and Helmet Displays

Gard

20°

2.5 IN → | ← 349 MR

1 MR
AT 50% BRIL

OPTICS
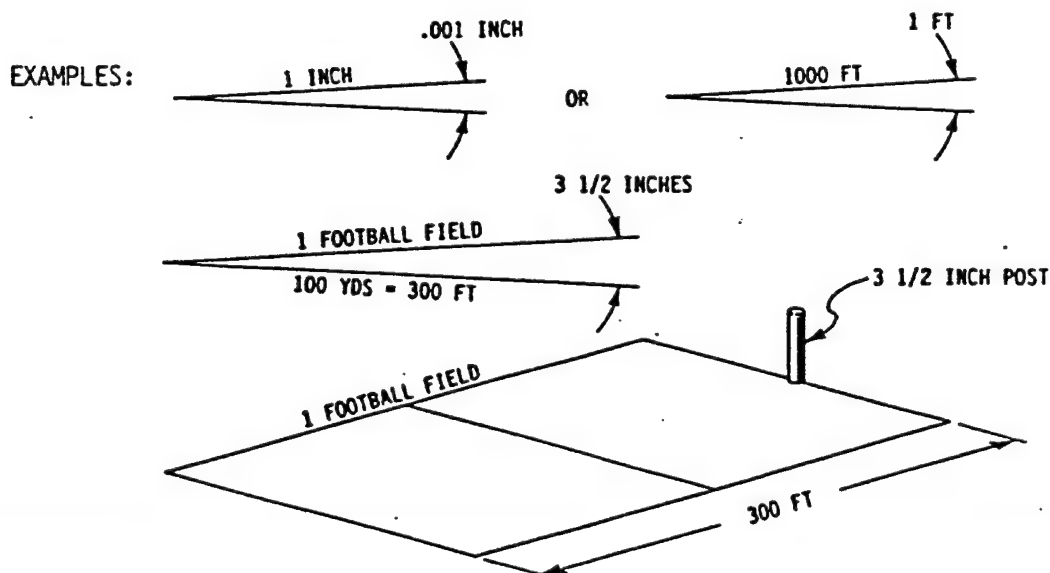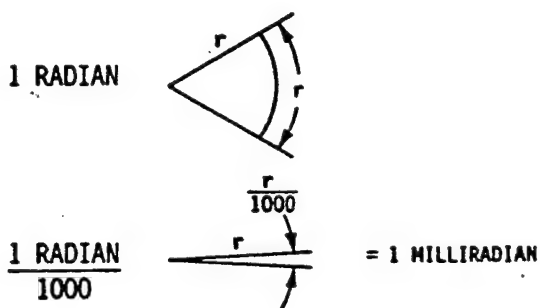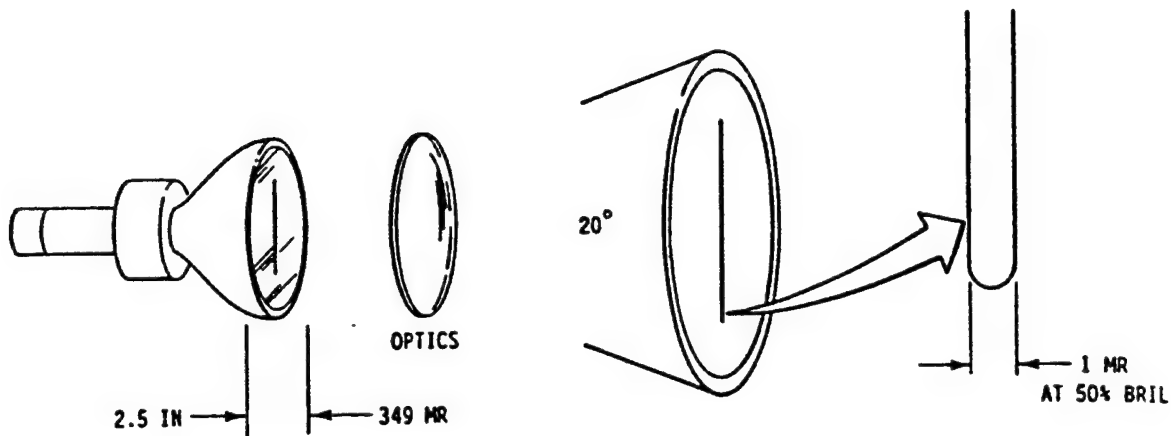
$$\therefore \text{CRT LINE} = \frac{1 \text{ MR}}{349 \text{ MR}} \ (2.5 \text{ IN}) = 0.007 \text{ IN}$$

- FOR SMOOTH MOTION, STEPS SHOULD BE NO
  MORE THAN 1/2 LINE WIDTH OR 0.0035 INCH

- FOR FLAT PANEL, PIXELS MAX AT 3.5 MILS
  WITH TWO LIT, MOVING ONE AT A TIME

HELMET BRIGHTNESS/CONTRAST

CRT

OPTICS (40%)

DAY
(DARK)
VISOR

CLEAR
VISOR

$\frac{40\% \ R}{500 \ FL} \rightarrow$

$$\frac{500 \ FL}{0.16} = 3500 \ FL$$
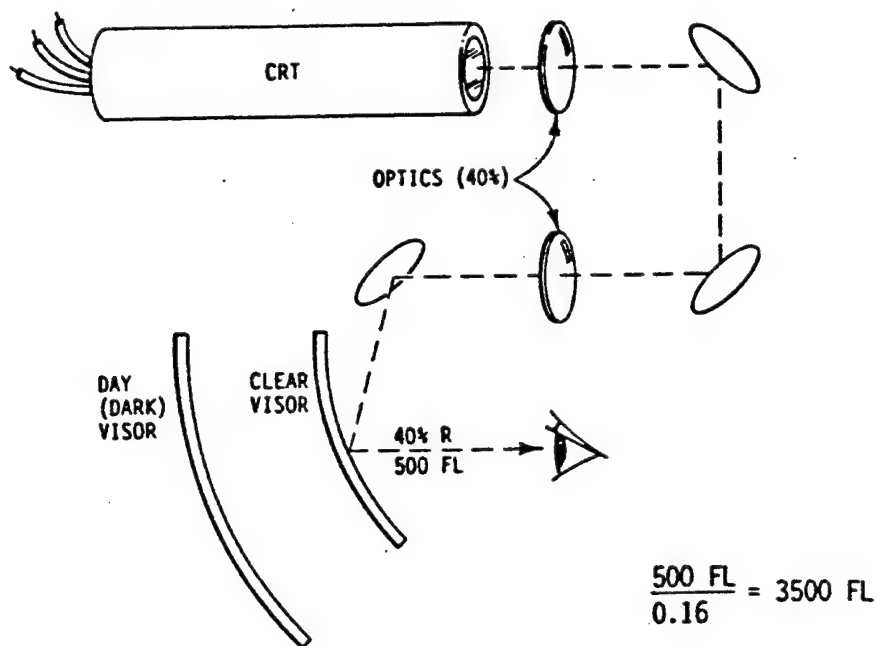
CONTRAST RATIO COMPLICATED BY VISOR
APPLICATIONS SO GENERALIZATION NOT POSSIBLE

HELMET IMAGE PLANES

1/2 INCH CRT   OPTICS
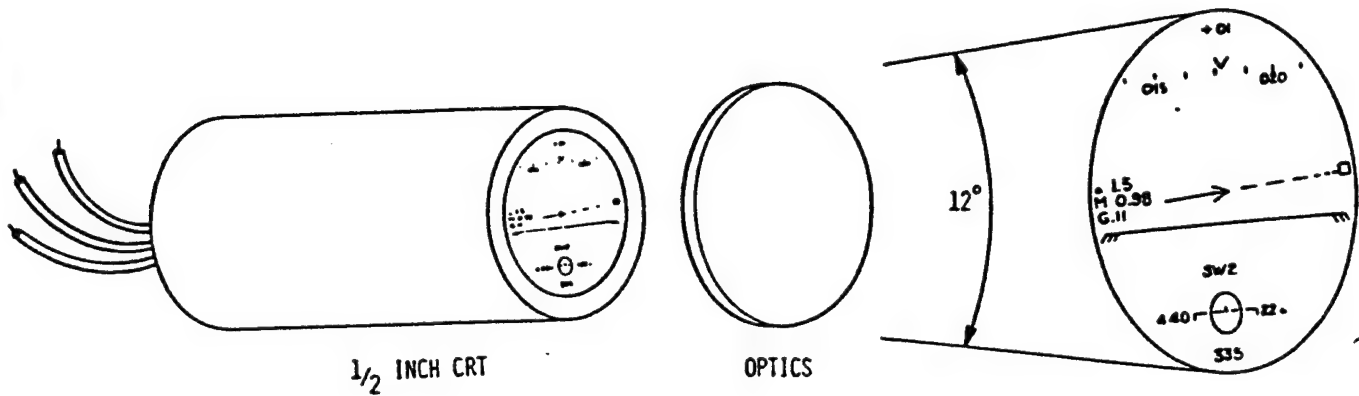
$$0.4 \text{ IN} = 12 \text{ DEG} = 209 \text{ MR}$$

$$\text{OR AT LINEWIDTH} = 1 \text{ MR} = \frac{0.4 \text{ IN}}{209 \text{ MR}} \approx 0.002 \text{ IN}$$

∴ FOR FLAT PANELS
- PIXELS AT 0.001 IN
- TWO LIT, MOVING ONE AT A TIME

(FOR LARGER FIELDS, IT GETS A LITTLE TOUGHER!)

SUMMARY OF IMAGE PLANE REQ'S

HUD

- PIXELS ABOUT 3 MILS (0.08 MM) SQUARE
- BRIGHTNESS 15,000 - 35,000 FTL

HELMETS

- PIXELS ABOUT 1 MIL (0.025 MM) SQUARE
- BRIGHTNESS 2,000 - 5,000 FTL

SECTION VIII

ELECTRO-OPTICAL SYSTEM PERFORMANCE
TEST AND EVALUATION

8.1 THE PHILOSOPHY OF TESTING

8.1.1 STAGES OF TESTING.   Testing can be categorized as developmental, functional, or operational, depending upon the stage of development of the test item. *Developmental testing* is concerned with the evaluation of design features for the purpose of design development.   The end result of developmental testing is the proposed final design.   *Functional testing* is concerned with the performance evaluation of the final design as a whole.   The principal method of evaluation is the quantitative measurement of the ability of the test item to perform its intended functions.   The end result of functional testing is final design acceptance or rejection. *Operational testing* is concerned with the evaluation of the final design and production implementation of the test item.   Of primary interest is the ability of the test item to accomplish its intended operational mission.   The end result of operational testing is acceptance or rejection of the test item for service use and the recommendation of operational procedures.

8.1.2 TESTING CRITERIA. The basic purpose of any stage of testing determines the criteria used to evaluate the test results. The testing criteria, in turn, are reflected in the tests to be performed and the test methods employed. Testing criteria derive from one of three objectives: data acquisition, determination of specification compliance, and evaluation of mission performance.   In developmental testing the intent is to acquire comprehensive information on the characteristics of the item under test.   Usually, no a-priori criteria are imposed for performance acceptance or rejection.   Functional testing, however, is primarily intended to evaluate the performance of the test item against specific criteria, ie. specification compliance. As previously indicated, operational testing is primarily concerned with mission performance.   While some specific, quantitative requirements are imposed, test criteria for operational testing often are of a qualitative nature.

It should be recognized that the three stages of testing; developmental, functional, and operational; are not mutually exclusive. That is, the differences are primarily ones

of emphasis. For example, functional testing often produces data that result in a design change. Thus, functional testing often takes on some aspects of developmental testing. For that reason, it is necessary, in functional testing, to test to a depth sufficient to allow engineering analysis of the problem. A "go" or "no-go" answer often is not sufficient. On the other hand, functional testing cannot ignore mission suitability in evaluating a new design. Compliance with published specifications is not sufficient if functional testing reveals an operational problem. Thus, while the following sections of this text will be concerned primarily with quantitative tests for specification compliance, it should be noted that functional testing should reflect mission requirements, including non-quantitative considerations when appropriate.

8.1.3 TEST REGIMES. Functional airborne system tests are performed in the *laboratory*, in the aircraft *on the ground*, and *in flight*. For various reasons, testing is usually performed in that order. Tests performed on the bench in the laboratory are most convenient, quickest, cheapest, and safest. Flight tests are least convenient, take the longest time, are most costly, and present the greatest danger to personnel and equipment. They also are most susceptible to uncertainties in the weather and availability of equipment. For the above reasons, tests should be performed in the laboratory, before installation in the aircraft, when feasible. After the laboratory, ground tests should be performed with the test item installed in the aircraft. Flight tests should be performed only when laboratory and ground tests have reduced the uncertainties to the greatest extent feasible.

Flight tests sometimes can be performed in a *test-bed aircraft*. Such an arrangement may allow in-flight tests to be performed with more extensive instrumentation than would be possible with the system installed in the aircraft for which it was intended. In addition, flight operations in a test bed aircraft are normally more convenient, less hazardous, and less costly. Testing in a test bed aircraft, however, cannot satisfy all flight testing requirements. The performance characteristics of all airborne systems are susceptible to the environment of the installation. Factors influenced by the vehicle are the electrical power, cooling, electromagnetic interference (EMI), vibration, acceleration, and other environmental effects. In a digital system, software interaction is also an important area for evaluation.

Simulator testing is very useful for finding and correcting problems in order to mature the system prior to beginning flight test. The most useful "simulations" incorporate actual flight hardware for the system under test while simulation is used for

generating external stimuli. These hybrid simulators are commonly called Systems Integration Laboratories (SILS). Simulators are advantageous in that tests can be rerun exactly, or with controlled modifications. The ability of a simulation to exactly duplicate test conditions is especially valuable in testing digital systems, where one-at-a-time modifications of the inputs are necessary to exercise the various logic branches of the software. Simulators have a great disadvantage in that it is very difficult to generate external stimuli equivalent to actual in flight conditions; thus, the simulator can generate problems unassociated with the system under test, while actual problems with the system will not be realized during ground testing.

This chapter is devoted to test methods peculiar to electro-optical system parameter determination and performance testing. In the following sections, brief descriptions are given of the methods employed to determine system compliance with the major electro-optical system functional specifications.

8.2   INFRARED SENSOR PERFORMANCE TESTING

8.2.1   ANGULAR RESOLUTION. The angular resolution of an infrared imaging system can be determined indirectly by determining its spatial frequency response. The angular resolution, θ_R, is related to the cut-off spatial frequency, $(SF)_{co}$, by the equation:

$$\theta_R = \frac{1}{(SF)_{co}} \qquad \text{(Radians)}$$

For a discussion of methods of determining spatial frequency response, see Sections 8.2.19 & 8.2.20. A direct, in-flight method of determining the angular resolution of an E/O sensor utilizes a resolution array of point source (small, high-intensity) targets as shown in Figure 8.1.   The process is as follows:

(a) Fly prescribed flight path toward E/O target array, at constant altitude.

(b) Determine aircraft position (range to target) by range instrumentation and record as a function of time.

(c) Acquire E/O target on sensor.

(d) Utilizing a video recorder or cockpit camera, record E/O sensor display imagery.

(e) Determine E/O sensor linear resolution, as a function of time, by noting the apparent number of E/O sources discernible at any given time.

(f) Correlate range and resolution data to obtain resolution as a function of

range.

(g) Calculate E/O sensor angular resolution, θ_R, as the ratio of linear resolution, W_R, to range, R. That is:

$$\Theta_R = \frac{W_R}{R}$$

where:

R = Slant range to target at time of observation

W_R = Minimum resolvable linear target separation

Air-to-Ground E-O Target Resolution Array
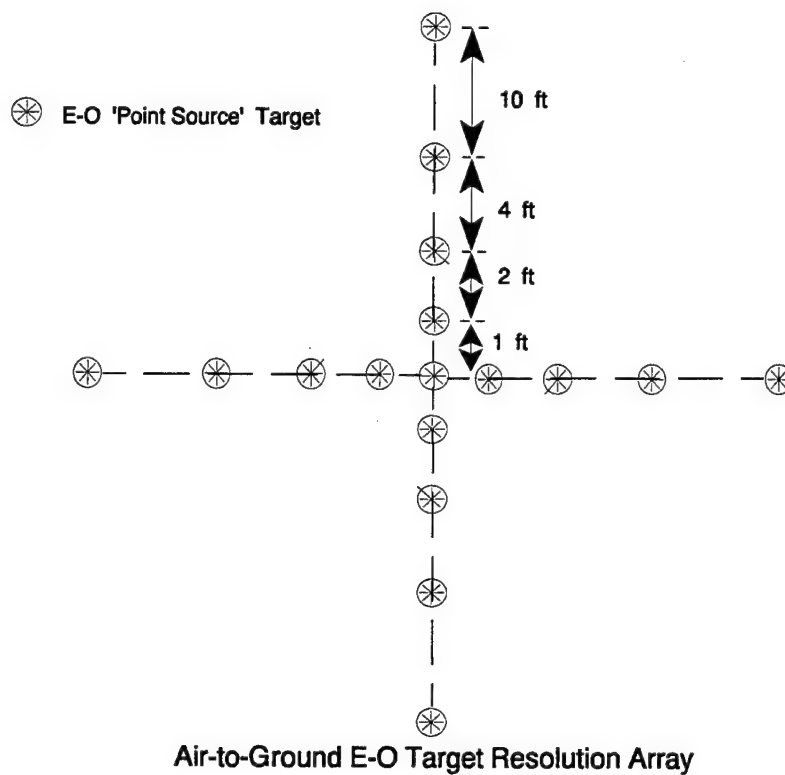
FIGURE 8.1

The minimum resolvable linear target separation is derived from the apparent number of discernible targets according to the following table. (Both azimuth and elevation resolution can be determined from the array shown in the figure. The table applies (separately) to either axis.)

No. Targets	1	3	5	7	9
Linear Resolution (Feet)	>10	<10	<4	<2	<1

If the target array is not oriented perpendicular to the sensor line-of-sight, a correction must be made for geometric distortion.

Angular resolution can be directly measured on the ground, utilizing a scaled-down version of the resolution array and an optical collimator. The collimator "collimates" the radiation from a nearby target so that it appears to the sensor as a distant target. An optically collimated E-O test target is described in Section 8.2.14.

Imaging "granularity" in some sensors produces inconsistent results in tests employing point sources. In such cases, the granularity itself should be evaluated.

8.2.2 BANDWIDTH (Optical Bandwidth, Temperature Bandwidth). The range of optical radiation frequencies to which an I/R sensor responds can be determined through the use of a suitable I/R source and a monochrometer as shown in Figure 8.2. The monochrometer is a device that transmits only radiation within a narrow bandwidth. In order to determine the response bandwidth of an I/R system, the source/monochrometer must be calibrated (the spectral radiant intensity determined as a function of frequency or wavelength). The bandwidth of the response of the I/R sensor is determined by the following procedure.

    (a)   Adjust monochrometer to desired wavelength and record wavelength.
    (b)   Record quantitative sensor output.
    (c)   Calculate ratio of sensor output to sensor input radiant flux.
    (d)   Repeat steps (a) through (c) to obtain data beyond the half-power points

of the sensor response curve in both directions.

(e)   Calculate bandwidth of sensor as the frequency span between the half power points.

I/R Source   Monochrometer   I/R Sensor under test

I/R SENSOR BANDWIDTH DETERMINATION TEST SETUP

BROAD-BAND I/R   NARROW-BAND I/R
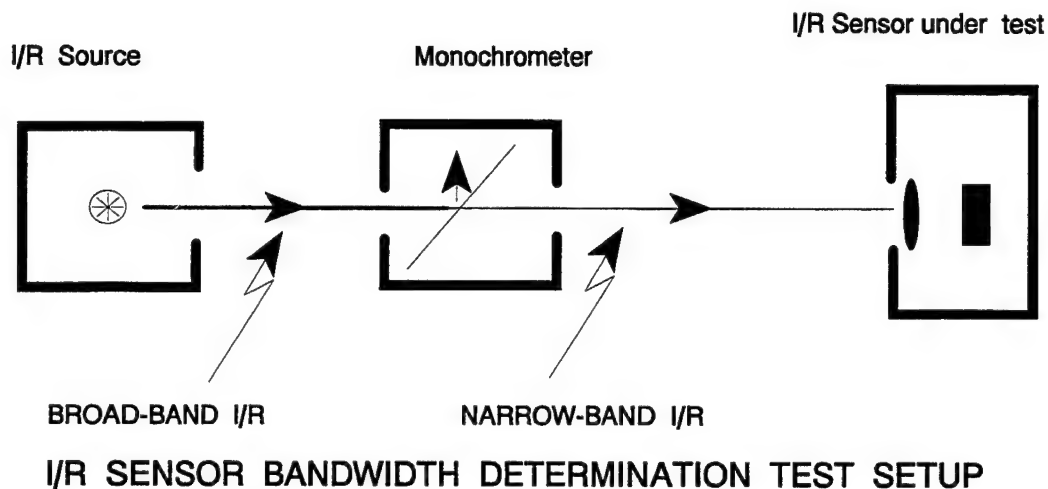
FIGURE 8.2

8.2.3 BEARING ACCURACY.   In-flight determination of bearing accuracy can be performed according to the following procedure.

(a) Fly prescribed flight path, at constant altitude, toward well-defined target of known position.
(b) Acquire target on sensor.
(c) Vary bearing to target and record indicated bearing as a function of time.
(d) Track aircraft using range instrumentation and calculate test aircraft-to-target bearing (truth data) from range data and aircraft heading.

(e) Compare target bearing indicated by sensor to truth data, by time correlating data.

8.2.4 BORESIGHT ACCURACY.

The alignment of the E/O sensor line-of-sight reference (boresight) with the aircraft armament datum line is determined employing a special test fixture, incorporating an I/R target and collimator (or autocollimator), which bolts to the airframe and provides an on-boresight target. The following procedure is employed.

(a) Affix test fixture to aircraft.
(b) Set sensor line-of-sight reference to zero azimuth and zero elevation.
(c) Note indicated position of test target in relation to sensor LOS reference (boresight).

8.2.5   POINTING ACCURACY.

The maximum error within which an E/O sensor line-of-sight reference can be aligned with a given direction (azimuth and elevation) can be determined utilizing a target of known orientation with respect to the aircraft datum line. Such a target is best provided by a collimating fixture similar to that employed for boresight accuracy measurements, but with the capability of providing off-boresight targets.

8.2.6 RELATIVE POINTING ACCURACY (Ground or In-flight)

The relative pointing accuracy of an E/O sensor with respect of other sensors (FLIR vs Laser, Laser vs navigation solution, etc) can be determined by simultaneously locking a known point target and slaving other sensors to the angle of the locked sensor in order to comparing their indicated positions.

(a) Setup with a low line-of-sight rate with a point target. (The target should be visible to each sensor being compared. For example if comparing radar to FLIR the target must be radar reflective with a significant ΔT.)
(b) Lock the point target with one sensor
(c) Slave the next sensor to the angle generated by the locked sensor
(d) Compare the indicated positions of each sensor. Maneuver to determine errors throughout the Field of Regard(FOR) of each sensor.

8.2.7 INSTANTANEOUS FOV (IFOV).

The instantaneous field-of-view of a scanned point-source-detecting E/O sensor can be determined indirectly by determining its angular resolution. The angular instantaneous field-of-view, Θ_{IFOV}, is related to the angular resolution, Θ_R, by the equation:

$$\Theta_{IFOV} = \Theta_{R} \qquad (Radians)$$

This equation neglects all resolution-limiting effects (such as detector bandwidth or frequency response) except the finite size of a detector element. In order to minimize the effects of other factors on resolution, and hence IFOV, the sensor response should be monitored directly at the detector output.

8.2.8   FIELD-OF-VIEW (FOV) and FIELD-OF-REGARD (FOR). The overall field-of-view of an E/O sensor can be determined on the ground utilizing a target and a collimator; on the ground using a fixed, distant target; or in flight. When a fixed target is employed, the sensor boresight line-of-sight is slewed until the target appears at the extremities of the field-of-view and the corresponding sensor slew angles are noted. When a target moving relative to the aircraft is employed, the target is moved to the extremities of the FOV and the angular FOV of the sensor is calculated from the known (measured) target positions.

The field-of-regard is the angle subtended during the maximum excursions of the sensors line-of-sight (LOS) in a scanned or slewed sensor. LOS limits are usually imposed by aircraft masking and mechanical limits. For a nonscanned or nonslewed sensor, the FOV is identical to the FOR. See Figure 8.3.

$$FOV = 2 \tan^{-1} \frac{W}{2H}$$
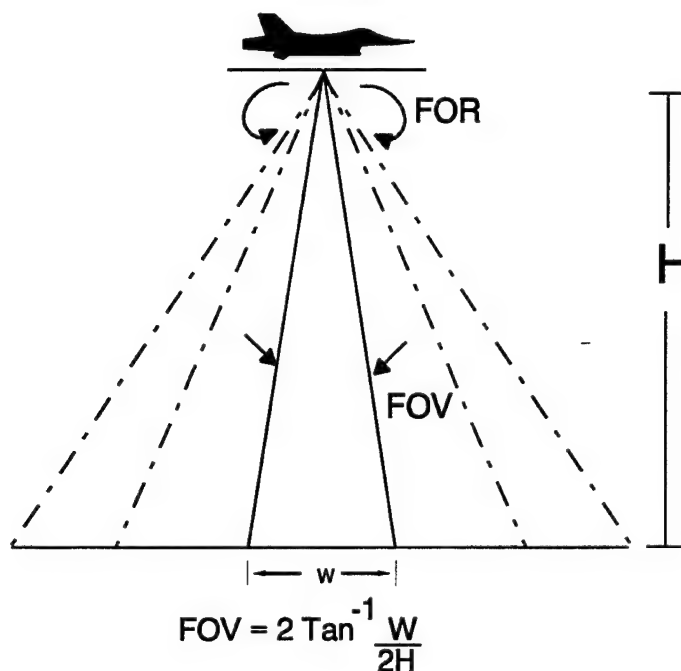
FIGURE 8.3

8.2.9 LINE-OF-SIGHT SLEW LIMITS. In order to determine the LOS slew angle limits, the E/O sensor is slewed to the limit of its travel about all axes. The angular limits can be measured directly from the sensor head gimbals or calculated from linear measurements from a reference to the sensor boresight. The azimuth and elevation look angles also can be read from the sensor direction indicators.

8.2.10 LINE-OF-SIGHT SLEW RATES. The maximum sensor line-of-sight slew rates are most readily determined by commanding sensor head slew from one limit to the opposite limit and timing the transit with a stop watch. In-flight determination of the maximum automatic (tracking) slew rates can be effected by flying a path with respect to the target calculated to produce a prescribed maximum LOS slew rate. (The maximum LOS slew rate is equal to the ratio of the ground speed of the aircraft to the aircraft-to-target distance-of-closest-approach. The distance-of-closest-approach is decreased, in successive runs, until target track is broken due to excessive LOS slew rate.

8.2.11 LINE-OF-SIGHT DRIFT RATE. The long-term LOS instability (drift rate) of an E/O sensor is best determined on the ground, utilizing the following procedure, illustrated in Figure 8.4.

(a) Align the sensor LOS reference (e.g., cross-hairs) on a prominent, fixed point target, at a known distance.
(b) After various time intervals, note the positions of the points in the target plane at which the sensor reference is then directed.
(c) Calculate the sensor drift rate according to the formula:

$$\theta = \frac{Tan^{-1}\ [D(t_1)/R]}{t_1 - t_o}$$

where: $D(t_1)$ = Linear Drift Distance at Range R at Time t.
  R = Range from sensor to Target Plane
  t_1 = Time of Measurement (Seconds)
  t_o = Time of Initial Alignment (Seconds)

The drawing in Figure 8.4 depicts a measurement of azimuth drift. The same procedure is employed to determine drift in elevation.

E-O SENSOR   TARGET PLANE

LOS Ref. at t = to

LOS Ref. at t = t1   D (t₁)

R
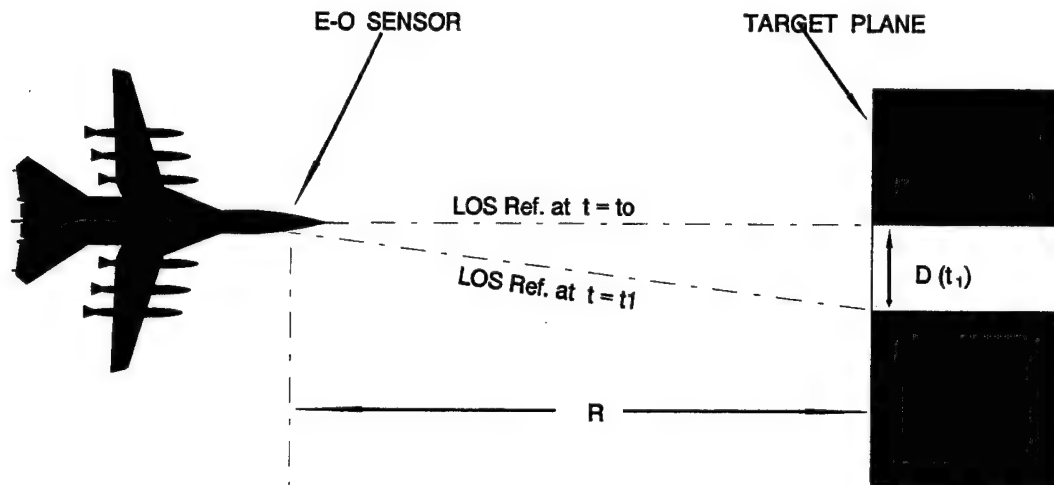
E-O SENSOR LOS DRIFT RATE TEST SETUP
FIGURE 8.4

8.2.12 LINE-OF-SIGHT JITTER. The short-term LOS instability (jitter) of an E/O sensor must be determined in flight since in-flight vibration is a major contributor to LOS jitter. The usual method of measurement of LOS jitter is indirect and utilizes the measurable loss of sensor angular resolution due to LOS jitter. The method of determination of angular resolution and the method of deriving LOS jitter from in-flight measurements are presented in Section 8.17 of this text. A direct method of determining the LOS jitter of an E/O imaging sensor is to record the displayed image of a well-defined source, (utilizing a camera or video recorder), and measure the actual jitter in the displayed image.

8.2.13 MAXIMUM RANGES FOR DETECTION AND RECOGNITION. The maximum ranges at which an E/O sensor provides detection and recognition of a target must be determined in flight and can utilize an E/O sensor bar target such as the Large IR Board, located in the PIRA, or a mission-related target. The E/O bar target has the advantage of known, controlled characteristics, whereas mission-related targets have the advantage of realism. Although the radiant intensity of some

mission-related targets can be measured by independent instrumentation, quantitative sensor evaluation generally requires the use of a specially designed target.

The Large IR Board is a billboard-like target, approximately 50 feet by 30 feet in size, and is used for dynamic testing of infrared sensors, television sensors, and photographic equipment where resolution and background information are required. See Figure 8.5. The white and black bars are painted with a special paint designed to provide three values of diffuse reflectance for illumination by an external source. In addition, the white faces are provided with electric heaters to provide temperature differentials for the testing of thermal sensors. By rotating the individual bars, various target patterns can be created. The target array is oriented 15° off the vertical so as to provide a more-nearly normal line-of-sight for an airborne sensor. The spacial frequency of the target is varied as the range changes between the test aircraft and the target.
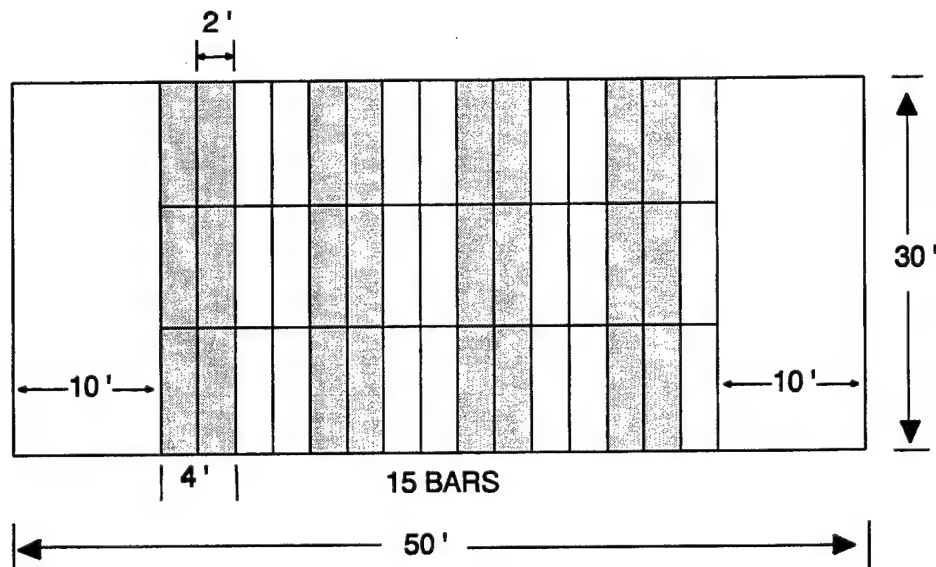
INFRARED TARGET BOARD

4 BAR PATTERN
7.5 TO 1 ASPECT
LAMBERTIAN SURFACE

FIGURE 8.5

The procedure for determining the maximum detection and recognition ranges is as follows:

(a)   Fly prescribed flight path, at constant altitude, toward well-defined target at known location.

(b)   Determine aircraft position (range to target) by range (ground) instrumentation or by on-board ranging system and record as a function of time.

(c)   Align sensor line-of-sight to place E/O target of known anticipated position in field-of-view of sensor.

(d)   Acquire target on sensor. (Note time of acquisition as time of detection.)

(e)   Continue observing E/O target on sensor until target features (bars for a bar-target) become distinguishable. (Note time of feature definition as time of recognition.)

(f)   Correlate aircraft-to-target range times with detection and recognition times to obtain maximum ranges for detection and recognition.   Note that the maximum detection and recognition ranges are a function of the radiant and spatial characteristics of the target, the ambient background illumination, and the atmospheric conditions at the time of the test.   To be meaningful, the maximum ranges must be associated with specific target characteristics and test conditions.

8.2.14 MINIMUM RESOLVABLE TEMPERATURE DIFFERENTIAL (MRΔT) (Thermal Resolution). The minimum target temperature differential resolvable by an imaging thermal detector is best determined by the combined angular resolution/thermal resolution test described in Section 8.2.17 of this text.

A simpler procedure for determining MRΔT can be performed as a ground test using an optically collimated E-O test target. The target can consist of a radiation source such as a laser or other illuminator, a reflective target to be illuminated by an external source, or a thermal bar target for I/R sensor testing. The arrangement of the collimated-target components is as shown in Figure 8.6. The E/O target is positioned at the focal point of the collimating mirror. The radiation from a single point on the target is thus reflected from the collimating mirror with all rays parallel to the line-of-sight from the E/O sensor under test to the point on the target. The image of the target therefore appears to the sensor as if it were at an infinite range.

FIGURE 8.6
OPTICALLY COLLIMATED E-O TEST TARGET
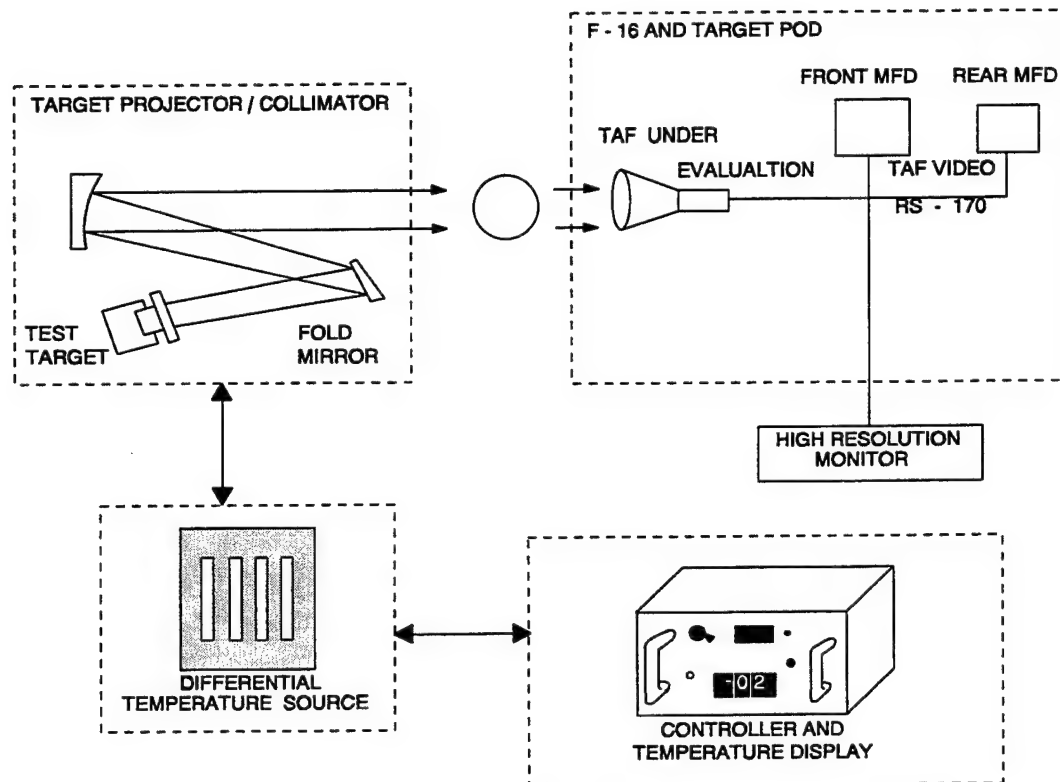
The purpose of the collimated source is to provide calibrated targets for long-range sensors without the difficulties associated with actually providing targets at large ranges. The spatial frequency of a collimated bar target image as seen by the sensor is given by the equation:

$$ SF_T \;=\; \frac{1}{\theta_{1c}} \;\cong\; \frac{FL_c}{W_{1c}} \qquad \text{(Cycles/Radian)} $$

where: FL_c = Focal Length of Collimator

W_{1c} = Width of one bar and space of Actual Target

The thermal bar target consists of a temperature-controlled surface (I/R source) with a slotted template mounted in such a way as to block part of the radiation from the source. The temperature of the template is held constant at ambient temperature by

virtue of its being mounted in a large block of aluminum (heat sink). A "bar" of the target is thus formed where a slot in the template allows the sensor under test to view the temperature-controlled source through the template. The "spaces" of the target are formed where the spaces between the slots in the template block the radiation from the temperature-controlled source. The spatial frequency of the collimated bar target image is adjusted by interchanging bar target templates with differing bar/space widths. The temperature-controlled source is electrically heated and thermoelectrically cooled to produce a bar-space temperature differentials. The temperature differential can be set to about 0.2 centigrade degrees and measured, by a radiometer, to about 0.05 centigrade degrees.

The MRΔT test is performed as follows:

(a)   Set the spatial frequency of the bar target to a value well below one-half of the sensor cut-off frequency.

(b)   Adjust the bar target temperature differential to a value well below the expected MRΔT of the sensor under test.

(c) Focus the sensor on the bar target and optimize the sensor control settings.

(d)   Gradually reduce the bar target temperature differential, allowing sufficient time for stabilization between changes, until the variations in radiant intensity due to the individual bars are no longer discernible on the sensor display.

(e)   Gradually increase the bar target temperature differential until the variations in radiant intensity due to the individual bars are just discernible.

(f) Record the bar target temperature differential attained in Step (e) as the MRΔT for the sensor.

8.2.15 NOISE EQUIVALENT TEMPERATURE DIFFERENTIAL (NEΔT). The noise-equivalent input temperature differential for a thermal detector can be determined by the following procedures:

(a)   Set the spatial frequency of a thermal bar target to a value well below one-half of the sensor cut-off frequency.

(b)   Adjust the bar target temperature differential to a value well above MRΔT for the sensor under test.

(c)   Focus the sensor on the target and optimize the sensor control settings.

(d)   Adjust the bar target temperature differential to a value that produces a target signal just large enough to be measured accurately in the presence of the noise.

(e)   Record the target temperature differential and resulting sensor video output voltage response attained in step d.

(f)   Block the target input to the sensor and measure the rms noise on the sensor video output voltage.

(g)   Calculate the sensor NEΔT according to the equation:

$$NE\Delta T \;=\; \frac{N\;\;\Delta T}{S} \quad (Degrees, Kelvin)\, 8.5$$

where:

N = RMS Noise Voltage on Sensor Video Output Signal. (Volts)
S = Peak-to-Peak Variation in Sensor Video Output Voltage due to
      Bar Target. (Volts)
ΔT = Bar Target Temperature Differential producing the Output
      Signal S (Kelvin, Degrees).

8.2.16 SPATIAL FREQUENCY RESPONSE. The spatial frequency response of an E/O sensor can be determined directly by viewing a target the radiance of which varies sinusoidally with position on the target. However, such a target is very difficult to construct and control. For that reason, spatial frequency response generally is determined utilizing a bar target (a target the radiance of which varies as a square wave with position on the target). Such a target can be an air-go-ground target such as the Large IR Board described previously is Section 8.2.13 or it can be a scaled-down optically collimated E-O test target as described in Section 8.2.14. Of course, the bar target yields not the response of the system to a sinusoidal variation in radiance, but the response to a square wave. The results, however, can be considered an approximation of the response to a sinusoidal variation with spatial

frequency equal to that of the fundamental Fourier component of the square wave.

A generalized procedure for determining the spatial response of an E/O sensor to a bar target during ground tests is as follows:

(a)   Adjust the differential radiance of the bar target (temperature difference between hot and cold bars for a thermal sensor) to a value well above the minimum resolvable differential for the sensor under test.

(b)   Adjust the spatial frequency of the target as seen by the sensor to a value well below one-half of the expected sensor cut-off frequency.

For ground tests, the spatial frequency of the collimated image of a bar target is independent of the actual sensor-to-target range and is given by:

$$SF_T = \frac{FL_c}{W_{1c}} \qquad\qquad 8.7$$

where: FL_c = Focal Length of Collimator
                        W_{1c} = Width of one Cycle of Target (One Bar and Space)

The spatial frequency in ground tests is usually changed by utilizing collimated-image targets with various target bar and space widths. Several targets ranging from wide bars (low spacial frequency) to narrow bars (high spatial frequency) are available with each ground test set.

(c)   Acquire the bar target on the sensor and focus the sensor on the target.

(d)   Observe the sensor video output signal and determine the maximum and minimum values of the output signal, as indicated in Figure 8.7.

(e)   Repeat steps (b) through (d), substituting increasingly greater target spatial frequencies in step (b), until the sensor response (Vmax-Vmin) is too small to measure.

The output of a scanning E/O sensor vanishes at the cut-off spatial frequency. At frequencies above the cut-off value, a "false" response occurs which is commonly called aliasing. An aliasing response will be at a lower frequency that the actual spatial

frequency of the target. Care must be taken to avoid mistaking "aliasing" for a true response.
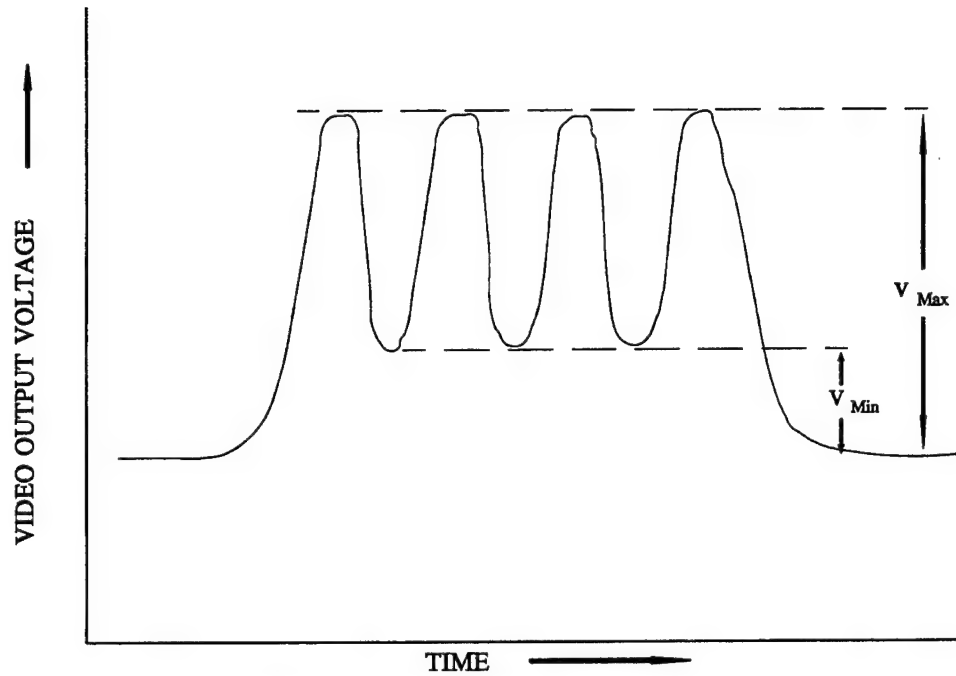
E-O Sensor Video Output Response to a 4-Bar Target

FIGURE 8.7

The spatial response of an E/O sensor to a bar target may be defined as the ratio given by the following equation.

$$SR = \frac{V_{\text{max}} - V_{\text{min}}}{V_{\text{max}} + V_{\text{min}}}$$

8.2.17 COMBINED ANGULAR RESOLUTION AND THERMAL RESOLUTION. The angular resolution and thermal resolution of an E/O sensor are best determined by the integrated test procedure presented below. In order to determine the effect of the in-flight environment on the sensor, the procedure consists of two parts. The ground test is performed first, followed by the in-flight test.

Ground Test Procedure

(a) Adjust the spatial frequency of a collimated bar target to a value well below one-half the expected cutoff frequency for the sensor under test.

(b) Adjust the bar target temperature differential to a value well above the expected MRΔT of the sensor under test.

(c) Focus the sensor on the target and optimize the sensor control settings.

(d) Reduce the bar target temperature differential to a value below the MRΔT of the sensor under test.

(e) Gradually raise the target temperature differential, while monitoring the sensor display, until the variations in radiant intensity due to the individual bars in the target just become discernible.

(f)   Measure the temperature differential attained in step (e).

(g)   Record the bar target temperature differential and spatial frequency attained in step (e).

(h)   Increase the spatial frequency of the bar target by a suitable increment.

(i)   Repeat steps (d) through (h) until the individual bars of the target can no longer be discerned even for the maximum target temperature differentials utilized in the test.

The data acquired in the preceding procedure provide measurements of the resolvable temperature differential, for the sensor, as a function of bar target spatial frequency. The results, when plotted as shown in Figure 8.8, yield the minimum resolvable temperature differential (MRΔT) and the spatial cutoff frequency (SF$_{co}$), of the sensor under test. As indicated in the figure, the asymptotic value of RΔT at low spatial frequencies represents the MRΔT for the sensor under test. The asymptotic value of SF$_T$ at high resolvable temperature differentials represents the spatial cutoff frequency for the sensor under test.

RESOLVABLE

ΔT (°c)

$\left(\begin{matrix}\text{THERMAL}\\\text{SENSITIVITY}\end{matrix}\right)$

LABORATORY RESOLUTION

MRΔT

^{f}s CUTOFF

SPATIAL FREQUENCY   (CYCLES / MR)

$\left(\begin{matrix}\text{ANGULAR}\\\text{RESOLUTION}\end{matrix}\right)$
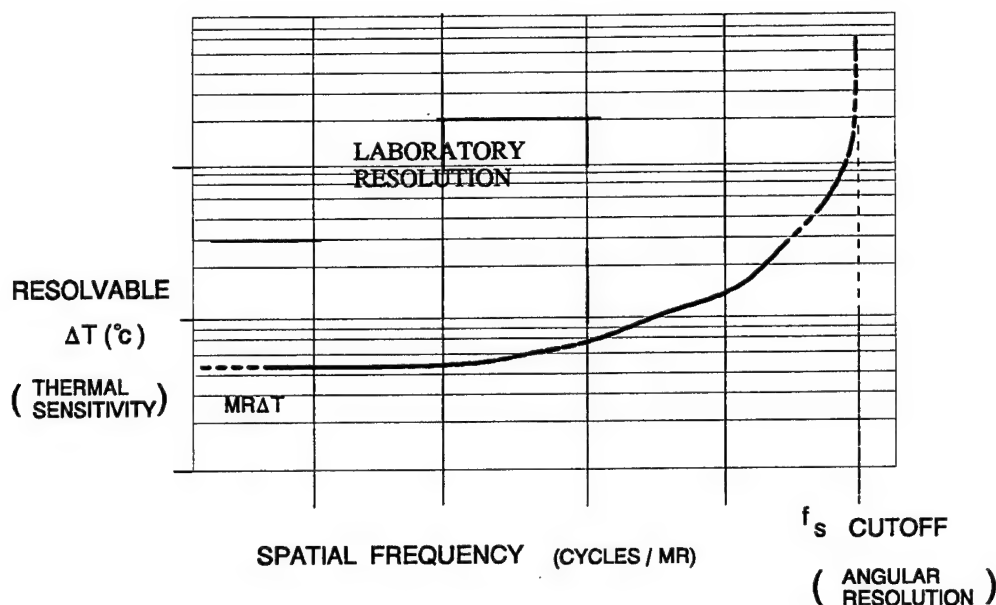
FIGURE 8.8

In-Flight Test Procedures

(a)   Set the bar/space width of a bar target to a value calculated to provide suitable spatial frequencies, at the planned test ranges, for the system under test. The (angular) spatial frequency of a bar target at an actual range R_T is given by the equation:

$$SF_T \;\; = \;\; \frac{R_T}{W_{1c}}$$

where:

R_T = Sensor-to-Target Range

W_{1c} = Width of one Cycle of Target (One Bar and Space)

The spatial frequency in tests utilizing such targets is usually adjusted by varying sensor-to-target range (ie. flying toward the target!) rather than target bar and space width.

(b)   Adjust the effective temperature differential of the bar target to the maximum value planned for the test.

(c)   Fly a prescribed flight path, at constant altitude and airspeed, on a heading designed to pass directly over the E/O target, and normal to the face of the target.

(d)   Determine the sensor/aircraft position (and, hence, sensor-to-target range) with suitable range instrumentation or an on-board ranging device.

(e)   Acquire the E/O target on the sensor under test.

(f)   Continue to observe the target on the sensor until the variations in radiant intensity due to the individual bars are just discernible.

(g)   Measure and record the resolvable temperature differential and the range (spatial frequency) attained in step (f).

(h)   Repeat steps (b) through (g), substituting, in step (b), increasingly small target temperature differentials, until the variations due to individual bars are no longer discernible even at the minimum sensor-to-target ranges planned for the test.

(i) During the inflight test, atmospheric conditions must be recorded in order to determine the atmospheric transmission factor (τ). ΔT must be multiplied by τ to get the normalized ΔT which is used for plotting test results. Additionally, thermovision should be used to record IR board differential temperature as truth data to ensure the IR board is operating properly. Figure 8.9 shows the MRΔT test setup.

The relationship between sensor cut-off spatial frequency, SF_{co}, and sensor angular resolution, θ_R, is given by the equation:

$$\theta_R = \frac{1}{(SF)_{co}} \qquad \text{(Radians)}$$

When the resolvable temperatures determined by the in-flight test are plotted versus the spatial frequency of the target, the results are very similar to those, shown in Figure 8.8, determined by the ground test. The only significant difference should be that the in-flight spatial cut-off frequency of the sensor should be somewhat lower than that attained in ground test. A plot showing both in-flight and ground test results is presented in Figure 8.10. For a properly-functioning sensor, the degradation of angular resolution in flight is due primarily to sensor line-of-sight jitter.

RESOLVABLE

ΔT (°c)

(THERMAL SENSITIVITY)

INFLIGHT RESOLUTION

MRΔT

LABORATORY RESOLUTION

SPATIAL FREQUENCY (CYCLES / MR)

f$_s$ CUTOFF

(ANGULAR RESOLUTION)
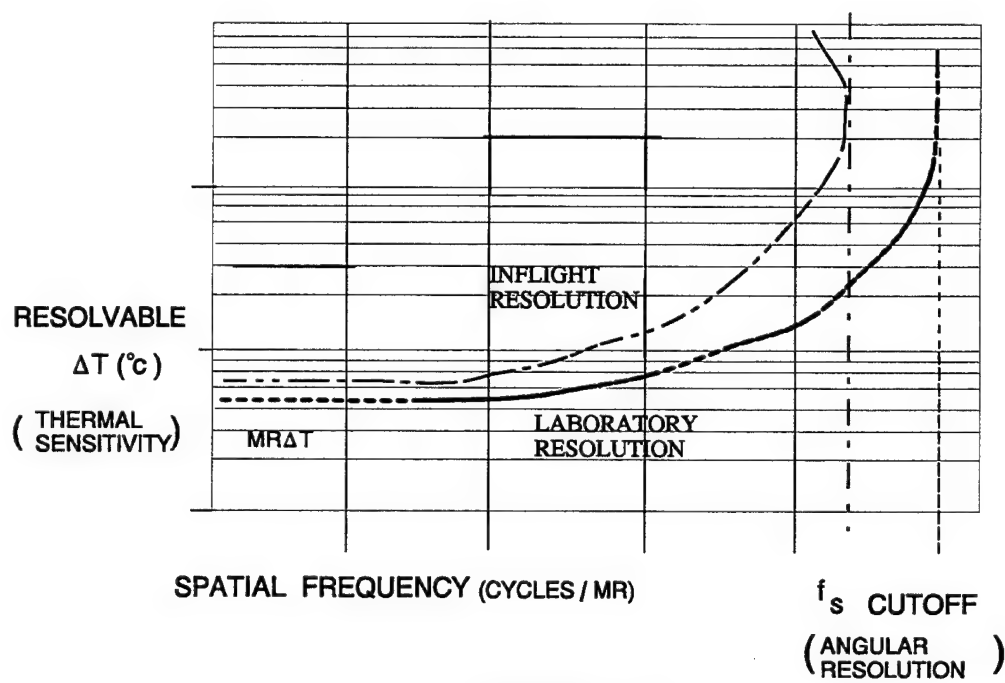
FIGURE 8.10

8.2.18 SENSOR TIME RESPONSE. The response of an E/O sensor to time-related variations in target radiant intensity can be determined as steady-state (sinusoidal) time-frequency response or transient (impulse or step-function) response. The time-frequency response can be determined by subjecting the sensor to a sinusoidal intensity modulated source and measuring the amplitude and phase variations in the video output signal from the sensor. The transient response can be determined by subjecting the sensor to a pulsed intensity modulated source and recording the sensor video output signal response as a function of time.

8.2.19 TRACKING PERFORMANCE. Three fundamentally different methods of "position tracking" are employed with E/O sensors. True image tracking utilizes the video signal produced by the target and tracks some feature of the target image as seen by the tracker (the centroid of the image, edge of the image, etc.). Inertial position tracking utilizes information from an inertial navigation system and tracks a fixed location on the surface of the earth. Target designator tracking tracks illumination from a laser target designator. In any case, the tracking error can be determined by the following procedure.

(a) Fly a prescribed flight path toward a prominent E/O target of known location.

(b) Determine the sensor/aircraft position and velocity with suitable range or on-board instrumentation.

(c) Acquire the E/O target on the sensor.

(d) Initiate target track at the earliest practicable instant. (Record corresponding range as maximum track acquisition range.)

(e) Alter flight path and attitude of aircraft in order to subject E/O sensor tracking line-of-sight to specified LOS rates.

(f) Measure and record E/O sensor video signal and tracking error signal as a function of time. (The E/O sensor display also can be recorded utilizing a cockpit camera.)

(g) Correlate derived tracking errors with LOS slew rates by time correlating

data obtained in steps (b) and (f).

8.3 LOW-LIGHT-LEVEL TELEVISION PERFORMANCE TESTING. The performance testing method outlined in Section 8.2 of this text, for scanning infrared sensors, are applicable to the performance testing of low-light level television sensors, with the comments, modifications, and exceptions noted below.

8.3.1 TESTS APPLICABLE WITHOUT MODIFICATION. The following test procedures, outlined in Section 8.2, are applicable without exception to the testing of low-light-level television sensors.

Test	Section
Angular Resolution	8.2.1
Bandwidth	8.2.2
Bearing Accuracy	8.2.3
Boresight Accuracy	8.2.4
Pointing Accuracy	8.2.5
Relative Pointing Accuracy	8.2.6
Instantaneous FOV	8.2.7
Field-of-View	8.2.8
LOS Slew Limits	8.2.9
Max. LOS Slew Rate	8.2.10
LOS Drift Rate	8.2.11
LOS Jitter	8.2.12
Max. Range for Detection and Recognition	8.2.13
Spatial Frequency Response	8.2.16
Time Response	8.2.18
Tracking Performance	9.2.19

8.3.2 TESTS APPLICABLE WITH MODIFICATION. The procedures outlined in Section 8.2.14 (Minimum Resolvable Temperature Differential), Section 8.2.15 (Noise Equivalent Temperature Differential), and Section 8.2.17 (Combined Angular Resolution and Thermal Resolution) are applicable to the testing of low-light-level television sensors with the substitution of the following photometric terms for radiometric terms.

Radiometric Term	Photometric Term
Radiant Flux (Watts)	Luminous Flux (Lumens)
Radiant Intensity (W/Sr)	Luminous Intensity (Lm/Sr)
Radiance (W/Sr-M^2)	Luminance (Lm/Sr-M^2)
Radiant Exitance (W/M^2)	Luminous Exitance (Lm/M^2)
Irradiance (W/M^2)	Illuminance (Lm/M^2)
Differential Temperature (C°)	Differential Luminous Exitance
Thermal Resolution (C°)	Luminosity Resolution (Lm/M^2)

8.4 LASER RANGER/DESIGNATOR PERFORMANCE TESTING.

The performance testing methods outlined in Section 8.2 of this text, for scanning infrared sensors, are applicable to the performance testing of laser ranger/designators, with the comments, modifications, and exceptions noted below.

8.4.1 TESTS APPLICABLE WITHOUT MODIFICATION.   The following test procedures, outlined in Section 8.2, are applicable without exception to the testing of laser/designators.

Test	Section
Line-of-Sight Slew Limits	8.2.9
LOS Slew Rates	8.2.10

8.4.2 BANDWIDTH.   The spectral characteristics of the radiation emitted by a laser/designator can be determined utilizing the test setup depicted in Figure 8.11. As indicated in that figure, the laser beam is locked onto a diffuse, uniformly reflecting target and the spectral radiant intensity is determined using a spectral radiometer. Although the figure indicates an in-flight test, the spectral characteristics of a laser beam are more conveniently and accurately determined on the ground and at short range to avoid atmospheric absorption.

FIGURE 8.11

E-O SENSOR AIBORNE TEST EMPLOYING E-O TARGET
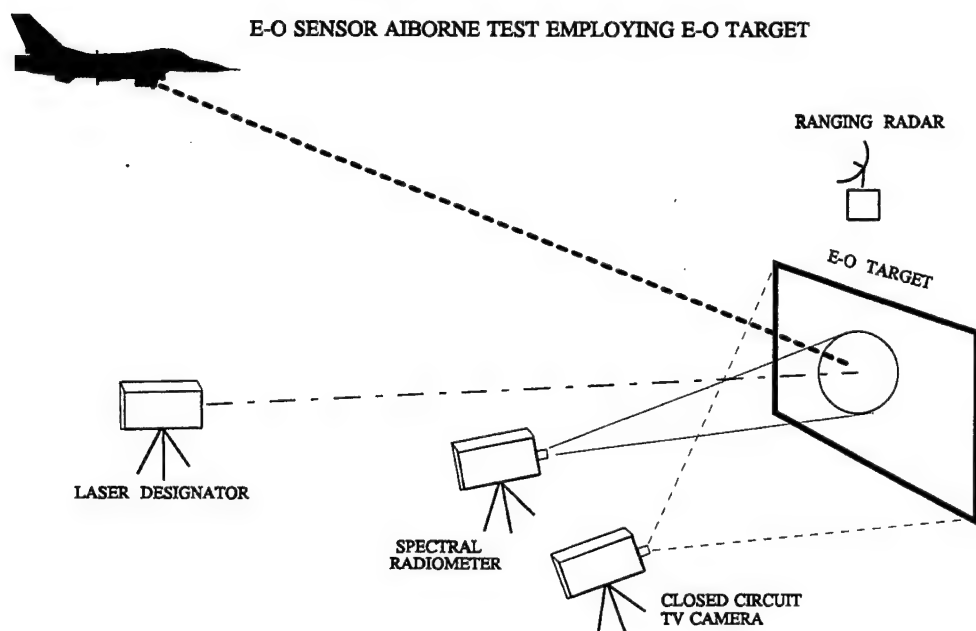
8.4.3 BORESIGHT ACCURACY. The boresight alignment of a laser/designator is best determined by ground test, utilizing a collimated-target test fixture similar to the one shown in Figure 8.6. The test procedure is listed below.

(a)   Acquire and focus E/O sensor on point-source target aligned with aircraft armament datum line (ADL).

(b)   Place a paper shield over target and mark ADL reference position on paper (Materials other than paper can be used.)

(c)   Fire laser, burning small spot on paper shield.

(d)   Measure displacement of laser burn spot from ADL reference mark.

(e)   Convert linear laser boresight error (D_e) to angular laser boresight error (δ_e) according to the equation:

$$\delta_e \;=\; Tan^{-1}\left[\frac{D_e}{FL_c}\right] \qquad \text{(Radians)}$$

where:

$\quad$ D_e $\;=\;$ Linear Laser Boresight Error

$\quad$ FL_c $\;=\;$ Focal Length of Collimator

The pointing accuracy of a laser/designator can be determined utilizing the above test procedure to check laser alignment with points off boresight (displaced from the aircraft armament datum line).

8.4.4 LINE-OF-SIGHT DRIFT RATE. The long-term line-of-sight instability (drift rate) of a laser/designator is best determined using the collimated target test setup employed in the boresight test described in Section 8.4.3 of this text. The procedure is as follows:

(a)   Conduct steps (a) through (d) of the boresight test, obtaining a laser burn spot on the paper target.

(b)   After a suitable designated time, fire the laser again, obtaining a second burn spot on the target.

(c)   Measure the relative displacement between the two laser burn spots.

(d)   Calculate the laser/designator LOS drift rate, θ_d , according to the equation:

$$\dot{\theta}_d = \left(\frac{1}{t_d}\right) Tan^{-1}\left[\frac{D_d}{FL_c}\right] \qquad \text{(Radians/Sec)}$$

where: D_d $\;=\;$ Relative Linear Displacement between Two Burn Spots

$\quad$ FL_c $\;=\;$ Focal Length of Collimator

$\quad$ t_d $\;=\;$ Time Interval between Two Laser Firings (Secs.)

8.4.5 LINE-OF-SIGHT JITTER. The short-term LOS instability (jitter) of a laser/designator must be determined by flight test since in-flight vibration is a

major contributor to LOS jitter. The test procedure employs the test setup depicted in Figure 8.11 of this text and consists of the following steps.

(a)   Fly prescribed flight path, at constant altitude and airspeed, on a heading designed to pass directly over the E/O target and normal to the face of the target.

(b)   Acquire the E/O target on an on-board sensor.

(c)   Designate the target (fire the designator laser).

(d)   Observe the (designated) target using the ground-based TV camera shown in Figure 8.11 and record the resulting video as a function of time.

(e)   Determine the airborne designator-to-target range using suitable onboard or range instrumentation.

(f)   Determine the laser designator LOS angular jitter by time correlating the jitter-induced movement of the laser spot on the target with the designator-to-target range data.

8.4.6 LASER RANGING ACCURACY. The ranging accuracy of a laser/designator is best determined by flight test employing an E/O target similar to the one described in Section 8.2.13 of this text. The procedure is as follows:

(a)   Fly prescribed flight path, at constant altitude and airspeed, on a heading designed to pass directly over the E/O target and normal to the face of the target.

(b)   Acquire the E/O target on an on-board sensor.

(c)   Designate the target and laser range on the target. Record the resulting data as a function of time.

(d)   Independently determine and record aircraft-to-target range using onboard or range instrumentation. (The highly accurate ranging provided by laser ranging makes it extremely difficult to obtain "truth" data of sufficient

accuracy.)

(e) Time correlate the laser range data with the "truth" data to determine ranging error.

The static ranging accuracy of a laser ranger can be determined by ground tests utilizing optical retro-reflectors positioned at known ranges from the test aircraft position.

8.4.7 LASER BEAM DIVERGENCE. The divergence of a laser beam is best determined by ground test employing the collimating apparatus described in Section 8.2.14 of this text. The laser is fired into the collimator as shown in Figure 8.12. Templates with various circular apertures are placed at the focal point of the collimator mirror as also shown in the figure. The size of the circular aperture is varied until the aperture just begins to occlude the beam as indicated by a reduction in the radiant flux received by the radiometer. (A reduction to 90% of the no-aperture value is taken as the reference point.) The angular beam width (divergence) of the laser beam is then equal to the diameter of the (90% flux) aperture divided by the focal length of the collimator.

FIGURE 8.12

LASER BEAM DIVERGENCE TEST SETUP

LASER BEAM DIVERGENCE TEST GEOMETRY
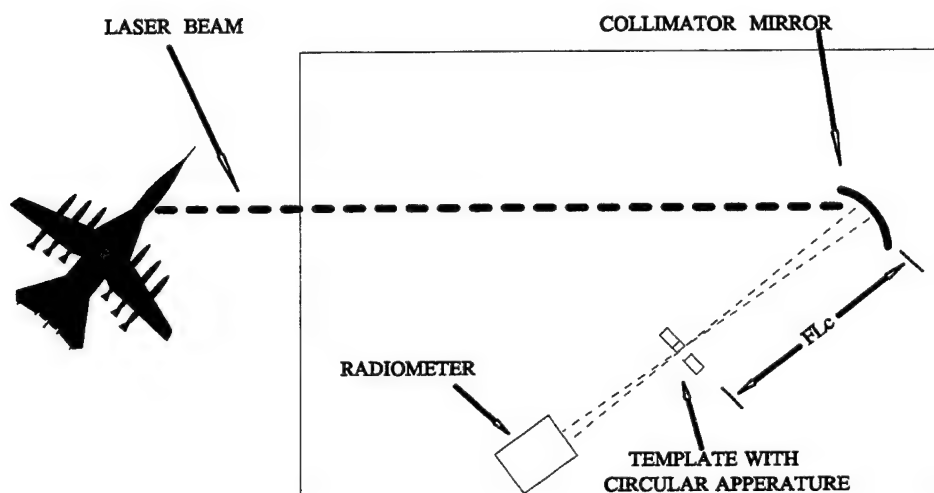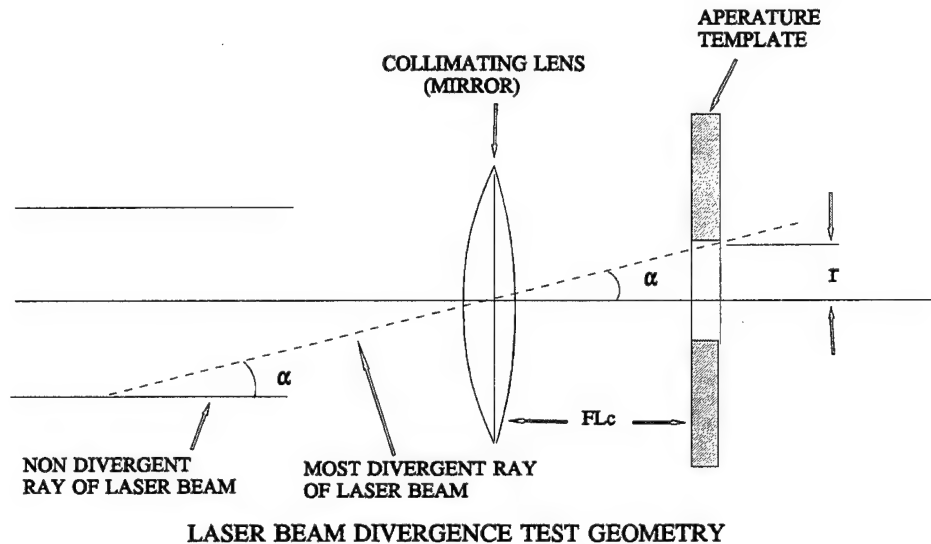
FIGURE 8.13

The geometry of the test is illustrated in Figure 8.13. If all of the rays in the laser beam were parallel ($\alpha = 0$), they would all be focused to a point at the focal point of the mirror. If the most divergent rays (edge of the beam) make an angle α with the beam axis, they will just graze the edge of the hole in an aperture plate of radius r as shown. Thus, the half-angle of the beam is equal to:

$$\alpha \;=\; \frac{r}{FL_c} \qquad\qquad \text{(Radians)}$$

where:

FL_c = Focal Length of Collimator (Meters)

r = Radius of aperture that just grazes the beam (Meters)

8.4.8 LASER OUTPUT POWER. The average output power of a laser ranger/designator is best determined in ground tests by firing the laser into a calorimeter.

The test procedure is as follows:

(a)   Align laser output beam with center of calorimeter.

(b)   Fire laser.

(c)   Record calorimeter output reading (laser average output power).

The pulse peak power and pulse energy of a pulsed laser can be calculated from the average power by means of the equations:

$$P_{peak} = \frac{P_{average}}{DC}$$
$$DC = \frac{\tau_p}{PRI}$$
$$E_{pulse} = P_{peak}\,\tau_p$$

where:

DC   = Duty Cycle (N.D.)
E_{pulse} = Energy in Single Pulse (Watt-Sec.)
$P_{average}$ = Laser Average Power (Watts)
P_{peak} = Laser Pulse Peak Power (Watts)
PRI   = Laser Pulse Repetition Interval (Secs)
τ_p = Laser Pulse Width (Secs)

8.4.9 LASER PULSE AMPLITUDE. The pulse amplitude and pulse amplitude stability of a pulsed laser ranger/designator is best determined by ground test employing the test setup depicted in Figure 8.14. The laser is fired into the radiometer and the output of the radiometer is recorded on the high-speed recorder as shown in the figure. Pulse amplitude stability can be determined by comparing the output recording over a specified time interval. Laser misfire rate (missing pulse rate) also can be determined by examination of the recorded radiometer output.

FIGURE 8.14

LASER PULSE PARAMETER TEST SETUP
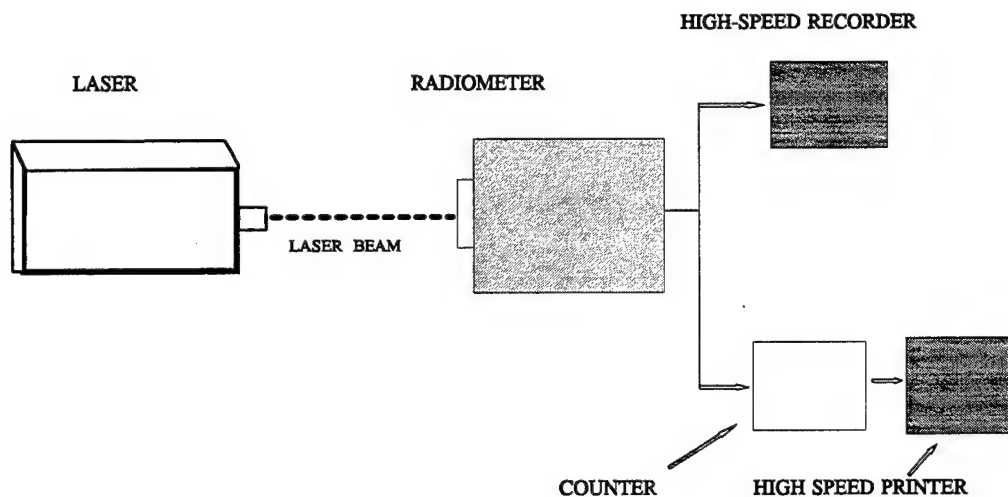
8.4.10 LASER PULSE WIDTH. The pulse width of a pulsed laser/designator is best determined by ground test employing the test setup depicted in Figure 8.14. The laser is fired into the radiometer and the output of the radiometer is recorded as shown. Because of the small pulse widths and the extremely fast rise and fall times associated with a laser pulse, an accurate determination of pulse width requires the use of special, fast-response detectors and recorders. In addition, corrections are generally made for the response times associated with the detector and recorder.

8.4.11 LASER PULSE REPETITION INTERVAL. The pulse repetition interval (or frequency) of a laser ranger/designator is best determined by ground test employing the test setup depicted in Figure 8.14. The laser is fired into the radiometer and the output pulses are counted and timed by the counter as shown. The output of the counter (pulse count and pulse rate) is recorded by the high-speed printer. Analysis of the high speed printout yields pulse repetition frequency (interval) and PRF stability.

8.4.12 BLIND RANGES. The blind ranges produced by eclipsing in an active, pulsed E/O sensor are generally greater than the maximum useful range of the sensor (because of the large pulse repetition interval usually employed). When significant blind ranges, including the minimum range, exist, they can be determined by the following procedure.

(a) Fly prescribed flight path, at constant altitude, toward well-defined target of known position.

(b) Acquire target on sensor.

(c) Continue to close on target monitoring sensor indication for dropouts.

8.5 PHOTOGRAPHIC CAMERA PERFORMANCE TESTING.

8.5.1 GENERAL E/O SENSOR TESTS. Many of the E/O sensor performance testing techniques discussed in Section 8.2 and 8.3 of this text apply, with only slight modification, to the evaluation of the photographic camera. The following tests, described in the sections indicated, are essentially applicable to photographic camera systems.

Test	Section
Bearing Accuracy	8.2.3
Boresight Accuracy	8.2.4
Pointing Accuracy	8.2.5
Field-of-View	8.2.8
LOS Slew Limits	8.2.9
LOS Slew Rates	8.2.10
LOS Drift	8.2.11
LOS Jitter	8.2.12

Some photographic system performance characteristics are highly dependent upon the photographic film employed. The results of testing for those characteristics are, thus, significant only for the specific films used in testing. Film-dependent characteristics include the following.

Angular Resolution
Bandwidth
Image Definition
Maximum Range
Minimum Resolvable Luminosity Differential

8.5.2 ANGULAR RESOLUTION. The angular resolution of a photographic system
should be evaluated in both static (ground) tests and flight tests. A comparison of
ground and flight test results provides an evaluation of line-of-sight stabilization
and motion compensation. A ground test of angular resolution can best be made
using a collimated target such as that described in Section 8.2.14 of this text. A
slight modification of the test procedure outlined in Section 8.2.17 of this text
determines both the angular resolution and the luminosity resolution of the
camera/film combination. The flight test for the determination of the angular
resolution of a photographic system utilizes a photogrammetric E/O target.

An example of an E/O test target used for the evaluation of photographic systems
is shown Figure 8.15. The target is oriented parallel to the ground and consists of
painted strips with the characteristics listed in Tables 8.1 and 8.2. In use, the
target is overflown and photographed from various altitudes.
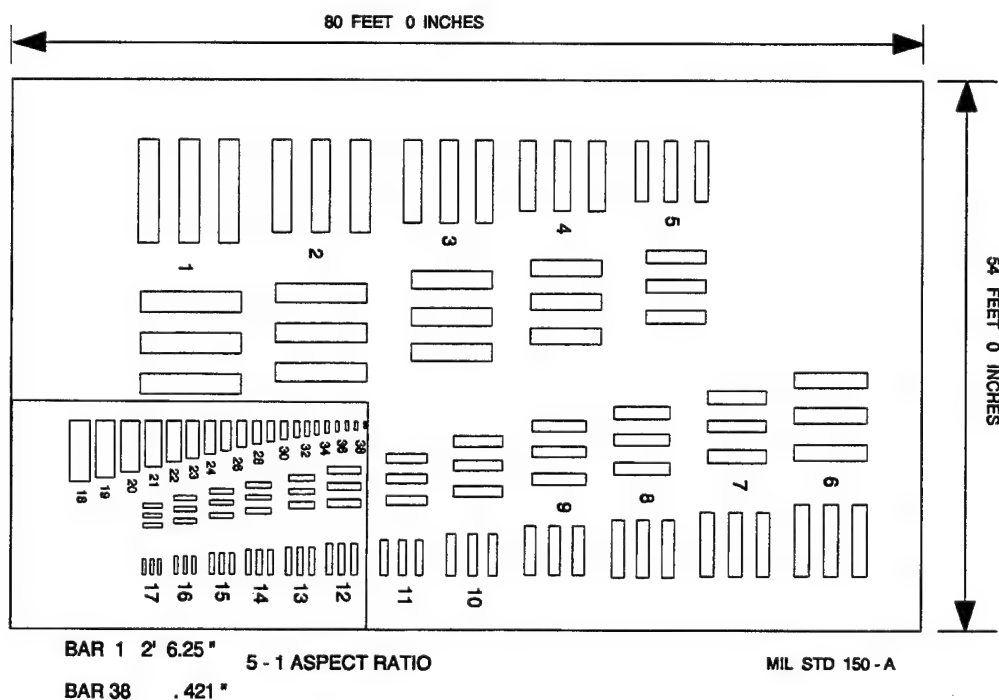
FIGURE 8.15

Table 8.1

Type "A" Photogrammetric Target Bar Widths

Bar/Group Number	Feet	Inches	Bar/Group Number	Feet	Inches
1	2	6.250	20	0	3.375
2	2	2.937	21	0	3.000
3	2	0.000	22	0	2.687
4	1	9.375	23	0	2.375
5	1	7.062	24	0	2.125
6	1	5.000	25	0	1.875
7	1	3.125	26	0	1.687
8	1	1.500	27	0	1.500
9	1	0.000	28	0	1.343
10	0	10.687	29	0	1.187
11	0	9.500	30	0	1.062
12	0	8.500	31	0	0.937
13	0	7.562	32	0	0.843
14	0	6.750	33	0	0.750
15	0	6.000	34	0	0.671
16	0	5.312	35	0	0.593
17	0	4.750	36	0	0.531
18	0	4.250	37	0	0.468
19	0	3.812	38	0	0.421

The lengths of the bars conform to MIL. STD. 150-A, that is, each has a length-to-width aspect ratio of 5-to-1.

The listed measurements are for the bar size only. For example using bar/group number 20:   Bar = 3.375 inches;   Bar + Space - 6.750 inches

Table 8.2

Type "A" Photogrammetric Target Characteristics

Target Characteristic	Values/Description
Designation	Type "A" Photogrammetric Target
Type	Photo Resolution Targets
Construction	Painted metal panels bolted to concrete
Reflectance	8% Black / 82% White (Vary with age)
Tone	Black and White

Photographic camera angular resolution tests can be conducted using the following procedure:

(a)   Fly prescribed flight path, at constant (specified) altitude and airspeed, on a heading designed to pass directly over the E/O target.

(b)   As aircraft overflys target, expose film.

(c)   Determine target luminance using ground instrumentation.

(d)   Calculate camera system angular resolution from the known bar size of the smallest resolvable bar-space group and the altitude.

APPENDIX A

GLOSSARY

ABSORBER. An object which readily "soaks up" radiation; a good absorber is a poor reflector and a good emitter.

ABSORPTION. The ratio of the radiant energy absorbed in a body of material to the radiant energy incident upon it.

ABSORPTION COEFFICIENT. A number characterizing the ability of given materials to absorb or attenuate radiations of specified energy. The linear absorption coefficient expresses this ability per unit thickness and is stated in units of reciprocal length or thickness. The mass absorption coefficient is equal to the linear absorption coefficient divided by the density of the absorbing material; it is the measure of absorption ability per unit mass.

ADIABATIC. A process that takes place without gain or loss of heat by the system involved.

ADIABTHERMENOUS. A material which absorbs a great deal of the radiation incident upon it.

AMBIENT TEMPERATURE. The temperature of the surrounding medium, such as gas or liquid.

AMPLIFIER. A device whose output is a function of an input signal and which draws power from a source other than the input signal.

ANGLE, DRIFT CORRECTION. The angular difference between the course and the heading (sometimes called the crab angle).

ANGSTROM (A). A distance to 10^{-8} centimeters. Visible light has a wavelength of a few thousand Angstroms (4,000-7,200).

ANGULAR VELOCITY. The time rate of change of the angle of rotation.

ANOMALY. Departure from regular arrangement, general rule, or usual method.

APERTURE. Any opening through which radiation may pass.

ASPECT ANGLE. The angle from the nadir at which a target is viewed.

ASSOCIATED FEATURES. The various apparent or recognizable detected emissions which support or are interrelated with a target.

ATMOSPHERE. A gaseous envelope surrounding a body, or a mass of gas occupying a region.

ATMOSPHERE WINDOW. Those spectral regions located between the principal absorption of the atmospheric gases which are regions of maximum transmission.

ATTENUATION. The reduction in the intensity of radiation, with distance from the source where the reduction is due to absorption and/or scattering; does not include the inverse-square decrease of intensity of radiation with distance from the source.

AXIS OF ROTATION, FIXED. The focus of points of a system along a straight line which remains stationary when the rest of the system undergoes rotational motion.

BACKGROUND. Any distribution or pattern of radiant flux external to the observing equipment, which may interfere with the process of frequencies or wavelengths.

BAND. A range of frequencies or wavelengths.

BANDWIDTH. The number of cycles per second required to convey the information being transmitted.

BIAS LEVEL. In infrared systems, the dc voltage applied to the light source used to expose the film. It establishes a reference brightness.

BLACKBODY. An ideal body which would, if it existed, absorb all and reflect none of the radiation falling upon it. The nearest approach to the ideal blackbody experimentally is an almost completely closed cavity in an opaque body.

BLACKBODY RADIATION. Radiation having a spectral distribution of energy according to the Planck radiation formula and such as would be given off by an ideal blackbody or complete radiator.

BOLOMETER. A sensitive thermometric instrument which utilizes the temperature coefficient of resistivity of some resistance element to measure radiation.

BOW-TIE EFFECT. Distortions caused by an increase in size of the ground area recorded by the instantaneous field of view (IFV) as the aspect angle approaches the horizon. IFV generates a bow-tie shape in one scan.

BRITISH THERMAL UNIT. Unit of work or energy required to raise the temperature of 1 pound of water through a temperature rise of 1°F, abbreviated BTU.

CAMOUFLAGE. The disguising of a target with paint, screens, reflectors, etc., also the disguise so applied.

CAPACITY, THERMAL. The amount of thermal energy required to raise the temperature of a system or substance by one degree equal to the product of mass times specific heat.

CATHODE-RAY TUBE (CRT). A funnel-shaped vacuum tube having in its neck an electron gun that directs a beam of electrons to a fluorescent screen.

CAVITY RADIATION. (See Blackbody)

CLOUD COVER. A measure of the area of sky covered by clouds, usually expressed in tenths of sky covered.

COMPARATIVE COVERAGE. Two or more sets of imagery taken over a given area which differ in at least one collection characteristic such as time of acquisition, altitude, focal length, or sensor.

CONDUCTION, THERMAL. Transfer of thermal energy from one part of an object to another by molecular motion.

CONDUCTIVITY, THERMAL. (See Conduction, Thermal)

CONTRAST. The tonal variation or ratio of tonal changes between adjacent fields of view.

CONVECTION, THERMAL. Transfer of thermal energy from one place to another by actual motion of materials caused by differences in materials densities.

COSINE EMISSION LAW. The energy emitted in any direction by a blackbody is proportional to the cosine of the angle which that direction makes with the normal to the surface.

CROSSOVER. Loss of contrast on infrared imagery occurring when two adjacent objects (such as a bridge and river) have identical radiometric temperatures. Also can refer to the thermal temperature crossover.

DECOY. An imitation of a target employed to lure or mislead.

DENSITY. 1. Photography--a measure of the opacity of photographic film; 2. Physics--mass of a substance per unit volume.

DETECTOR, INFRARED. A device which transduces the energy of electromagnetic radiation falling upon it into some other form of energy, in most cases electrical.

DETECTOR TIME CONSTANT. (See Time Constant)

DETECTIVITY D*. A figure of merit for infrared detectors; obtained by dividing the detector noise equivalent power into the square root of the product of the detector area and the bandwidth.

DEWAR. A "vacuum bottle" designed to hold refrigerant coolants.

DIATHERMANEOUS. A material that absorbs little of the radiation _____ upon it.

DISTORTION FACTORS. Those influences which affect the geometric and tonal fidelity of infrared system displays.

DISTORTION, INHERENT. The distortion of the display of the received infrared radiation caused by characteristics of the infrared set and the scan geometry.

DOPING. Addition of impurities to a semiconductor to achieve a desired characteristic.

DRIFT. The horizontal displacement of an aircraft, under the action of the wind, from the track it would have followed in still air.

DRIFT ANGLE. The angular difference between aircraft heading and aircraft track.

DRIFT ERROR. The difference between actual aircraft drift and calculated (set) aircraft drift.

ELECTROMAGNETIC RADIATION. The energy propagated through space or through a material medium as waves of variations of electric and magnetic fields. They are known as radio waves, heat waves, light waves, etc., depending on frequency.

ELECTROMAGNETIC SPECTRUM. The continuum consisting of the ordered arrangement of radiation according to wavelength, frequency, or photon energy.

EMISSIVE POWER. The total radiation from a blackbody per unit area of radiation surface. Emissive Power = (Stefan Boltzmann Constant) X (Kelvin Temp)^4. Emissive power of a graybody is equal to its absorptivity as emissivity times the emissive power of a blackbody at the same temperature.

A-5

EMISSIVITY. The ratio of the radiation emitted by any surface to the radiation emitted by a blackbody at the same temperature under similar conditions: May be expressed as total emissivity for all wavelengths, spectral emissivity--as a function of wavelength, or geometric emissivity as a function of angle.

EMITTANCE, SPECTRAL-RADIANT. Radiant power emitted from a surface, per unit surface area, per unit wavelength.

EMITTANCE, TOTAL RADIANT. Integral of total power radiated per unit area of a surface over all wavelengths.

ENERGY, RADIANT. Energy which is transferred by electromagnetic waves without a corresponding transfer of matter.

EQUILIBRIUM, THERMAL. A system is said to be in thermal equilibrium if the temperature is uniform throughout the system and is the same as that of the surroundings.

FAR INFRARED. That portion of the electromagnetic spectrum between the wavelengths of 5.6 and 1,000 microns, or 25 and 1,000 microns, depending on the criterion of definition being used.

FIELD OF REGARD. The field-of-regard is the angle subtended during the maximum excursions of the sensors line-of-sight (LOS) in a scanned or slewed sensor. LOS limits are usually imposed by aircraft masking and mechanical limits.

FIELD OF VIEW. The area or solid angle visible through an optical instrument.

FILTER. A device for eliminating or reducing certain waves or frequencies while leaving others relatively unchanged.

FOCUS. The point toward which rays of light converge to form an image after passing through a lens or having been reflected by mirrors. The condition of sharpest imagery.

FREQUENCY. The number of repetitions of a periodic process per unit time. In the case of electromagnetic radiation, frequency is so enormous that wavelengths are ordinarily used instead.

GAIN CONTROL. That portion of a system which adjusts the gain of a single circuit to obtain desired relative output levels from two or more sequential unequal input signals.

GAMMA. A numerical measure of the extent to which a negative has been developed, indicating the proportion borne by the contrast of the negative to that of the subject on which it was exposed. The numerical figure for gamma is the tangent of the straight line (correct exposure) portion of the curve resulting from plotting exposure against density. A gamma of 1.0 indicates a negative which has the same contrast as the subject photographed. A gamma of 1.2 indicates a negative which has greater contrast than the subject photographed.

GLOW TUBE. An electronic tube whose light intensity is proportional to the voltage input. It is used in an infrared scanner to expose the film at a light intensity proportional to the detector voltage.

GOLAY PNEUMATIC CELL. A small transparent cell containing gas which is used to detect radiation.

GRAYBODY. Any object which absorbs less than all incident radiation and which emits less than the theoretical maximum amount at a given temperature.

HAZE. Very small particles of salt, dust, and/or water in the air.

HEAT CAPACITY. (See Capacity, Thermal)

HEAT, LATENT. Thermal energy gained by a substance without an accompanying rise in temperature during a change of state.

HEAT, SPECIFIC. The amount of heat in BTU required to raise the temperature of 1 pound of a substance 1°F.

HEAT TRANSFER. Heat can be transferred by three different methods: conduction, convection and radiation.

HUMIDITY, ABSOLUTE. The mass of water vapor at a specific volume.

HUMIDITY, RELATIVE. The fraction of percentage of the actual vapor pressure of the water vapor contained in the atmosphere at a given temperature, to the maximum or saturated vapor pressure of water vapor at the same temperature.

IMAGE PLANE. The plane perpendicular to the optical axis of an optical system in which the image is formed.

INFRARED RADIATION. Electromagnetic radiation of wavelength between 0.72 microns (7,200 Angstroms) and about 1,000 microns (1 millimeter). Frequently divided into near, middle and far infrared. All bodies (not at absolute zero temperature) radiate in this wavelength region.

INSTANTANEOUS FIELD OF VIEW (IFV). The smallest solid angle resolvable by a scanner when expressed in degrees. When expressed in feet, it is the projected area of the detector image on the ground and is a measure of the resolution of a scanner. Ground area recorded has characteristic bow-tie shape.

INTEGRATION, VIDEO. A method of utilizing the redundancy of repetitive signals to improve the output signal-to-noise ratio, by scanning the successive video signals.

INTENSITY MODULATION. The changing of density or tonal quality.

INVERSE SQUARE LAW. The intensity of radiation from a point source decreases as the reciprocal of the distance from the source, squared, in a nonabsorbing medium.

IRRADIANCE. The radiation power incident on the unit area of a surface.

JOULE. A unit of work or energy. The work done when a force of one newton produces a displacement of 1 meter in the direction of the force.

JUNCTION P-N. The boundary surface between donor type and acceptor type semiconduction materials. These junctions have high rectifying properties.

KELVIN TEMPERATURE SCALE. (See Temperature scale Kelvin)

KEYS. Reference materials which facilitate identification and determination of significance of objects or conditions found in reconnaissance presentations.

KIRCHHOFF RADIATION LAW. The emissivity of a surface at a given temperature is equal to the absorptivity which the surface exhibits for radiation from a source at the same temperature.

LAMBERT COSINE LAW. (See Cosine Emission Law)

LIGHT. That form of radiation that is detected by the human eye.

LIGHT, SPEED OF. Speed of light in empty space is about 2.99776×10^{10} cm/s (about 186,000 miles per second). The speed in other media is this figure divided by the index of refraction of the media.

LIGHT, TRANSMITTED. Light that has traveled through a medium without being lost through absorption or scattering processes.

MAGNIFICATION. Enlargement of photographic images by an optical instrument or photographic process.

MALFUNCTION. A failure in the normal operation of an infrared system.

MERCURY-DOPED GERMANIUM. A photoconductive detector which is sensitive to infrared radiation in the spectral region between 2 and 14 microns.

MICRON. Unit of length, abbreviation μ. Exactly 10^{-6} meters and 10^{-4} centimeters (1/1,000,000 meters or 1/10,000 centimeters).

MICROWAVE. An electromagnetic wave having a wavelength longer than far infrared and shorter than conventional radio wavelengths (1 mm to 30 cm wavelength).

MILLIRADIAN. One thousandth of a radian (see Radian). It is approximately the angle subtended by an arc 1 foot in length at 1,000 feet. (Often abbreviated to "mil" and defined as resolution achievable at a given range, usually 1,000 feet: a 1 mil system infers 1 foot resolution at 1,000 feet altitude).

NEAR INFRARED. That portion of the infrared region of the electromagnetic spectrum between 0.72 and 1.5 microns.

NEUTRAL DENSITY FILTER. A light filter which reduces the intensity of the light without changing the relative spectral distribution of the energy.

NOISE EQUIVALENT POWER. The radiation power needed to produce a signal-to-noise ratio of one, or the radiation power needed to produce a signal equal to the noise level of the detector.

PARAMETER. A factor, such as cloud cover, temperature, altitude, or focal length, whose presence, condition or size affects the final product of a system.

PASSBAND (OF A FILTER). That band of frequencies that are passed with little or no attenuation.

PHOTOCONDUCTIVE DETECTOR. Apparatus used to detect or measure radiant energy by generating an electrical potential across a boundary of two types of material.

PITCH. The alternate lurch or rise and fall of the nose of the aircraft: the rapid up/down motion of the aircraft from level flight.

PLANCK'S LAW. A law of physics which gives the spectral energy distribution of the heat radiation emitted from a blackbody at any temperature.

POWER, RADIANT. The rate of transfer of radiant energy.

QUANTUM THEORY OF RADIATION. The energy of radiation emitted or absorbed is concentrated in quanta, or photons, each with an energy in ergs of 6.624 X 10 times the frequency of the radiation in cycles per second.

RADIAN. That angle which intercepts an arc in a circle equal to the circle's radius. A unit for measuring angles π radians = 180 degrees. There are approximately 0.0175 radians per 1 degree.

RADIANCE, APPARENT. Radiant power per unit solid angle from a source as witnessed by an airborne detector. Apparent radiance is directly related to tone on infrared imagery.

RADIANT ENERGY. Energy transmitted as electromagnetic radiation.

RADIANT FLUX. The time rate of low or radiant energy.

RADIANT INTENSITY. The energy emitted per unit time, per unit solid angle.

RADIATION. (See Thermal radiation)

RADIATION TEMPERATURE. That temperature of a complete radiator, or blackbody, which has a total radiant emittance equal to that of the object being measured.

RADIATION, THERMAL. Measure of continuous radiation of energy from surfaces of all objects above absolute zero.

RADIOMETER. An instrument for detecting and usually also for measuring radiant energy.

RADIOMETRIC. Having to do with radiant energy.

RANGE, SLANT. The distance measured along the line of sight from the aircraft to an object on the ground.

RANKINE TEMPERATURE SCALE. A temperature scale which corresponds to the Kelvin scale but is based on the absolute zero of the Fahrenheit system, so that 0° Rankine = 459.69°F.

REFLECTIVITY. The ratio of the reflected radiant intensity of the incident radiant intensity.

RESOLUTION, ANGULAR. The angle subtended by two objects which just allows the two to be recognized as two objects rather than one. In an infrared system the resolution is equal to the scanner's instantaneous field of view.

ROLL. The revolving of the aircraft first to one side, then to the other, about its longitudinal axis.

SATURATING SIGNAL. A signal of an amplitude greater than the dynamic range of the system.

SCALE. The ratio of image size to object size, often called the "representative fraction." A scale of 1:30,000 means that 1 inch on the map equals 30,000 inches on the ground.

SCAN LINE. An image line corresponding to one revolution of a single plane mirror. A four-sided mirror system will create four scan lines on the resultant imagery during a single revolution.

SCATTERING. The diffuse reflection of light due to the interposition in the light steam of objects of varying sizes.

SENSITIVITY, SPECTRAL. The sensitivity of a photoelectric device in relation to the wavelength of the incident radiant energy.

SIGNAL-TO-NOISE RATIO. The ratio of the value of the signal to that of the noise.

SIGNATURE. An anomaly resulting from a known object or event. Identifiable image characteristics of recorded objects or events.

SINK, HEAT. A body that can absorb heat without change in the intrinsic properties of the body.

SOLAR RADIATION. The radiation from the sun comprises a very wide range of wavelengths from the long infrared to the short ultraviolet within a maximum intensity in the visible region at about 0.5 microns.

SPECIFIC HEAT. (See Heat, specific)

SPECIFIC HEAT CAPACITY. Same as Specific heat.

SPECTRAL CHARACTERISTIC. A relation, usually shown by a graph, between wavelength and some other variable.

SPECTRAL IMAGERY. Imagery obtained in specific portions of the electromagnetic spectrum using selected bandwidth limiting techniques, e.g., using film/filter combinations for visible and near visible spectrum.

STEFAN-BOLTZMANN LAW. The total radiant emittance into a hemisphere from a blackbody is directly proportional to the fourth power of the absolute temperature of the blackbody source. The constant of proportionality is 5.673×10^{-12} watts/cm^2 deg^4 Stefan Boltzmann constants.

STERADIAN. A solid range which subtends an area equal to the square of the radius.

STEREOSCOPIC IMAGE. That impression of a three-dimensional model which combines two perspective images on the retina of the viewer's eyes.

STRIP IMAGERY. Continuous image presentation displayed on long strips of film. Normally associated with side-looking radar, infrared scanning systems, and in photography, shutterless cameras.

TEMPERATURE, ABSOLUTE. The temperature measured from the absolute zero that temperature at which the volume of an ideal gas would become zero. Degrees centigrade 273.16° = degrees absolute or degrees Kelvin.

TEMPERATURE SCALE; CENTIGRADE. A temperature scale with the freezing point of water defined as 0°C and the boiling point as 100°C under conditions of normal atmospheric pressure.

TEMPERATURE SCALE; FAHRENHEIT. A temperature scale based upon the freezing point of water defined at 32°F and the boiling point as 212°F under conditions of normal atmospheric pressure.

TEMPERATURE SCALE; KELVIN. A temperature scale based upon absolute zero temperature, with the freezing point of water defined at 273.16°K under conditions of normal atmospheric pressure.

THERMAL CONDUCTION. (See Conduction, Thermal)

THERMAL CONVECTION. (See Convection, Thermal)

THERMAL RADIATION. All bodies that are not at absolute zero emit radiation excited by the thermal agitation of their molecules or atoms. This thermal radiation depends upon the nature of the body and its temperature. The Planck radiation formula results in the best description of thermal radiation.

THERMOLUMINESCENCE. The property possessed by many minerals of emitting visible light when heated. Results from release of energy stored as electron displacement in the crystal lattice.

TIME CONSTANT. All photon detectors require a certain time to respond to a radiation pulse and continue to respond for a small time after the radiation ceases. The time constant is a measure of this time lag.

TONE. Each distinguishing shade variation from black to white.

TRANSMISSION COEFFICIENT. The ratio of transmitted to incident radiation per unit thickness for a given material.

TRANSMISSIVITY. The fraction of the incident radiation power which is transmitted by the medium.

TUBE, CATHODE RAY. (See Cathode-Ray Tube)

WASHOUT. A condition during which the total energy radiated from a unit area of most objects on the ground is essentially the same. When this happens, it becomes impossible to distinguish boundaries between such objects as land and water or to see roads on infrared imagery (see also Crossover).

WATT. A unit of power. The rate of energy consumption or conversion when one joule of energy is consumed or converted per second.

WAVELENGTH. The displacement of a wave which occurs during one complete period. Wave velocity = frequency X wavelength.

WIENS DISPLACEMENT LAW. The wavelength at which the radiation from a blackbody has it greatest intensity is inversely proportional to the absolute temperature of the body, i.e., $\lambda_m T$ = constant, thus as the temperature rises, the peak of the distribution curve is shifted toward the short wavelength of the spectrum.

WIENS LAW. The power emitted by a blackbody within the maximum intensity wavelength interval is proportional to the fifth power of the absolute temperature.

WIENS RADIATION LAW. An attempt to describe the spectral distribution of energy from a blackbody which agrees with experimental data for short wavelengths and low temperatures.

YAW. The unplanned rapid changing of aircraft heading.